PRECLINICAL SAFETY ASSESSMENT OF INDIGENOUS PROBIOTIC *Limosilactobacillus fermentum* NCDC 400

THESIS SUBMITTED TO THE

ICAR-NATIONAL DAIRY RESEARCH INSTITUTE, KARNAL

(DEEMED UNIVERSITY)

IN PARTIAL FULFILMENT OF THE REQUIREMENTS

FOR THE AWARD OF THE DEGREE OF

DOCTOR OF PHILOSOPHY

IN

DAIRY MICROBIOLOGY

BY

BASAVAPRABHU H N
M. Tech. (Dairy Microbiology)

DIVISION OF DAIRY MICROBIOLOGY

ICAR-NATIONAL DAIRY RESEARCH INSTITUTE

(DEEMED UNIVERSITY)

KARNAL-132001 (HARYANA), INDIA

2023

Regn. No. 19-P-DM-01

PRECLINICAL SAFETY ASSESSMENT OF INDIGENOUS PROBIOTIC *Limosilactobacillus fermentum* NCDC 400

BY

BASAVAPRABHU H N

THESIS SUBMITTED TO THE
ICAR-NATIONAL DAIRY RESEARCH INSTITUTE, KARNAL
(DEEMED UNIVERSITY)
IN PARTIAL FULFILMENT OF THE REQUIREMENTS
FOR THE AWARD OF THE DEGREE OF

DOCTOR OF PHILOSOPHY

IN

DAIRY MICROBIOLOGY

Approved by:

06/03/2023

(Prof. Neeraj Kumar)
(EXTERNAL EXAMINER)

06/03/2023

Dr. PRADIP V BEHARE
MAJOR ADVISOR & CHAIRMAN

MEMBERS OF ADVISORY COMMITTEE		
1.	**Dr. Anil Kumar Puniya** Principal Scientist, DM Division	
2.	**Dr. Diwas Pradhan** Scientist (SS), DM Division	7/3/2023
3.	**Dr. Suman Kapila** Principal Scientist, ABC Division	On International Tour
4.	**Dr. Sudarshan Kumar** Principal Scientist, ABTC	06.03.2023
5.	**Dr. Sachinandan De** Principal Scientist, ABTC (Director's Nominee)	6/3/2023

DAIRY MICROBIOLOGY DIVISION
NATIONAL DAIRY RESEARCH INSTITUTE
(DEEMED UNIVERSITY)
KARNAL-132001 (HARYANA), INDIA

Dr. Pradip V Behare
Senior Scientist

CERTIFICATE

This is to certify that the thesis entitled **"PRECLINICAL SAFETY ASSESSMENT OF INDIGENOUS PROBIOTIC *Limosilactobacillus fermentum* NCDC 400"** submitted by **Mr. BASAVAPRABHU H N** towards the partial fulfilment of the requirements for the award of the degree of **DOCTOR OF PHILOSOPHY in DAIRY MICROBIOLOGY** of the **ICAR- National Dairy Research Institute (Deemed University)**, **Karnal (Haryana), India**, is a bonafide research work carried out by him under my supervision and guidance and no part of the thesis has been submitted for any other degree or diploma.

Dated:

(Dr. Pradip V Behare)
Major Advisor & Chairman
(Guide)

Dedicated

to

my breath and my almighty

"Amma and Ajji" . . .

Acknowledgments

The journey of my fruitful and challenging life would never start with acknowledging the valuable suggestions and well wishes of numerous people and it's a great time to express my deepest sense of gratitude to a few of them. It is all due to accompany and support of many people in my academic and personal life, which made me possible to bring out the efforts and hard work into a thesis. It obviously gives me immense pleasure to dedicate my extreme sense of respect and gratitude.

First of all, I take the privilege to dedicate my deepest sense of gratitude to my major advisor ***Dr. Pradip V. Behare****, Senior scientist, Dairy Microbiology Division, NDRI, Karnal for his constant support and care throughout my Ph.D. journey which made it possible to shape this thesis. I am very fortunate to obtain scholarly guidance from sir.*

I would like to acknowledge ***ICAR-National Dairy Research Institute,*** *Karnal for providing me Institutional Fellowship during this Ph.D. program and* ***Dr. Dheer Singh****, (Director), and* ***Dr. M. S. Chauhan (Former Director),*** *ICAR-NDRI, for proving necessary research facilities to carry out my research work. Further I would like to extend my gratitude to the Head, Dairy Microbiology Division for kind support throughout my doctoral degree programme.*

I would like to acknowledge the members of the advisory committee, ***Dr. Anil Kumar Puniya, PS,*** *DM Division,* ***Dr. Diwas Pradhan,*** *Sci (SS), DM Division,* ***Dr. Suman Kapila, PS, ABC Division, Dr. Sudarshan Kumar,*** *Sr. Sci, ABTC, and* ***Dr. Sachinandan De****, PS, ABTC (Director's Nominee), for their valuable suggestion throughout my research work.*

Special thanks to ***Dr. A. K Dang,*** *PS, AP Division, and* ***Dr. Raju*** *(LRC) for providing the blood analyzer for my research work. I would like to express my extreme gratitude to* ***Dr. Rubina K, Baithalu****, Sci, LPM Division, and* ***Dr. Rashmi H. M.****, Sr. Sci, DM Division for providing the transwell plates and bead beater facility, respectively. Further, I would like to express my deepest thanks to* ***Dr. Rajan Sharma****, PS, DC*

Division, for proving me with an opportunity to use the ATR-FTIR facility located in the National Referral Center for Milk Quality and Safety, NDRI, Karnal.

I wish to express my deepest sense of gratitude to ***Dr. Jeevan K****, Scientist-1, ICMR-Regional Ayurveda Research Institute, and* ***Dr. S K, Niranjan****, PS, ICAR-NBAGR, Karnal,* ***Dr. Ravinder Nagpal****, Assistant Professor, FSU College of Health and Human Sciences, USA, for their kind assistance in histopathological analysis, genotoxicity assays, and gut microbiome analysis, respectively.*

My academic life has no meaning without acknowledging my inspiration and guru ***Dr. R. Prabha****, former associate professor and Head, the Department of Dairy Microbiology, Dairy Science College, Hebbal, Bengaluru for her constant encouragement and intellectual support in my entire student life. I always bow to her blessings and well wishes, which otherwise would never be possible to shape my academic carrier. As my inspiration, madam's simplicity and humbleness made it possible to shape my personal life too.*

It's my great pleasure to express my sincere thanks to TFSL lab members ***Soniya****,* ***Dr. Manorama Kumari****,* ***Nishu****,* ***Shashank****, and* ***Rishab*** *for their immense support throughout my research tenure and made my stay comfortable in TFSL. A special thanks to* ***Yogita ma'am, Mr. Satish, and Mr. Rajveer*** *for their help throughout my research tenure in TFSL.*

*Finally, I would like to thank my almighty "****Mother****" for introducing me to this wonderful world with her constant support and her divine blessings, which are making me reach my goals. I thank my special members* ***Ajji****,* ***Thata****,* ***Loki mama****,* ***Shivu mama****,* ***Sahana akka****,* ***Manju attae****,* ***Shashu****,* ***Preru****, for their endless support throughout my life. Finally, I thank all my cousins* ***Pradhi anna****,* ***Chida anna****,* ***Babu anna****,* ***Prathima akka,*** *and* ***Nagaraj anna*** *who stood with me in all the sorrows and joys of my life.*

Date: ***(BASAVAPRABHU H N)***

CONTENTS

LIST OF TABLES

LIST OF FIGURES

LIST OF ABBREVIATIONS

AFLP	Amplified Fragment Length Polymorphism
AI	Atherogenic index
AIDS	Acquired Immunodeficiency Syndrome
ALT	Alanine Aminotransferase
AMR	Antimicrobial Resistance
ANOVA	Analysis of Variance
ARDB	Antibiotic Resistance Genes Database
ARDRA	Amplified Ribosomal DNA Restriction Analysis
ARG-ANNOT	Antibiotic Resistance Gene-ANNOTation
AST	Aspartate Aminotransferase
ASVs	Amplicon sequence variants
ATCC	American Type Culture Collection
ATR	Attenuated Total Reflectance
BD	Basal Diet
BLAST	Basic Local Alignment Search Tool
BMCs	Bone Marrow Cells
bp	Base pair
BSA	Bovine Serum Albumin
BSH	Bile Salt Hydrolase
BW	Body Weight
CARD	Comprehensive Antibiotic Resistance Database
CAT	Catalase
CDS	Coding Sequences
CFU	Colony Forming Unit
CGE	Center for Genomic Epidemiology
CIA	Critically Important Antimicrobials
CLSI	Clinical and Laboratory Standards Institute
CON	Control
ConA	Concanavalin A
COVID	Coronavirus Disease
CRISPR	Clustered Regularly Interspaced Short Palindromic Repeats
CT	Closure Time
Cy	Cyclophosphamide
DBT	Department of Biotechnology
DE	Dimensional gel electrophoresis
D-gal	D-galactose
DGGE	Denaturing Gradient Gel Electrophoresis
dL	Deciliter
DLC	Differential Leukocyte Count
DMEM	Dulbecco's Modified Eagle Medium
DNA	Deoxyribonucleic Acid
ECM	Extracellular Matrix
EDTA	Ethylenediaminetetraacetic Acid
EFSA	European Food Safety and Standards Authority
ELISA	Enzyme-Linked Immunosorbent Assay
EPS	Exopolysaccharides

ESI-Q-TOF-MS	Electrospray Ionization-Quadrupole-Time of Flight Mass Spectrometry
EtBr	Ethidium Bromide
EU	European Union
EUCAST	European Committee on Antimicrobial Susceptibility Testing
FAO	Food and Agricultural Organization
FF	Faecal flora
fl	Femtoliter
FSSAI	Food Safety and Standards Authority of India
FTIR	Fourier Transform Infrared
g	Relative Centrifugal Force
g	Gram
G	Gauge
GpX2	Glutathione peroxidase
GRAN	Granulocytes
GRAS	Generally Recognized as Safe
h	Hour
H and E	Hematoxylin and Eosin
Hb	Hemoglobin
HCT	Hematocrit Test
HD	High Dose
HDL	High-density lipoprotein
Hfr	High-Frequency Recombination
HHT	Hereditary Hemorrhagic Telangiectasia
HLP	Hemolysin-Like Protein
HPLC	High-Performance Liquid Chromatography
HRESI-MS	High-Resolution Electrospray Ionization Mass Spectrometry
IAEC	Institute Animal Ethics Committee
ICAR	Indian Council of Agricultural Research
ICMR	Indian Council of Medical Research
IDF	International Dairy Federation
IE	Infective Endocarditis
Ig	Immunoglobulin
IL	Interleukin
IP/ i.p.	Intraperitoneally
ISO	International Organization for Standardization
kb	Kilo base
KEGG	Kyoto Encyclopedia of Genes and Genomes
Kg	Kilogram
LAB	Lactic Acid Bacteria
LC-MS/ MS	Liquid Chromatography- Mass Spectrometry
LD	Lethal Dose
LD	Low Dose
LDH	Lactate Dehydrogenase
LDL	Low-density lipoprotein
LPS	Lipopolysaccharide
LYM	Lymphocytes
M	Mole

MALD-TOF-MS	Matrix-Assisted Laser Desorption Time Of Flight Mass Spectrometry
MC	Model Control
MCH	Mean Corpuscular Hemoglobin
MCP	Monocyte chemoattractant protein
MCV	Mean Corpuscular Volume
MIC	Minimum Inhibitory Concentration
min	Minute
mL	Milliliter
MLST	Multilocus Sequence Typing
mm	Millimetre
MON	Monocytes
MRS	deMan, Rogosa, and Sharpe
MTCC	Microbial Type Culture Collection and Gene Bank
NC	Normal Control
NCBI	National Centre for Biotechnology Information
NCCS	National Centre for Cell Sciences
NCDC	National Collection of Dairy Cultures
NDRI	National Dairy Research Institute
NGS	Next Generation Sequencing
NO	Nitric oxide
NOAEL	No Observed Adverse Effect Level
NOEL	No Observable Effect Level
OECD	Organization for Economic Cooperation and Development
ORF	Open Reading Frame
OriT	Origin of Transfer
PAS	Periodic acid-Schiff
PBS	Phosphate Buffered Saline
PCoA	Principal coordinate analysis
PCR	Polymerase Chain Reaction
PCT	Procalcitonin Test
PFGE	Pulse-Field Gel Electrophoresis
pg	Picogram
PHASTER	PHAge Search Tool Enhanced Release
PLT	Platelets
QPS	Qualified Presumption of Safety
QPS	Qualified Presumption of Safety
RAPD	Random Amplified Polymorphic DNA
RAST	Rapid Annotation Subsystem
RBCs	Red Blood Cells
rDNA	Ribosomal-Deoxyribonucleic Acid
Rep-PCR	Repetitive Extragenic Palindromic PCR
RGI	Resistance Gene Identifier
RH	Relative Humidity
rpm	Revolutions Per Minute
RPMI	Roswell Park Memorial Institute
SCFAs	Short Chain Fatty Acids
SDS-PAGE	Sodium dodecyl-sulfate polyacrylamide gel electrophoresis

sec	Second
SET	Sodium EDTA Tris
SNP	Single Nucleotide Polymorphism
SOD	Superoxide dismutase
T4CP	Type IV Coupling Protein
T4SS	Type IV Secretion System
TAE	Tris-Acetate EDTA
TEE	Transesophageal Echocardiography
TGF-beta	Transforming growth factor
TGGE	Temperature Gradient Gel Electrophoresis
TLC	Thin Layer Chromatography
TNF-alpha	Tumour Necrosis Factor alpha
tPA	Tissue-type Plasminogen Activator
UV	Ultra-Violet
v/v	Volume by volume
VFDB	Virulence Factors Database
VLDL	Very low-density lipoprotein
w/v	Weight by volume
w/w	Weight by weight
WBC	White Blood Cells
WGS	Whole-Genome Sequencing
WHO	World Health Organization
µg	Microgram
µL	Microliter
µL	Microliter

ABSTRACT

Regardless of the long and safe use of lactic acid bacteria throughout human evolution, the safety assessment of potential probiotic strains has become a pragmatic regulatory obligation before clinical translation. The present study was undertaken to evaluate the pre-clinical safety and toxicology of *Limosilactobacillus fermentum* NCDC 400, an in-house industrially important and potential probiotic strain, using a battery of *in vitro*, *in silico*, and *in vivo* approaches. *In vitro* tests suggest that the strain was devoid of debilitating phenotypes/ activities of hemolysin, coagulase, urease, DNase, gelatinase, β-glucuronidase, β-glucosidase (harmful enzymes), platelet aggregation, mucin and phenylalanine degradation. Overproduction of adverse metabolites such as biogenic amines, D-lactate, ammonia, and indole was also not witnessed by this strain. The test strain was sensitive to the antagonistic property of human serum (> 3 $\log_{10}$ reductions at 3 h). Under the purview of regulatory guidelines, *L. fermentum* NCDC 400 was sensitive to all the antibiotics enlisted by EFSA guidelines for obligate heterofermentative lactobacilli. The targeted PCR assays using genomic and plasmid DNA of *L. fermentum* NCDC 400 against the genes conferring unusual antibiotic resistance *viz*. tetracycline, erythromycin, chloramphenicol, and beta-lactams were found absent. The virulence genes encoding coagulase (*Coa*), nuclease (*nucA*), and gelatinase (*gelE*) were also unseen. Further, an in-depth analysis of the whole genome of *L. fermentum* NCDC 400 using suitable bioinformatics pipelines and their subsequent validation through multiple databases inferred that this bacterium is non-pathogenic to humans as well as absence of potential antibiotic resistance genes (extrinsic resistance) bearing lateral transferability. In cell culture assays, *L. fermentum* NCDC 400 was found to be non-cytotoxic to Caco-2 cells even at a concentration as high as 10^{11} CFU/ mL as well as did not alter their cellular integrity when cultured on transwell inserts. In oral toxicity tests, the daily oral administration of *L. fermentum* NCDC 400 at 10^8 (low dose) and 10^{10} (high dose) cells/ mouse for 14 (acute), 28 (subacute), and 90 (subchronic) days did not induce treatment-related toxicity either in terms of physiological behaviors or clinical parameters (hematology, clinical biochemistry, histopathology, and immune status) of mice. Episodes of *L. fermentum* NCDC 400-mediated bacterial translocation to extra-intestinal organs were unnoticed in all three oral toxicity studies. Safety and efficacy evaluation of *L. fermentum* NCDC 400 in an immunocompromised mice model revealed no test strain related adverse effect on the physiological behaviors or clinical parameters of mice; rather it augmented the immune status of mice by immune stimulation (cytokine balance). *L. fermentum* NCDC 400 was well tolerated in the immunocompromised mice model and did not foster any adverse effects like genotoxicity even at a high dose (10^{10} CFU/mice/day). Owing to these findings, a dose of 10^{10} CFU/mice/day may be considered NOEL (No Observable Effect Level) in both healthy and immunocompromised mice. Moreover, NCDC 400 intervention resulted in enhancing the richness and diversity of gut bacteria by fostering beneficial saccharolytic microbes including potential next-generation probiotics (NGPs) while declining the pathobionts. Overall, the results that emerged from this study underscore the safe and non-toxic behavior of *L. fermentum* NCDC 400 and thereby call for and should facilitate further human clinical trials.

सारांश

मानव विकास के दौरान लैक्टिक एसिड बैक्टीरिया के लंबे और सुरक्षित उपयोग के बावजूद संभावित प्रोबायोटिक स्ट्रेनों का सुरक्षा मूल्यांकन नैदानिक कार्य करने के लिए दिए जाने से पूर्व एक व्यावहारिक नियामक बाध्यता बन गई है। वर्तमान अध्ययन लिमोसिलैक्टोबैसिलस फेरमेंटम एनसीडीसी 400 जो इन-हाउस औद्योगिक रूप से महत्वपूर्ण और संभावित प्रोबायोटिक स्ट्रेन है, जो इन-विट्रो, इन सिलिको और इन विवो दृष्टिकोणों की बैटरी का उपयोग करते हुए पूर्व-नैदानिक सुरक्षा और विष विज्ञान का मूल्यांकन करने के लिए किया गया था । इन विट्रो परीक्षणों से पता चलता है कि स्ट्रेन कमजोर करने वाले फेनोटाइप / हेमोलिसिन, कोगुलेज़, यूरेज़, DNase, जिलेटिनस, β-ग्लूकोरोनिडेज़, β-ग्लूकोसिडेज़ (हानिकारक एंजाइम), प्लेटलेट एकत्रीकरण, म्यूसिन और फेनिलएलनिन के गिरावट की गतिविधियों से रहित था। बायोजेनिक एमाइन, डी-लैक्टेट, अमोनिया और इंडोल जैसे प्रतिकूल मेटाबोलाइट्स का अधिक उत्पादन भी इस स्ट्रेन में नहीं देखा गया। परीक्षण किया जाने वाला स्ट्रेन मानव सीरम(3 एच पर 3 लॉग कमी) की विरोधी गुण के प्रति संवेदनशील था । विनियामक दिशानिर्देशों के दायरे में एल. फेरमेंटम एनसीडीसी 400 ईएफएसए दिशानिर्देशों द्वारा सूचीबद्ध सभी एंटीबायोटिक दवाओं के प्रति संवेदनशील था, जो विषमलैंगिक लैक्टोबैसिली को बाध्य करते हैं। एल. फेरमेंटम एनसीडीसी 400 के जीनोमिक और प्लास्मिड डीएनए का उपयोग कर लक्षित पीसीआर जांच असामान्य एंटीबायोटिक प्रतिरोध में टेट्रासाइक्लिन, एरिथ्रोमाइसिन, क्लोरैम्फेनिकॉल और बीटा-लैक्टम अनुपस्थित पाए गए को प्रदान करने वाले जीन के खिलाफ होती है। कोगुलेज़ (सीओए), न्यूक्लियस (एनयूसीए), और जिलेटिनेज़ (जेलई) को एन्कोडिंग करने वाले विषाणु जीन भी अनदेखी थे। इसके अलावा, उपयुक्त जैव सूचना विज्ञान पाइपलाइनों का उपयोग करके एल. फेरमेंटम एनसीडीसी 400 के पूरे जीनोम का गहन विश्लेषण और कई डेटाबेस के माध्यम से उनके बाद के सत्यापन से यह निष्कर्ष निकला कि यह जीवाणु मनुष्यों के लिए रोगजनक नहीं है और साथ ही संभावित एंटीबायोटिक प्रतिरोध जीन (बाहरी प्रतिरोध) की अनुपस्थिति के बावजूद बाद में हस्तांतरणीयता देखी गई | सेल कल्चर एसेज़ में, L. फेरमेंटम एनसीडीसी 400 को Caco-2 कोशिकाओं के लिए गैर-साइटोटोक्सिक पाया गया, यहां तक कि 10^{11} सीएफयू/एमएल जितनी अधिक सांद्रता के साथ-साथ ट्रांसवेल इंसर्ट पर सुसंस्कृत होने पर उनकी सेलुलर अखंडता में बदलाव नहीं किया। मौखिक विषाक्तता परीक्षणों में, 10^8 (कम खुराक) और 10^{10} (उच्च खुराक) कोशिकाओं/माउस पर एल. फेरमेंटम एनसीडीसी 400 का दैनिक मौखिक प्रशासन 14 (एक्यूट), 28 (सबएक्यूट), और 90 (सबक्रोनिक) दिनों के लिए प्रेरित नहीं किया जबकि उपचार से संबंधित विषाक्तता या तो चूहों के शारीरिक व्यवहार या नैदानिक मापदंडों (हेमेटोलॉजी, नैदानिक जैव रसायन, हिस्टोपैथोलॉजी और प्रतिरक्षा स्थिति) के संदर्भ मेंदेखी गई। तीनों ओरल टॉक्सिसिटी स्टडीज में एल. फेरमेंटम एनसीडीसी 400-मध्यस्थता वाले बैक्टीरियल ट्रांसलोकेशन के एक्सट्रा-इंटेस्टाइनल ऑर्गन्स पर ध्यान नहीं दिया गया। प्रतिरक्षा में अक्षम चूहों के मॉडल में एल. फेरमेंटम एनसीडीसी 400 की सुरक्षा और प्रभावकारिता के मूल्यांकन से पता चला कि चूहों के शारीरिक व्यवहार या नैदानिक मापदंडों पर कोई परीक्षण स्ट्रेन संबंधी प्रतिकूल प्रभाव नहीं पड़ा; बल्कि इसने प्रतिरक्षा उत्तेजना (साइटोकिन संतुलन) द्वारा चूहों की प्रतिरक्षा स्थिति को बढ़ाया। एल. फेरमेंटम एनसीडीसी 400 को प्रतिरक्षा में अक्षम चूहों के मॉडल में अच्छी तरह से सहन किया गया था और उच्च खुराक (10^{10} सीएफयू/चूहे/दिन) पर भी जीनोटॉक्सिसिटी जैसे किसी प्रतिकूल प्रभाव को बढ़ावा नहीं दिया। इन निष्कर्षों के कारण, 10^{10} सीएफयू/चूहे/दिन की खुराक को स्वस्थ और प्रतिरक्षा में अक्षम चूहों दोनों में NOEL (नो ऑब्जर्वेबल इफेक्ट लेवल) माना जा सकता है। इसके अलावा, एनसीडीसी 400 के हस्तक्षेप के परिणामस्वरूप संभावित अगली पीढ़ी के प्रोबायोटिक्स (एनजीपी) सहित लाभकारी सैक्रोलाइटिक रोगाणुओं को बढ़ावा देकर पेट के बैक्टीरिया की समृद्धि और विविधता में वृद्धि हुई है, जबकि पैथोबियोन में कमी आई है। कुल मिलाकर, इस अध्ययन से जो परिणाम सामने आए हैं, वे एल. फेरमेंटम एनसीडीसी 400 के सुरक्षित और गैर-विषैले व्यवहार को रेखांकित करते हैं और इस तरह आगे के मानव नैदानिक परीक्षणों की मांग करते हैं यदि उन्हें सुविधाजनक बनाना चाहिए।

Introduction

INTRODUCTION

The beneficial microbes, especially the lactic acid bacteria (LAB), have been safely used over the years. As progress is being made in gut microbiota and probiotic science, today, there is ample evidence to brace the numerous health-beneficial properties of probiotics. This escalated the probiotic interventions to prevent, ameliorate, or treat specific disease manifestations. Hitherto, the clinical use of probiotics as live biotherapeutic agents perpetuated among adults as well as infants of various health and physiological conditions. However, the safety of probiotics in varying human health and physiology is questionable because of inconsistent outcomes reported in a multitude of clinical trials, case reports, and experimental models. In addition, the preponderance of probiotics in fostering various theoretical risks, such as systemic bloodstream infections, production of harmful metabolites and enzymes, virulence factors, drug resistance, gastrointestinal side effects, and excessive immune stimulation in susceptible human subjects, have been increasingly reported (Doron and Snydman, 2015; Sotoudegan *et al*., 2019). Regardless of a history of long and safe use of LAB throughout human evolution, the growing market demand, as well as consumer consciousness on probiotics, has necessitated advancement in safety standards and disclosure of validated scientific proofs for the mentioned health claims on all probiotic products. This perhaps calls for an in-depth and comprehensive safety assessment of potential probiotic strains before introduction into the food system or clinical translation. Hence, it is paramount to appraise the benefit-to-risk ratio of any potential probiotic strain before their human administration. To achieve this, an amalgamation of suitable *in silico* tools, *in vitro* tests, and *in vivo* models may help nominate the probiotic strains devoid of potential risk factors. In congruence, both national and international regulatory apex bodies, such as the Indian Council of Medical Research/ Department of Biotechnology (ICMR/ DBT) and the Food and Agricultural Organization/ World Health Organization (FAO/ WHO) have formulated *in vitro* and *in vivo* guidelines to investigate the safety and efficacy of all potential probiotics (Ganguly *et al*., 2011).

Limosilactobacillus fermentum NCDC 400 is an in-house heterofermentative lactic acid bacteria isolated from *Dahi* (Indian fermented milk). The strain has been deposited at the Microbial Type Culture Collection and Gene Bank (MTCC), Chandigarh, and designated as *L. fermentum* MTCC 25407. The strain has an impending to emerge as an allochthonous probiotic bacterium since it demonstrated desirable probiotic attributes,

such as acid and bile tolerance, cell surface hydrophobicity, auto-aggregation, co-aggregation, antimicrobial activity, etc. (Panicker *et al*., 2018). Further understanding of the gastrointestinal resilience of this strain at the proteome level indicated that it imbibes an array of cellular mechanisms to survive and establish in the gastrointestinal milieu (Pragya *et al*., 2017; Kaur *et al*., 2017). Besides, *L. fermentum* NCDC 400 has shown various health benefits such as cholesterol-lowering, anti-oxidant and anti-inflammatory activities, and demonstrated protective effects on reproductive health, and obesity-induced hepatic steatosis in suitable experimental models (Akram *et al*., 2022; Gawande *et al*., 2021; Rani *et al*., 2022). From an industrial perspective, *L. fermentum* NCDC 400 is technologically a robust strain, well-known for its ability to produce exopolysaccharides "EPS 400" which improves the rheological properties of fermented dairy foods (Behare *et al*., 2013). Therefore, the strain with dual properties of being a potential probiotic as well as industrially important, offers a two-fold advantage for futuristic applications as functional probiotics.

After deciphering the functional and therapeutic efficacy of *L. fermentum* NCDC 400 under *in vitro* and *in vivo* conditions, it was pragmatic and obligatory that this strain must adhere to the existing probiotic guidelines (ICMR/ DMBT) of the country before utilization as food supplements/ nutraceuticals. Accordingly, the next step was to understand how best the strain is tolerated in healthy and immunocompromised animals at various doses. This would be possible only by conducting bio-safety directed pre-clinical trials to unknot any ill effects on health. Henceforth, the present research program has been designed to assess the safety of NCDC 400 by amalgamating the *in vitro* approaches, contemporary omics-based approaches, as well as the probiotic-specific conventional toxicology involving laboratory animals, particularly rodents. Owing to the fact that the safety of probiotics among immunocompromised subjects is a matter of concern, this study also investigates the safety and efficacy of *L. fermentum* NCDC 400 in an immunocompromised mice model. In this context, the present investigation was formulated with three following objectives;

1. Assessment of *Limosilactobacillus fermentum* NCDC 400 for safety aspects using *in vitro* methods.
2. Toxicological evaluation of *Limosilactobacillus fermentum* NCDC 400 in the murine model.
3. Evaluation of safety and efficacy of *Limosilactobacillus fermentum* NCDC 400 in an immunocompromised murine model.

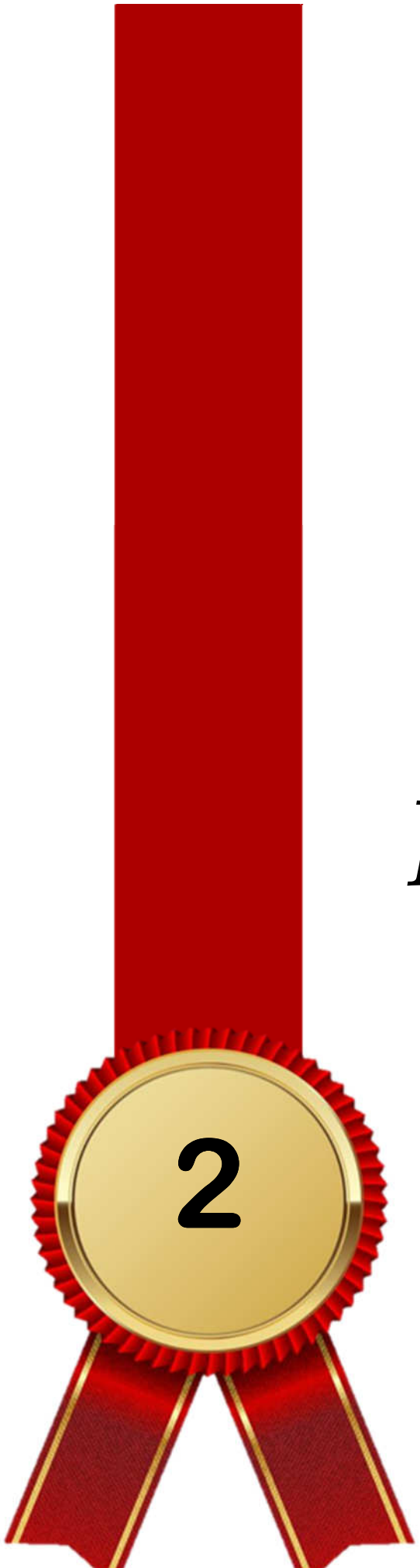

Review of Literature

REVIEW OF LITERATURE

2.1. Prologue

Viable microorganisms have become an inseparable part of the human diet and are frequently consumed in various fermented foods. The etymology of the use of beneficial microorganisms was lost with centuries of antiquity. Though there were no solid scientific evidences, beneficial microorganisms, such as lactic acid bacteria, have long been used as foods and biotherapeutic agents to ameliorate gastrointestinal disturbances (Prajapati and Nair, 2008). Amid this Metchnikoff's view, the scientific advancements in the microbial sciences have paved the way to conceptualize probiotics as "a traditional concept with the modern facet." *Lactobacillus* and *Bifidobacterium* are the conventionally used probiotic genera owing to their Qualified Presumption of Safety (QPS) status accorded by the European Food Safety and Standards Authority (EFSA). Similarly, a yeast probiotic, *Saccharomyces boulardii,* holds a significant market value in the human and animal probiotics sector (Sen and Mansell, 2020). On the other hand, the probiotic candidature of unconventional genera has recently gained wide popularity as next-generation probiotics (*Akkermansia muciniphila, Bacteroides fragilis, Gordonibacter urolithinfaciens, Clostridium beijerinckii, Faecalibacterium prausnitzii, Parabacteroides goldsteinii*) (Lin *et al*., 2019). Besides the proven roles of probiotics in gastrointestinal disorders, comprehensive investigations have been made to decipher the underlying mechanisms of probiotics in mitigating both infectious and lifestyle diseases associated with the brain (Ansari *et al*., 2020), lung (Forsythe, 2011), urogenital tract (Ballini et *al*., 2018), kidney (Tao *et al*., 2019), liver (Xue *et al*., 2017), pancreas (Lutgendorff *et al*., 2008), and including oral health (Nadelman *et al*., 2018).

Although the term probiotics portray a beneficial connotation on human health, the safety assessment of potential probiotic strains has become a pragmatic and mandatory criterion for clinical translation irrespective of the genera or their historic safe use. This is perhaps because of their unusual behaviors reported in patients immunocompromised (diseased subjects or critically ill patients) (Gore and Tucker, 2020; Rossi *et al*., 2019; Singhi and Baranwal, 2008). An escalating shift from traditional probiotics to next-generation probiotics (organisms with no safety background) also demands an initial idea on safety perspectives (Xu *et al*., 2020). On top of this, the

enduring threat of antibiotic resistance, horizontal gene transfer, virulence determinates, and adverse metabolites among food-grade bacteria have become practical safety concerns in this era of antimicrobial resistance (Kim and Kang, 2020; Rastogi *et al*., 2019). Considering these undesirable properties, Food and Agriculture Organization/ World Health Organization (FAO/ WHO) drafted international guidelines to reconcile the attributes of candidate probiotic strains for human applications (FAO, 2002). Since then, several regional regulatory bodies have framed safety evaluation guidelines following FAO/ WHO guidelines. For example, the Food Safety and Standards Authority of India (FSSAI) regulate the probiotic category of foods in India by complying with Indian Council of Medical Research- Department of Biotechnology (ICMR-DBT) guidelines (Ganguly *et al*., 2011), the European Food Safety Authority (EFSA) guidelines in Europe and Norwegian Food Safety Authority guidelines in Norway (Yazdankhah *et al*., 2014). These guidelines commonly suggest evaluating intrinsic and adoptive antibiotic-resistant traits and virulence determinants (*in vitro* and *in vivo*) (**Fig. 2.1**).

2.2. The art of fermentation to the science of probiotics

Although the process of microbial fermentation was majorly focused on preserving the surplus food, the knowledge on health benefits upon the consumption of fermented foods was entrenched throughout human evolution. The history of human consumption of fermented foods dates bakes to several years ago (10,000 BC). The art of fermentation was reported to be originated in the Indian subcontinent during the Indus valley civilization. The occurrence of such fermented products in the pre-Vedic (Harappan civilization) and Vedic era was also evidenced in the holy scripture of the Hindu eternal religion "Veda". The artifacts from various parts of the world, such as Egypt and the Middle East, depict that fermentation was practiced across the globe from the old days (Prajapati and Nair, 2008). Most of the fermented products have been prepared from the traditional know-how, representing the geographical culture and region where they originated. For instance, archeological studies during ancient history suggest that microorganisms were used to produce fermented beverages even during 7,000 BC in the city of Jiahu, located in the southwestern part of the Chinese Republic (Ozen and Dinleyici, 2015).

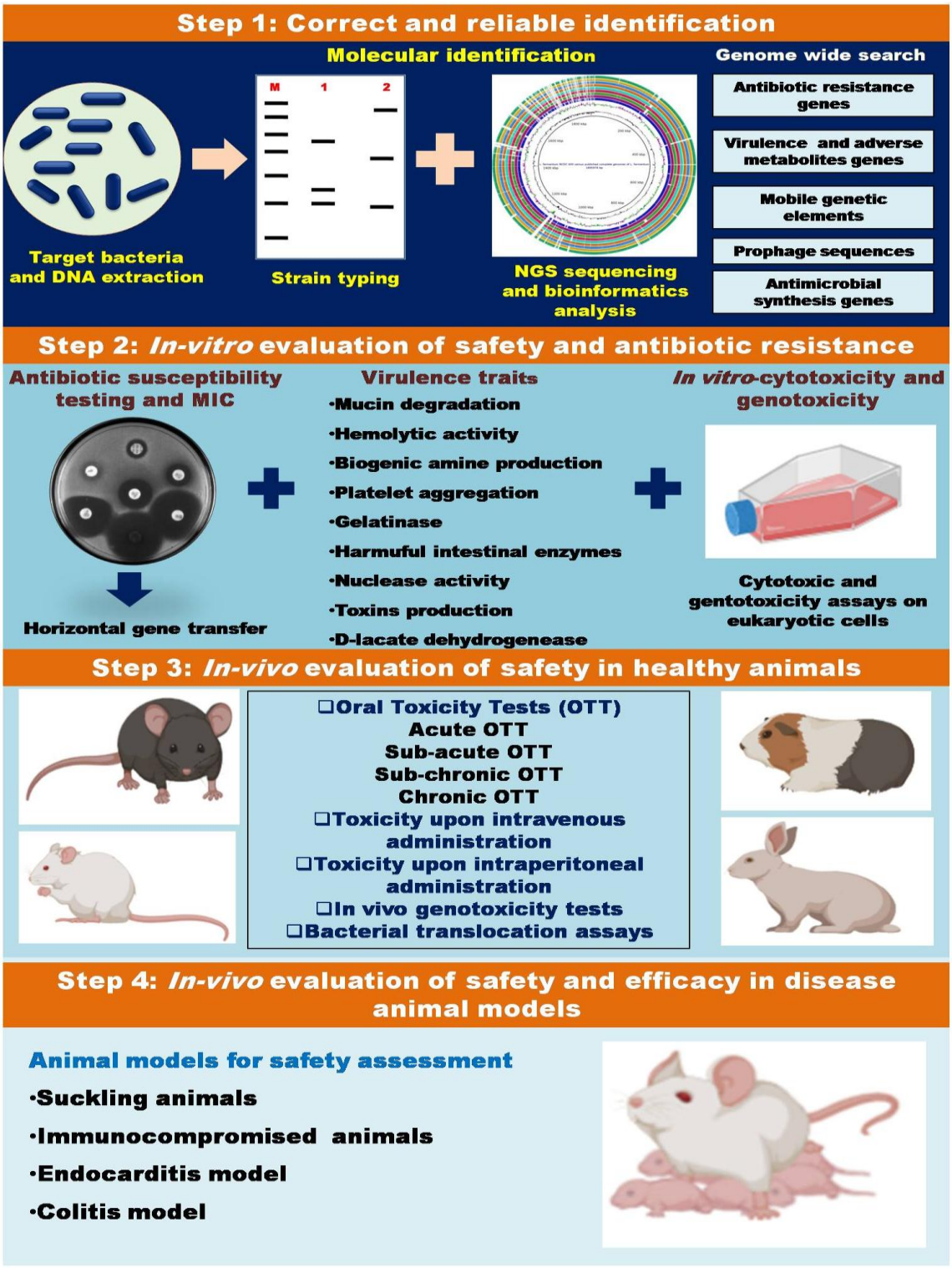

Fig. 2.1: Route-map for the preclinical safety assessment of potential probiotic strains

With the discovery of lactic acid bacterial fermentation by Pasteur in 1857, the notion of using beneficial microorganisms became more popular in microbiological history. Since then, several beneficial microbes have been isolated and characterized,

including *Bifidobacterium* spp. in 1889 by Henry Tissier (Kusumitha *et al*., 2020). Of note, the discovery and the industrial application of two strains *viz. Escherichia coli* Nissle 1917 by Alfred Nissle (1917) and *Lacticaseibacillus casei* strain by Shirota and Dr. Minoru Shirota (1935) were the milestones in probiotic history. The term "probiotic" has been derived from the Greek/Latin word "*for life*", indicating a precisely opposite meaning of antibiotics lineage, i.e., "*against life*" (Akram *et al*., 2017). The usage of probiotic terminology was not so common until 1965 when Lilley and Stillwell used it for the first time to describe the substances secreted by one microorganism, which later stimulated another's growth. Nearly a decade after (1974), Parker's first attempt was made to define this concept as "*organisms and substances which contribute to intestinal microbial balance*". However, Parker's definition was amended and redefined to highlight the importance of live microbiota in defining probiotics by Fuller in 1989 as "*a live microbial feed supplement that beneficially affects the host animal by improving its intestinal microbial balance*" (Fuller, 1992). Lately, an attempt was made in 2001 to define probiotics by an expert consultation working on behalf of the FAO/ WHO as "*live microorganisms which when administered in adequate amounts confer a health benefit on the host*". Nevertheless, an expert panel in the International Scientific Association for Probiotics and Prebiotics (2013) has bought some trivial grammatical changes in the existing definition without recasting the meaning proposed by FAO/WHO in 2001. Accordingly, the newly amended and internationally agreed definition of probiotics can be defined as "*live microorganisms that, when administered in adequate amounts, confer a health benefit on the host*" (Hill *et al*., 2014).

2.3. Probable risks associated with probiotics

Though the historic background describes the safe usage of live fermentative microbes, the mounting evidence supported by clinical trials or case reports on the risk associated with consumption of probiotics among a few segments of the population has made the consumer choice problematic task (**Table 2.1**). Contrary to the episodes on safe usage of probiotics in healthy individuals, the potential risks in the critically ill or immunocompromised patients or preterm infants are still worthy of attention as patients may be fraught with danger (Chiang *et al*., 2021). Adverse effects of certain strains of probiotics include bacteremia, sepsis, endocarditis, systemic bloodstream infections, gastrointestinal side effects (vomiting, nausea, spasms, diarrhea, bloating, thirst, and taste disturbance), skin side effects (such as skin rashes or mild acne), extreme immune stimulation (autoimmune disease or inflammation reaction), production of harmful

metabolites (D-lactate metabolite and deconjugation of bile salts), unnatural antibiotic resistance, and horizontal transfer of antibiotic resistance (Sotoudegan *et al*., 2019). Hence, probiotics cannot be considered risk-free and should be carefully evaluated in pre-clinical studies using suitable animal models before translating for clinical trials.

2.4. Need of taxonomical identification of probiotics

Particular attention should be given to correctly identifying probiotic strains since it is a foremost step in avoiding misleading information about the strain (Wang *et al*., 2021). Taxonomical identification of any potential probiotic strains is crucial as probiotic effects are strain-specific. Therefore, correct and reliable identification of probiotic strains to the strain level would aid in claiming the good benefits. Taxonomic classification assigns the microorganism to correct taxa, which predicts the genetic relatedness between the microbes of known taxa. On the other hand, bacterial identification confirms the identity of a strain, and such information can also be exploited to draw a conclusive opinion on the origin of a particular strain. For example, *Lactobacillus kefiranofaciens* is generally isolated from kefir, while *Lactobacillus crispatus* is commonly isolated from the human female lower genital tract (Zheng *et al*., 2020). Nomenclature of a strain helps in naming the bacteria with genus, species, and strain and therefore facilitates the appropriate labeling of commercialized probiotic products with up-to-date nomenclature as per the labeling requirements. Moreover, it explicitly helps the food/pharmaceutical industries with in-house laboratory facilities to ensure the intended strain in the final product.

According to international guidelines, the specification of microorganisms must be established using combined phenotypic and genotypic methods (e.g., 16s rDNA sequencing) (https://www.who.int/foodsafety/fs_management/en/probiotic_ guidelines. pdf). However, the methods of classification of newer strains solely based on phenotypic approaches or by 16s rDNA sequencing or DNA/ DNA hybridization is impossible because these methods cannot discriminate a bacterium at the strain level. Therefore, numerous molecular fingerprinting tools *viz*. ribotyping, amplified ribosomal DNA restriction analysis (ARDRA), random amplified polymorphic DNA (RAPD), amplified fragment length polymorphism (AFLP), pulse-field gel electrophoresis (PFGE), repetitive extragenic palindromic PCR (Rep-PCR), denaturing (D)/ temperature (T) gradient gel electrophoresis (DGGE/ TGGE), and multilocus sequence typing (MLST) have been proposed for typing lactic acid bacteria (Sharma *et al*., 2020).

Table 2.1: Reports on potential risks upon probiotic administration in diseased or immunocompromised human subjects

Strain	Health state of subjects	Adverse effects	References
Lactobacillus spp.	Comorbid 82-year-old female *Clostridium difficile* colitis	Liver abscess and bacteremia	Sherid *et al*. (2016)
Lacticaseibacillus rhamnosus GG	Adult patient affected by severe active ulcerative colitis	Bacteremia	Meini *et al*. (2015)
Saccharomyces boulardii	Patient with *Clostridium difficile*-associated diarrhoea	Fungemia	Santino *et al*. (2014)
Saccharomyces boulardii	An elderly patient with *Clostridium difficile* colitis	Fungemia	Cherifi *et al.* 2004)
Lactobacillus acidophilus	51-year-old man with AIDS	Bacteremia	Haghighat and Crum-Cianflone, 2016
Saccharomyces cerevisiae	76 and 73 years old patients with COVID-19	Bloodstream infection	Ventoulis *et al*. (2020)
Saccharomyces ceravisiae	3.5-month-old infant	Fungemia	Chakravarty *et al*. (2019)
Saccharomyces ceravisiae	79-year-old woman with rheumatoid arthritis	Fungemia	Thygesen *et al*. (2012)
Saccharomyces cerevisiae	Immunosuppressed patients	Fungemia	Riquelme *et al*. (2003); Sonpal *et al*. (2010)
Lacticaseibacillus rhamnosus	24-year-old female cardiosurgical patient	Sepsis	Kochan *et al*. (2011)
Lacticaseibacillus rhamnosus	36-year-old woman with alcoholic cirrhosis (Child's Pugh Class B) complicated by refractory ascites, spontaneous bacterial peritonitiss, and grade 1 oesophageal varices	Endocarditis	Naqvi *et al*. (2018)
Lacticaseibacillus rhamnosus	50-year-old Caucasian male	Bacteremia, mitral aortic valve infective endocarditis (IE), and splenic infarction	Pasala *et al*. (2020)

Strain	Health state of subjects	Adverse effects	References
Lacticaseibacillus rhamnosus	84-year-old male patients with acute myeloid leukemia, large granular lymphocytic leukemia	Recurrent bacteremia	Ambesh *et al*. (2017)
Lacticaseibacillus rhamnosus	57-year-old healthy man	Endocarditis	Campagne *et al*. (2020)
Lacticaseibacillus rhamnosus and *Lactobacillus acidophilus*	74-year-old man	Bacteremia and endocarditis	Zeba et al. (2018)
Lacticaseibacillus rhamnosus	Patients with hereditary hemorrhagic telangiectasia (HHT)	Infective endocarditis	Boumis *et al*. (2018)
Lacticaseibacillus paracasei	65-year-old male who underwent a dental extraction	Endocarditis	Osman *et al*. (2019)
Lacticaseibacillus paracasei	75-year-old woman with history of Birt-Hogg-Dube syndrome and bioprosthetic aortic valve replacement	Bacteremia and evidence of bacterial vegetations noted on transesophageal echocardiography (TEE) along with evidence of severe aortic insufficiency	Ajam *et al*. (2019)
Lacticaseibacillus rhamnosus	Healthy adults	Brain fogginess, gas, bloating, D-lactic acidosis	Rao *et al.* (2018)
Lacticaseibacillus paracasei	Consumer of probiotics with severe bicuspid aortic valve stenosis and diffuse mid-layer fibrosis in the left ventricular myocardium on computed tomography	Endocarditis	Kato *et al*. (2016)
Lactobacillus species	Healthy adults	Endocarditis and bacteremia	Agrawal *et al*. (2020)
Lacticaseibacillus rhamnosus GG	Preterm infants	Sepsis	Chiang *et al*. (2021)
Lacticaseibacillus rhamnosus GG	Infant with aortic coarctation	Sepsis	Aydoğan *et al*. (2022)
Clostridium butyricum (*C. butyricum*) MIYAIRI 588	74-year-old man with gallbladder cancer	Sepsis	Shimura *et al*. (2021)

Amongst the non-molecular methods, MALD-TOF-MS (matrix-assisted laser desorption time of flight mass spectrometry) and FTIR (Fourier Transform Infrared) spectroscopy have also been used by a few groups of researchers (Samelis *et al*., 2011; Wenning *et al*., 2010). Amid the several existing methods, Pulsed Field Gel Electrophoresis (PFGE) is has been suggested by FAO/ WHO guidelines since it is a gold standard method with higher discriminative power at the strain level (FAO/ WHO, 2002). RAPD may also be considered a better approach, provided the researcher has optimized protocol with standardized DNA quality, PCR buffer, primer concentration, and annealing temperature (Sharma *et al*., 2020).

It is essential to consider that no strain typing methods can replace whole-genome sequencing (WGS) through the shotgun approach to identify probiotic strains accurately. WGS data provide information for the unequivocal taxonomic identification of the strain by the similarities among the strains: single nucleotide polymorphism (SNP)- and gene by gene-based approaches. It is mandatory to sequence the whole genome of potential probiotic strains and deposits them in publicly accessible genetic sequence databases such as NCBI GenBank and the same bacterial strain to an internationally recognized microbial culture collection centers with International Depositary Authority under the Budapest Treaty (EFSA, 2012). The development of high throughput next-generation sequencing platforms has made whole-genome sequencing an easy task. Today, there are two major next generation sequencing (NGS) platforms, i.e., short-read platforms (including Illumina and Ion Torrent) and long reads platforms, including single-molecule real-time sequencing (Pacific Biosciences) and nanopore (Oxford Nanopore) sequencing (Motro and Moran-Gilad, 2017). However, selecting suitable platforms generally depends on several factors such as cost, read length, coverage, Phred quality score (quality of the data), etc. (Quail *et al*., 2012). For instance, sequencing through a few platforms like PacBio may not cover smaller-sized plasmids, and therefore the presence of small plasmids and their associated risk may not be determined. By contrast, the Illumina platform has been observed to cover the complete whole genome, including smaller plasmids (Chokesajjawatee *et al*., 2020). The regular strain typing or whole-genome analysis of the probiotic stain would also reflect the genome stability regarding susceptibility to genome shuffling or rearrangements. Such rearrangements may introduce minor variations through mutations, deletions, and insertions, but that can easily pass on by vertical inheritance and rarely through horizontal gene transfer

episodes. Genome shuffling may also cause severe issues like losing specific health-promoting characteristics (Sanders *et al*., 2010).

2.5. *In vitro* safety evaluation assays

2.5.1. Hemolytic activity

Hemolytic activity is considered an essential bio-safety aspect. Even if the particular genera has QPS status or is traditionally consumed over the years, it is mandatory to measure the hemolytic activity as strongly recommended by the EFSA (Yasmin *et al*., 2020). Production of hemolysin that causes the lysis of the erythrocytes generally depends on one bacterium to another. Culturing the strain of interest on blood agar or quantification of released hemoglobin by measuring the spectrophotometric absorbance at 415 or 570 nm is the typically followed laboratory protocol (Banerjee *et al*., 2017; Lefevre *et al*., 2017). In this regard, several enterococci strains showed hemolytic activity (α-hemolysis and β-hemolysis) on blood agar (Zhang *et al*., 2016). On the contrary, some enterococci strains were harmful to hemolysis (Al Atya *et al*., 2015). Although *Lactobacillus* species are typically non-hemolytic, some researchers have observed partial or γ -hemolytic activity in some *Lactobacillus* strains, which might be due to hydrogen peroxide production or surfactants. γ -hemolysis in lactobacilli may also occur due to the fulfillment of the iron requirement of bacteria for pyrimidine and purine metabolism in an environment with limited or specific nucleotide sources (Vesterlund *et al*., 2007). This wide disparity in the hemolytic ability of potential probiotic strains further recommends evaluating the hemolytic activity of putative probiotic strains.

2.5.2. Mucin degradation

Probiotics are generally applied to tissues where the cells express mucus. Mucus membrane harbors dynamic commensal microbiota and acts as a physical barrier against invading pathogens. Thus the mucin-gut microbiota interaction plays a paramount role in shaping the mucus barrier by enhancing mucin expression in the host (Ravcheev and Thiele, 2017; Shin *et al*., 2019). Dysbiosis in the gut microbiota has been linked to mucin degradation and other health disorders. Hence, mucin degradation by probiotic strains is considered a virulent determinant. However, the emergence of next-generation probiotics has made it controversial regarding the classification of mucin degradation property of probiotics as a beneficial or virulence trait since *Akkermansia muciniphila*, a next-

generation probiotic, often shown mucin degradation to continue the cross-feeding mechanisms or may utilize mucin as carbon and nitrogen source (Shin *et al*., 2019; Van Herreweghen *et al*., 2020). This necessitates the need for the scientific and regulatory recommendations to reclassify mucin degradation phenotype in context to traditional versus next-generation probiotics. Though numerous investigators have highlighted the inability of conventional or traditional probiotics to degrade mucin, the collateral reports pertinent to the mucolytic property of *Bifidobacterium* strains urges the strict incorporation of mucin degradation assay while assessing the safety of potential probiotic strains (Ruas-Madiedo *et al*., 2008; Shekh *et al*., 2016). Three approaches have been employed to evaluate the mucin depletion capability of probiotics. These include growth in liquid medium supplemented with partial purified hog gastric mucin (spectrophotometric measurement), SDS-PAGE analysis of degraded mucin residues (visualization by coomassie blue and/or periodic acid–Schiff staining for visualization of glycoprotein pattern), and degradation assay in Petri dish (visualization by amido black staining) (Abe *et al*., 2010).

2.5.3. Gelatinase activity

Gelatinase is one of the microbial pathogenic determinants by which bacteria invade the host tissue by their protein degradation ability. Although not frequently observed in beneficial microbes, the tissue invading pathogens (*Pseudomonas, Proteus, Listeria, Bacillus, Clostridium)* often display gelatinase activity (Abfalter *et al*., 2015). However, few reports indicate the gelatin liquefaction ability of gut-derived lactic acid bacteria (enterococci) (Birri *et al*., 2013). Contrary to this, several probiotic *Lactobacillus* strains have shown negative manifestations towards this assay, thus suggesting their inability to degrade and invade the proteinaceous host tissue (Saif and Sakr, 2020). Though *Enterococcus faecalis* had *gelE*, the gene responsible for gelatinase activity, the strain did not phenotypically express the gelatin liquefaction ability (Wang *et al*., 2019). This underscores the need for proteome-level studies to validate genotypic findings with the corresponding phenotype. The methods like streaking the test culture on nutrient gelatin agar and observing the clear zone after flooding saturated ammonium sulfate for the positive response (Kaktcham *et al*., 2018) or gelatin liquefaction tube assay are the commonly preferred assays (Kang *et al*., 2019; Wang *et al*., 2019).

2.5.4. DNase activity

This activity determines the catalytic activity of microbially expressed deoxyribonuclease that cleaves the phosphodiester linkages in the DNA backbone. At the laboratory level, the microbial DNase activity is determined by culturing the test culture on the DNase test agar supplemented with a specific concentration of tollidium blue (Ragul *et al*., 2019). Though several pathogens are known to secrete this enzyme either extracellularly or intracellularly, this phenotype is undesirable for lactic acid bacteria since probiotics are most commonly intended for human and animal consumption. However, a handful of *Lactobacillus* and *Enterococcus* strains have shown positive reactions for extracellular DNase activity in a strain-dependent manner (Câmara *et al*., 2020; Romero, 2020). By contrast, probiotic strains of *Lactobacillus, Bacillus, Weissella* genera did not reveal the DNase activity (Mercha *et al*., 2020; Ragul *et al*., 2019). These reports suggest that virulence property may be a species-strain-specific property and needs careful evaluation of all the potential probiotic strains.

2.5.5. Biogenic amines

Biogenic amines are the low molecular thermostable organic nitrogen compounds produced either by the decarboxylation of specific amino acids or by amination and transamination of aldehydes or ketones during metabolic processes (Ruiz-Capillas and Herrero, 2019). Microbial decarboxylase activity expels carbon dioxide from amino acids to produce biogenic amines (Doeun *et al*., 2017). Biogenic amines have been classified into three types based on their molecular structures. They include aromatic and heterocyclic compounds (histamine, tryptamine, tyramine, phenylethylamine, and serotonin), aliphatic compounds (ethylamine, methylamine, isopentylamine, and ethanolamine), and aliphatic polyamines (putrescine, cadaverine, spermine, spermidine, and agmatine). Though several of these amines act as precursor amines for hormone synthesis and are found to have some pharmacological effect, the consumption of few biogenic amines at higher concentrations has shown adverse effects like hypotension, bradycardia, headaches, migraine, neurological disorders, nausea, vomiting, respiratory disorders, nasal secretion, bronchospasm, tachycardia, extrasystoles, hypotension, edema (eyelids), urticaria, pruritus, flushing, and asthma (Tofalo *et al*., 2016). This necessitates quantifying the biogenic amines in the foods or pharmaceutical compounds intended for human consumption. Lactic acid bacteria are a potential source of biogenic amines (histamine, tyramine, tryptamine, putrescine, cadaverine, and phenylethylamine) since

they possess decarboxylase activity in a strain-specific manner (Lorencová *et al*., 2012). The methodologies for qualitative assessment of biogenic amines include TLC and culturing the bacteria of interest on the decarboxylase agar medium with or without the precursor amino acids. The bacteria that produce the biogenic amine increases the pH (due to the production of alkaline products) of the decarboxylase medium that can qualitatively be determined by the color change (yellow to purple) in the basal medium. On the other hand, TLC and High-performance liquid chromatography (HPLC) fitted with a C-18 column, and UV detector has been used to quantitatively assess biogenic amines (Deepika *et al*., 2011; Ku *et al*., 2020; Muñoz-Atienza *et al*., 2011).

2.5.6. Adverse metabolites

Probiotic bacteria's typical D-lactic acid production phenotype is regarded as undesirable characteristics as the human body can poorly metabolize and excrete D-lactate. This causes D-lactic acidosis or D-lactic acid-associated encephalopathy in the potentially ill patients or neonates, or patients with co-morbidities such as mesenteric thrombosis, mid-gut volvulus, or Crohn's disease (Sanders *et al*., 2010). Despite these potential illnesses, no standards recommend the upper levels for D-lactic acid concentration in probiotics. Most LAB, including commercially available probiotic strains, have reported producing D-lactate (Meleh *et al*., 2020). Therefore, any potential probiotic strains that produce D-lactate in excess amount compared to commercial reference strains may be considered unsafe temporally. Albeit not all probiotic strains may directly produce D(-)-lactic acid, DL-lactate racemase enzyme activity in lactobacilli may convert L-form to D-form.

BSH activity is generally considered a beneficial property since it edifies bacteria to dwell under bile stress. It may also lower the serum cholesterol levels of the host (Bustos *et al*., 2018). However, the excessive bile salt deconjugation or dehydroxylation of primary bile salts by 7α-dehydroxylase active strains has been noted as an adverse effect on the host. Deconjugated secondary bile acids (deoxycholic and lithocholic acids) promote colon carcinogenesis, oxidative stress, and DNA damage (Louis *et al*., 2014; Ocvirk and O'Keefe, 2017). In a study, such biotransformation of primary bile acids (cholic acid and chenodeoxycholic acid) to secondary bile acids (deoxycholic acid and lithocholic acid) by test probiotic culture was confirmed by TLC (Aryantini *et al*., 2017). Several *Lactobacillus plantarum* strains isolated from various fermented foods formed

secondary bile acid deoxycholic acid, lithocholic acid, and ursodeoxycholic acid A as well as a range of intermediates (Prete *et al*., 2020).

2.5.7. Harmful intestinal enzyme

The occurrence of fecal enzymes *viz*. azoreductase, beta-glucosidase, beta-glucuronidase, nitrate reductase, nitroreductase, and urease among the candidate probiotic strains have been considered as potential safety concern since they show pro-carcinogenic activity (Verma and Shukla, 2013). Besides, α-chymotrypsin and N-acetyl-β-glucosaminidase activities may have also observed to have negative effects on the colon (Rzepkowska *et al*., 2017). These enzymes belong to the hydrolase and reductase categories. Their excessive activity may lead to disorders in the functioning of the digestive tract and ultimately may lead to colon cancer (Koppel *et al*., 2017; Nagpal *et al*., 2012). Several potential probiotic *Lactobacillus* and *Enterococcus* strains from the human-origin have shown β-glucosidase and β-glucuronidase activity (Mroczynska and Libudzisz, 2010; Todorov *et al*., 2017). In another study, lactic acid bacteria isolated from both fecal sources and food matrix expressed β-glucuronidase and β-glucosidase activity in a strain-specific manner (Rzepkowska *et al*., 2017). On the contrary, β-glucosidase activity is generally considered a beneficial property in the fermentation sciences due to its bioconversion ability of isoflavone glucosidases (Son *et al*., 2017). Hence, further explicit scientific opinions are necessary to include β-glucosidase activity either as a techno-functional attribute or a safety indicator.

2.5.8. Virulence factor genes

The studies that lack whole-genome analysis for unraveling safety-related genes have adopted a targeted approach of confirming the absence of virulence genes via the polymerase chain reaction (PCR) approach. For such studies, the rational selection of genes based on the particular organism with appropriate experimental controls is paramount to interpret the findings. For assessing the safety of enterococcal probiotic strains, investigators targeted genes that code for enterococcal surface protein (*esp*), hemolysin (*cyl*A, *cyl*B, and *cyl*M), gelatinase (*gel*E), aggregation substance (*agg*), endocarditis antigen (*efa*Afm), sex pheromone (*cpd*, *ccf*, and *cob*), adhesion of collagen (*ace*) and hyaluronidase (*hyl*) (Bhardwaj *et al*., 2012; Nascimento *et al*., 2019). Similarly for *Lactobacillus* probiotics, the genes encoding gelatinase (*gelE*, *fsrA*, *fsrB*, *fsrC*), hyaluronidase (*hyl*), aggregation substance (*asa1*), virulence of *Enterococcus* spp. (*mur-2*) enterococcal surface protein (esp), cytolysin (*cylA*), endocarditis antigen (*efaA*),

adhesion of collagen (*ace*), serine protease (*sprE*), sex pheromones, chemotactic for human leukocytes; facilitate conjugation (*ccf, cob, cpd*), and biogenic amines (*hdc1*, *hdc2, tdc, odc*) have been frequently investigated and reported a strain-specific response (Casarotti *et al*., 2017; de Souza *et al*., 2019).

2.5.9. Platelet aggregation, plasminogen binding, and activation tests

Platelet aggregation phenotype is determined to investigate the ability of a bacterium to aggregate platelets and cause sepsis and infective endocarditis (Zhou *et al*., 2005). Microbes can bind to the host plasminogen via lysine residues of cell surface proteins and use them to degrade the host's extracellular matrix (ECM) proteins for their invasion. Plasminogen is activated either by tissue-type plasminogen activator (tPA) and urokinase (u-PA) or by bacterial enzymatic activators such as staphylokinase and streptokinase that converts plasminogen to active plasmin (Nitzsche *et al*., 2016). Such pathogenic phenotype in probiotic strains was investigated in a handful of studies and found negative for the test (Aryantini *et al*., 2017). Nevertheless, the platelet aggregation phenotype of probiotics may depend on the previous niche of the isolates. For instance, *Lactobacillus* strains from human blood or septicemia patients manifested positive reactions, whereas the isolates of dairy or human gut origin showed negative aggregation phenotype (Collins *et al*., 2012; Nissilä *et al*., 2017; Pradhan *et al*., 2019a). In fact, the administration of probiotic *Lacticasibacillus casei* CRL 431 has improved the platelet functionality in the *Streptococcus pneumonia*-infected *in vivo* model (Haro and Medina, 2019; Zhou *et al*., 2005). Likewise, the co-treatment of *Limosilactobacillus reuteri* with cancer cells that overexpress the uPA/uPA receptor (uPAR) has been found to downregulate the expressions of uPA and uPAR (Rasouli *et al*., 2017). Closure time (CT) measurement method (platelet function analyzer) or aggregometer mediated assessment of platelet aggregation in platelet-rich plasma and platelet-poor plasma is commonly employed to assess the platelet functioning or disorders (Kang *et al*., 2019).

2.5.10. Genotoxicity and mutagenicity

Genotoxicity assays determine the effect of test compounds on genome stability or integrity in eukaryotic cells. *In vitro* genotoxicity assessment aids in screening a large number of test compounds possessing potential toxicity. *In vitro* genotoxicity assays for probiotic safety, evaluation have frequently been carried out on eukaryotic cells. Chinese hamster ovary cells (CHO-K1) using comet assay (Liao *et al*., 2019) or chromosomal aberration assay with and without metabolic activation by S9 (Lin *et al*., 2018).

Chromosomal aberration assay accounts for different types of chromosomal eccentricity, such as chromatid break, gaps, and centromeric association. An exposure to a probiotic formulation of *Latilactobacillus curvatus* WiKim 38 at different concentrations (19.53-5000 μg/ mL) did not inhibit cell growth of CHO-K1 cells by more than 50% at doses up to 5000 μg/ mL. Moreover, there was no significant increase in the number of metaphases with structural or numerical aberrations in the WiKim 38-treated groups at any concentration in the presence or absence of the metabolic activation system compared to the vehicle control group (Han *et al*., 2021). Similarly, SOS-Chromotest is another method used to study the genotoxic effect on prokaryotic cells (Bocci *et al*., 2015; Caldini *et al*., 2008). On the other hand, *in vitro* mutagenicity is carried out by plate incorporation assay using *Salmonella typhimurium* histidine-auxotrophic strains TA97a, TA98, TA100, TA102, and TA1535 through Ames test or bacterial reverse mutation assay (with or without S9 activation) (Chiu *et al*., 2013; Lin *et al*., 2018). The outcomes of various genotoxicity and mutagenicity assays of probiotics have been presented in **Table 2.2**. However, most of the tested probiotic strains did not show either genotoxicity or mutagenicity. Rather probiotic interference protected the cells from the genotoxic or mutagenic effects that were previously induced by various chemicals (Prete *et al*., 2017).

2.5.11. Cytotoxicity

Cytotoxicity assays provide a crucial means of selecting the therapeutic compounds for further drug discovery or research. Moreover, these tests are generally assessed on eukaryotic cells, and thus the results obtained from such experiments may be considered for the dose selection for further *in vivo* toxicity experiments (Ukelis *et al*., 2008). A compound is considered cytotoxic if it significantly alters the cellular attachment, morphology, and growth rate, or causes cell death. Besides classical dye inclusion or exclusion and colony formation assays, an array of cytotoxicity testing methods has been developed based on various principles; i) viability based on metabolic reductase activities (tetrazolium and resazurin reduction to formazan); ii) viability by bioluminescent ATP assays; iii) cytotoxicity based on released metabolic enzymes into the culture medium; iv) measurement of DNA fragmentation by DNA laddering (genotoxic); v) measurement of caspase activity by caspase quantification assay (Ukelis *et al*., 2008).

Table 2.2: Outcomes of assays on cytotoxicity, genotoxicity and mutagenicity of various potential probiotic strains

Probiotic strain	Test	Outcome	References
	***In vitro* tests**		
Escherichia coli strain Nissle 1917	Ames test	Non-mutagenic	Dubbert, *et al*., 2020
Lactiplantibacillus plantarum strain PS128	Ames test and chromosomal aberration test using Chinese hamster ovary cells	Non-mutagenic and Non-genotoxic	Liao *et al*. (2019)
Bacillus amyloliquefaciens B-1895 and *B. subtilis* KATMIRA1933	Ames test	Non-mutagenic	AlGburi *et al*. (2016)
Lacticaseibacillus paracasei subsp. *paracasei* NTU 101.	Ames Test and chromosomal aberration test using Chinese hamster ovary cells	Non-mutagenic and Non-genotoxic	Tseng *et al*. (2015)
Akkermansia muciniphila	Ames test and micronucleus test	Non-mutagenic/genotoxic	Druart *et al*. (2020)
Lacticaseibacillus rhamnosus MP108	Ames test	Non-mutagenic	Zhang *et al*. (2020)
Bacillus mojavensis KJS-3	Ames test and chromosomal aberration test using Chinese hamster lung cell line	Non-mutagenic and Non-genotoxic	Kim *et al*. (2012)
Bifidobacterium strains	MTT assay on Caco-2 cells	Significant decrease in the viability of the cells at 24 h	Yasmin *et al*. (2020)
Saccharomyces boulardii RC009	Neutral red uptake assay on Vero-cells	Non-cytotoxic	Poloni *et al*. (2021)
Lacticaseibacillus rhamnosus MTCC-5897	MTT, neutral red uptake, and LDH release assay on Caco-2 cells	Non-cytotoxic	Bhat *et al*. (2019a)
Lactiplantibacillus plantarum strain PS128	MTT assay on CHO-K1 cell	Non-cytotoxic	Liao *et al*. (2019)
Lactobacillus strain MTCC 5690	Trypan blue exclusion assay on HT-29 cells	Non-cytotoxic	Rokana, Mallappa, Batish, & Grover (2017)

Probiotic strain	Test	Outcome	References
Lacticaseibacillus rhamnosus GG	MTT assay on Caco-2 cells	Non-cytotoxic	Singh *et al*. (2018)
Lactiplantibacillus plantarum KP894100 and *Lactobacillus acidophilus* KP942831	MTT assay on U-87 and MCF-7 cells	Cytotoxic to cancer cells	Bharti *et al*. (2015)
Saccharomyces cerevisiae RC016 (Sc) and *Lacticaseibacillus rhamnosus* RC007	Neutral red absorption assay on Vero cells	Non-cytotoxic	Fochesato *et al*. (2020)
In vivo tests			
Escherichia coli strain Nissle 1917	Comet Assay	Non-genotoxic	Dubbert *et al*. (2020)
Lacticaseibacillus paracasei subsp. *paracasei* NTU 101.	Micronucleus assay	Non-genotoxic	Tseng *et al*. (2015)
Lactiplantibacillus plantarum MTCC 5690 and *Limosilactobacillus fermentum* MTCC 5689	*In vivo* chromosomal aberration and micronucleus assay	Non-genotoxic	Pradhan *et al*. (2019a)
Saccharomyces cerevisiae RC016	Micronuclei assay and comet assay	Non-genotoxic	Gonzalez Pereyra *et al*. (2014)
Liquorilactobacillus mali APS1	*In vivo* micronucleus (MN) assay	Non-genotoxic	Lin *et al*. (2018)
Lacticaseibacillus rhamnosus LCR177, *Bifidobacterium adolescentis* BA286, and *Pediococcus acidilactici* PA318	*In vivo* micronucleus assay	Non-genotoxic	Chiu *et al*. (2013)
Bacillus licheniformis Me1	Micronucleus Assay	Non-genotoxic	Nithya *et al*. (2012)
Lacticasesibacillus rhamnosus MP108	*In vivo* mouse micronucleus, and *in vivo* mouse spermatocyte chromosome aberration assays	Non-genotoxic	Zhang *et al*. (2020)
Lactiplantibacillus plantarum strain PS128	*In vivo* micronucleus Assay	Non-genotoxic	Liao *et al*. (2019)

Cytotoxicity assays measure collateral parameters proportional to the degree of cell viability or death (Niles *et al*., 2008). The assays based on the metabolic reductase activities include MTT (3-(4,5-dimethylthiazolyl)-2,5- diphenyltetrazolium bromide) (a gold standard method of assessing the viability/cytotoxicity of compounds), XTT (2,3-bis(2-methoxy4-nitro-5-sulphophenyl)-5-carboxanilide-2H-tetrazolium), MTS (5-(3-carboxymethoxyphenyl)-2-(4,5-dimethylthiazoly)- 3-(4-sulfophenyl)tetrazolium, inner salt) and WST-1 ((4-[3-4-iodophenyl]-2-(4-nitrophenyl)-2H-5-tetrazolio)- 1,3-benzene disulfonate). The cytotoxicity by enzymes released is based on the fact that cells leak the intracellular components after death. The lactate dehydrogenase (LDH) assay that works on this principle is generally preferred for drug discovery research as the presence of specific biomarker activity is typically proof-positive while assessing cytotoxicity (Niles *et al*., 2008). With this regard, several potential probiotic strains have been assessed for their cytotoxicity on various eukaryotic cell lines and found to alter the cellular viability in a strain and dose-specific manner, as presented in **Table 2.2.**

2.5.12. Transferable antibiotic resistance

In the era of antibiotic, antimicrobial resistance (AMR), resistance exhibited by food-grade lactic acid bacteria deserves special attention as equally as clinically relevant pathogens since the resistance genes located on the mobile genetic elements such as plasmids, transposons, integrons, IS elements may possess the equal propensity to transfer laterally among the commensal microbes/pathogens. It is now generally accepted that natural resistance due to intrinsic mechanisms does not pose a higher risk than the acquired resistance gained by horizontal gene transfer. Therefore, antibiotic resistance *per se* is not a safety issue unless it is laterally transferable. To target the specific antibiotics against the particular bacterial genera, the EFSA provided the specific breakpoints against various antibiotics. EFSA guideline suggests investigating the resistance towards ampicillin, vancomycin, gentamicin, kanamycin, streptomycin, erythromycin, clindamycin, tetracycline, and chloramphenicol antibiotics against various probiotics genera (EFSA, 2012). Resistance phenotype of probiotic bacteria can be assayed according to the Clinical and Laboratory Standards Institute (CLSI) or European Committee on Antimicrobial Susceptibility Testing (EUCAST) or International Dairy Federation/ International Organization for Standardization (IDF/ ISO) methodologies which are based on agar dilution method, broth dilution method, minimal inhibitory concentration (MIC), Kirby-Barer disk-diffusion method, the

Epsilometer test (E-test), or advanced molecular methods such as microarray and PCR (Aristimuño *et al*., 2018; Neut *et al*., 2017). The presence of transferable antibiotic resistance can be identified either by profiling individual plasmids or whole-genome analysis for mobile genetic elements and subsequent conjugate experiments (Plate, filter, and broth mating techniques) (Hummel *et al*., 2007; Toomey *et al*., 2009). In recent days, the whole genome sequencing of target probiotic strain and subsequent genome analysis to unfold the resistance genes (CARD or ResFinder databases), prophage sequence (PHASTER), and insertion sequences (ISfinder) are emerging as a more validated and spectacular approach.

2.5.12.1. Intrinsic resistance

Intrinsic resistance is a natural feature of bacterial biology, which is generally considered as chromosomally encoded and lacks lateral transferability to other bacteria. The best example for inherent resistance is the vancomycin resistance phenotype displayed by *Enterococcus, Lactobacillus,* and *Bifidobacterium* because of specific alteration in peptidoglycan architecture (D-lactate or D-serine replaces D-alanine residue in the muramylpentapeptide to prevent vancomycin binding) (Gueimonde *et al*., 2013). **Table 2.3** shows the resistance phenotype to aminoglycoside antibiotics (kanamycin, gentamicin, neomycin, and streptomycin) among *Lactobacillus*, *Bifidobacterium*, *Lactococcus,* and *Streptococcus* is also an intrinsic property due to the absence of cytochrome-mediated electron transport that mediates drug uptake (Hummel *et al*., 2007). At the same time, reports also suggest that lactobacilli are also intrinsically resistant to metronidazole, cefoxitin, ciprofloxacin, and trimethoprim (Erginkaya *et al*., 2018; Ma *et al*., 2017). Similarly, intrinsic resistance to mupirocin in bifidobacteria is because mupirocin competes with isoleucine as a substrate for isoleucyl-tRNA synthetase thus affecting protein synthesis (Zielińska *et al*., 2018). However, the low concentrations of macrolides, vancomycin, chloramphenicol, beta-lactams, rifampicin, spectinomycin, ampicillin, penicillin G, cephalosporin, bacitracin, chloramphenicol, erythromycin, clindamycin, nitrofurantoin, and tetracycline have been reported to inhibit bifidobacterial growth (Clelia, 2017; Li *et al*., 2020). Despite being intestinally resistant to aminoglycosides and glycopeptide (vancomycin), bifidobacteria is also resistant to quinolones (nalidixic acid and norfloxacin), sulfonamides, fusidic acid, trimethoprim, metronidazole, polymyxin B, and colistin (Li *et al*., 2020).

Table 2.3: Resistance or sensitivity pattern of different probiotic strains towards different antibiotics

Probiotic strains	Resistant	Susceptible	Resistance genes	Virulence genes	References
Limosilactobacillus reuteri VB4	-	-	*vanA*	*Agg*	Dlamini *et al*. (2019)
Lactobacillus isolates	Vancomycin (4/6), Erythromycin (2/6), Sulphamethoxazole/trimethoprim(6/6), Gentamicin (6/6), Clindamycin(1/6), Amikacin (6/6), Kanamycin (6/6), Cefoxitin (5/6), Ciprofloxacin (6/6), Tetracycline (2/6), Polymyxin B (6/6)	Penicillin G (5/6), Ampicillin (6/6), Amoxicillin/clavulanate (6/6), Chloramphenicol (6/6), Streptomycin (6/6)	-	-	Meleh *et al*. (2020)
Lacticaseibacillus rhamnosus MTCC-5897	Nitrofurantoin and Vancomycin	Amoxyclav, Ampicillin, Co-trimoxazole, Norfloxacin (NX), Oxacillin, Erythromycin, Tetracycline, Chloramphenicol, Clindamycin, Gentamycin, Penicillin, Netillin	-	-	Bhat *et al*. (2019a)
Limosilactobacillus mucosae	Gentamycin, Vancomycin, Tobramycin	Ampicillin, Cefoxitin, Chloramphenicol, Tetracycline, Penicillin, Erythromycin, Linezolid, Cefotaxime	-	-	Rastogi *et al*. (2019)

Probiotic strains	Resistant	Susceptible	Resistance genes	Virulence genes	References
Limosilactobacillus fermentum, *Lacticaseibacillus casei*, *L. delbrueckii* subsp. *bulgaricus*	-	-	*van A, van B, vanC1, vanC-2,vanC-3, vanC1, tet(M), tet(L), tet(K), tet (O), bcr(B), bcr(R), erm(C), ant(4')-Ia, aph(3')-III-a, aph(2")-Ib, aph(2")-Ic, aph(2")-Id, aac(6')-Ie-aph(2")-Ia, aac(6')-Ii, catA(PIP501), int-Tn, int*	*gelA, hyl, asa1, esp, cylA, fsrA, fsrB, fsrC, sprE, ccf, cob, cpd, hdc1, tdc*	Casarotti *et al*. (2017)
Lacticaseibacillus rhamnosus DTA 79 and *L. paracasei* DTA 83		Amoxicillin + clavulanic acid, Ampicillin, Cephalexin, Ciprofloxacin, chloramphenicol, nalidixic acid, tetracycline	-	-	Junior *et al*. (2019)
Ligilactobacillus salivarius	Kanamycin, streptomycin, Gentamycin, cotrimoxazole, tetracycline, ceftazidime, ceftriaxone	Cefotaxime, amoxicillin, chloramphanical, penicillin,	-	-	Li *et al*.(2020)
*Enterococcus faecium*394 and 894	Erythromycin, gentamycin, kanamycin, streptomycin,	Ampicillin, chloramphenicol, penicillin, tetracycline, vancomycin	-	*asa*1, *gel*E*Cyl*A, *cyl*$L_{L,S,}$ *cyl*M, *Hyl*$_{efm}$, *gel*E, and *Cyl*A	Özkan *et al*. (2021)
Limosilactobacillusreuteri IDCC 3701	Gentamicin, kanamycin	Ampicillin, streptomycin, erythromycin, clindamycin, tetracycline, chloramphenicol	Not detected	Not detected	Lee *et al*. (2021)

Probiotic strains	Resistant	Susceptible	Resistance genes	Virulence genes	References
Levilactobacillusbrevis KU15147, KU15148, and KU15154	Kanamycin, Streptomycin, Ciprofloxacin	Ampicillin, Gentamicin, Tetracycline, Chloramphenicol, Doxycycline	-	-	Kim *et al*. (2021)
Bacillus spp.	Lincomycin, tetracycline.	Erythromycin, streptomycin, gentamicin, florfenicol, linezolid; CIP, ciprofloxacin; VAN, vancomycin	-	*nheA*, *nheB*, *nheC*, *hblC*, *hblD*, *hblA* , *cytK2*, *ces*	Deng *et al*. (2021)
Limosilactobacillus vaginalis MA-10	Ampicillin, vancomycin and linezolid	Amikacin, Gentamicin, Kanamycin, Ofloxacin	-	-	Asan-Ozusaglam and Gunyakti (2021)
Lacticaseibacillus paracasei, *Limosilactobacillus fermentum*, and *Levilactobacillus brevis*	Ampicillin, erythromycin, clindamycin, tetracycline, and chloramphenicol	Vancomycin, kanamycin, and streptomycin	-	-	Sornsenee *et al*. (2021)
Enterococcus spp.	-	-	-	*hyl*, *esp*, *gelE*, *agg*, *ace*, *efa*, *CylL*, *cob*, *cpd*, and *ccf*	Lengliz *et al*. (2021).
Latilactobacillus sakei L4, *Enterococcus hirae* E5, *Pediococcus acidilactici* P7, *Weissella confusa* W8	Vancomycin (4/4), polymyxin B (4/4), gentamicin (3/4), ciprofloxacin (4/4), amikacin (4/4), enrofloxacin (4/4), ofloxacin (4/4), lincomycin (4/4), cephalexin (3/4),	Doxycycline (4/4), tetracycline (1/4), Florfenicol (4/4), rifampin (4/4), midecamycin (4/4), kitasamycin (4/4), clindamycin (4/4),	Not detected (Van A and VanB)	-	Liu *et al*. (2020)

"-" not determine

2.5.12.2. Acquired resistance

Acquired resistance is either due to horizontal gene transfer or mutations and drug selection. The horizontal transfer of resistance genes from one bacterium to another is facilitated through conjugation, transduction, or transformation, thereby contributing to transforming sensitive bacteria into resistant ones (Bonham *et al*., 2017). Several LAB have shown unnatural resistance by exhibiting the presence of genes such as *blaZ*(beta-lactams), *cat*(chloramphenicol), *erm*(A, B, C, T, LF, GT) (erythromycin, macrolides, lincosamides, and streptogramins), *mef*(A) (macrolides), *tet*(W), *tet*(M), *tet*(S), *tet*(O), *tet*(Q), *tet*(Z), *tet*(W/O), *tet*(K), *tet*(O/W/32/O/W/O), *tet*(L) (tetracycline). Most importantly, chloramphenicol (plasmid), tetracycline (plasmid, transposon, and chromosome), and erythromycin (plasmid, transposon, and chromosome) have been reported to be housed in mobile genetic elements (Gueimonde *et al*., 2013). These genes tend to transfer horizontally between closely related organisms such as *erm*(B) from lactobacilli to enterococci (Toomey *et al*., 2009), *tet*(M), and *erm*(B) from lactobacilli to *Enterococcus faecalis* (Nawaz *et al*., 2011).

2.6. Omics based safety analysis

2.6.1. Genomics

Unraveling the safety-related genes across the whole genome using bioinformatics tools (genome mining) has emerged as an easy, quick, and feasible method. By harnessing the bacterial complete genome sequence, the presence of any antibiotic resistance genes, virulence and stress-related genes, prophage sequences, tolerance to heavy metals, and adverse metabolic genes can be mapped using various databases such as Basic Local Alignment Search Tool (BLAST) with the Virulence Factors Database (VFDB), Antibiotic Resistance Genes Database (ARDB), etc. (Senan *et al*., 2015). However, several investigators have used different databases with acceptable e-values/ identity/ coverage scores to predict the genes conferring antibiotic resistance and virulence phenotypes (**Table 2.4)**. Since there are no clear procedural guidelines for microbial safety assessment, Chokesajjawatee *et al*. (2020) have recently proposed the guidelines for conducting safety evaluation via whole-genome analysis as outlined below.

- ***Determination of the smallest extra-chromosomal DNA size***

Since corroborative evidence suggest that most of the antibiotic resistance and virulence genes are located on the plasmid DNA, it is therefore essential to unravel the presence of any small plasmids. A simple laboratory method of plasmid extraction and subsequent visualization through agarose gel electrophoresis would provide complete insights into the target bacterium's genome.

- ***Selection of the whole-genome sequencing platform***

The sequencing platform should generate complete insights into the genome. However, most of them fail to recognize the extra-chromosomal DNA. Hence, hybrid sequencing via Oxford Nanopore Technologies and Illumina platform (ONT-Illumina hybrid sequencing) may be helpful to gather comprehensive genome information.

- ***Identification of virulence and undesirable genes***

Functional annotation of genes accountable for virulence and undesirable properties may be disclosed in association with publicly available databases [Kyoto Encyclopedia of Genes and Genomes (KEGG) database (available at https://www.kegg.jp)] and can further confirm manually. However, it is pertinent to note that survival and adaptation-related genes under virulence genes should not be considered under this category.

- ***Identification of functional and transferrable AMR genes***

The presence of any AMR genes should be annotated using the KEGG database under "Brite ko01504: Antimicrobial resistance genes". It is also crucial to identify their genome locations if detected since gene location determines the transferability. A web-based tool, oriTfinder (https://bioinfo-mml.sjtu.edu.cn/oriTfinder/), can discover the origin of transfer (*oriT*) regions that are necessary to classify the self-transmitted conjugative plasmids. Similarly, a genome-scale search for existing prophages sequences can be accomplished by the PHASTER web tool (http://phaster.ca/).

- ***Identification of antimicrobial drug production capability***

By the World Health Organization's List of Critically Important Antimicrobials for human medicine (WHO CIA list), a search for antimicrobial drug production ability of target probiotic strains should be annotated using the KEGG database.

Table 2.4: Various sequencing platforms and databases used in the genome-scale assessment of safety and resistance genes

Bacterial strain	NGS Platform for WG analysis	Database or web servers	References
Lactiplantibacillus plantarum BCC9546	Hybrid Oxford Nanopore Technologies and high-throughput Illumina platform	VFDB, KEGG database, CARD (RGI 5.0.0, CARD 3.0.3), ResFinder (ResFinder 3.2), KEGG database (Release 90.1) using Blast KOALA search tool, "Brite ko01504: Antimicrobial resistance genes, PHASTER tool, oriTfinder	Chokesajjawatee *et al*. (2020)
Lactobacillus helveticus MTCC 5463	Pyrosequencing (454 Life Sciences technology) based on a high-throughput sequencer (GS-FLX, Roche)	BLAST with the VFDB (http://www.mgc.ac.cn/VFs/main.htm) and ARDB (http://ardb.cbcb.umd.edu/)	Senan *et al*. (2020)
Limosilactobacillus reuteri PNW1 (Contig-wise genome analysis)	Illumina MiSeq Platform1	ResFinder v. 3.1, RAST, CARD (RGI 5.1.0), VirulenceFinder v. 2.0, PathogenFinder v. 1.1, PHASTER, ISfinder search tool, Insertion Sequence Semi-Automatic Genome Annotation (ISsaga V. 2.0) and OASIS	Alayande *et al*. (2020)
Lactiplantibacillus plantarum strains	Not disclosed	BLAST	Arellano *et al*. (2020)
Bacillus coagulans GBI-30, 6086	Illumina GAIIx sequencer	CARD, local Protein-protein Basic Local Search Tool (BLASTP). Putative virulence factors were identified by local BLASTP, VFDB, ProphageFinder, and CRISPRFinder	Salvetti *et al*. (2016)
Lactobacillus crispatus, L. jensenii, Lacticaseibacillus paracasei, Limosilactobacillus reuteri, Ligilactobacillus salivarius	Not disclosed	CARD (http://arpcard.mcmaster.ca/), ResFinder (https://cge.cbs.dtu.dk/services/ResFinder/) and ARG-ANNOT (https://www.mediterranee-infection.com/acces-ressources/base-de-donnees/arg-annot-2/)	Sirichoat *et al*. (2020)
Enterococcus durans KLDS6.0930	PacBio RSII platform	CARD, VFDB (http://www.mgc.ac.cn/VFs/main.htm), ResFinder 3.0 (https://cge.cbs.dtu.dk//services/ResFinder/), PathogenFinder 1.1 (https://cge.cbs.dtu.dk/services/PathogenFinder/), CRISPR Finder and PHASTER	Li *et al*. (2018)
Lactobacillus crispatus YIT 12319 (LcY)	MiSeq (Illumina)	MiFuP Safety (http://www.bio.nite.go.jp/mifup_safety/])	Terai *et al*. (2020)

Bacterial strain	NGS Platform for WG analysis	Database or web servers	References
Bacillus coagulans strain LBSC	MinION Mk1b (Oxford Nanopore Technologies, Oxford, UK)	CARD, VFDB, PHASTER web based server, CRISPR Finder	Saroj and Gupta (2020)
Bacillus fragilis HCK-B3	Illumina	Island Path-DIMOB, Islander, CARD, VFDB	Tan *et al*. (2020)
Lactobacillus acidophilus NCFM®, *Lactica seibacillus paracasei* Lpc-37®, *Bifidobacterium animalis* subsp. *lactis* strains Bl-04®, and Bi-07®	PacBio technology	RAST, CARD, MvirDB, BLASTp	Morovic *et al*. (2017)
Lactobacillus helveticus, D75 and D76 strains (Vitaflor, Russia)	PacBio RS II	InterPro, KEGG, NCBI, and CRISPRfinder	Toropov *et al*. (2020)
Limosilactobacillus reuteri IDCC 3701	Illumina	VFDB, ResFinder, PHASTER web-based program	Lee *et al*. (2021)
Enterococcus faecium LBB.E81	Illumina	ResFinder, VirulenceFinder, CARD	Urshev and Yungareva (2021)
Bacillus coagulans IDCC 1201	Illumina	VFDB, antibiotic resistance genes database (ARDB), PHASTER	Bang *et al*. (2021)
Limosilactobacillus fermentum (ATCC 23271)	Illumina platform	RAST, VFDB, PHASTER	Dos Santos *et al*. (2021)
Lactiplantibacillus plantarum strain GS083, GS086, and GS090	Life Ion S5	VFDB, CARD, ResFinder	Zeng *et al*. (2020)

Note: VFDB: Virulence factor database, KEGG: Kyoto Encyclopedia of Genes and Genomes, CARD: Comprehensive Antibiotic Resistance Database, BLAST: Basic Local Alignment Search Tool, RAST: Rapid Annotation using Subsystem Technology, MvirDB: Microbial Virulence Database, MiFuP Safety: Microbial Functional Potential for Safety, ARGD: Antibiotic Resistance Genes Database, OASIS: Optimised Annotation System for Insertion Sequences,_ARG-ANNOT: Antibiotic Resistance Gene-ANNOTation, CRISPR finder: Clustered regularly interspaced short palindromic repeats finder.

Nevertheless, it should be considered that *in silico* analysis is only a first step in the probiotic safety assessment, and it may not completely replace the *in vivo* safety assessment for scrutinizing the undesirable effects. *In silico* analysis would be used to screen many strains to eliminate the high-risk strains without the need for animal studies. Genome-scale analysis may demonstrate the possible future direction on identifying potential risks associated with specific strain and the specific areas that need to be addressed during *in vivo* research concerning the pathogenicity.

2.6.2. Transcriptomics

Transcriptomics deals with quantifying a total set of coding and non-coding RNA in a probiotic bacterium. This helps to comprehend the gene expression patterns and genome dynamics like gene structure and regulation. Microarray has been traditionally used to investigate the mRNA expression of targeted genes (Endo *et al*., 2020). However, RNA sequencing (RNA seq) has flourished rapidly as advances are being made in next-generation sequencing platforms (ABI SOLiD 4 sequencing platform, Illumina, and Ion Torrent) (Bisanz *et al*., 2014). This offers a great potentiality to determine the expression and regulation of all possible genes and thus confirm the functionality of virulent or pathogenic, or antibiotic resistance genes. Moreover, it offers the researchers to understand the mRNA expression profile of virulence genes upon exposure to various stress that probiotics undergo in the *in vivo* system (acid/ bile/ enzymes). Nevertheless, limited studies have been focused on validating the virulence/ pathogenicity of probiotic strains until the transcriptome level. In this regard, upregulation of genes encoding an ABC-type multidrug/antibiotic transport system has been noted in bile stress-induced *Lactobacillus acidophilus* NCFM (Koskenniemi *et al*., 2011). Similarly, bile stress induced the hemolysin-like protein (HLP) gene expression in the *Bifidobacterium longum* BBMN68 (An *et al*., 2014).

2.6.3. Proteomics

Proteomics offers comprehensive information on the proteome of a cell at its any growth phase, and thus it aids in establishing a link between transcriptome and functionally active proteome. The techniques like gel-based proteomics (SDS-PAGE, 2-DE, immunological methods like western blot) and chromatography coupled with mass-spectrometry such as MALDI-TOF MS/ ESI Q-TOF-MS/ capillary electrophoresis coupled to mass spectrometry have gained momentum in identifying the targeted or

overall proteins of a cell (Klein *et al*., 2013; Mbye et al., 2020). Amongst various virulence determinants, biogenic amines have been characterized from multiple potential probiotic strains using the techniques like high-resolution electrospray ionization mass spectrometry (HRESI-MS) analysis, high-pressure liquid chromatography (HPLC), LC-MS/ MS (Priyanka *et al*., 2021; Saroj and Gupta, 2020; Ku *et al*., 2020). A recent study by Cirrincione *et al*. (2019) have used a proteomics approach to study the safety of food-isolated strain *E. faecalis* D27 (dairy-isolate) using LC-MS/MS. They identified several proteins of potential pathogenic nature *viz*. serine proteases, von Willebrand factor, serine hydrolase with beta-lactamase activity, efflux transporter, and proteins involved in horizontal gene transfer. Further, the proteins involving bacterial communication, such as pheromones and conjugative elements and proteins able to interact with human components have been identified. Currently, comparative proteomics and functional genomics are the two necessary fields that the researchers are exploiting to elucidate novel genes related to antibiotic resistance and infer biological functions in food-grade bacteria such as probiotics (Muñoz *et al*., 2016; Zheng *et al*., 2017). Several resistance mechanisms/proteins (up-regulation of protein synthesis, NADH peroxidase (Npx) and a small heat shock protein, and the down-regulation of carbohydrate metabolism and energy production) in probiotic *Lactobacillus pentosu*s MP-10 have been identified in response to the antibiotics (amoxicillin, chloramphenicol, and tetracycline) using comparative proteomics (Muñoz, *et al*., 2016). Researchers used the proteomics approach to study the proteome of probiotic *Enterococcus durans* under aerobic and anaerobic conditions. The authors observed the differential expression of several proteins of safety concern, such as penicillin-binding proteins, decarboxylase, etc. (Comerlato *et al*., 2020). Therefore proteomics may serve as a quality control tool to investigate the safety of probiotics before human applications.

2.6.4. Metabolomics

Metabolomics deals with the outcome of a gene or gene product and is directly related to the functional genome (**Fig. 2.2**). Thus, it deals with quantifying and identifying various metabolites of a cell in its entire growth cycle. Advanced chemometric analytical techniques like spectrophotometric methods, Attenuated Total Reflection- Fourier-Transform Infrared Spectroscopy (ATR-FTIR), chromatography [liquid chromatography (LC)/ gas chromatography (GC) coupled with mass spectrometry (MS) or MS/ MS], and (nuclear magnetic resonance) NMR have been used to generate

high throughput and reliable data on identification and quantification of the metabolome of a cell (Liang *et al*., 2018). Concerning probiotic safety, harmful metabolites like D-lactate or biogenic amines or ammonia production can be quantified through a targeted metabolomics approach (Ban *et al*., 2020; Bang *et al*., 2021). Various researchers have confirmed the presence/absence of tyramine, histamine putrescine, cadaverine, and 2-phenethylamine in the cell-free supernatant of probiotic bacteria through the HPLC/ TLC approach (Božič *et al*., 2021). However, untargeted methods may provide a comprehensive idea of overall metabolites. Further, the production of toxic metabolites by converting primary bile acids to secondary bile acids has been studied in *Weissella cibaria* by analyzing the bile salt deconjugation by HPLC. *Weissella cibaria* hydrolyzed the conjugated bile acids taurocholic acid (TCA) and glycocholic acid (GCA) by 96.97% and 98.14%, respectively. Thin-layer chromatographic (TLC) analysis confirmed the inability to convert primary bile acids (cholic acid and chenodeoxycholic acid) to secondary bile acids (deoxycholic acid and lithocholic acid) (Kang *et al*., 2020).

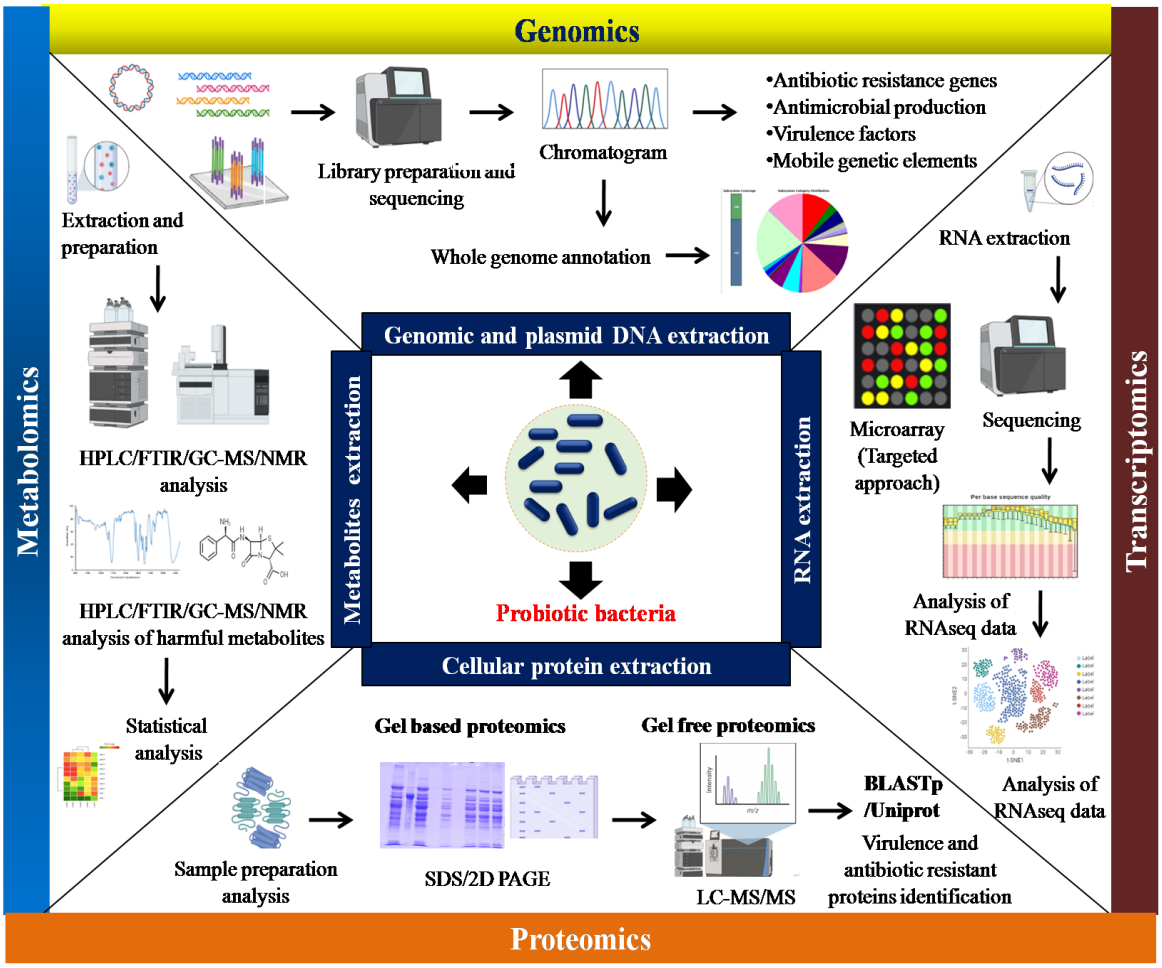

Fig. 2.2: An overview on integration of various omics approaches in the safety assessment of probiotics

2.7. *In vivo* safety studies

2.7.1. Toxicity studies in healthy animals

Toxicity studies in animals are conducted before the clinical trials to assess the degree to which the test compounds are toxic and investigate the toxicity mechanisms. Animal studies may hint the insights into a safe starting dose for clinical studies, target organ toxicity, and other similar insights on a treatment that produces the most minor toxicity (Soltani *et al*., 2021). However, most preclinical studies are generally carried out to meet regulatory requirements as they often emphasize the necessity of toxicity tests to preserve current levels of human health and environmental protection. The emergence of test guidelines program of the Organization for Economic Cooperation and Development (OECD) has harmonized the safety testing guidelines for different chemicals across 37 OECD member countries (Source: https://www.nap.edu/read/11523/chapter/4; https://www.nuffieldbioethics.org/wp-content/uploads/Animals-Chapter-9-Animal-Use-in-Toxicity-Studies.pdf). Since there are no standardized and uniform guidelines prescribed by international scientific association for *in vivo* safety appraisal of probiotic strains, several researchers have used the OECD test guidelines with slight modifications in doses (**Table 2.4**). OECD guidelines are framed to assess the adverse effects that occur on first exposure to a single dose of a substance (acute toxicity studies), to assess the potential of substances to interact with genetic material (genotoxicity), and to identify whether toxicity occurs after continuous exposure to a substance (repeated-dose toxicity studies).

2.7.1.1. Acute Toxicity (single or repeated dose)

Acute toxicity is an integral step in assessing the toxicity of test compounds in typical rodents (rats or mice) for two weeks (OECD Test guideline-425). Historically, the test compounds are administered in different dosages to determine the lethal dose (LD_{50}), which induces death in 50% of the test animals (OECD, 2008a). However, using a single high amount is commonly practiced (Qureshi *et al*., 2020) over multi-dose (Lu *et al*., 2021). Despite accounting for the unusual animal behavior, growth, and mortality (if any), both external and internal bleeding, diarrhea, loss of appetite, vomiting (in non-rodents), changes in the mucous membranes, respiratory and somatomotor activity, behavior pattern, tremors, convulsions, salivation, diarrhea, lethargy, sleep and changes in gait and posture, aggression, salivation, changes in blood pressure, coma, loss of fur and hair, dehydration, or nasal discharge are by far experimental parameters

(Shokryazdan *et al*., 2016). On the other hand, separate tests are generally recommended to assess test compounds' local and systemic toxicity. At the end of the experiment, it is also paramount to record the morphological and biochemical changes with gross necropsy examination. Effects of oral administration of various probiotic strains (oral toxicity) at different concentrations have been presented in **Table 2.5.** Acute oral toxicity of *Lactiplantibacillus plantarum* MF405176, *Limosilactobacillus fermentum* MF033346, *Lactococcus lactis* spp. *lactis* MF480428, *Enterococcus faecium* MF480431, and *Pediococcus acidilactici* MF480434 were evaluated in Wistars rats with three individual doses (10^8 CFU/g, 10^{10} CFU/g, and 10^{12} CFU/g) of each probiotic strain at a single oral dose of 5000 mg/kg bw. No animals demonstrated signs of toxicity at 14^{th} day (Divisekera *et al*., 2021). Oral administration of *Lacticaseibacillus casei* IDCC 3451 (300 or 2000 mg of freeze-dried *Lacticaseibacillus casei* IDCC 3451 powder in 10 mL sterilized water per kg BW) to rats did not induce any necropsy and abnormal clinical signs with no mortalities during the study period (14 days) (Shin *et al*., 2021). Similarly, single-dose oral administration of *Lactococcus lactis* IDCC 2301 (300 or 2000 mg of free-dried *Lactococcus lactis* IDCC 2301 powder in 10 mL sterilized water per kg BW) did not show mortality, signs of body weight changes, and toxicity in female rats (Kim *et al*., 2021).

2.7.1.2. Repeated dose oral toxicity studies

2.7.1.2a Subacute toxicity

Subacute toxicity of the test compound is based on the repeated oral administration during one limited period (one dose level daily for 28 days). This study has three objectives (i) to recognize toxicity that develops only after a certain length of continuous exposure (ii) to investigate the most affected organs (iii) to determine the toxic doses (Source: https://www.nuffieldbioethics.org/wp-content/uploads/Animals-Chapter-9-Animal-Use-in-Toxicity-Studies.pdf). According to OECD Test guideline 407, the toxicity response is considered by recording weekly bodyweight variations, feed intake, biochemical and cardiovascular changes, and behavioral changes. Similar to acute toxicity testing, the histopathological changes in the major organs or tissues are examined (OECD, 2008b). In this regard, oral administration of *Lactiplantibacillus paracasei* IBRC-M 11110 at two doses of 6×10^8 CFU/ day and 6×10^9 CFU/ day for 28 days did not affect the general health and body weight of the rats with no significant alteration in serum biochemical parameters.

Table 2.5: Outcomes of studies on probiotic safety evaluation in healthy animals (Oral Toxicity Tests)

Probiotic strains	Dosage of probiotics in different tests	Animals	Outcomes	References
Bacillus coagulans IDCC 1201	Acute oral toxicity (8.5×10^{10} CFU/g at 300 mg/kg body weight or 2000 mg/kg BW once daily for 14 days)	Female rats	No adverse effects	Bang *et al*. (2021)
Limosilactobacillus reuteri IDCC 3701	Acute oral toxicity (13.8×10^{10} CFU/g) per kg body weight (BW) (i.e., 300 mg/kg BW or 2000 mg/kg BW)	Rats	No adverse effects	Lee *et al*. (2021)
Lactiplantibacillus pentosus IBRC11143	Acute oral toxicity (1×10^{8} and 1×10^{9} CFU/rat)	Wistar rats	No adverse effects	Bahrehvar, Khezri, Barzegari, and Nejati (2021)
Limosilactobacillus fermentum NCMR 2826 and FIX	10^{16} CFU/ mL for Acute Oral Toxicity (Single dose) and 10^{7}, 10^{8}, 10^{10} CFU/mL for subchronic 13-week (90-day) study	Male Wistar rats	No toxic effects	Thumu and Halami (2020)
Lab4 consortium consists of *Lactobacillus acidophilus* CUL21 (NCIMB 30156), *Lactobacillus acidophilus* CUL60 (NCIMB 30157), *Bifidobacterium bifidum* CUL20 (NCIMB 30153) and *Bifidobacterium animalis* subsp. *lactis* CUL34 (NCIMB 30172)	90-day oral toxicity (1×10^{11} cfu/kg/day, 2×10^{11} cfu/kg/day or 5×10^{11} cfu/kg/day	Wistar rats	No adverse effects	Baker *et al*. (2021)
HOWARU® probiotic product (*Lactobacillus acidophilus* NCFM (ATCC SD5221), *Lacticaseibacillus paracasei* Lpc-37 (ATCCSD5275), *Bifidobacterium animalis* sub sp. *lactis* Bl-04 (ATCC SD5219) and *B. animalis* subsp. *lactis* Bi-07 (ATCC SD5220)	Acute toxicity test with a study dose of 5000 mg/kg body weight (mg/kg) or $1.7–4.1 \times 10^{12}$ CFU/kg body weight	Rats	No adverse effects	Morovic *et al*. (2017)
Bacteroides fragilis HCK-B3	Acute toxicity study with a dose of 10^{9} CFU/mice	Mice	No adverse effects	Tan *et al*. (2020)
Lactobacillus helveticus KLDS1.8701	Acute toxicity (6×10^{10} CFU/kg body weight) and subacute oral toxicity [1×10^{9} CFU/kg BW (Low) and 1×10^{10} CFU/kg BW (High)]	Rats	No adverse effects	Li *et al*. (2017)

Probiotic strains	Dosage of probiotics in different tests	Animals	Outcomes	References
Lactiplantibacillus plantarum LAB12	Acute (11 log CFU/ kg BW) and subchronic toxicity test (low dose) (8 log CFU/kg BW), medium dose (9 log CFU/kg BW) and high dose (10 log CFU/kg BW)	Rats	No adverse effects	Fareez *et al*. (2019)
Limosilactobacillus reuteri 29B	Acute oral toxicity study (1×10^8, 1×10^9, and 1×10^{10} CFU/mouse/day)	BALB/c mice	No adverse effects	Meleh *et al*. (2020)
Lentilactobacillus buchneri FD2, *Limosilactobacillus fermentum* HM3	Acute (6×10^{10} CFU /kg BW) and subacute toxicity (1×10^{10} CFU /kg BW and 1×10^9 CFU/kg BW)	Rats	No adverse effects	Shokryazdan *et al*. (2016)
Enterococcus durans KLDS6.0930	Subacute toxicity using the test dosage 1×10^9 CFU/kg body weight (BW)	Rats	No adverse effects	Li *et al*. (2018)
Enterococcus faecium 2C	1×10^{11} CFU/kg of animal body weight for modified acute toxicity test (21 consecutive days) (Sub acute)	Male Wistar rats	No adverse effects	Khalkhali and Mojgani (2018)
Lactobacillus rhamnosus MTCC- 5897	Subacute toxicity (10^7, 10^9, 10^{11} , and 10^{13} CFU/animal/day)	Mice	No adverse effects	Bhat *et al*. (2019)
Limosilactobacillus fermentum MTCC-5898	Subacute toxicity (10^7, 10^9, 10^{11} CFU/animal/day)	Mice	No adverse effects	Samtiya *et al*. (2020)
Saccharomyces cerevisiae RC016	Subchronic toxicity (10^8 CFU/animal/day)	Wistar rats	No adverse effects	Gonzalez Pereyra *et al*. (2014)
Limosilactobacillus fermentum NCMR 2826 and FIX	10^7, 10^8, 10^{10} CFU/mL for Subchronic 13-week (90-day) study	Male Wistar rats	No toxic effects	Thumu and Halami (2020)
Bacteroides uniformis CECT 7771	10^{10} CFU/day (sub-chronic 90 day trial in animals)	Wistar rats	No adverse effects	Gómez del Pulgar *et al*. (2020).
Bacillus licheniformis Me1	Subchronic toxicity (1.1×10^{10} and 1.1×10^{11} CFU/ kg body weight/day)	Wistar rats	No adverse effects	Nithya *et al*. (2012)
GanedenBC$^{30™}$ (A probiotic product containing *B. coagulans*) product containing *B. coagulans* at 6.88×10^{10} CFU/g	One year chronic toxicity by feeding 600-2000 mg/kg BW/day	Wistar rats	No adverse effects	Endres *et al*. (2011)

However, a substantial decrease in mean corpuscular volume and mean corpuscular hemoglobin of male rats was recorded (Bahrevar *et al*., 2021a). This variation suggests including both male and female rats in the study to nullify the observations influenced by the individual sex. In another study, the oral administration of *Lactiplantibacillus pentosus* (IBRC=11143) 1×10^8 and 1×10^9 CFU/ rat in a subacute study (28-days) showed a significant difference in urea and creatinine levels between the control and the experimental groups. Some blood parameters (lymphocyte, red blood cell, hematocrit, and hemoglobin) were also showed a significant change in the groups that received IBRC=11143. Moreover, a significant increase in alkaline phosphatase levels was observed in male rats (Bahrehvar *et al*., 2021b). These findings are suggested that *Lactiplantibacillus pentosus* (11143) was not entirely safe, and strain may not be the right choice as a probiotic for human consumption. However, several other putative probiotic strains (*Bifidobacterium lactis* BL-99 and *Lacticaseibacillus paracasei* K56 and ET-22) were safe/non-toxic on a dose-dependent basis multidose oral administration of test strains in the murine model (Lu *et al*., 2021). Subacute toxicity of a next-generation probiotic *Butyricicoccus pullicaecorum* 25-3T (10^9 CFU/ mL) was evaluated in rats and found safe without hematological and biochemical alteration (Steppe *et al*., 2014). However, the strain had several antibiotic resistance genes as predicted by CARD/RAST with the risk of horizontal transfer (Steppe *et al*., 2014).

2.7.1.2 b Subchronic toxicity

After gathering the insights on safety dose in the acute and sub-acute toxicity tests, this test is generally carried out. Subchronic toxicity test is conducted in rodents with at least three concentrations for the prolonged tenure of 90 days. The outcomes of this test allow measuring the highest safe dose without significant effects on viability (the 'no observed adverse effect level', or NOAEL). This may also aid in risk analysis by limiting the acceptable exposure of humans to a fraction of the NOAEL. The general observations and physical parameters (body weight, feed intake, and local injuries) are observed during the study. A detailed examination of hematology, clinical or blood/serum biochemistry, gross necropsy, and histopathology provides a satisfactory safety level estimation (OECD Test guideline 408) (OECD, 1995). In a study conducted by Divisekera *et al*. (2021), repeated dose exposure of *Lactiplantibacillus plantarum* MF405176, *Limosilactobacillus fermentum* MF033346, *Lactococcus lactis* sub sp. *lactis* MF480428, *Enterococcus faecium* MF480431, and *Pediococcus acidilactici* MF480434

by oral administration (10^8 CFU/g, 10^{10} CFU/g, 10^{12} CFU/g) of each probiotic strain at 1000 mg/kg bw/day for consecutive 90 days indicated safe status by demonstrating no changes in animal behavior, biochemical and hematological parameters, feed or water intake and adverse effects on body weight observed. In addition, bacteremia or bacterial translocation and histopathological changes in rat organs were not observed. In yet another study, repeated exposure of *Latilactobacillus curvatus* WiKim 38 at 0, 500, 1500, and 5000 mg/kg b.w (9.42×10^8 CFU/g counts) for 90 days had no adverse effects up to 5000 mg/kg b.w./day (Han *et al*., 2021). Rats administered with microencapsulated *Lactiplantibacillus plantarum* LAB12 at a low dose (8 log CFU/kg bw), medium dose (9 log CFU/kg bw), and high dose (10 log CFU/kg bw) for 90 days did not show mortality or treatment-related findings in terms of impairment in blood and tissue marker enzymes, clinical body weight, water intake, or food consumption (Fareez *et al*., 2019).

2.7.1.2 c Chronic toxicity

Chronic toxicity characterizes the toxicity of orally administered substances of interest in the mammalian species (preferably rodents) upon exposure to prolonged and repeated (daily). Continuous exposure of test compounds in high doses may be lost for a minimum of 12 months. The variability in the baseline parameters such as feed and water intake and hematological examination, urinalysis, clinical chemistry), gross necropsy, and histopathological analysis are recorded (OCED Test guideline 452) (OECD, 2018a). One year chronic oral toxicity of probiotic GanedenBC^{30}™ containing *Bacillus coagulans* at a concentration of 15×10^9 CFU/g was studied in Wistar rats using different doses varying from 0, 600, 1200, and 2000 mg/kg bw/day (Endres *et al*., 2011). It was found that the lowest NOEL of 1948 mg/kg (6.88×10^{10} CFU/g) was concluded to have a 100-fold safety factor. However, only a handful of studies have been conducted to understand the toxicological safety upon long-term and repeated exposure of probiotic strains. Hence, future studies should focus on evaluating the effect of probiotic administration on long-term exposure in healthy and diseased animal models.

2.7.2. Bacterial translocation assay

Under a healthy milieu, the intestinal environment constitutes a balanced and dynamic gut microbiota. Intestinal epithelial cells act as a physical barricade and thus

abrogate the translocation of intestinal lumen content or bacteria across the epithelium. The immune defenses in the healthy subjects typically eliminate pathogenic bacteria that would otherwise translocate across the mucosal epithelium (Liong, 2008). The structural and functional intactness of the gut may alter under immunocompromised conditions (disease conditions or a state of hyper-inflammation or drug interventions), the perturbed gut integrity in such episode may lead to lumen bacterial translocation (both pathogenic and beneficial) through either paracellular or transcellular routes to different organs via systemic circulation of blood and lymph, and thus eventually instigate sepsis or bloodstream infections (Nagpal and Yadav, 2017). Therefore, profiling the specific microbial load in the lymphatic organs of gut-associated lymphoid tissue (GALT) such as mesenteric lymph nodes (MLN) or spleen may be potential targets to assess the pathway by which probiotic entry to the systemic circulation (Abe *et al*., 2020).

Accounting for the mounting evidence on probiotics-mediated sepsis and bloodstream infections in human subjects (**Table 2.1**), several attempts have been made to study the translocation ability of probiotic strains both in healthy and diseased models. Studies conducted in the healthy animals concluded that probiotic strains (*Bifidobacterium longum* BB536, *Bifidobacterium breve* M-16V, *Bifidobacterium infantis* M-63, *Lactobacillus delbreuckii* 45E, *L Limosilactobacillus fermentum* 28E, *Limosilactobacillus mucosae* 28C, *Limosilactobacillus reuteri* 29A & 29B) had no translocation ability from the lumen to different organs including blood, liver, spleen, kidney, and MLN with no disturbance to epithelial cells and mucosal layer in the ileum, cecum, and colon (Abe *et al*., 2010; Meleh *et al*., 2020). Similarly, a probiotic safety study in an immunocompromised and immunocompetent rodent model indicates the absence of *Bacillus uniformis* CECT 7771 translocation to mesenteric lymph node (MLN), blood, and liver, therefore indicating that such strain has the tremendous potentiality to enter clinical trials (Fernández-Murga and Sanz, 2016; Gómez del Pulgar *et al*., 2020).

2.7.3. Genotoxicity

Genotoxicity assays are carried out to study the effect of test compounds on the genetic alterations in somatic and/or germ cells. Such studies are generally designed to find out the genetic material damages either by recording gene mutation, clastogenicity (i.e., structural chromosome changes) and aneuploidy (occurrence of one or more extra or missing chromosomes leading to an unbalanced chromosome complement) (Source:

https://www.who.int/docs/default-source/food-safety/ehc-240-chapter-4-5-genotoxicity-draft-dec-2019.pdf?sfvrsn=e6f002fb_2). The various methods employed to study the *in vivo* genotoxicity have been discussed below.

2.7.3.1. Micronucleus assay

This assay evaluates the formation of micronuclei in the erythroblasts sampled from the bone marrow (usually measured in immature erythrocytes) or peripheral blood (measured in reticulocytes) of animals (rats or mice). This test is based on the principle that when the bone marrow erythroblast develops into an immature erythrocyte (sometimes also referred to as a polychromatic erythrocyte or reticulocyte), it may migrate into the peripheral blood by extruding its nucleus. Thus, visualization of micronuclei formed due to genotoxic effect can be seen in erythrocytes because normal and matured erythrocyte lacks the central nucleus. Nevertheless, care should be taken while opting for the tests since the *in vivo* micronucleus test using bone marrow cells has the probability of obtaining false-positive results as the cells in the bone marrow are rapidly dividing pro-erythrocytes (OECD Test guideline 474) (OECD, 2016a). Supplementation of a probiotic consortium of *Lacticaseibacillus rhamnosus* LCR177, *Bifidobacterium adolescentis* BA286, and *Pediococcus acidilactici* PA318 (1.25, 2.5, and 5.0 g/kg bw) to ICR male mice did not foster reticulocytes formation in blood cells (Chiu *et al*., 2013). Oral administration of *Latilactobacillus curvatus* WiKim 38 at 500, 1000, and 2000 mg/kg bw of rats for a day (twice at 24-h intervals) resulted in no change in the frequencies of micronucleated polychromatic erythrocytes (MNPCEs) compared to the negative control (vehicle/ saline). But, there was a significant increase in the frequency of MNPCEs in the positive control group (cyclophosphamide) (Han *et al*., 2021).

2.7.3.2. Mammalian alkaline comet assay

As per the OECD Test guideline 489, this method is also called an alkaline single-cell gel electrophoresis assay. This method identifies substances that induce DNA damage either by single or double-strand breaks in rodents. The comet assay may be applied to any tissue of an animal, including a specific site of tissues and germ cells, making this assay useful in assessing DNA damage upon exposure to target tissues. The assay result is expressed in terms of % tail DNA (or other measures, tail length and tail moment) and median values per slide, mean values per animal, and mean values per

group (OECD, 2016b). Oral administration of *Escherichia coli* strain Nissle 1917 (EcN) at 10^9–10^{11} CFU/rat for 28 days did not induce DNA-strand breaks and therefore, in turn suggested the inability to foster detectable genotoxic potential in Wistar rats (Dubbert *et al.*, 2020). The intestinal cells of Wistar rats fed with *Lactobacillus acidophilus* strain Er-2317/402 Narine (1.0×10^8 CFU/mL) did not induce double-strand breaks in the DNA thus suggesting that administered probiotic strain was safe (Pepoyan *et al*., 2019). In a similar study, probiotic *Saccharomyces cerevisiae* RC016 (daily oral dose of 10^8 viable cells) intervention for 90 days did not provoke genotoxicity in Wistar rats as estimated by comet assay (Gonzalez Pereyra *et al*., 2014).

2.7.3.3. Chromosomal aberration assay

According to OECD Test guideline 475, *in vivo* chromosomal aberration assay is generally conducted in rodents to determine the effect of test compound on structural aberrations in chromosome (OECD, 2016c). While asessing the aberrations, this test considers the chromosome or chromatid type aberrations in the metaphase spread such as chromosomal gap, chromosomal break, dicentric, ring, chromatid gap, chromatid break, multiple aberrations, and acentric fragment. The chromosomal damage or related aberrations induced by the test substances may foster genetic diseases and cancer. Hence, it is most relvent and appropriate to assess the genotoxicity of any potential probiotics intended for human consumption. In this regard, the oral administration of two indigenous probiotic *Lactiplantibacillus plantarum* MTCC 5690 and *Limosilactobacillus fermentum* MTCC 5689 at 1012 CFU/mouse for 21 days induced no strcutral chromosomal aberrations (Pradhan *et al*. 2019a).

2.7.4. Teratogenicity or developmental toxicity, or reproductive toxicity

Developmental toxicity assesses the effect of a test compound to cause the adverse effects to the developing embryo or fetus either by directly on cells of the embryo causing cell damage and thus leading to abnormal organ development or by induction of mutations in a parental germ cell. OECD Test guideline 414 has outlined the test procedures to assess prenatal developmental toxicity in pregnant animals, which covers the assessment of maternal effects and death, structural abnormalities, or altered growth in the fetus (OECD, 2018b). However, only limited studies have been carried out to evaluate such effects of probiotics during safety appraisal. A study conducted by Endres *et al*. (2011) has illustrated the no observed reproductive toxicity in the parents or in their

F_1 generation upon oral administration of GanedenBC^{30}™ (containing multiple strains of probiotic *Bacillus coagulans*) for a year. In another study, maternal oral administration of APS1 powder (1×10^{10} CFU/g) had been observed to have no related reproductive toxicity and fetal development when the *Liquorilactobacillus mali* APS1 dosage was 1,670 mg/kg/day in rats (Lin *et al*., 2018). *Clostridium butyricum* MIYAIRI 588®, a well studied anaerobic probiotic strain, had no reproductive toxicity or teratogenicity and did not adversely influence the development of F_1 mice when maternal administration of probiotics at a maximum dose of 4800 mg/kg during 6–15 days of gestation (Isa *et al*., 2016). A recent finding suggests that probiotic *Lacticaseibacillus rhamnosus* can significantly modulate the fecundity in the Zebrafish coadministration with perfluorobutanesulfonate (PFBS) compared to PFBS alone (Tang *et al*., 2020). Effect of probiotic preparations contained *Bacillus subtilis* (10^9 CFU/mL), *Propionibacterium* 10^7 CFU/mL, *Lactiplantibacillus plantarum* 10^7 CFU/mL) on the physiological state and reproductive functions was studied in rats and their offsprings. Interestingly, long-term oral administration of the studied doses did not lead to a decrease in the reproductive function of laboratory animals during the experimental period (Skvortsov *et al*., 2021). However, further studies are warranted to comprehend such effects of different strains of probiotics in different animal species.

2.8. Safety assessment in diseased animal models

Since most potential probiotic strains are generally safe under healthy conditions, it is necessary to create diseased animal models that imitate the human pathophysiology and favor the probiotic bacteria to demonstrate the virulence properties. So far, several animal models have been used to assess the safety of probiotics. Amongst, experimental small animals *viz*. mice, rats, guinea pigs, rabbits, rabbit pups, and weaning piglets of various health statuses (healthy, endocarditis, pathogens infected, congenitally immunodeficient gnotobiotic, acute pancreatitis, induced immunocompromised) have been often reported in the literature (Adawi *et al*., 2002; Barba-Vidal *et al*., 2017; Bhat *et al*., 2020; Baloch *et al*., 2019; Copeland *et al*., 2008; Fernández-Murga and Sanz, 2016; Muftuoglu *et al*., 2006, Saleh *et al*., 2017). In relevance to the evidence of probiotics-mediated endocarditis and bacteremia in human subjects, two major experimental *in vivo* models, *viz*. experimental endocarditis and immunocompromised murine models, have been proposed by the EU-PROSAFE expert committee (Vankerckhoven *et al*., 2008). Since the vast majority of the probiotic applications are focused on improving gut health,

researchers have employed colitis-induced murine models to investigate probiotics' safety and efficacy (Pradhan *et al*., 2019b). Therefore, we aimed at elaborating experimental endocarditis, immunocompromised, and colitis models as below.

2.8.1. Immunocompromised model

An immunocompromised animal model mimics the physiology of immunocompromised humans. Immunosuppressive drugs *viz*. glucocorticoids, cytostatics, calcineurin inhibitors (cyclosporine A), etc., have been used for *in vivo* research (Diehl *et al*., 2017). Several of these drugs target to inhibit the proliferation of immune and non-immune cells. However, different doses of cyclophosphamide and cytostatics (azathioprine) have been most commonly used in creating an immunocompromized model in probiotic research. The immunosuppressive ability of such drugs depends on the type of animals, bodyweight of animals, dosage, route of administration, and time duration (Huyan *et al*., 2011; Saleh *et al*., 2017). Cyclophosphamide is an alkylating anti-tumor drug with cytotoxic and immunosuppressive effects by targeting B-cells and T-suppressor cells. Cytochrome P450 (CYP450) converts cyclophosphamide to 4-hydroxyphosphamide (Cy), which interconverts to another tautomeric form i.e., "aldophosphamide". These interconvertible tautomers can passively diffuse into target cells, wherein the aldophosphamide is converted to phosphoramide mustard, which exerts DNA-crosslinking properties. On the other hand, azathioprine acts as a purine analog and thus can interfere with DNA synthesis (Diehl *et al*., 2017). So far, little efforts have been made to study the safety of probiotics using this model. Accordingly, the safety of potential probiotic *Bacteroides uniformis* CECT 7771 was evaluated in this Cy-induced immunocompromised model and found safe (no bacterial translocation) upon their oral administration at 2×10^9 CFU/day/mice for six days. Moreover, *B. uniformis* CECT 7771 also downregulated gene and protein expression (*iNOS* and *PPAR-γ*) and inflammatory cytokines induced by immunosuppression (Fernández-Murga and Sanz, 2016). A study by Saleh *et al*. (2017) established the safety of orally administered probiotics in an azathioprine-induced immunosuppressed rabbit model. While evaluating the safety of *Bacillus* probiotic strains in immunocompromis mice, Cui *et al*. (2020) have challenged immunosuppressed mice with *B. cereus* 4 (an isolate for treating human diarrhea) to mimic immunodeficient patients or children. Infected mice without treatment all died with an inflammatory ededema on the submucosa and increased goblet cells in

the intestine. These results indicate that *Bacillus* probiotic isolates can produce multiple functional virulence factors. On the contrary, a recent probiotic safety study in immune-deficient mice demonstrated that *B. fragilis* HCK-B3 had been found immunologically safe in an acute toxicity study. Still, the authors did not evaluate the bacterial translocation to extra-intestinal organs (Tan *et al*., 2020).

2.8.2. Endocarditis model

Endocarditis is a rare disease characterized by severe infection and inflammation of the heart muscles and valves. It is classified as native valve endocarditis, prosthetic valve endocarditis , right-sided endocarditis, and device-related endocarditis. It has been suggested that creating this model would just replicate the pathophysiology of infective endocarditis in humans as three similar events occur in this model; (i) a preexisting valve lesion (induced by catheterization) become colonized during transient bacteremia (intravenous bacterial inoculation); (ii) bacterial persistence, colonization, and growth within the cardiac lesions; and (iii) dissemination of septic emboli to distant organs (Vankerckhoven *et al*., 2007). Extensive valve damage by surgical procedure and catheter-related model (a polyethylene catheter is introduced into the left ventricle through the aortic valve or introduced into the right ventricle through the tricuspid valve, followed by intravenous injection of bacteria, to produce a left-sided or right-sided endocarditis model) are the two fundamentally used methods to create endocarditis model (Wang *et al*., 2013). Nevertheless, the catheter-based model has been extensively used in probiotic research, and it has been found that lactobacilli isolates derived from bloodstream infections had tenfold lower infective dose (ID_{90}) (10^6 and 10^7 CFU) compared to the isolates from non-bloodstream sources (10^8 CFU) with inferior adhesion ability to cardiac vegetations (Vankerckhoven *et al*., 2007). In another study, *Lactiplantibacillus plantarum* 299v injected through intravenous route was not found in the major organs (no bacterial translocation) thus suggesting that *Lactiplantibacillus plantarum* 299v is safe in the endocarditis rat model (Adawi *et al*., 2002).

2.8.3. Colitis model

The colitis model simulates the pathophysiology of human colitis, where probiotics are widely recommended as biotherapeutic agents to ameliorate colitis. However, the safety of probiotics before the therapeutic application of probiotics is paramount since the intestine in colitis is characterized by epithelial hyper-permeability

(leaky gut) that may favor bacterial translocation (Cuffaro *et al*., 2020). Although probiotics resuscitate the pathological conditions of colitis by reinforcing epithelial barrier function, the collateral translocation of probiotic bacteria across the intestinal barrier is an event of concern. In such cases, careful examination of changes in the organ index, histopathology, feed intake, body weight, general animal behaviours, mortality (if any) is paramount in deducing a final decision (Pradhan *et al*., 2019b). Therefore, it is important to evaluate the safety of probiotics in the colitis model that are meant for futuristic applications as biotherapeutics to curb colitis. Dextran sulfate sodium and 2,4,6-trinitrobenzene sulfonic acid induced colitis mouse model are widely used in assessing the safety of probiotics *in vivo* (Daniel *et al*., 2006; Geier *et al*., 2007). Findings of such experiments were highly variable and showed strains specific effects in terms of betterment of gut health and translocation efficiency (de LeBlanc *et al*., 2016; Pavan *et al*., 2003; Pradhan *et al*., 2019b). These outcomes suggest the safety of probiotics under diseases or immunocompromised conditions is unclear and therefore necessitates precise and extensive biosafety characterization of all potential probiotic strains attributes both in healthy and diseased states, irrespective of their superior health beneficial attributes.

Overall, although probiotics are one of the fastest-growing areas of functional foods, the coaxial clinical reports underscoring the dark sides of probiotics that need to be addressed for every candidate strain. Most studies on probiotics are incomplete using their paucity in the comprehensive safety assessment. On the other hand, evidence on probiotics-mediated adverse effects in the vulnerable group of population necessitate the safety insights by short to long time exposure of probiotic strains using suitable animal models of differential health and immune status under the purview of regulatory guidelines. Hence, complete safety studies, including integrating *in vitro* and *in vivo* methods, generate sufficient safety data for clinical translation. Additionally, integration of genome-wide analysis of probiotic strains indicates the occurrence of safety-related genes and highlights the genome stability that alters over time due to various factors. Taken together, it is very clear from the above review that the all probiotic features are strain specific, and all the potential probiotic strains should be subjected for detailed safety evaluation before the clinical translation or studies in clinical milieu.

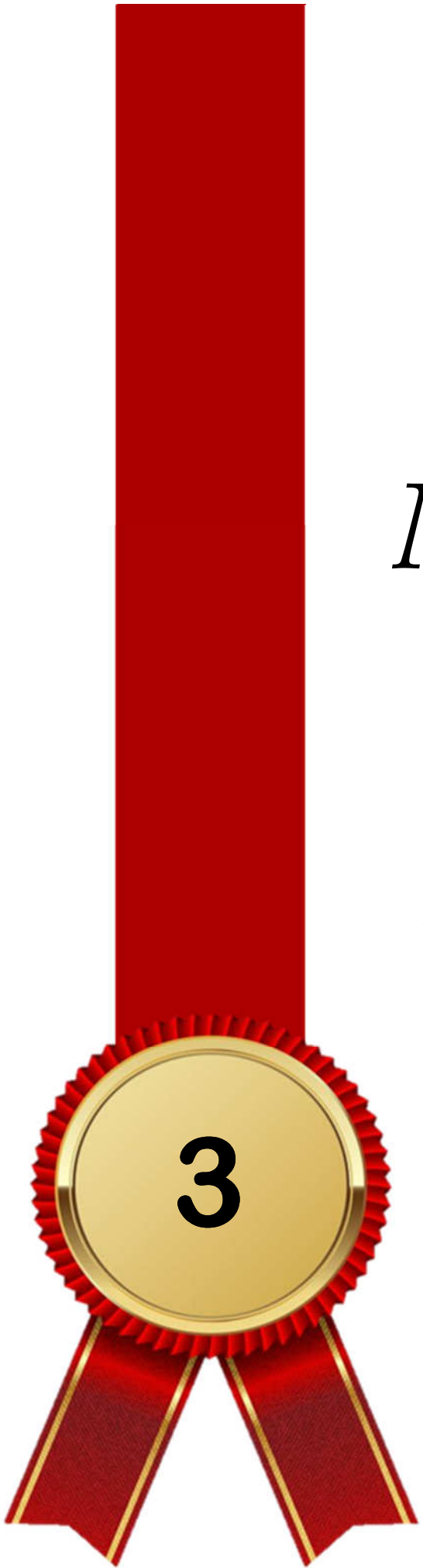

Materials & Methods

Objective 1

Assessment of *Limosilactobacillus fermentum* NCDC 400 for safety aspects using *in vitro* methods

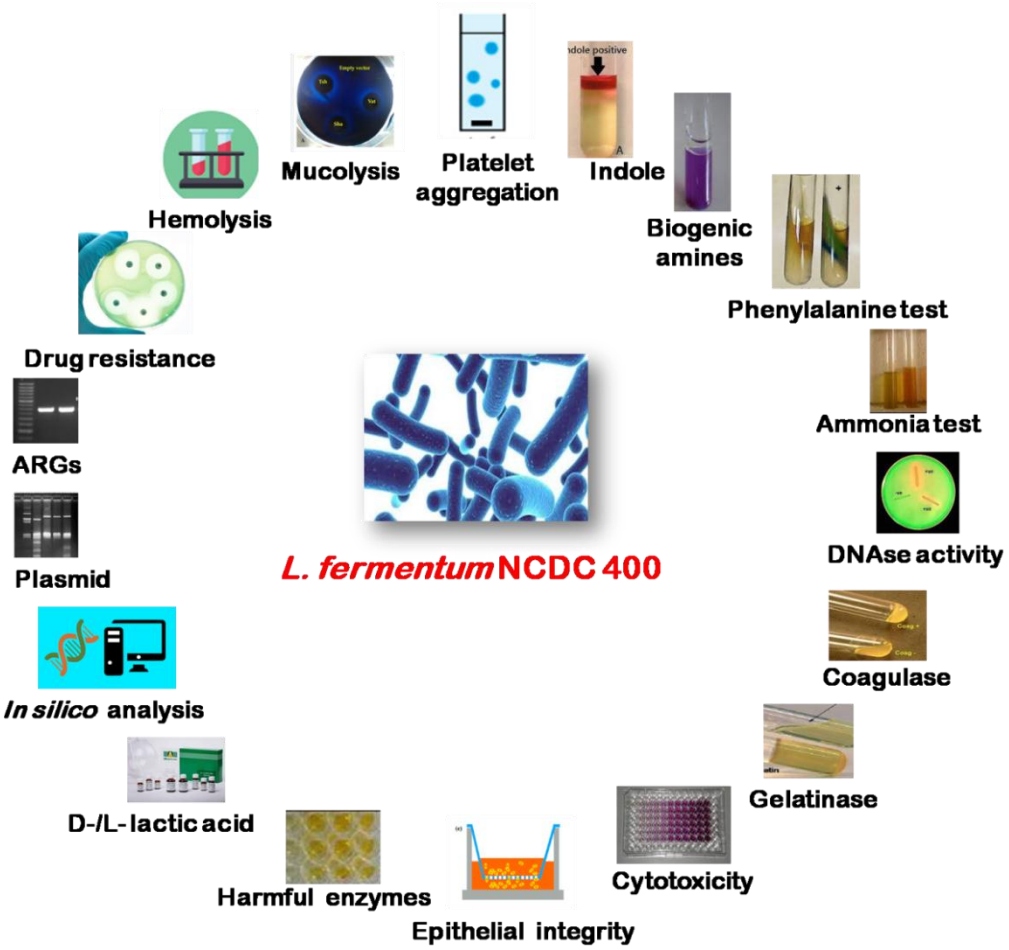

Fig. 3.1: Pictorial illustration on various *in vitro* and *in silico* assays used to investigate the bio-safety of *Limosilactobacillus fermentum* NCDC 400

3.1. Collection and reconfirmation of purity and identity *L. fermentum* NCDC 400 by polyphasic approach

3.1.1. Procurement, propagation, and purity assessment of the test strain

A freeze-dried ampoule of *L. fermentum* NCDC 400 was collected from the National Collection of Dairy Cultures (NCDC), Dairy Microbiology Division, ICAR-

National Dairy Research Institute, Haryana, Karnal. The obtained culture was activated in sterile deMan, Rogosa, and Sharpe (MRS) broth (HiMedia, India) by incubating at 37 ˚C/ 16-18 h. The active culture was subjected to a series of biochemical tests such as Gram's staining, negative staining, and catalase test as follows.

3.1.1.1. Microscopic examination

The morphology of NCDC 400 was examined by Gram's staining and negative staining using commercial kits (HiMedia, India) according to the manufacturers' guidelines.

3.1.1.2. Catalase test

A loopful of NCDC 400 was mixed with 3% hydrogen peroxide (H_2O_2) (Merck, Mumbai, India) on a clean and dry glass slide. The appearance of brisk effervescence was considered positive while its counterpart was considered negative for the test. Provided that the members of the genus *Limosilactobacillus* generally do not exhibit catalase activity, this test would aid in ascertaining the purity of the strain under investigation.

3.1.2. Procurement and propagation of other cultures used in the investigation

Several cultures were used as positive controls in various arrays through the research activities, and their source of procurement and propagation conditions are provided here. NCDC 167 (mixed *dahi* culture) was procured from the NCDC and activated in the M-17 broth (Himedia, India) at 30 ˚C/ 18 h. Similarly, other pathogenic cultures *viz*. *Staphylococcus aureus* NCDC 110, *Pseudomonas aeruginosa* NCDC 105, *Serratia marcescens* NCDC 108, *Proteus vulgaris* NCDC 73, *Bacillus cereus* NCDC 66, *Enterococcus faecalis* NCDC 114, and *Escherichia coli* NCDC 135 were procured from NCDC and were propagated in nutrient broth or Brain Heart Infusion (BHI) broth (Himedia, India) at 37 ˚C/ 18-24 h. On the other hand, *S. aureus* ATCC 25923 was received from the Bio-remediation and Synbiotic Functional Food Research Laboratory, Dairy Microbiology Division, ICAR-NDRI, Karnal and propagated in Brain Heart Infusion (BHI) broth at 37 ˚C/ 18-24 h. *Salmonella arizonae* ATCC 13314 was procured from the Rumen Biotechnology Laboratory, Animal Nutrition Division, ICAR-NDRI Karnal and propagated in Brain Heart Infusion (BHI) broth at 37 ˚C/ 18-24 h.

3.1.3. Reconfirmation of the identity of *L. fermentum* NCDC 400 by genotypic approaches

3.1.3.1. Extraction of genomic DNA from *L. fermentum* NCDC 400

The genomic DNA from NCDC 400 was extracted according to the method of Pospiech and Neumann (1995). Briefly, 1.5 mL active test culture was centrifuged at 6,000 rpm for 15 min to harvest the cell pellet. The cell pellet was washed using 1 mL sterile milli-Q water and the obtained cell pellet was suspended in 0.5 mL Sodium EDTA Tris (SET) buffer (pH 8.0) containing 5 mg/ mL of lysozyme (BIO BASIC CANADA INC., Canada). The cell suspension was incubated at 37 ˚C for 1 h with intermittent mixing. Fifty microliters of 10% SDS were added to the above cell suspension and incubated for 30 min at room temperature with intermittent mixing. Further, 200 µL of 5 M NaCl and 800 µL Phenol: Chloroform: Isoamyl alcohol mixture (25:24:1) (HiMedia, India) was added to the above solution and incubated for 30 min at room temperature with frequent intermittent mixing. The cell suspension was centrifuged at 4,500 rpm for 15 min and the top aqueous phase was transferred to 1.5 mL fresh microcentrifuge tube containing 500 µL of isopropanol. The above cell suspension was incubated at -20 ˚C overnight and centrifuged at 12,000 rpm for 15 min at 4 ˚C. The obtained pellet was washed with 100 µL of 70% ethanol and the traces of ethanol were removed by incubating at room temperature for 2 h. Thus obtained DNA was dissolved in 50 µL of Tris EDTA (TE) buffer (pH 8.0) and preserved at -20 ˚C. The extracted DNA was quantified and checked for its purity using Synergy H1 Multimode Reader (BioTeK, Winooski, VT).

3.1.3.2. Species-level identification of *L. fermentum* NCDC 400 by polymerase chain reaction (PCR) approach

The genomic DNA as well as the PCR reagents such as 2 X DreamTaqTM Green PCR Master mix (Thermo Scientific, Lithuania), nuclease-free water (Thermo Scientific, Lithuania), and a set of previously published (Dickson *et al.,* 2005) *Limosilactobacillus fermentum* specific forward primer: LF1 (5′-AATACCGCA TTACAACTTTG-3′) and reverse primer: LF2 (5′-GGTTAAATACCGTCAACGTA-3′) (custom synthesized by Eurofins Genomics, India) were thawed on ice. Initially, a standard mixture of master mix, primers, and nuclease-free water was added to the microcentrifuge tube (**Table 3.1**) and mixed well by a short spinning. Eleven microliters of the master mix were carefully

transferred to the 200 µL PCR tubes containing 1 µL template DNA. Thereafter, the samples were vortexed and transferred to PCR Thermal cycler heating blocks (BIO-RAD S1000^{TM} thermal cycler). The PCR steps were carried out at specific conditions of the aforesaid primers as displayed in **Table 3.2.**

Table 3.1: Reagents used in the PCR-based identification of *L. fermentum* NCDC 400

Reagents	Volume (µL)	Concentration
Green PCR Master mix	6.25	2 X
Forward primer	0.5	0.05-1 µM
Reverse primer	0.5	0.05-1 µM
Template DNA	1	100 ng/ µL
Nuclease free water	4.25	-
Total	12.5	-

Table 3.2: PCR cycling steps for species-level identification of *L. fermentum* NCDC 400

PCR steps	Conditions
Initial denaturation	94˚C/ 5 min
Final denaturation	94˚C/ 1 min
Annealing	50˚C/ 1 min
Extension	72˚C/ 1 min
Final extension	72˚C/ 10 min
No. of cycles	30

3.1.3.3. Molecular typing of *L. fermentum* NCDC 400

Random Amplified Polymorphic DNA (RAPD) PCR was used to establish the strain level identity of *L. fermentum* NCDC 400. The template DNA was independently amplified with four arbitrary primers such as OPA5 (5′-AATCGGGCTG-3′), M-13 (5′-GAGGGTGGCGGT TCT-3′), OPA18 (5′-AGGTGACCGT-3′), and OPA20 (5′-GAGGGTGGCGGTTCT-3′) synthesized by Eurofins Genomics, India (Jarocki *et al*.,

2020). The standard PCR mix was prepared by mixing the PCR reagents like 2 X DreamTaqTM Green PCR Master mix (Thermo Scientific, Lithuania), nuclease-free water (Thermo Scientific, Lithuania), and a single arbitrary primer (**Table 3.3**). The obtained mix was vortexed and transferred to the PCR tube containing 1 µL template DNA. The samples were mixed and transferred to a PCR Thermal cycler (BIO-RAD S1000^{TM} thermal cycler). The PCR steps were carried out at specific conditions according to the time and temperature stringency of the different primers (**Table 3.4)**. The obtained PCR amplicons were separated on the 1.5% agarose gel and stained with EtBr to generate a bacterial fingerprint.

Table 3.3: Reagents used in RAPD-PCR for molecular typing of *L. fermentum* NCDC 400

Reagents	Volume (µL)	Concentration
Green PCR Master mix	7	2 X
Primer	2.5	0.05-1 µM
Template DNA	1	100 ng/ µL
Nuclease free water	2	-
Total	12.5	-

Table 3.4: PCR cycling steps for generating RAPD fingerprint of *L. fermentum* NCDC 400

Steps	Temperature/ time conditions			
	OPA5	**M13**	**OPA18**	**OPA20**
Initial denaturation	94˚C/ 5 min	95˚C/ 7 min	95˚C/ 7 min	95˚C/ 7 min
Final denaturation	94˚C/ 1 min	95˚C/ 30 sec	95˚C/ 30 sec	95˚C/ 30 sec
Annealing	39˚C/ 1 min	35˚C/ 30 sec	33˚C/ 30 sec	40˚C/ 30 sec
Extension	72˚C/ 2 min	72˚C/ 4 min	72˚C/ 4 min	72˚C/ 4 min
Final extension	72˚C/ 10 min	72˚C/ 10 min	72˚C/ 10 min	72˚C/ 10 min
No. of cycles	34	40	40	40

3.2. Plasmid profiling of *L. fermentum* NCDC 400

The plasmid DNA from *L. fermentum* NCDC 400 was extracted and purified using ZR Plasmid Miniprep-Classic Kit (ZR plasmid MiniPrep-Classic, Irvine, USA) with slight modifications. In brief, 1.5 mL of bacterial culture was centrifuged at 6,000 rpm for 10 min. The supernatant was discarded and the cell pellet was suspended in 200 µL of P1 Buffer containing 5 mg/ mL lysozyme. Further, 200 µL of P2 Buffer was added and mixed by vortexing the tubes to lyse the cells. After 2 min, 400 µL of P3 Buffer was transferred to the above cell suspension and mixed thoroughly to neutralize completely (yellow color). Further, the suspension was incubated at room temperature for 1-2 min for complete lysis. The samples were then centrifuged for 2 min and the supernatant was transferred to Zymo-Spin™ IIN column in a collection tube. The Zymo-Spin™ IIN/ Collection Tube assembly was centrifuged for 30 sec and the flow-through in the collection tube was discarded. Exactly 200 µL of Endo-Wash Buffer was added to the column and centrifuged for 30 sec. Further, 400 µL Plasmid Wash Buffer was added to the column and centrifuged for 1 min. Finally, the column was transferred to a clean microcentrifuge tube and plasmid DNA was eluted with 30 µL DNA Elution by subjecting to the centrifugation process for 30 sec. The obtained plasmid DNA was stored at -20˚C. The plasmid DNA was confirmed by conducting agarose electrophoresis using 1% agarose gel stained with ETBr.

3.3. Characterization of NCDC 400 for the possible virulence determinants using *in vitro* approaches

3.3.1. Hemolytic activity

3.3.1.1. Blood agar method

Briefly, an active culture of NCDC 400 was streaked on the blood agar base (HiMedia, India) supplemented with 5% human blood. After incubation at 37˚C for 16-18 h, the plates were observed for a clear zone around the streaked area for the positive reaction (beta hemolysis). *Staphylococcus aureus* NCDC 110 was used as a positive control.

3.3.1.2. Spectrophotometric method

The method for spectrophotometric-based assessment of hemolytic activity of NCDC 400 was adopted from Deng *et al*. (2021). Accordingly, 10 mL of human blood

was collected in EDTA-coated tubes and centrifuged at 3,000 rpm for 10 min. The blood plasma was discarded and RBC was washed twice in PBS (pH 7.4). The suspension of 8% (v/v) RBC was then prepared by suspending RBC in PBS (pH 7.4). An aliquot of 0.5 mL of 8% RBC suspension and 0.5 mL overnight grown bacterial cell-free supernatant was mixed in a microcentrifuge tube and incubated at 37˚C for 0, 2, 4, 6, and 8 h. This mixture was then centrifuged at 3,000 rpm for 10 min at 4˚C to collect the supernatant. The obtained supernatant was used to determine the optical density (OD) spectrophotometrically (Epoch microplate reader, China) at 576 nm to measure the hemoglobin released as a function of RBC lysis. During this experimentation, 1% (v/v) Triton X (HiMedia, India) was used as positive control while 4% RBC suspension was used as a negative control. On the other side, the entire assay was also repeated with a known beta-hemolytic *Staphylococcus aureus* NCDC 110. Finally, the percentage of hemolysis was determined using the following equation.

$$\%\ Hemolytic\ activity = \frac{OD_{sample} - OD_{negative\ control}}{OD_{positive\ control} - OD_{negative\ control}} \times 100$$

3.3.1.3. RBC staining

The hemolytic activity of the test culture was investigated by visualizing the morphology of erythrocytes upon Giemsa staining according to Dey *et al*. (2019). Briefly, 10 µL of the RBC cell suspension exposed to the cell-free suspension of test culture for different time intervals was made into a thin smear on a clean and dry glass slide. The prepared smear was air-dried and fixed with 70% (v/v) ethanol for 5 min. The smear was stained with 1 X Giemsa stain (NICE Chemicals Pvt. Ltd., India) for 20-30 min. The excess dye was removed by rinsing the glass slides with distilled water. Finally, the changes in the morphology and membrane integrity of RBC were visualized under an oil immersion objective of an inverted microscope (Radical Scientific, India).

3.3.2. DNase activity

Six-millimeter wells were punched on the sterile solidified DNase agar supplemented with 0.1% Toluidine Blue (HiMedia, India). Exactly 200 µL cell-free supernatant obtained from active test culture as well as a positive control (*S. aureus* ATCC 25923) was transferred into the wells and incubated at 37˚C for 18-24 h. The appearance of pink color with a halo zone around the wells was considered positive for the test.

3.3.3. Coagulase test

Approximately 15 mL of blood was drawn into EDTA-treated tubes from a healthy adult in the Dr. Lal Path's laboratory, Karnal, Haryana. The blood samples were immediately brought to the laboratory under ice-cold conditions and subjected to centrifugation at 2,000 x *g* for 10 min at 4˚C to separate plasma. Further, 1 mL of plasma was inoculated with the 2% active test culture as well as *S. aureus* ATCC 25923 (positive control) and incubated at 37˚C for 4 h. Finally, the tubes were examined for plasma coagulation every 30 min interval. The presence of clots within 4 h was considered coagulase positive.

3.3.4. Ammonia production test

The ammonia production by the test culture was performed according to the previously described indophenol reaction method of Kim *et al*. (2018). Briefly, NCDC 400 as well as *Pseudomonas* spp. NCDC 105 (positive control) was independently cultured in Brain Heart Infusion (BHI) broth (HiMedia, India) at 37˚C for 5 days. The cell suspension was centrifuged at 10,000 rpm for 30 min at 4˚C. The supernatant was collected and the pH of the medium was adjusted to 7 using 1 N NaOH. Further, 10 µL solution 1 (2 g phenol and 0.01 g sodium nitroferricyanide dehydrate dissolved in 200 mL distilled water) and 10 µL solution 2 (1 g NaOH and 0.08 g sodium hypochlorite (NaClO) dissolved in 200 mL distilled water) were added to 96 well plates with the subsequent addition of 100 µL pH neutralized cell-free supernatant. The plate was incubated at room temperature for 1 h and the absorbance was noted at 625 nm. The absorbance value derived from the only BHI medium was used as a negative control. Finally, the results are interpreted using the standard curve developed using different concentrations of ammonia **(Annexure I)**.

3.3.5. Gelatin liquefaction assay

Overnight grown active test culture was inoculated (2%) into the sterile nutrient broth (HiMedia, India) tubes supplemented with 5% of gelatin. The tubes were incubated at 37˚C/ 48 h and further transferred to a refrigerator (4 ˚C) for 4 h. The solidification of the gelatin tubes after refrigerated storage was considered gelatinase negative while its counterpart was considered negative. The various pathogenic cultures such as *Serratia* spp. NCDC 108, *Pseudomonas* spp. NCDC 105, *Proteus vulgaris* NCDC 73, and *Bacillus cereus* NCDC 66 were used as positive control (Kang *et al*., 2019).

3.3.6. Urease test

The activity of urease was determined according to Kang *et al*. (2019) by stabbing the test culture into Christensen Urea Agar (HiMedia, India) slants supplemented with 20% (w/v) urea. The slants were incubated at 37 ˚C for 18-24 h and observed for a color change from yellow to deep pink for a positive reaction. The community-type microflora isolated from human fecal matter as well as *Proteus vulgaris* NCDC 73 was used as the positive control.

3.3.7. Indole test

The indole production was determined by culturing the test bacterium in tryptophan media (Kang *et al*., 2019). Briefly, 2% active culture of NCDC 400, as well as *E. coli* NCDC 134 (positive control), were inoculated into sterile tryptophan media (HiMedia, India) and subsequently incubated at 37 ˚C for 18-24 h. After said incubation, 1-2 drops of Kovac's reagent (HiMedia, India) were added to the media, and the appearance of a red ring on the top of the medium was considered positive for the indole test.

3.3.8. Phenylalanine degradation test

The phenylalanine degradation ability of the test culture was evaluated on phenylalanine slant agar (0.5% NaCl, 0.3% yeast extract, 0.2% DL-phenylalanine, 0.1% Na_2HPO_4, 1.0% agar-agar) (Kang *et al*., 2019). Initially, the NCDC 400 strain was subcultured twice in MRS broth supplemented with 0.2% (w/v) DL-phenylalanine (HiMedia, India). The obtained strain was streaked on phenylalanine slant agar and incubated at 37 ˚C/ 18-24 h. Further, 3-5 drops of 10% (w/v) ferric chloride was dropped on the slant to observe a color change to green within 1 to 5 min for a positive reaction. *Proteus vulgaris* NCDC 73 was used as a positive control.

3.3.9. Harmful intestinal enzymes assay

The activities of harmful intestinal enzymes such as beta-glucosidase and beta-glucuronidase were determined by the color change upon reaction with specific substrates (Kim *et al*., 2019). Briefly, the test culture (NCDC 400), as well as positive controls (community-type faecal flora and *E. coli*), were concentrated by centrifugation (5,000 rpm/ 10 min), suspended in PBS (pH 7.4) and the OD_{600} was adjusted to 2.0. Further, 100 µL of 0.1 M p-nitrophenyl-β-D-glucopyranoside (for β-glucosidase activity) (HiMedia, India) and 0.1 M p-nitrophenyl-β-D-glucuronide (Sigma, St. Louis, USA) (for

β-glucuronidase activity) were added to an equal volume of bacterial cell suspension in 96-well plate and incubated at 37 ˚C for 16 h. The appearance of yellow color was considered positive for the reaction.

3.3.10. D-/ L- lactic acid production test

The production of D-/ L- lactic acid by NCDC 400 was quantified using the D-/ L-Lactic acid assay kit (Megazyme, Wicklow, Ireland). Briefly, the cell-free supernatant derived from an overnight cultured NCDC 400 was used to assay the lactic acid production. The different reagents as well as samples were mixed in a cuvette as presented in **Table 3.5.**

Table 3.5: Details of reagents used in quantification of D-/ L- lactic acid from NCDC 400

Sample/ Reagent	Blank	Sample	Sample/ Reagent	Blank	Sample
D-lactic acid			**L-lactic acid**		
Distilled water	1.60 mL	1.5 mL	Distilled water	1.60 mL	1.5 mL
Sample	-	0.10 mL	Sample	-	0.10 mL
Solution 1 (Buffer)	0.50 mL	0.5 mL	Solution 1 (Buffer)	0.50 mL	0.5 mL
Solution 2 (NAD^+)	0.10 mL	0.10 mL	Solution 2 (NAD^+)	0.10 mL	0.10 mL
Suspension 3 (D-GPT)	0.02 mL	0.02 mL	Suspension 3 (D-GPT)	0.02 mL	0.02 mL
The mixture was mixed and the absorbance (A_1) after 3 min was noted at 340 nm					
Suspension 5 (D-LDH)	0.02 mL	0.02 mL	Suspension 4 (L-LDH)	0.02 mL	0.02 mL
After the addition of suspension 5, the content was mixed and the absorbance (A_2) was measured after 5 min at 340 nm					

After the sequential addition of sample, solution 1 (buffer), solution 2 (NAD^+), and suspension 3 (D-GPT), the entire suspension was mixed and the absorbance "A_1" after 3 min was noted at 340 nm. Further, suspension 4 and suspension 5 were added to

the cuvettes to quantify the L- and D-lactic acid, respectively. After the addition of suspension 5 or 4, the entire content was mixed and the absorbance (A_2) was measured after 5 min at 340 nm. Finally, the concentration of D-/L-lactic acid is determined using the following equation.

$$c = \left(\frac{V \times MW}{\in \times d \times v}\right) \times \Delta A$$

Where,

c = Concentration of D-/ L-lactic acid (g/L)

V = Final volume (mL) [2.26]

MW = Molecular weight of D-/ L- lactic acid (g/ mol) [90.1]

ε = Extinction co-efficient of NADH at 340 nm [6300]

d = Light path (cm) [1]

v = sample volume (mL) [1]

ΔA = A_2-A_1

3.3.11. Determination of human serum resistance

The ability of NCDC 400 to dwell in the blood serum was tested by the pour plating method (Vesterlund *et al*., 2007). At the outset, 20 mL of human blood was collected from the healthy adult donor and allowed to clot. The serum was separated from the blood by centrifuging at 2,500 rpm/ 5 min. The sterility of the serum was checked by plating method using nutrient agar. Further, 5 mL active culture of NCDC 400 was centrifuged and the supernatant was discarded. The cell pellet was washed twice with PBS (pH 7.4) and re-suspended in the same volume of serum. The bacterial count was checked immediately at 0 h by the pour-plating method (MRS agar). The serum suspension containing the bacterial cells was incubated at 37˚C for 3 h. The reaction was stopped by incubating on ice for 10 min. After said incubation, 1 mL of the suspension was further plated on MRS agar to determine the bacterial survivability. On the other hand, brain heart infusion (BHI) agar (HiMedia, India) was used to enumerate the faecal flora (positive control).

3.3.12. Platelet aggregation test

The method of Huang *et al*. (2016) was used to determine the platelet aggregation ability of NCDC 400. In brief, the blood samples were drawn into the EDTA tubes as

detailed under 3.3.3 and immediately processed for plasma separation by subjecting to centrifugation at 200 ×g for 10 min at 4˚C. The initial platelet count (PC) in the plasma was determined using a blood analyzer (Byovet, Smart-3Dx, Vet-Hematology analyzer, UK, Model No. CONU CELL 23 Excel). The obtained platelet-rich plasma (PRP) (3.81×10^{11}/ L) (0.5 mL) was treated with 10^8 CFU/ mL NCDC 400, collagen (1.0 mg/ mL) (Sigma-Aldrich, USA) as a positive control, only PRP (negative control) and incubated at 37 °C for 15 min. Finally, the number of platelets in the topmost layer of the suspension was performed by blood analyzer and the percentage of platelet aggregation was calculated using the following equation;

$$\%\, Platelet\ aggregation = \frac{PC_{negative\ control} - PC_{sample}}{PC_{negative\ control}} \times 100$$

3.3.13. Biogenic amines production test

3.3.13.1. Colourimetric assay

The formation of biogenic amines by the test culture was investigated by qualitative approaches. Briefly, NCDC 400 was sub-cultured four times in the MRS broth supplemented with 0.005% pyridoxal-5-phosphate and 0.1% of individual amino acids (histidine, tyrosine, lysine, and arginine, HiMedia, India). To further evaluate the biogenic amine production by colorimetric method (qualitative method), the test culture (NCDC 400) as well as positive controls *viz*. *Salmonella arizonae*, fecal flora, and *Enterococcus faecalis* NCDC 114 were streaked onto the decarboxylase agar plates supplemented with different precursor amino acids and incubated at 37°C for 48 h. Similarly, the test culture was inoculated (2%) to Moeller decarboxylase broth (HiMedia, India) and incubated at 37°C for 48 h to measure the change in the pH and color (pale yellow to purple) due to the formation of respective biogenic amines that are alkaline in nature.

3.3.13.2. High-performance liquid chromatography (HPLC) analysis

The sample preparation and quantification of biogenic amines through HPLC were performed according to the method of Kim *et al*. (2018) and Singracha *et al*. (2017). Accordingly, the NCDC 400 was repetitively sub-cultured four times in the MRS broth supplemented with 0.005% pyridoxal-5-phosphate and 0.1% precursor amino acids (histidine, tyrosine, lysine, arginine, HiMedia, India) for overnight. Further, 5 mL of cell-free culture supernatant collected by centrifuging at 6,000 rpm for 10 min, was mixed by

vortexing with 25 mL of 0.1 N HCl for 5 min. The mixture was centrifuged at 10,000 rpm for 15 min at 4˚C and the aqueous layer was collected. The residue was re-extracted one more time and filtered with Whatman No. 4 filter paper. One mL of the above filtrate, 500 µL saturated sodium carbonate, and 1 mL of dabsyl chloride (Supelco, Bellefonte, PA, USA) in acetone (10 mg/ mL) were transferred to a screw-capped glass tube and mixed by proper vortexing. This mixture was incubated at 70˚C for 30 min in a hot bath and the excess dabsyl chloride was precipitated by adding 100 µL of 30% ammonium hydroxide. The supernatant was adjusted to 5 mL with acetonitrile and filtered through 0.45 µm membrane filter before HPLC analysis. The samples were stored at -20˚C until analysis. Finally, the HPLC analysis of the biogenic amines was performed as described in **Table 3.6.** Finally, the obtained peaks and their retention time have been compared with the standards (1 mg/ mL) such as tyramine, putrescine, and cadaverine (Sigma Aldrich, USA).

Table 3.6: Details of HPLC conditions used for quantification of biogenic amines

Parameters	**Conditions**		
HPLC	RP-HPLC-UV/VIS (Shimadzu Corporation, Japan)		
Column	Ascentis® C18 column (5 µL, 250 × 46 mm, 100˚A, Supelco, Bellefonte, Pa., USA)		
Mobile solvent	**Time (min)**	**HPLC water (%)**	**Acetonitrile (%)**
	0	40	60
	1	40	60
	20	0	100
	25	0	100
	26	40	60
	30	40	60
Flow rate	0.8 mL		
Column temperature	30˚C		
Injection volume	20 µL		
Detector	UV 250 nm		

3.3.14. Mucin degradation test

The mucin degradation ability of the test strain (NCDC 400), in contrast to fecal flora (positive control), was evaluated by four different methods such as growth in mucin-containing liquid medium (spectrophotometric method), SDS-PAGE analysis, mucin degradation assay in Petri dish, and Attenuated Total Reflectance-Fourier-Transform Infrared (ATR-FTIR) spectroscopy analysis of mucin according to Abe *et al*. (2010).

3.3.14.1. Spectrophotometric method

Overnight cultured NCDC 400 was inoculated (2%) into 10 mL of basal medium (devoid of carbon source) composed of 0.5% Peptone, 0.5% Trypticase Peptone, 1% yeast extract, 0.05% L-cysteine-HCl, 4 mL of mineral solution-A (0.78% K_2HPO_4 solution) and 4 mL of mineral solution-B (0.47% KH_2PO_4, 1.18% NaCl, 1.2%. $(NH_4)_2CO_4$, 0.12% $CaCl_2$, 0.25% $MgSO_4.H_2O$) supplemented with 0.5 and 1.0% porcine mucin (Type II, Sigma Aldrich, USA) with or without glucose (0.5 and 1.0%). After following an incubation period of 48 h at 37˚C, the bacterial growth was determined spectrophotometrically by recording the absorbance at 600 nm.

3.3.14.2. Mucin degradation assay in Petri dish

The solidified agar plates were prepared by supplementing the basal medium with agar-agar (2%) as well as mucin (0.5 and 1.0%) and glucose (1%). Further, 10 µL of the test culture was spotted on the agar surface and the plates were incubated at 37˚C/ 48 h. Subsequently, the plates were stained with 0.1% amido black (HiMedia, India) prepared in 3.5 M acetic acid for 30 min, and the excess dye was washed with 1.2 M acetic acid. The presence of discoloration around the colony was considered positive for mucolytic properties.

3.3.14.3. ATR-FTIR spectroscopy

The test strain was incubated in a basal medium supplemented with 1% mucin. After incubation at 37˚C for 16 h, the medium was centrifuged (10,000 × *g*; 30 min; 4 ºC) and the supernatant fluid was collected and precipitated repetitively with chilled ethanol (1.5 times of supernatant). Thus obtained pellet was freeze-dried and subjected to FTIR analysis using a scanning range of 400-4000 cm^{-1} at a resolution of 4 cm^{-1} (ATR–FTIR, IRAffinity, Shimadzu, Japan). The spectra of a freeze-dried sample of basal medium supplemented with 1% mucin (without bacterial inoculation) as well as only

porcine mucin were used to compare the spectral differences that occur due to mucolytic activity of test strain (if any).

3.3.14.4. SDS-PAGE analysis

The mucolytic activity of the test strain was profiled by following the Laemmli SDS-PAGE technique (He, 2011). The test strain was inoculated into 10 mL basal medium (supplemented with 1% mucin) and incubated at 37˚C for 16 h. After said incubation, the medium was centrifuged (10,000 × *g*; 30 min; 4 ºC) and the obtained supernatant was collected and precipitated repetitively with chilled ethanol (1.5 times of supernatant). Thus obtained pellet was suspended in the 0.5 mL of 10 mM Tris-HCl and mixed with an equal amount of loading dye (mixture of 0.1% bromophenol blue and beta-mercaptoethanol; 475:25 µL), and heated in boiling water bath for 5-10 min. The heated samples were subjected to a short spin to remove the insoluble debris and the 10 µL clear sample was separated on 4% stacking and 10% separating gel with an aid of electrophoresis at 90 V. After electrophoresis, the gel was stained using silver staining protocol as reported elsewhere (Wray *et al*., 1981). In order to further clarify the mucin-degrading ability of NCDC 400, the Periodic acid-Schiff (PAS) staining of gel, a method used to identify the glycoproteins, was also performed. Briefly, the gel fixed with 12.5% trichloroacetic acid (TCA) for 1 h was immediately exposed to 1% periodic acid for 2 h. The gel was washed with 15% acetic acid for 2 h and placed in the Schiff reagent for 2 h at 4 ˚C. Finally, the gel was destained three times with 7% and 15% over 24 h. The obtained gel was scanned using the 2 D gel documentation system (Epson Scanner; Proteomics images and spot picker, M/S GE Health care bioscience Pvt Ltd., New Delhi).

3.3.15. Evaluation of *in vitro* adhesion and cytotoxicity of NCDC 400 on eukaryotic cell line

3.3.15.1. Procurement and propagation of Caco-2 cells

The human colon carcinoma Caco-2 cells (P-35) exhibiting distinctive features of gut enterocytes were procured from the National Centre for Cell Sciences (NCCS), Pune, India. The cells were cultured in Dulbecco's Modified Eagle Medium (DMEM) (Sigma, USA) supplemented with Fetal Bovine Serum (FBS; 10% v/v), sodium carbonate (2% v/v), L-Glutamine (2 mmol/ L), and antibiotics (Penicillin, 100 U/ mL; Streptomycin, 30 µg/ mL; and Amphotericin, B-25 µg/ mL) (HiMedia, India) in a 25 cm^2 (T-25) tissue-

culture flask (Tarsons, Korea). The cells were incubated in a 5% CO_2 incubator (HealForce, China) maintained at 37 °C in a humidified atmosphere. The spent medium was replaced every alternative day with a fresh medium. The cells were routinely maintained in a fresh T-25 flask using DMEM and the cells were trypsinized when they reach 50-60% confluency.

3.3.15.2. Evaluation of adhesion of NCDC 400 on Caco-2 cells and mucin surface

Caco-2 cells were seeded (~1 x 10^5 cells/ well) in 6 well tissue culture plates and allowed to form a confluent monolayer (80-90% confluency) by incubating at 37 °C for 15 days in 5% CO_2 incubator. The spent medium was replaced with antibiotic-free DMEM one day before the experiment. Before the start of the experiment, the spent medium was removed and the cells were washed twice with PBS (pH 7.4). Similarly, 1 mL of filter-sterilized 1% (w/v) porcine gastric mucin-type III (Sigma, USA) solution, prepared by suspending in PBS (pH 7.4) at 4ºC for 2 h with intermittent mixing, was transferred to the 6 well tissue culture plate (Thermo Fisher Scientific, China) and incubated overnight at 4ºC. Thereafter, the plates were rinsed twice with 1 mL of PBS to remove the unbound mucin. The unevenness on the mucin surface was blocked by incubating with 1mL of 2% BSA (Sigma, USA) at 4 ºC for 4 h. The unbound fractions of BSA were removed by washing twice with 500 µL of PBS. The Caco-2 cells and mucin-coated wells were incubated with 1 mL of NCDC 400 cells (2.5×10^9) [prepared by washing and dissolving the cell pellet in PBS (pH 7.4)] at 37ºC for 4 h. After the specified incubation, the unbound fractions were removed by washing twice with PBS (pH 7.4). The adhered cells were recovered by treating the cells with 1 mL triton-X-100 (0.5% v/v). The bound cells were quantified by plating using MRS agar. The results were expressed as % relative adhesion using the following equation.

$$\%\ Relative\ adhesion = \frac{CFU/mL\ after\ adhesion}{CFU/ml\ before\ adhesion} \times 100$$

3.3.15.3. MTT assay

MTT dye reduction was performed to check the effect of test bacteria on cellular viability by considering that viable cells metabolize tetrazolium colorless salt to blue formazan crystals in mitochondria (Bhat *et al.*, 2019a). Caco-2 cells were seeded at 1×10^5 concentrations into each well of the 96-well plate. The plate was incubated at 37°C for 24 h in a CO_2 incubator for cell attachment. Different concentrations of NCDC 400

(10^8-10^{11} CFU/ mL) solubilized in DMEM were added to the wells in triplicates (0.1 mL/ well) and incubated for 24 h. While the cells treated with only DMEM served as control. Later, the spent media was removed and the cells were gently washed with PBS (pH 7.4). Exactly, 90 µL of DMEM media and 10 µL of MTT dye (5 mg/ mL) (HiMedia, India) was added to each well and the plate was gently shaken and incubated for 3 h at 37°C. After incubation, 70 µL of supernatant was removed and 100 µL of dimethyl sulphoxide (SRL Pvt. Ltd., Mumbai, India) was added to each well in order to solubilize the formazan crystals. Finally, the absorbance was measured at 570 nm and the cell viability was calculated using the following equation.

$$\%\, Viability = \frac{Test\ OD}{Control\ OD} \times 100$$

3.3.15.4. Neutral red assay

The neutral red uptake assay was performed to evaluate the cellular viability by considering that viable cells accumulate neutral red dye in the lysosomes (Bhat *et al*., 2019a). The seeding of cells into the 96-wells and the treatment of test compounds for 24 h were performed as described in section **3.3.15**.2. After rinsing of Caca-2 cells with PBS (pH 7.4), the cells were treated with 200 µL of cell culture grade neutral red dye (0.4% w/v) (Sigma, St. Louis, USA) and incubated at 37°C for 3 h. The internalized dye was removed by adding 200 µL wash solution (a mixture of 7.5 mL milli-Q water, 7.5 mL absolute alcohol, and 150 µL acetic acid) to each well and incubated at 37°C for 30 min. Optical density was determined with a microplate reader using an absorption spectrum at 540 nm as previously described by Bhat *et al*. (2019a). The viability of cells was estimated using the following equation.

$$\%\, Viability = \frac{Test\ OD}{Control\ OD} \times 100$$

3.3.15.5. Trypan blue exclusion assay

Caco-2 cells were seeded into each well of 6-well tissue culture plate (cell density; 1×10^5) and incubated at 37 °C overnight for cellular attachment to plate. The preparation and exposure of the test culture to the Caco-2 cells are provided in the previous section (**3.3.15.2**). The spent media as well as the test bacterial debris

were aspirated and the cells were washed twice with PBS (pH 7.4). Therefrom, the Caco-2 cells attached to the plate surface were detached by trypsin digestion. The devastating effect of trypsin treatment on the Caco-2 cells was neutralized by adding DMEM media (1 mL/ well). An aliquot of 100 µL cell mixture was mixed with 100 µL of trypan blue (0.4% v/v) (HiMedia, India) in a microcentrifuge tube. Later, 10 µL of the aforementioned mixture was loaded onto a Neubauer's chamber and examined with 10 X objective of an inverted microscope. The live/ viable (colorless) and dead (blue color) cells were counted and the percentage viability of cells was computed using the following equation.

$$\%\, Viability = \frac{Number\ of\ viable\ cells}{Total\ number\ of\ cells} \times 100$$

3.3.16. Effect of NCDC 400 on cellular barrier integrity of Caco-2 cells

3.3.16.1. Culturing Caco-2 cells on transwell plate and measurement of monolayer integrity

Caco-2 cells (1 x 10^6 cells) suspended in DMEM were added (500 µL) to an apical chamber of the 24-well polystyrene transwell plate (Corning Costar, USA) and 1 mL growth medium was supplemented to the basal chamber of the transwell plate. The cells were allowed to proliferate by incubating at 37 °C for 15 - 20 days in a 5% CO_2 incubator. The spent medium was aspirated every alternate day and supplemented with the fresh medium until a confluent and completely polarized monolayer of Caco-2 cells was attained. After ensuring a near complete confluence (visualization through an inverted microscope) of Caco-2 cells on the apical chamber, the integrity of the cell monolayer was tested by phenol red dye diffusion assay. In brief, after rinsing both the apical and basal chamber with PBS (pH 7.4), an aliquot of 250 µL DMEM with phenol red was added to the apical chamber while the same volume of DMEM without phenol red was added to the basal chamber. Finally, the plate was incubated at 37 °C for 1 h in a CO_2 incubator and exactly 100 µL medium from the apical and basal chambers was pipette out to measure the absorbance spectrophotometrically at 558 nm. The % phenol red transflux across the Caco-2 monolayer was calculated using the following equation:

$$Transflux\ (\%) = \frac{Absorbance\ of\ basal\ chamber}{Absorbance\ of\ apical\ chamber} \times 100$$

3.3.16.2. Evaluation of the effect of NCDC 400 on transwell permeability of Caco-2 cells

The transwell inserts with less than 2% transflux (Sowmya *et al*., 2019) were exposed to different concentrations of test culture suspended in antibiotic-free DMEM (10^8-10^{11} CFU/ mL) and the plates were incubated at 37˚C for 24 h (5% CO_2, 90% humidity). The cells treated with *E. coli* NCDC 135 (10^8 CFU/ mL) served as positive cells while the cell treated only with DMEM served as the negative control. The basal chamber was filled with 1 mL DMEM (antibiotic-free). After said incubation, the spent medium was removed from apical and basal chambers and the monolayer was rinsed gently with PBS and subjected to phenol red diffusion across the Caco-2 monolayer as described in the preceding section **3.3.16.1**.

3.3.17. Antibiotic resistance profiling of NCDC 400

3.3.17.1. Antibiotic susceptibility test

The phenotypic resistance to different antibiotics was tested by antibiotic susceptibility test (AST) by following the protocol of disc diffusion assay as given by Bhat *et al*. (2019a) with minor modifications. In brief, 16-18 h grown active culture of NCDC 400 was diluted using the sterile physiological saline to attain the equivalent turbidity to 0.5 McFarland (~1-2x10^8 CFU/mL). The cell suspension having 0.5 McFarland has been swabbed on the MRS agar (2% agar) plates and an array of antibiotic discs (**Annexure 2**) (Icosa G-1 plus, Icosa Universal 1, Icosa Universal 2, Octa disc G Plus-17, Octa disc G-VII-minus, HiMedia, India) were placed on the solid agar surface. The plates were incubated at 37˚C for 16-18 h and observed for a zone of clearance around the disc. Since there are no standard guidelines available for the interpretation of AST results of *Lactobacillus*, the findings were interpreted based on published literature.

3.3.17.2. Determination of minimum inhibitory concentrations

The minimum inhibitory concentration (MICs) of different antibiotics was determined using commercial strips. Overnight grown NCDC 400 was diluted using the sterile physiological saline to attain the equivalent turbidity to 0.5 McFarland (~1-2x10^8 CFU/mL). The cell suspension equivalent to 0.5 McFarland has been swabbed on the MRS agar (2% agar) plates and antibiotic MIC strips (HiMedia, India) (**Annexure 2**) were placed on the agar surface. The plates were incubated at 37˚C for 16-18 h. The zone

of clearance against the lowest antibiotic concentration of antibiotics was regarded as MIC. Results were interpreted according to the EFSA guidelines (https://www.efsa.europa.eu/ sites/ default/files/engage/170615_0.pdf).

3.3.18. PCR-based identification of antibiotic resistance and virulence genes

The presence of genes confirming antibiotic resistance and virulence factors, selected through a wide literature search, was tested in NCDC 400 through a targeted conventional PCR approach. Both chromosomal and plasmid DNA was used as the template DNA to locate the position of these genes, if present. The DNA samples and PCR reagents were thawed on ice. Initially, a standard mixture of master mix, primers, and nuclease-free water was added to the microcentrifuge tube (**Table 3.1**) and mixed well by a short spinning. Eleven microliters of the master mix were carefully transferred to the 200 µL PCR tubes containing 1 µL template DNA. Thereafter, the samples were vortexed and transferred to PCR Thermal cycler heating blocks (BIO-RAD S1000^{TM} thermal cycler). The PCR conditions, primer sequences against the targeted gene, and amplicon size are presented in **Table 3.7**.

Table 3.7: Primer sequences and their annealing conditions used in the PCR-based identification of virulence or ARGs

Target gene	Primer code	Primer sequence (5′-3′)	Annealing condition	Amplicon size (bp)
TetO	tet(O)-F	AACTTAGGCATTCTGGCTCAC	62˚C/ 1 min	515
	tet(O)-R	TCCCACTGTTCCATATCGTCA		
TetM	tet(M)-F	GTTAAATAGTGTTCTTGGAG	54˚C/ 45 sec	576
	tet(M)-R	CTAAGATATGGGCTCTAACAA		
ant(6')-Ia	ant(6′)-Ia-F	ACTGGCTTAATCAATTTGGG	56˚C/ 30 sec	**577**
	ant(6′)-Ia-R	GCGTTTCCGCCACCTCACCG		
catA8	catA8-F	GGATATGAACTGTATCCTGCT	58˚C/ 1 min	461
	catA8-R	AATGAAACATGGTAACCATCAC		
emeA	emeA-F	GTGACAGCCTTTGTGGCAGAT	57˚C/ 60 sec	697
	emeA-R	TAGTCCGTTGATGGTTCCTTG		
Int-Tn (Tn916/Tn 1545)	Int-Tn-F	GCGTGATTGTATCTCACT	55˚C/ 45 sec	1028
	Int-Tn-R	GACGCTCCTGTTGCTTCT		

ermB	erm(B)-F	GAAAAGRTACTCAACCAAATA	55˚C/ 1 min	639
	erm(B)-R	AGTAACGGTACTTAAATTGTTTAC		
msrA	msr(A)-F	GCAAATGGTGTAGGTAAGACAACT	52˚C/ 1 min	399
	msr(A)-R	ATCATGTGATGTAAACAAAAT		
ermA	erm(A)-F	TCTAAAAAGCATGTAAAAGAA	53˚C/ 1 min	645
	erm(A)-R	CTTCGATAGTTTATTAATATTAGT		
ermC	erm(C)-F	GCTAATATTGTTTAAATCGTCAAT	47˚C/ 1 min	642
	erm(C)-R	GCTAATATTGTTTAAATCGTCAAT		
ermF	erm(F)-F	GAGATCGGRCCAGGGAAGC	59˚C/ 1 min	309
	Erm(F)-R	GTGTGCACCATCGCCTGA		
blaTEM	blaTEM-F	TCCGCTCATGAGACAATAACC	60˚C/ 15 sec	931
	blaTEM-R	TTGGTCTGACAGTTACCAATGC		
aac(6')-le-apha (2'')-Ia	10F	CCAAGAGCAATAAGGGCATA	55˚C/ 1 min	220
	10R	CACTATCATACCACTACCG		
aph(3')-IIIa	11F	GCCGATGTGGATTGCGAAAA	60˚C/ 1 min	292
	11R	GCTTGATCCCCAGTAAGTCA		
Coa	CoaF	GCGCTAGGCGCATTAGCAGTTGC	61˚C/ 15 sec	173
	CoaR	CGCTGGTTCTCTAGATTTTCAATTATTCCCC		
NucA	NucF	GATGGCTATCAGTAATGTTTCGAAAGGGC	60˚C/ 15 sec	561
	NucR	ACATAAGCAACTTTAGCCAAGCCTTGACG		
GelE	gelE-F	TATGACAATGCTTTTTGGGAT	55˚C/ 90 sec	213
	gelE-R	AGATGCACCCGAAATAATAATATA		

3.3.19. *In silico* prediction of virulence and antibiotic resistance genes

3.3.19.1. DNA sequences and circular genome map

The whole genome sequences of NCDC 400 (137 scaffolds) were obtained in the FASTA format from National Center for Biotechnology Information (NCBI) (BioProject: PRJNA398455; BioSample: SAMN07510693; Accession: PDKX00000000), published in previous work (Azmal *et al*., 2018). The circular map

was developed using the Proksee genome visualization tool. The obtained sequences were sequentially subjected to a series of publically available databases or bioinformatics tools to decipher the genes of safety interest as shown in **Fig.3.2**.

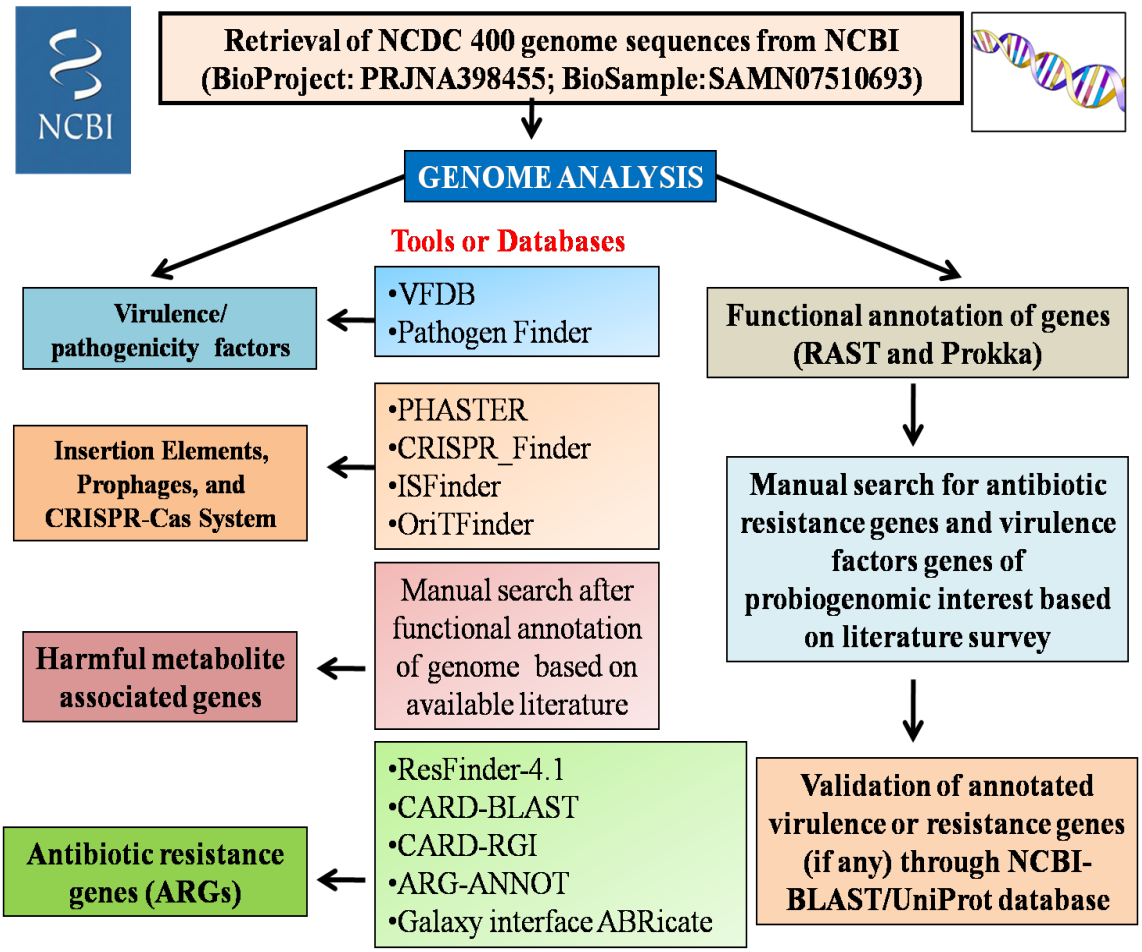

Fig. 3.2: Sequential steps and various bioinformatics tools used in genome-wide safety analysis of NCDC 400

3.3.19.2. Identification of virulence genes

PathogenFinder and VirulenceFinder (version 2.0) hosted by the Center for Genomic Epidemiology (CGE), were used to unravel the possible pathogenic factors of NCDC 400 towards the human host. Also, the potential virulence genes associated with the NCDC 400 whole genome were ruled out through an alignment via BLASTp against the VFDB (Virulence Factor Database) (http://www.mgc.ac.cn/VFs/main.htm). A coverage and identity of > 60% with an E-value of 0.00001 was used as the criteria for this analysis.

3.3.19.3. Identification of antibiotic resistance-related genes

The genes conferring the antibiotic resistance to NCDC 400 were mined by performing BLASTn analysis against the CARD (Comprehensive Antibiotic Resistance Database) database (https://card.mcmaster.ca/analyze/blast). A coverage > 70%, identity > 80%, and E-value > e−6 were used as criteria to identify the possible antibiotic resistance genes. The presence of single nucleotide polymorphisms (SNP)-based mutations that confer the resistance to NCDC 400 was identified by Resistance Gene Identifier (RGI) (https://card.mcmaster.ca/analyze/rgi) which detects the resistome from nucleotide based on homology and SNP models. The obtained hits were classified as perfect, strict, and loose based on 100%, 90-100%, and 50-90% sequence similarity, respectively. Further, as pointed out by EFSA, the whole genome scaffolds NCDC 400 were also subjected to ARG-ANNOT (Antibiotic Resistance Gene-ANNOTation), a new bioinformatic tool that detects existing and putative new ARGs (https://ifr48.timone.univ-mrs.fr/blast/arg-annot_nt.html). In addition, the whole genome search for ARGs was performed by annotating the genome via ABRicate (https://usegalaxy.org/), a galaxy interface used for mass screening of contigs for antimicrobial and virulent genes.

3.3.19.4. Insertion Elements, Origin of Transfer, Prophages, and CRISPR‑Cas System

The annotation of insertion sequences (IS) was performed by ISFinder (Insertion Sequence Finder) (https://isfinder.biotoul.fr/). The prophecy of prophage arrangements was carried out using the PHASTER (PHAge Search Tool Enhanced Release) (https://phaster.ca/). The CRISPR-Cas system was predicted using the CRISPRCasFinder (https://crisprcas.i2bc.paris-saclay.fr/CrisprCasFinder/Index). Finally, a genome search for the origin of transfer (OriT) regions was performed using the OriTFinder tool (https://bioinfo-mml.sjtu.edu.cn/oriTfinder/).

3.3.19.5. Functional annotation of NCDC 400 using RAST and Prokka

The whole genome sequences were subjected to Rapid Annotation Subsystem (RAST) and a Galaxy interface Prokka (a prokaryotic genome annotation server) for functional annotation of genome. RAST-assisted whole genome annotated file was further investigated for any functional genes that code for antibiotic resistance and virulence factors by considering the subcategories (resistance to antibiotics and toxic

compounds as well as invasion and intracellular resistance) and subsystems under the category of virulence, disease, and defense. To check the analogy, the confirmed subsystems that encode either virulence or resistance were also meanwhile verified in the Prokka annotated files. Likewise, the Prokka-based genome annotated files (.tsv, .fna, and .faa) were mined for searched for the presence of any virulence factors or resistance-conferring factors using standard keywords such as virulence, toxin, resistance, antibiotics, efflux, drug, efflux pump, gelatinase, cytolysin, hyaluronidase, aggregation substance, enterococcal surface protein, sex pheromones, endocarditis antigen, and integration factors. The presence of any ARGs or other virulence factors was validated through BLASTp search using the UniProt database set at E=0.0001 (https://www.uniprot.org/blast).

3.3.19.6. Identification of harmful enzymes and metabolite-associated genes

The genes associated with the production of harmful enzymes and metabolites were identified by the functional annotation of the genome by Rapid Annotation Subsystem (RAST) and Prokka. Further, the existence of any harmful enzymes or metabolites coding genes was identified by a manual search with the assistance of published literature on probiogenomics (de Jesus *et al*., 2022; Mann *et al*., 2021a; Senan *et al*., 2015). Further, the identified genes were validated for the accuracy of genome annotations by an alignment using VFDB as well as the BLASTp algorithm of the UniProt database with an E-value set at 0.0001. If the genome, on the other hand, portrays one more related gene for harmful metabolite production, the insights into the completeness of genes required to produce the end metabolite were identified by predicting the canonical pathways using RAST and KEGG server (https://rast.nmpdr.org/rast.cgi;).

Objective 2: Toxicological evaluation of *Limosilactobacillus fermentum* NCDC 400 in the murine model

3.4. Animals for oral toxicity tests

After prior approval from the institutional animal ethics committee regarding the animal care procedures and experimental protocols to conduct animal trials, a total of 81 male Swiss albino mice of about 4-5 weeks (approx. 25-30 g) age were received from and housed in Small Animal House of the ICAR-National Dairy Research Institute, Karnal, Haryana, India. Experiments were conducted after an acclimatization period of 1

week. All mice were housed in polypropylene cages in climate controlled room maintained at a temperature of 25 ± 1 °C, RH 55 ± 10%, and 12: 12 light-dark cycle. The animals had free access to tap water and a standard basal diet (BD) containing 15% wheat crushed, 58% Bengal gram crushed, 10% groundnut cake crushed, 4% refined oil, 5% skimmed milk powder, 4% casein, 4% mineral mixture, 0.2% vitamin mixture, and 0.2% choline chloride on w/w basis.

3.5. Experimental designs

With slight modifications in the OECD (The Organization for Economic Cooperation and Development) guidelines, a total of three *in vivo* oral toxicity studies *viz*. acute (14-days repeated dose toxicity test) (OECD 407), subacute (OECD 407), and subchronic toxicity (OECD 408) studies were conducted sequentially (**Fig. 3.3**). For each study, a total of 27 mice were randomly divided into three groups having nine mice each. Group 1 served as control (hereafter referred to as CON) and received only sterile PBS (pH 7.4), which served as a vehicle to carry test compound in other groups.

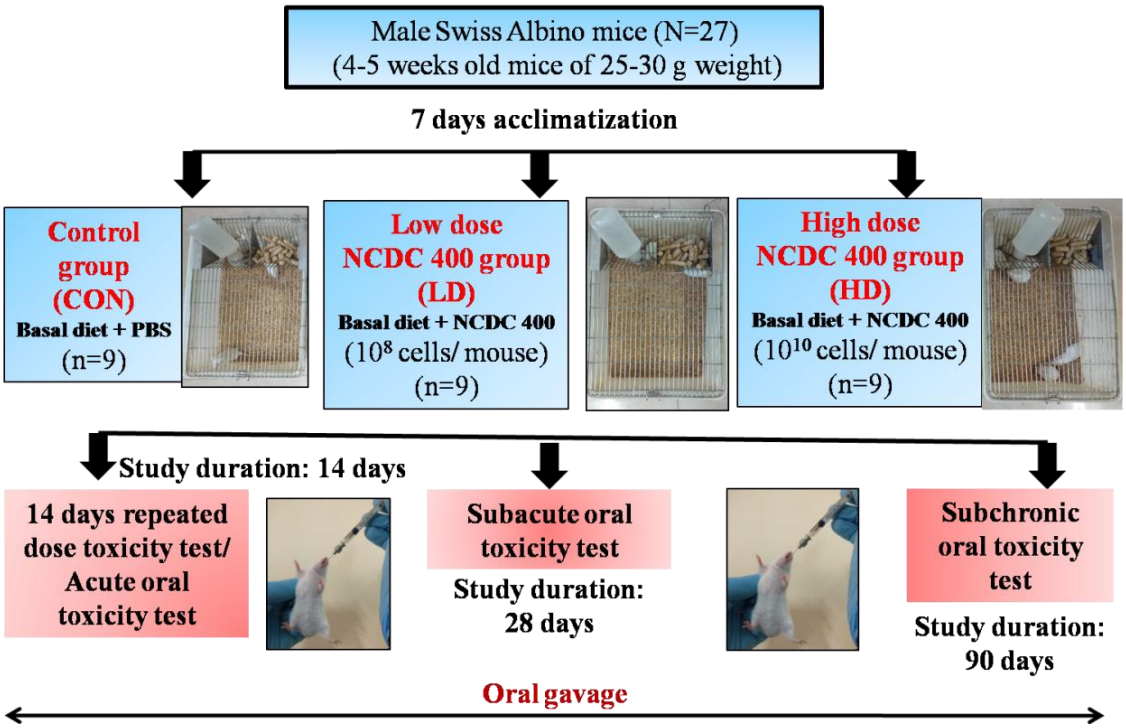

Fig. 3.3: Schematic representation of experimental design for oral toxicity tests (acute, subacute, and subchronic toxicity)

Group 2 mice received a low dose of NCDC 400 at 10^8 CFU/ mouse (hereinafter referred to as LD), and Group 3 was fed with a high dose of NCDC 400 at 10^{10} CFU/

mouse (referred to as HD) through daily oral gavage (20–22G needles) for a different duration as per the test requirements. During the experimental period, the feed and water were provided *ad libtum*. Although the experimental design in all three studies remains the same, the experimental duration or the period of exposure of test bacterium to animals varied depending on the type and aim of the study. In accordance with OECD guidelines, the different doses of test bacterium (NCDC 400) were administered to animals for a total duration of 14, 28, and 90 days for acute, subacute, and subchronic toxicity studies, respectively

3.6. General observations

Animals were strictly supervised after 30 min and 4 h of the first exposure to test bacterium as well as on daily basis after the dosing. The signs of toxicity and any changes in skin and fur, eyes and mucous membranes, respiratory, and somatomotor activity, and the behavior pattern of the animals were monitored. Further, keen observations were made on the tremors, convulsions, salivation, diarrhea, lethargy, and sleep of animals. In addition, the physical parameters such as body weight, feed and water intake, local injuries, and mortality (if any) were systematically recorded throughout the experimental period.

3.7. Gross necropsy, tissue, and faeces collection

After the end of the feeding schedule, all animals were fasted overnight (only the food was withheld with a provision for water) and the animal faeces were collected from the individual mouse by transferring animals into clean cages covered with sterile aluminum foil. The animals were examined for an external body check and including orifices and further euthanized with diethyl ether over dose. The postmortem observations of a body, including the internal organs and other structures, were performed as necropsy. The changes in the gross appearance of organs or tissue like color, size, or lesions were noted. Further, the blood and tissue samples were aseptically collected for further analysis. A portion of blood was collected (EDTA tubes) from the heart of animals by direct cardiac puncture. Whereas the blood collected in the non-EDTA tubes was allowed to clot and centrifuged at 2,000 × *g* for 10 min at 4°C to separate the serum. All the organs were excised, examined, weighed, and stored in sterile saline tubes on an ice-bath. While the organs meant for histopathological analysis were preserved in 10% neutral buffered formalin. On the other hand, the caecal content of the

animals was collected into a fresh microcentrifuge tube for further analysis. In the entire process, every care was taken to minimize the external or environmental contamination of extra intestinal tissues and other organs.

3.8. Body weight and organ indices

The body weight of every animal in both experimental and control groups was monitored based on a daily or weekly basis as per the study requirements. The average weight of each animal in the respective group was compared. After terminal scarifies of the animals, the major organs (brain/ heart/ kidney/ spleen/ liver/ lungs) were collected, adherent fat was trimmed off, and their weights were measured to determine the organ indices as given below.

$$Organ\ index\ (\%) = \frac{Organ\ weight\ (g)}{Total\ body\ weight\ (g)} \times 100$$

3.9. Hematology

The hematological assessment of blood was carried out immediately after the collection of the blood from the animals. The analysis was performed on an automated hematological analyzer (MS4Se-Melet Schloesing Lab, New Delhi, India) and the parameters like Red Blood Cell (RBC), Hemoglobin (Hb), Hematocrit Test (HCT), Mean Corpuscular Volume (MCV), Mean Corpuscular Hemoglobin (MCH), Mean Corpuscular Hemoglobin Concentration (MCHC), Mean Platelet Volume (MPV), White Blood Cells (WBC), and other differential leukocyte counts (DLC) were estimated.

3.10. Serum biochemistry

The fasting blood glucose level was checked before the terminal sacrifice of animals. The blood was drawn from the tail vain and the glucose level was measured using a glucometer (GlucoOne, Himachal Pradesh, India). The serum biochemical parameters including kidney functioning markers (urea and creatinine), the markers for liver functioning [alanine aminotransferase (ALT) and aspartate aminotransferase (AST)], lactate dehydrogenase (LDH), a marker for myocardial toxicity were determined using commercial kits (Liquid stable, Recombigen Laboratories Pvt. Ltd., New Delhi, India) following the manufacturer's instructions. While the parameters like calcium, phosphorus, and total serum protein were estimated using an automatic clinical chemistry analyzer (TRANSASIA, EM-200, Mumbai, India). On the other hand, the total serum lipids were profiled by determining the triglycerides, high-density lipoprotein (HDL), and total cholesterol using commercial kits (Liquid stable, Recombigen

Laboratories Pvt. Ltd., New Delhi, India) following the manufacturer's instructions. Besides, the levels of low-density lipoprotein (LDL) and very low-density lipoprotein (VLDL) were also determined using Friedewald's equations while an atherogenic index (AI) was computed using the following equations.

$$VLDL = \frac{Triglycerides}{5}$$

$$LDL = Total\ cholesterol - (HDL + VLDL)$$

$$Atherogenic\ index = \frac{LDL}{HDL}$$

3.11. Histopathological analysis

Gross pathological examination of tissues or organs (brain, liver, lungs, heart, spleen, kidney, small and large intestine) from at least three animals from each group was carried out at the end of the study. The tissues were fixed in 10% (v/v) neutral buffered formalin and further processed by cassetting, mounting, and stained with hematoxylin and eosin (H and E) at the National Liver Disease Biobank U/o Institute of Liver and Biliary Sciences, D-1, Vasant Kunj, New Delhi-110070. The slides were assessed for microscopic tissue manifestations (if any) by a veterinary pathologist.

3.12. Harmful intestinal enzyme assay

Freshly collected caecal content was immediately assessed for harmful intestinal bacterial enzymes (β-glucosidase and β-glucuronidase) according to Shokryazdan *et al*. (2016). Briefly, 1g of caecal content was suspended in 10 mL PBS (pH 7.4) and centrifuged (3,000 × *g* for 5 min) at room temperature to collect supernatants. Further, 0.2 mL supernatant was mixed either with 0.8 mL of 2 mM p-nitrophenyl-β-D-glucopyranoside (for β-glucosidase activity) or 2 mM p-nitrophenyl-β-D-glucuronide (for β-glucuronidase activity) and incubated at 37°C for 1 h. The reaction was ended by adding 1 mL of 0.5 mol/ L NaOH. The mixture was centrifuged at 4,000 × *g* for 10 min. The activities of β-glucosidase and β-glucuronidase were determined in the supernatant by recording the absorbance at 405 nm. Further, a standard curve of different concentrations (0, 0.1, 0.2, 0.5, 1, and 10 mmol/ L) of p-nitrophenol (HiMedia, India) (**Annexure 1**) was used to interpret the results as unit/ g cecal content. One unit is defined as the activity required for releasing 1 μmol/ L of p-nitrophenol in 1 h.

Tryptophanase activity in the caecal content was assayed according to the method of An *et al*. (2011). Briefly, 0.1 mL supernatant was mixed with 0.5 mL reaction mixture

consisting of 0.2 mL of complete reagent solution (2.75 mg pyridoxal phosphate, 19.6 mg disodium EDTA dihydrate, and 10 mg bovine serum albumin in 100 mL of 0.05 M potassium phosphate buffer, pH 7.5) and 0.2 mL of 20 mM tryptophan. The mixture was incubated at 37˚C for 1 h and then the reaction was stopped by adding 2 mL color reagent (14.7 g p-dimethyl-amino-benzaldehyde in 52 mL H_2SO_4 and 948 mL 95% ethanol). Thus obtained mixture was centrifuged at 3,000 rpm/ 10 min and enzyme activity was measured by recording the absorbance at 550 nm.

3.13. Bacterial translocation assay

The ability of NCDC 400 to translocate from the intestine to blood and other extra-intestinal organs was tested by colony PCR (Singer *et al*., 2018). Briefly, the extra-intestinal organs (liver, lung, heart, spleen, brain, and kidney) excised from the mice were immediately transferred to 5 mL sterile normal saline and further homogenized to obtain the tissue homogenates. Aliquots of tissue homogenates were plated using MRS agar. Whereas the blood sample drawn from the heart was directly plated on MRS agar and the plates were incubated at 37˚C for 18-24 h. The colonies that appeared on MRS were counted and randomly selected for genotypic identification. The colony PCR was performed using *L. fermentum*-specific LF1 and LF2 primers using similar reagents and thermal cycler conditions, as presented in **Tables 3.1** and **3.2,** except for the template DNA. In this PCR, the bacterial colonies that were formed on the MRS agar were picked up through sterile pipette tips and suspended in nuclease-free water (5 µL) served as template DNA. If any colonies were found positive for *L. fermentum*, the RAPD-PCR using M-13 primer was then performed to generate the molecular fingerprint to discriminate between the strains as described in **section 3.1.2.3**.

3.14. Estimation of selective gut health indices

3.14.1. Faecal pH

One gram of fresh faeces was dissolved in 10 mL distilled water and the pH was measured using a pre-calibrated pH meter (PHS-3BW Bench top pH meter. Biolinkk, India).

3.14.2. Faecal ammonia

A. Reagent preparation

- **Solution A:** 1 g phenol and 5 mg sodium nitroprusside were dissolved in 100 mL distilled water.

- **Solution B:** 0.5 g NaOH and 0.84 mL sodium hypochlorite were dissolved in 100 mL distilled water, and finally the solution was stored in the amber color reagent bottle.
- **Standard ammonium sulphate:** 0.048 g ammonium sulphate was dissolved in 100 mL distilled water to get a final concentration of 10 mg ammonium nitrogen per 100 mL. A working standard was obtained by diluting 10 mL of the above stock solution up to 100 mL. The solution contains 0.01 mg ammonium nitrogen/ mL.

B. Procedure:

The faecal ammonia estimation assay protocol was adapted from Singh *et al*. (2021). Briefly, 2 g of fresh faeces was suspended in 6 mL of 6 N HCl and stored at -20˚C till further analysis. The preparation of the standard curve as well as the sample for estimation of ammonia has been presented in **Table 3.8**. After the addition of the standard solution or the sample, 5 mL of solution A and 5 mL of solution B was added to all the tubes and the content was mixed well. The tubes were incubated at 40˚C for 15 min and the optical absorbance was noted at 625 nm. The results were interpreted based on the developed standard curve.

Table 3.8: Different concentrations of ammonia used for developing standard curve

Tube No.	1	2	3	4	5	6	7	8	9
Distilled water (mL)	1	0.95	0.90	0.80	0.60	0.40	0.2	0.0	0.9
Std. solution (mL)	-	0.05	0.10	0.20	0.40	0.60	0.80	1.0	-
Sample (mL)	-	-	-	-	-	-	-	-	0.1
Ammonia (N) (µg)	0	05	1.0	2.0	4.0	6.0	8.0	10.0	?

3.14.3. Faecal lactate

A. Reagents preparation

- **p-hydroxy diphenyl reagent:** 1.5 g of p-hydroxy diphenyl was taken in a 100 mL volumetric flask and to which 10 mL each of 5% NaOH and distilled water was added. The mixture was warmed in a boiling water bath with constant

stirring until all the solutes get completely dissolved. The final volume was made up to 100 mL and stored in an amber-colored reagent bottle.

- **Standard lactic acid:** 0.1065 g of lithium lactate was dissolved in 50 mL of distilled water in a volumetric flask and 0.1 mL of concentrated H_2SO_4 was added to it. Ultimately, the final volume was made up to 100 mL using distilled water to make the stock solution of standard lactic acid. Whereas the working standard lactic acid solution was prepared just before the start of the experiment by diluting 1mL stock solution to 100 mL using distilled water which contained 0.01mg lactate/ mL.

B. Procedure

The method for faecal lactate quantification was adapted from Singh *et al*. (2021). Accordingly, 1 g of fresh faeces was suspended in 2 mL of distilled water. The slurry was centrifuged at 10,000 rpm/ 10 min. The supernatant was separated and stored at -20˚C until further analysis. One milliliter supernatant was mixed with 1 mL of 20% $CuSO_4$ in a test tube and the volume was made up to 10 mL using distilled water. To this, 1 g of $Ca(OH)_2$ was added and mixed well to obtain the homogenous suspension. The mixture was incubated at 37 ˚C/ 90 min with intermittent mixing and centrifuged at 3,000 rpm for 10 min. Further, 1 mL of obtained supernatant was taken in the test tube and prepared similarly as followed for the standard curve development, shown in **Table 3.9.**

Table 3.9: Different concentrations of lactate used for developing standard curve

Tube No.	1	2	3	4	5	6
Distilled water (mL)	1	0.9	0.8	0.6	0.4	0.2
Std. lactic acid (mL)	0	0.1	0.2	0.4	0.6	0.8
Total lactic acid in tube (µg)	0	1.0	2.0	4.0	6.0	8.0

Furthermore, 0.05 mL of 4% $CuSO_4$, as well as 6 mL concentrated H_2SO_4 was added to all tubes containing samples or standards. The tubes were heated in the boiling water bath for 5 min and cooled to room temperature. Further, the tubes were incubated at 30˚C for 30 min following the addition of 0.1 mL of p-hydroxydiphenyl reagent.

Later, the tubes were heated in the boiling water bath for 90 sec and further cooled to room temperature in order to measure the absorbance at 560 nm against a reagent blank.

3.14.4. Caecal short-chain fatty acids

One gram of caecal content was suspended in 2 mL of 25% (w/v) metaphosphoric acid and further vortexed to obtain a homogenous suspension. The suspension was centrifuged at 10,000 rpm for 10 min at 4˚C and the supernatant was analyzed for SCFAs using Gas Chromatography (GC) (5765 Nucon, New Delhi, India) fitted with N_2 flame ionization detector. The separation of SCFAs was achieved with Chromosorb 101 column with the standard operation conditions as follows: injection volume: 1 µL, injection port temperature: 200˚C, column temperature: 145˚C, carrier gas N_2, detector temperature: 180˚C, and run time: 10 min. Finally, the results were interested based on the chromatograms obtained after analyzing the standard comprising acetate, propionate, and butyrate in the concentration of 0.065, 0.015, and 0.010 M, respectively.

3.15. Effect of oral supplementation of NCDC 400 on immune homeostasis

The immunoglobulins (IgG and IgA) inflammatory cytokines (IL-6, TNF-alpha, TGF-β, IL-10) and chemokine (MCP-1) in serum were measured using commercially available mouse sandwich enzyme-linked immunosorbent assay (ELISA) kits (BT Bioassay, China; Krishgen BioSystems, Mumbai, India), according to the manufacturers' protocol. Briefly, mouse antibody-coated 96-well plates were added with serially diluted respective standards (50-100 µL/ well) or undiluted serum sample (40 µL/ well) for 2 h at room temperature. Then, 10 µL/ well biotin-conjugated detection antibodies of respective cytokines or immunoglobulins and 50 µL/ well streptavidin-conjugated HRP was added as detection enzyme and incubated at 37˚C for 1 h. The wells were aspirated and washed 4 times with 1 X wash buffer. Finally, TMB substrate (3,3,5,5-tetramethyl diamine benzidine containing 0.03% H_2O_2) solution was added for the color development and the plates were spectrophotometrically recorded at 450 nm before 10 min of adding stop solution (100 µL). Finally, the results were expressed based on the developed standard curves (**Annexure 1).**

Objective 3: Evaluation of safety and efficacy of NCDC 400 in an immunocompromised murine model

3.16. Development of cyclophosphamide (Cy) induced immunocompromised mice model

3.16.1. Animals

After the IAEC approval, a total of 60 male Swiss Albino mice of age 4-5 weeks (25-30 g) were procured from and housed in the Small Animal House of the ICAR-National Dairy Research Institute, Karnal. Experiments were conducted after an acclimatization period of 7 days. All mice were housed in polypropylene cages in climate controlled room marinated at a temperature of 25 ± 1 °C, RH 55 ± 10%, and 12: 12 light-dark cycle. The animals had free access to sterile drinking water and a standard basal diet (BD) containing 15% wheat crushed, 58% Bengal gram crushed, 10% groundnut cake crushed, 4% refined oil, 5% skimmed milk powder, 4% casein, 4% mineral mixture, 0.2% vitamin mixture, and 0.2% choline chloride on w/w basis. Every care was taken to avoid secondary infections from animal handling procedures. Cleaning and sanitation of cages and experimental house were effectively monitored.

3.16.2. Experimental design

As shown in **Fig. 3.4**, a total of sixty animals were divided into 4 groups containing 15 mice each. Group 1 served as control and it does not received Cy treatment. While the injections only sterile milli-Q water (vehicle control) was provided intraperitoneally (IP). On the other hand, Groups 2, 3, & 4 received different doses of Cy (HiMedia, India) treatment (IP) ranging from 50, 100, and 150 mg/ Kg body weight (BW), respectively. In the entire study of 17 days, animals received different doses of Cy three times between 7 days intervals. On the other hand, three animals from each group were dissected on the 3, 6, 9, 12, and 17^{th} day to evaluate the effect of administration of Cy doses and frequency of Cy administration on various hematological and oxidative markers. Thus, this design would provide us an idea that which Cy dose and its number of administrations are effective in fostering the immune-suppressed state, so as to facilitate the conduct of any pre-clinical safety studies in such an immunocompromised model, for a desirable period.

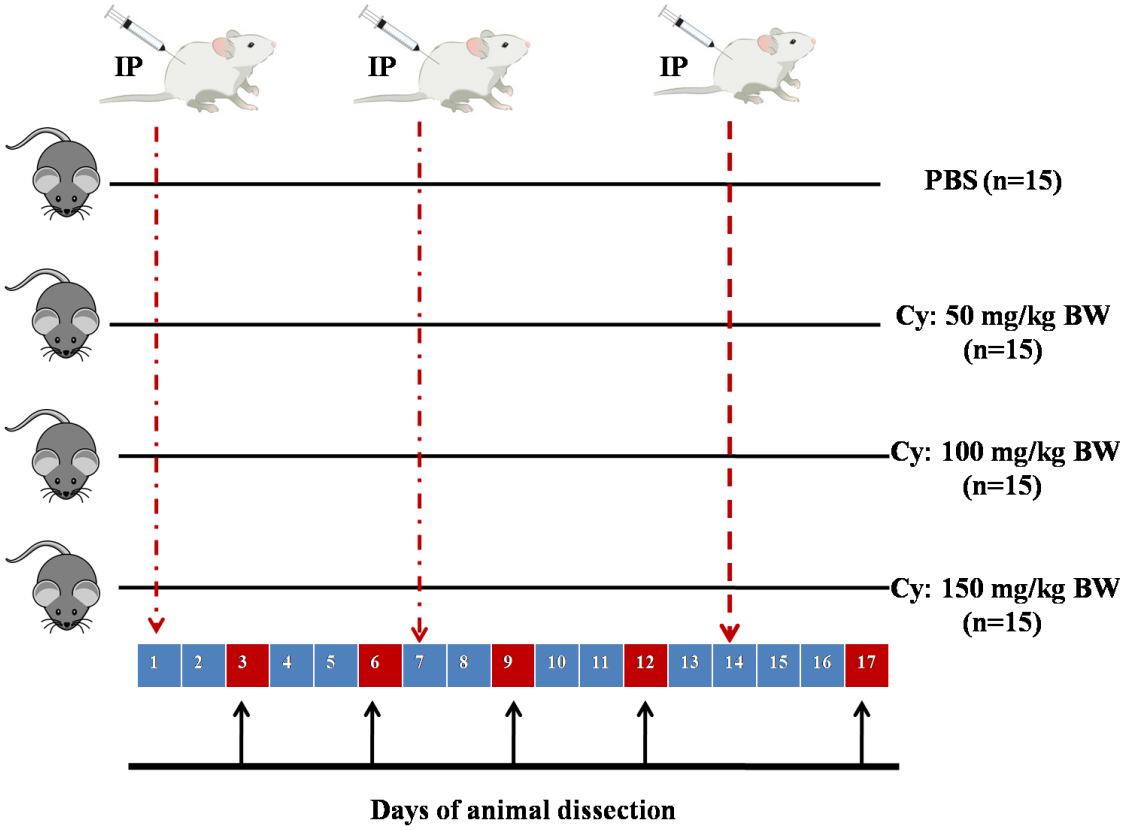

Fig. 3.4: Experimental design and grouping of animals for the development of Cy induced an immunocompromised murine model

3.16.3. Blood and tissue collection

After the end, all animals were fasted overnight, and the animals were examined for an external body check and including orifices. Animals were euthanized with ether over dosing, exsanguinated (blood was collected from the heart in the EDTA and non-EDTA treated tubes), and subjected to necropsy. The blood collected in the non-EDTA tubes was allowed to clot and centrifuged at 2,000 × *g* for 10 min at 4 °C to separate the serum. All the organs were excised, examined, weighed, and stored in sterile saline on an ice-bath.

3.16.4. Body weight and organ indices

The body weight of each animal in all groups was monitored daily. However, the final weight of the animal was measured before the animal is euthanized. The average weight of each animal in the respective groups was compared. After terminal scarifies of the animals, the major immune organs/ tissues (spleen/ thymus) were collected, adherent fat was trimmed off, and their weights were measured to determine the organ indices as given below.

$$Organ\ index\ (\%) = \frac{Organ\ weight\ (g)}{Total\ body\ weight\ (g)} \times 100$$

3.16.5. Hematology

The hematological assessment of blood was carried out immediately after the collection of the blood from the animals. The analysis was performed on an automated hematological analyzer (Byovet, Smart-3Dx, Vet-Hematology analyzer, UK, Model No. CONU CELL 23 Excel). The parameters like WBC, Lymphocytes, Granulocytes, Monocytes, HCT, and RBC were recorded.

3.16.6. Determination of oxidative markers (SOD, CAT, GpX2)

The activities of superoxide dismutase (SOD), catalase (CAT), and glutathione peroxidase (GpX2) in the serum samples were measured using commercial mouse ELISA kits (Krishgen BioSystems, Mumbai, India), according to the manufacturers' protocol for sandwich ELISA, detailed under **section 3.15**. The standard curves for each ELISA assay have been presented in **Annexure 1.**

3.17. Evaluation of safety and efficacy of NCDC 400 in Cy-induced immunocompromised mice model

3.17.1. Animals

After the IAEC approval, a total of 44 male Swiss Albino mice of age 4-5 weeks (25-30 g) were procured from and housed in the Small Animal House of the ICAR-National Dairy Research Institute, Karnal. Experiments were conducted after an acclimatization period of 7 days. Animal housing and diet patterns followed in this study were similar to our previous study as described in **section 3.16.1**.

3.17.2. Experimental design

Forty-four mice were randomly divided into 4 groups with 11 mice each. Group 1 served as normal control (hereafter referred to as NC) and received only sterile PBS, which served as a vehicle to carry test compound (NCDC 400) in other groups. The animals in this group did not receive Cy treatment. Group 2 served as model control (hereinafter referred to as MC) and received only sterile PBS. Group 3 received a low dose of NCDC 400 at 10^8 CFU/ mouse (hereinafter referred to as LD), and Group 4 was fed with a high dose of NCDC 400 at 10^{10} CFU/ mouse (referred to as HD) through daily oral gavage (20–22G needle) for 15 days. At the same time, animals in the MC, LD, and

HD groups were administered intraperitoneally with 3 doses of cyclophosphamide at 150 mg/ kg BW at an interval of 5-6 days between each dose. However, oral administration of NCDC 400 was started after 2 days of Cy administration to ensure that the safety study of NCDC 400 was conducted in a completely validated immune-suppressed mice model (**Fig. 3.5**). During the experimental period, the animals were provided with feed and sterile water were provided *ad libtum*.

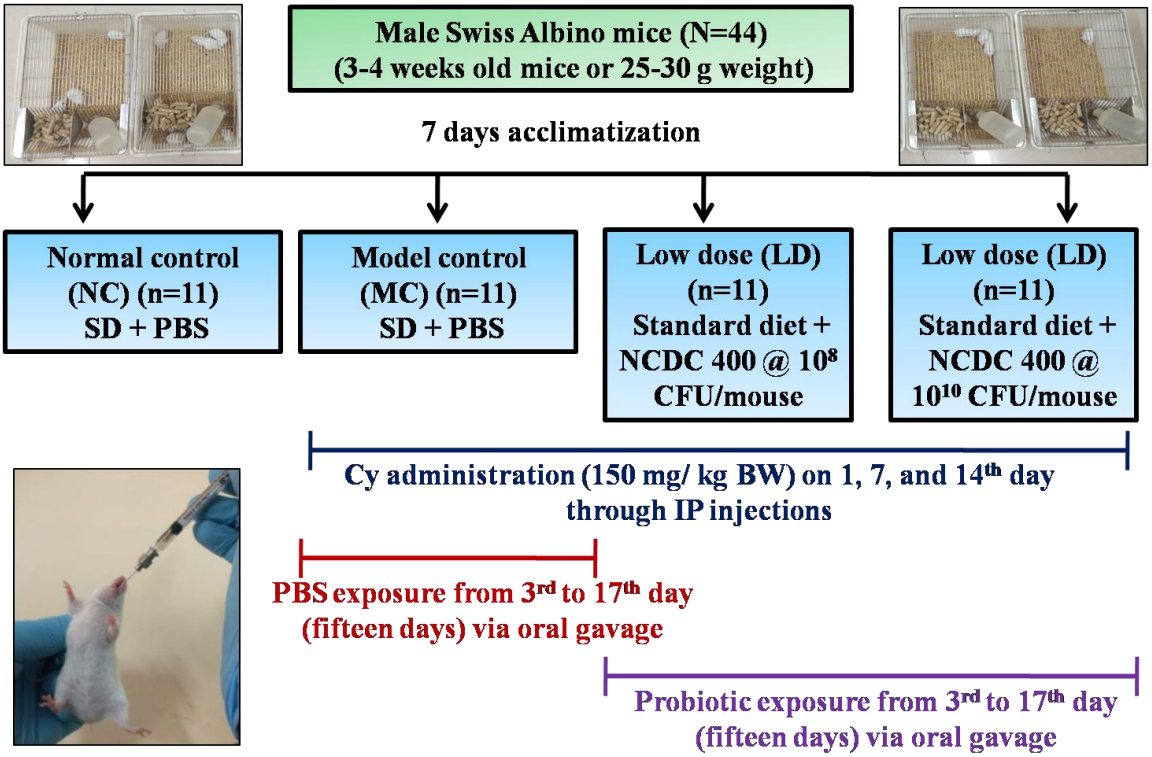

Fig. 3.5. Diagrammatic representation of experimental design used in the safety assessment of NCDC 400 using an immunocompromised mice model

3.17.3. General observations

All the general health and visible toxicity signs included in the oral toxicity tests (**section 3.6**) were also included in this study. In addition, the feed and water intake in the animals of each group was recorded on the daily basis.

3.17.4. Gross necropsy, tissue, and faeces collection

All animals fasted overnight at the experimental schedule and the faeces were collected from the individual mice by transferring them into clean cages covered with sterile aluminum foil. The examination of external surfaces of the body, all orifices, cranial, thoracic, and abdominal cavities, and their contents was done, and findings (if any) were recorded. The changes in the gross appearance of organs or tissue by virtue of

their color, size, or lesions were noted. On completion of the gross examination, the animals were euthanized with diethyl ether over dose. The blood and organs collection following their subsequent processing for various experiments is as followed under **section 3.7.**

3.17.5. Body weight and organ indices

The body weight of every animal in all the groups was monitored on daily basis. The average weight of each animal in the respective group was compared. Further, the final weight of animals before the terminal scarifies was noted. Finally, the weights of major organs (brain/ heart/ kidney/ spleen/ liver/ lungs/ thymus) were measured to determine the organ indices using the formula described in **section 3.8.**

$$Organ\ index\ (\%) = \frac{Organ\ weight\ (g)}{Total\ body\ weight\ (g)} \times 100$$

3.17.6. Hematology

The hematological assessment of fresh blood was carried out using an automated hematological analyzer (Byovet, Smart-3Dx, Vet-Hematology analyzer, UK, Model No. CONU CELL 23 Excel). The following parameters were determined; Red Blood Cell (RBC), Hemoglobin (Hb), Hematocrit Test (HCT), Mean Corpuscular Volume (MCV), Mean Corpuscular Hemoglobin (MCH), Platelets (PLT), Procalcitonin Test (PCT), White Blood Cells (WBC), Lymphocytes (LYM), Monocytes (MON), and Granulocytes (GRAN).

3.17.7. Serum biochemistry

As described previously, the various serum biochemical markers that suggest acute hepatocellular**,** renal, and cardiac toxicity were tested. In addition, the fasting blood glucose, total serum proteins, (minerals) phosphorous, calcium, and total lipids were profiled as described in **section 3.10.**

3.17.8. Histopathological analysis

Histopathological examination was carried out on collected organs from 3 randomly selected animals of each group. The tissues were fixed in 10% neutral buffered formalin and further processed for routine paraffin embedding (Dehydration using ascending grades of alcohol, clearing with xylene, paraffin impregnation, and paraffin

embedding). Sections of 4-5 micron thickness were taken using a microtome, stained with Haematoxylin and Eosin stain the National Liver Disease Biobank U/o Institute of Liver and Biliary Sciences, D-1, Vasant Kunj, New Delhi-110070. Additionally, the spleen was subjected to Perl's Prussian blue staining for hemosiderin at the Central Council for Research in Ayurvedic Sciences, Regional Ayurveda Research Institute, Gwalior. Finally, the slides were assessed for microscopic tissue manifestations (if any) by a veterinary pathologist.

3.17.9. Harmful intestinal enzyme assay

The activities of harmful intestinal enzymes viz. β-glucosidase and β-glucuronidase in the caecal content/ slurry were tested as detailed under **section 3.12.**

3.17.10. Bacterial translocation assay

The translocation ability of NCDC 400 from the gut to blood and other organs *viz*. (liver, lung, heart, spleen, brain, and kidney) was investigated as described in **section 3.13.**

3.17.11. Estimation of selective gut health indices

The few important gut health markers *viz*. faecal pH, ammonia, lactate, and SCFAs (acetate, butyrate, propionate, and total SCFA) were estimated as previously explained in **section 3.14.**

3.17.12. Effect of NCDC 400 on immune markers

The levels of immunoglobulins (IgG and IgA), inflammatory cytokines (IL-6, TNF-alpha, TGF-β, and IL-10), and chemokine (MCP-1) in serum were measured using commercially available mouse sandwich enzyme-linked immunosorbent assay (ELISA) kits (BT Bioassay, China; Krishgen BioSystems, Mumbai, India), as previously detailed under **section 3.15**.

3.17.13. Determination of oxidative markers

The serum enzymic oxidative markers such as superoxide dismutase (SOD), catalase (CAT), and glutathione peroxidase (GpX2) were measured using commercial mouse ELISA kits (Krishgen BioSystems, Mumbai, India), according to the manufacturers' protocol of sandwich ELISA, as previously detailed under **section 3.15**.

3.17.14. Determination of serum nitric oxide

Nitric oxide (NO) content in the serum was measured using the Griess reaction method (Srivastava *et al*., 2022). Initially, the serum was deproteinized by mixing equal volumes of serum and acetonitrile for 1 min and the mixture was centrifuged at 10,000 × g for 10 min at 4 °C (Ghasemi *et al*., 2007). The supernatant was used for NO estimation. Briefly, 50 µL supernatant as well as 50 µL 1 X Griess reagent (Sigma, USA) were mixed and incubated at room temperature for 45 min. Finally, the absorbance was measured at 550 nm. The amount of nitrite in the serum was determined using the sodium nitrite standard curve (**Annexure 1**).

3.17.15. Effect of NCDC 400 on macrophage functioning tests

3.17.15.1. Isolation of peritoneal macrophages

After the experimental duration, the mice were humanly sacrificed by ether overdosing and the peritoneal cavity macrophages were collected via intraperitoneal injection of 5 mL serum-free RPMI-1640 (HiMedia, India) containing L-glutamine and antibiotics *viz.* penicillin (5000 U/ mL) and streptomycin (5 mg/ mL) (HiMedia, India). The obtained cell suspension was centrifuged at 350 × *g* for 5 min and resuspended in RPMI-1640. The viability of macrophages in the suspension was determined using the trypan blue exclusion assay.

3.17.15.2. Phagocytic activity

The phagocytic activity of macrophages was investigated using the previous method (Kapila *et al*., 2007). Briefly, the macrophages were seeded to a 6-well tissue culture plate (Thermo Scientific, USA) at a concentration of 1×10^5 cells/ well. Cells were allowed to attach to the bottom of the culture plate by incubating at 37 °C for 2 h. After the incubation, 100 µL yeast suspension (10^8 cells/ mL) was added to each well and incubated for 1 h at 37 °C in 5 % CO_2 incubator. The spent medium was collected and stored at -20 ˚C for the estimation of markers of phagocytic activity of macrophages. Further, the cells were rinsed twice using PBS (pH 7.4) and stained with May–Grünwald dye (Himedia, India) for 10 min. Then, the cells were rinsed in the buffer and restained with 1 X Giemsa solution (NICE Chemicals Pvt. Ltd., India) for 10 min each. Finally, the excess stain was removed by rinsing with PBS (pH 7.4) and cells were observed using an inverted light microscope (Radical Scientific, India). The per cent phagocytosis

was calculated by considering the number of macrophages with internalized yeast per hundred macrophages.

3.17.15.3. Pinocytosis activity

Pinocytosis activity of macrophages was carried out according to the method of Wang *et al*. (2018). The macrophages were seeded in 96-well tissue culture plates (Thermo Scientific, USA) at a concentration of 1×10^5 cells/well. Cells were incubated for 2 h at 37 °C in 5 % CO_2 incubator with 95 % RH (Heal Force, HF90, China). The unbound cells were removed by rinsing two times with PBS. Further, 0.075% (*w*/*v*) neutral red (Sigma, St. Louis, USA) dissolved in PBS (pH 7.4) was added into each well and incubated for an additional 2 h at 37 °C. Subsequently, the cells were washed three times with PBS (pH 7.4) and 200 µL lysis or de-staining solution (glacial acetic acid: ethanol = 1: 1) was added to extract the dye inside the macrophages by incubating the 96-well plate overnight at 4 °C. The pinocytosis ability of macrophages was measured by recording the absorbance at 570 nm.

3.17.15.4. NO release

Nitrite release during the process of phagocytosis was measured in the culture supernatant of macrophages using the Griess reaction. Briefly, 100 µL of culture medium obtained after the yeast-induced phagocytic reaction **(section 3.17.15.2)** was mixed with an equal volume of 1 X Griess reagent (Sigma, USA) and incubated at room temperature for 45 min. Finally, the absorbance was measured at 550 nm. The amount of nitrite in the sample was determined using the sodium nitrite standard curve (**Annexure 1**).

3.17.15.5. β-glucosidase and β-glucuronidase activities

In this assay, 0.2 mL culture medium obtained after the yeast-induced phagocytic reaction **(section 3.17.15.2)** was mixed either with 0.8 mL of 2 mM p-nitrophenyl-β-D-glucopyranoside (for β-glucosidase activity) or 2 mM p-nitrophenyl-β-D-glucuronide (for β-glucuronidase activity) and incubated at 37 °C for 1 h. The reaction was ended by adding 1 mL of 0.5 mol/ L NaOH and the mixture were centrifuged at 4,000 × *g* for 10 min. The activities of β-glucosidase and β-glucuronidase were determined in the supernatant by recording the absorbance at 405 nm. The results were expressed based on the previously developed p-nitrophenol (PNP) standard curve described under **section 3.12.**

3.17.16. Splenocytes proliferation assay

3.17.16.1. Isolation of splenocytes

After the animal is sacrificed, the spleen from three representative animals per group was transferred to a sterile RPMI medium (HiMedia, India) containing L-glutamine and antibiotics *viz.* penicillin (5000 U/ mL) and streptomycin (5 mg/ mL) (HiMedia, India). For the isolation of splenocytes, the spleen was minced using a scissor and passed through a sterile cell strainer to obtain the homogenous cell suspension. The suspension was centrifuged at 350 × *g* for 10 min and the supernatant was discarded and the cell pellet was twice treated with 1 X RBC lysis buffer (0.154M ammonium chloride [NH_4Cl], 10mM potassium bicarbonate [$KHCO_3$], and 0.1 mM ethylenediaminetetraacetic acid [EDTA]) in order to lyse erythrocytes. After centrifugation at 200 × *g* for 10 min, the supernatant was discarded and the splenocytes were suspended in RPMI medium, and cells were counted by trypan blue exclusion assay using an inverted light microscope.

3.17.16.2. Splenocytes proliferation index

Splenocytes proliferation index was determined according to the method of Park and Lee (2018) as well as Wang *et al*. (2018). Accordingly, the splenocytes were seeded to the 96-well plates at 1×10^5 cells/ well and stimulated with 100 µL B-cell mitogen lipopolysaccharide (LPS) (Sigma-Aldrich, USA) at 5 µg/ mL and T-cell mitogen concanavalin A (ConA; HiMedia, India) at 10 µg/ mL in RPMI medium supplemented with 10% FBS, penicillin (5000 U/ mL) and streptomycin (5 mg/ mL) for 48 h. Following incubation, 10 µL of MTT dye (5 mg/ mL) was added and further incubated at 37˚C for 4 h in CO_2 incubator. The spent medium was replaced with 150 µL of DMSO and incubated at 37 ˚C/ 30 min. Finally, the plates were spectrophotometrically recorded at 570 nm. The stimulation index of splenocyte proliferation was calculated from the absorbance at 570 nm by splenocytes cultured in RPMI 1640 medium with ConA or LPS, divided by those cultured in RPMI 1640 medium alone.

3.17.17. *In vivo* genotoxicity assays

3.17.17.1. Micronucleus assay

After the removal of muscle adhered to the bone, the femur bone was separated and flushed by injecting the PBS (pH 7.4). The obtained bone marrow cell suspension was centrifuged at 1,000 rpm for 10 minutes. The obtained cell pellet was suspended in

100 µL of fetal bovine serum (FBS). A thin smear of bone marrow cell suspension was made on a glass slide. The slide was air dried, methanol fixed, and stained with 5% Giemsa stain (NICE Chemicals, Kochi, India) for 10-15 min. Finally, slides were visualized under an inverted light microscope. A total of 300 bone marrow erythrocytes were investigated per mouse to evaluate for any micronuclei (Pradhan *et al*., 2019a).

3.17.17.2. Chromosomal aberration assay

At the end of the study, 2 h before the animal dissection, three animals per group were intraperitoneally injected with mitotic inhibitor i.e., Colchicine (4 mg/ kg/ BW) (Sigma, St. Louis, USA) (Pradhan *et al*., 2019a). After the dissection, the bone marrow cells (BMCs) were flushed from the femur bone using 0.56% KCl solution. The cells were incubated at 37 ˚C for 20 min in the KCl solution. The cell suspension was centrifuged at 1,000 rpm/ 10 min. The cell pellet of BMCs was then fixed with Carnoy's fixative (methanol and acetic acid at 3:1). Further, the cells were burst open by dropping the cell suspension onto a pre-chilled glass slide from at least 1 meter height. The slides were air-dried and stained with 5% Giemsa stain for 15-20 min. The slides were visualized under an inverted microscope under 100 X objective. Finally, 100 well-separated metaphase arrested plates (metaphase stage of the chromosome) per mouse were evaluated for structural aberrations, and the results were expressed as % chromosomal aberrations (CA).

3.17.18. Faecal bacterial analysis

3.17.18.1. Extraction of metagenomic DNA

The faecal samples were thawed on ice before metagenomic DNA extraction. The community DNA was extracted from 3 samples per group using Quick-DNA Faecal/Soil Microbe DNA Miniprep Kit (Zymo Research, USA) as per the manufacturer's instructions given below with some modifications.

- Exactly 150 mg of faecal sample was transferred to a ZR BashingBead™ Lysis Tube (0.1 & 0.5 mm) and 750 µL BashingBead™ buffer was added to the same tube.
- The tube was fitted onto a holder assembly of bead homogenizer (MP Biomedicals LLC, Solon, OH, USA) and processed for cycling protocol of 3

cycles (4m/ sec) of 40 sec each with 5 min rest and cooling of samples in ice after each cycle.

- The ZR BashingBead™ Lysis Tube (0.1 & 0.5 mm) was centrifuged at ≥ 10,000 × *g* for 1 min.
- The resultant supernatant was transferred to a Zymo-Spin™ III-F Filter in a Collection Tube and further centrifuged at 8,000 × *g* for 1 min.
- An aliquot of 1,200 µL of Genomic Lysis Buffer (previously added with beta-mercaptoethanol at 500 µL/ 100 mL) was added to the same filtrate in the Collection Tube and mixed well.
- Exactly 800 µL of the above mixture was transferred to a Zymo-Spin™ IICR Column in a Collection Tube and centrifuged at 10,000 × *g* for 1 min. The flow-through was discarded from the Collection Tube and this step was repeated for another 800 µL mixture.
- An aliquot of 200 µL DNA Pre-Wash Buffer was added to the Zymo-Spin™ IICR Column in a new Collection Tube and centrifuged at 10,000 × *g* for 1 min. Further, 500 µL g-DNA Wash Buffer was added to the Zymo-Spin™ IICR Column and centrifuged at 10,000 × *g* for 1 min.
- Zymo-Spin™ IICR Column was transferred to a clean 1.5 mL microcentrifuge tube and 50 µL DNA Elution Buffer was added to the column matrix. The content was centrifuged at 10,000 × *g* for 30 sec to elute the DNA.
- A Zymo-Spin™ III-HRC Filter was placed in a clean Collection Tube and 600 µL Prep Solution was added and centrifuged at 8,000 × *g* for 3 min.
- The eluted DNA was transferred to a Zymo-Spin™ III-HRC Filter in a clean 1.5 mL microcentrifuge tube and centrifuged at exactly 16,000 x *g* for 3 min. Thus obtained metagenomic DNA was stored at -20˚C until further analysis.

3.17.18.2. Evaluation of quantity, purity, and integrity of metagenomic DNA

The purity and quantity of metagenomic DNA were determined spectrophotometrically using SYNERGY H1 Hybrid Multimode Reader (BioTEK, Winooski, VT). An aliquot of 2 µL extracted DNA was loaded onto the NanoQuant Plate and scanned at the wavelength of 260 and 280 nm. The concentration of DNA (nucleic

acid quantification) was determined by considering the absorbance at A_{260}. On the other hand, the purity of metagenomic DNA was determined by calculating the A_{260}/ A_{280} ratio.

The integrity of metagenomic DNA was analyzed by conducting agarose gel electrophoresis. Agarose gel (0.8% concentration) was prepared by dissolving an appropriate quantity of agarose in 1 X TAE buffer (pH 8.0) added with EtBr of 0.5 µg/ mL before casting the gel. The gel was moulded on a casting try and placed in a horizontal electrophoresis tank (Mini submarine, Hoeffer, USA). The electrophoresis tank was filled with 1 X TAE electrophoresis buffer to cover the gel to a depth of about 1 mm. An aliquot of 2 µL DNA was mixed with 2 µL of loading dye and loaded into the wells of the gel. Electrophoresis was carried out in 1 X TAE running buffer (pH 8.0) at 90 V. Finally, the gel was examined under Gel Documentation (Gel-Doc) system (Gel Doc XR+, BIO-RAD).

3.17.18.3. 16S rDNA amplicon sequencing and data analysis

Faecal 16S rDNA amplicon sequencing and data analysis was performed according to Kumari *et al*. (2022). Briefly, the profiling of the 16S rRNA V3-V4 hypervariable region of faecal samples was performed using Illumina (Novaseq 6000) platform to compare the microbiota diversity and composition across the faecal DNA samples of different groups. The obtained sequences (.fastq files) were processed with the QIIME2 (version 2.2021.2) bioinformatics pipeline, in a miniconda environment, followed by quality-filtering, adapter-trimming, denoising, and removal of non-chimeric amplicons by using the dada2 pipeline using default parameters. The Amplicon sequence variants (ASVs) were assigned bacterial taxonomic nomenclature by using the Naive Bayes classifier natively installed in dada2 workflow and pre-trained with SILVA reference database (version 138.1) with 99% sequence identity threshold. The obtained sequence reads were filtered to exclude features annotated as 'mitochondria' and 'chloroplast'. Community richness (alpha-diversity) indices included Chao1 index and Shannon index and were calculated within QIIME2. Community dissimilarities (β-diversity) were estimated using principal coordinate analysis (PCoA) of the Bray–Curtis dissimilarity index within QIIME2. The resultant dataset was analyzed in two output forms: the raw abundance tables for ASVs and their respective taxonomic assignments. The raw read counts were transformed to relative abundances by dividing each value by the total reads per sample and collapsed to taxonomic levels by summing their respective

relative abundances. Finally, the bacterial community composition was measured at taxonomic levels of phylum, family, and genus.

3.18. Statistical analysis

A minimum of three independent trials were carried out in all experiments and the results are expressed as mean ± standard error of the mean (SEM). One-way analysis of variance (ANOVA) followed by Duncan Post hoc test or t-test was performed wherever appropriate by IBM SPSS (Version 26.0, Chicago, IL, USA) and GraphPad Prism (version 8), to consider the significance at $p < 0.05$. The graphs were prepared using GraphPad Prism (version 8) and Microsoft Office (2007).

Results & Discussion

RESULTS AND DISCUSSION

Albeit nearly most of the probiotic strains are isolated from conventional eco-systems like dairy and human sources, it is inevitable to subject them to para and pre-clinical trials focusing on safety and efficacy to endorse their health claims and human compatibility. As evidenced by the literature, these bacteria, unless carefully studied, cannot be declared to be safe because they may possess harmful factors that deem them unfit for human consumption. Rather, a comprehensive battery of *in vitro* and *in vivo* toxicology testing may help eliminate the potentially hazardous strains from the human food chain. Accordingly, *in vitro* safety tests are the preliminary tests that endow basic knowledge of strain on human blood compatibility, drug resistance, compatibility with extracellular matrix (mucin), metabolic capabilities concerning the production of harmful enzymes and metabolites, and so on. Hitherto, considerable progress has been made in whole genome sequencing (WGS) technologies, and candidate probiotic strains are generally sequenced using cost-effective next-generation sequencing (NGS) technologies. Hence, analyzing the genome data using suitable bioinformatics tools enables us to comprehend the molecular mechanism underlying the physiological functions including the key features of virulence, antibiotic resistance, and adverse metabolites. Moreover, the virulence phenotypes can be linked and validated by functional annotation of the genome architecture. More importantly, such whole genome-based safety studies also provide an idea of bacterial genome stability by uncovering the possible mobile genetic elements, prophage sequences, and CRISPR sequences in the complete genome. In the second phase, pre-clinical trials are conducted to establish the safety and efficacy of the strain trials in animals (most preferably rodents). *In vitro* toxicology trials are generally well-designed to determine the safer dose. Such studies provide clear knowledge of changes in body weight, clinical signs of toxicity, feed consumption, clinical pathology, etc. Additionally, these studies are aimed at; (i) determining the safe starting dose for clinical trials, (ii) providing insights on probiotic administration regime that results in the least chronic toxicity, (iii) offering knowledge on biomarkers for clinical monitoring, and (iv) estimate the effects of long-term exposure on organ/ tissue toxicity and carcinogenicity as well as its reversibility (efficacy). Considering these facts, the present study, herein, evaluated the safety and efficacy perspectives of *L. fermentum* NCDC 400 using appropriate *in vitro*, *in silico*,

and *in vivo* approaches. The results obtained from the current investigation are discussed in this chapter.

Objective 1: Assessment of *Limosilactobacillus fermentum* NCDC 400 for safety aspects using *in vitro* methods.

4.1. Reconfirmation of purity and identity of NCDC 400

The purity of NCDC 400 was evaluated by microscopic and biochemical tests. Upon negative straining, the culture appeared to be long rods arranged in chains. In differential staining, the bacterium was found to be Gram-positive by exhibiting purple color. NCDC 400 did not show brisk effervesces upon treatment with hydrogen peroxide, indicating that it is negative for the catalase test. These manifestations indicate that the culture used throughout the experimentation process was devoid of contamination. Lately, the identity of NCDC 400 was confirmed by species-specific PCR. For this purpose, the genomic DNA was extracted from the active culture and used as a template for the PCR reaction. The amplification of the specific region of genomic DNA with a set of *L. fermentum*-specific primers (LF1 and LF2) (the primer specificity was confirmed by NCBI-BLAST) resulted in the formation of a desirable amplicon size of 337 bp (**Fig. 4.1)** (Dickson *et al.,* 2005). This reconfirms the molecular identity of the strain under investigation as *L. fermentum*.

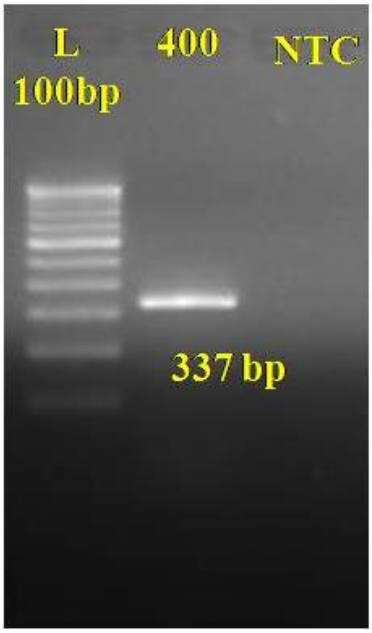

Fig. 4.1: Gel image re-confirming the molecular identity of test strain as *L. fermentum* by species-specific PCR approach. (L: DNA ladder 100 bp; 400: NCDC 400; NTC: Non-template control).

4.2. Molecular typing of NCDC 400

In this study, RAPD-PCR was used to identify and discriminate the NCDC 400 at strain level. The amplification of genomic DNA with four different single arbitrary primers (M13, OPA5, OPA18, and OPA30) resulted in different RAPD fingerprints (DNA band patterns) due to the random hybridization of these primers to DNA. The amplification with M13 resulted in the formation of two intense bands of above 1 kb and one at 400 bp. Three prominent faint bands appeared between 300-400 bp (**Fig. 4.2**). Although OPA5 could not able to hybridize the several regions of genomic DNA, it could amplify two regions of genomic DNA resulting in the two faint bands above 1 kb. In contrast, OPA18 and OPA20 could not amplify the genomic DNA. This could be due to the absence of primer homology with that of the chromosomal DNA to detect the polymorphs. It is important to mention that the RAPD-based PCR amplification of genomic DNA with a minimum of ten times resulted in the generation of the same band pattern, thereby indicating that the method is reproducible and can be applicable for strain level discrimination. Overall, the developed RAPD fingerprint would be useful in the strain-specific identification of test stain wherever required in this study. RAPD is quite a rapid and effective molecular typing tool with several advantages like good discriminative power, ease of execution, inexpensive, and general applicability. Although this technique is blamed to have poor reproducibility, it can be overcome by an accurate optimization of assay protocol such as quality and quantity of DNA, primer concentration, annealing conditions, etc. (Sharma *et al*., 2020). However, poor reproducibility was not witnessed in this study because we found uniformity in the RAPD fingerprint generated even as high as ten times using the optimized conditions.

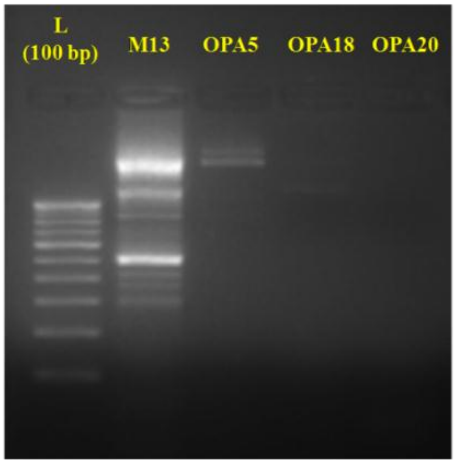

Fig. 4.2: Gel image depicting the RAPD fingerprint of *L. fermentum* NCDC 400

4.3. Plasmid profiling of *L. fermentum* NCDC 400

The plasmid DNA extraction from NCDC 400 using the conventional alkali lysis method or ZR plasmid MiniPrep-Classic yielded no plasmids. Hence, slight modifications in the kit protocol to include the addition of lysozyme (5 mg/ mL) to the P1 buffer, and an additional incubation step at 37 °C yielded two plasmids of approximate size 8 kb (plasmid A) and 5 kb (plasmid B) (**Fig. 4.3**). However, NCDC 167 (Dahi culture), which was used as a positive control to validate the accuracy of the assay protocol, demonstrated 6 plasmids of varying size and band intensity. The plasmid band intensity generally depends on the copy number at the present physiological state. Plasmids are the important extra-chromosomal self-replicating DNA molecules present in bacteria. These encode, but not necessarily, several metabolic and resistance-providing functions. Of them, the plasmid-associated antibiotic resistance genes (ARGs) are of major concern as these plasmids may have lateral transferability. However, it should be noted that not every plasmid is mobile unless they are equipped with F-factor. Moreover, the stability of these plasmids is debatable as bacteria may eliminate the plasmid whenever the plasmid-encoded function is necessary for survival or the absence of selective pressure may also promote plasmid loss (Cui *et al*., 2015). LAB frequently possess the plasmids in varying numbers. Amongst, the genus *Lactobacillus* has been reported to carry 1-10 plasmids of smallest to largest size. The species like *L. plantarum*, *L. salivarius*, and *L. acidophilus* have been reported to exhibit megaplasmids of 120-490 kb (Cui *et al*., 2015). In comparison, NCDC 400 had two extractable plasmids (<10 kb) at the current physiological state. These results are consistent with the findings of Chin *et al*. (2005), who reported the 2-5 plasmids of < 12 kb in *L. fermentum* strains.

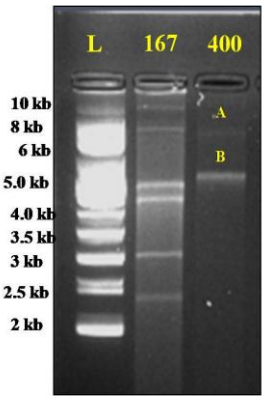

Fig. 4.3: Agarose gel displaying the plasmids of NCDC 400

(L: supercoiled DNA ladder, 167: Dahi culture NCDC 167, 400: NCDC 400)

4.4. Characterization of NCDC 400 for the possible virulence determinants using *in vitro* approaches

4.4.1. Hemolytic activity

EFSA strongly recommends assessing the hemolytic activity of probiotic strains intended for food applications even if they have a long history of safe use or are known to have Generally Recognized as Safe (GRAS) or Qualified Presumption of Safety (QPS) status. In accordance, NCDC 400 demonstrated the ɣ-hemolytic property (no hemolysis) as it did not show the clear zone around the streaked area on the blood agar. In contrast, *S. aureus* NCDC 110 (positive control) revealed strong beta-hemolytic properties by demonstrating a clear zone around the streaked area.

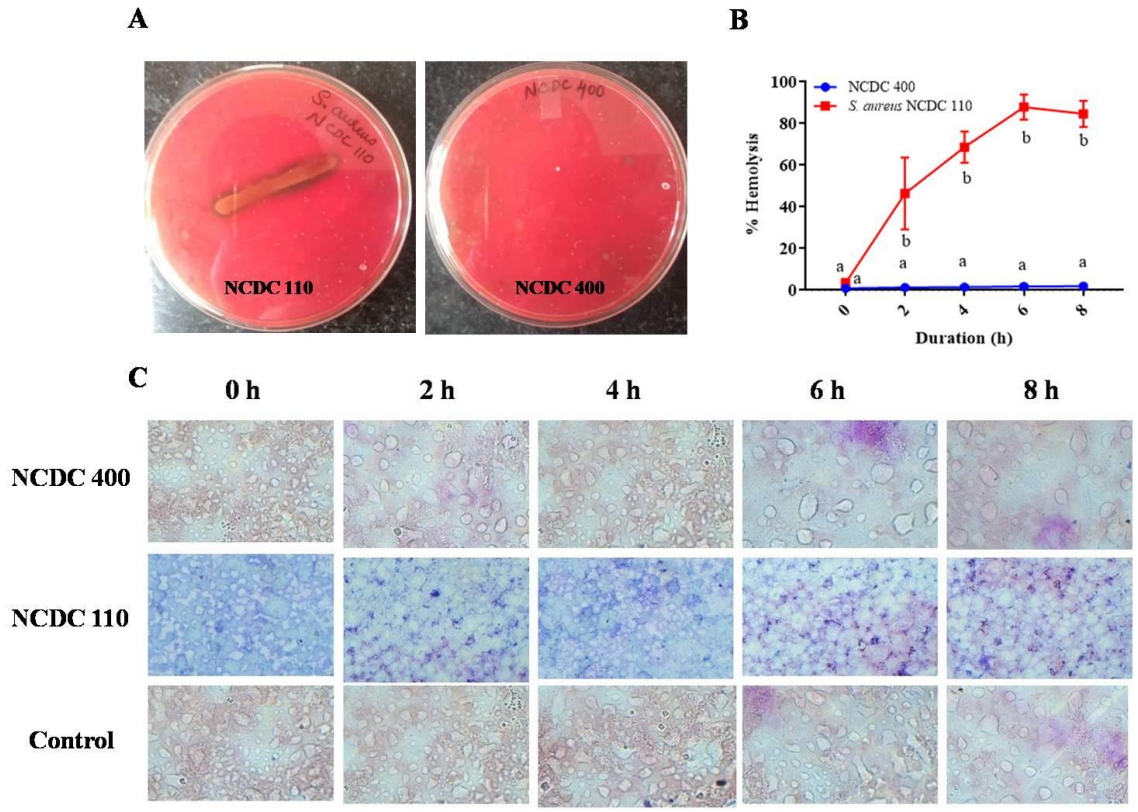

Fig. 4.4: Representative images and microphotographs (100 X) depicting the non-hemolytic property of NCDC 400. (A) Streak assay; (B) Spectrophotometric method; (C) Giemsa staining of RBC. Error bars indicate the variations of three determinations in terms of the standard error of mean. Superscripts (a and b) represent the significant differences ($p < 0.05$) between the NCDC 400 and *S. aureus* at different time interval (*t-test was performed to compare two means*).

In the spectrophotometric assay, *S. aureus* NCDC 110 showed a time-dependent increase in the hemolytic activity to as high as 87.91±3.42% at 8 h. In contrast, NCDC

400 showed negligible hemolysis contributing less than 1.5% over 8 h of exposure, clearly signifying its safe use. There was no constant increase in the RBC lysis phenomenon with an increase in the exposure time. This indicates that NCDC 400 typically lacks the hemolytic property. In analogy with these findings, the RBC treated with NCDC 400 revealed no damage in the membrane integrity even after 8 h of exposure while the treatment with *S. aureus* NCDC 109 demonstrated a severe loss of integrity as evidenced upon Giemsa staining of RBC after post-exposure to the cell-free supernatant of the bacterial culture. Overall, these results conclusively suggest that NCDC 400 typically lacks the hemolytic phenotype. Our results are in agreement with Tarrah *et al*. (2019), who also reported the absence of alpha-hemolysis in a few *Lactobacillus* strains. In contrast, another group of researchers witnessed alpha hemolysis (partial hemolysis or green hemolysis) by most *Lactobacillus* strains (93%) due to the formation of methemoglobin upon the hydrogen peroxide-induced oxidation of hemoglobin (Domingos-Lopes *et al*., 2017). Hence, considering the metabolic features of LAB, alpha-hemolysis may be considered generally acceptable for this category of microbes.

4.4.2. DNase activity

NCDC 400 did not exhibit DNase activity, which was confirmed by the absence of a pinkish zone around the wells added with the cell-free supernatant of NCDC 400. On its counterpart, *S. aureus* ATCC 25923 demonstrated DNase activity which was visible on the DNase assay plate showing the clear zone with a pale pinkish appearance (**Fig. 4.5**). These observations are in agreement with the previous report indicating the absence of DNase activity in probiotic *Lactobacillus* cultures (Somashekaraiah *et al*., 2019). Though several pathogens are known to secrete this enzyme extracellularly, a handful of *Lactobacillus* and *Enterococcus* strains have shown positive for extracellular DNase activity in a strain-dependent manner (Romero, 2020; Câmara *et al*., 2020).

4.4.3. Coagulase test

The exposure of human plasma to the NCDC 400 did not foster plasma coagulation. *S. aureus* ATCC 25923 (positive control), on the other hand, could rapidly coagulate the plasma within 2 h of co-incubation (**Fig. 4.5**). Similarly, researchers have also reported the absence of coagulase activity among a majority of *Lactobacillus* strains (Abe Sato *et al*., 2021). Although coagulase expression is most commonly reported in

pathogens, few *Lactobacillus* isolates have been reported to display coagulase activity (Razmgah *et al*., 2016). This calls for the researchers to include coagulase activity as one of the bio-safety parameters to be investigated for probiotic strains. However, the NCDC 400 has been tested to be devoid of coagulase activity.

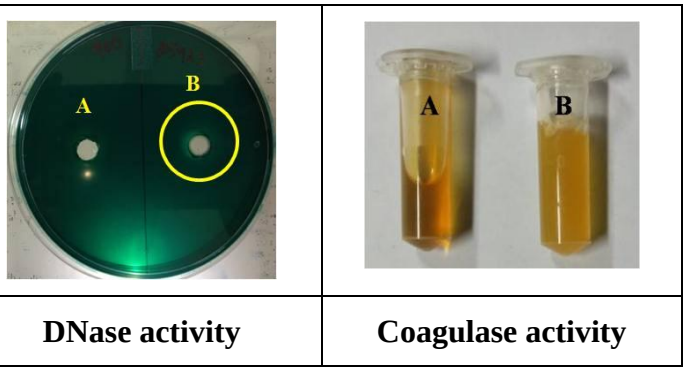

Fig. 4.5: Agar plate and plasma tube displaying the absence of DNase and coagulase activities in NCDC 400. (A) NCDC 400; (B) *S. aureus* ATCC 25923

4.4.4. Ammonia production test

The ammonia production by NCDC 400 was estimated by indophenol reaction method. Accordingly, NCDC 400 could produce relatively lesser ammonia which may not be harmful at such a lower concentration (**Fig. 4.6a**). In contrast, the metabolic activity of *Pseudomonas* spp. (proteolytic strain) could produce a significantly ($p < 0.0001$) higher amount of ammonia (0.69 ± 0.09 µg/mL) compared to NCDC 400 (0.02 ± 0.01 µg/mL). However, the ammonia production by NCDC 400 was relatively lesser than that reported for probiotic *L. fermentum* OK (68 ± 1 µg/mL) (Mann *et al*., 2021a). It is worth pointing out that the concentration of ammonia produced by NCDC 400 is far below the toxic level mentioned by South Korea's Ministry of Food and Drug Safety's milk product quality (Sohn, 2016). The lower ammonia production by NCDC 400 may be correlated to the absence of urease activity which converts urea to carbamate and ammonia (Solga, 2003). These results are in close agreement with earlier work demonstrating negligible ammonia production by *L. gasseri* HHuMIND, a strain designated as oral probiotics (Mann *et al*., 2021b). The level of ammonia production by food-grade microbes and commercial probiotics should be carefully monitored since excess ammonia is closely linked to human health. The decomposition of protein in the intestine may produce toxic end products like amines, phenol, ammonia, and indole that may damage the liver and induce the activation of co-factors that damages the cell,

ultimately resulting in chronic hepatic toxicity and hepatic encephalopathy (Ishibashi and Yamazaki, 2001).

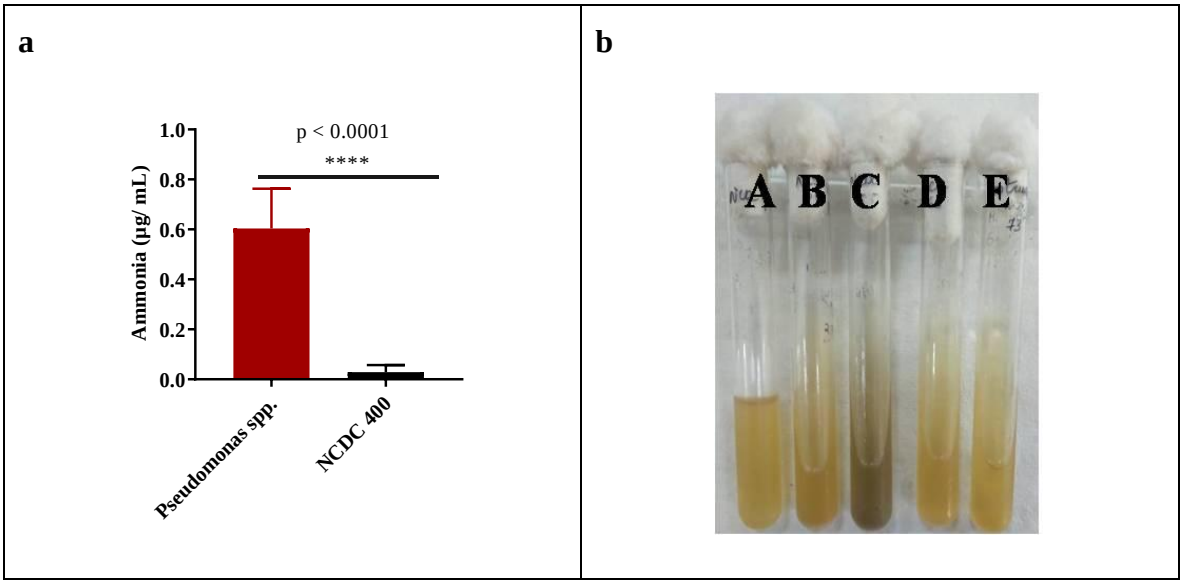

Fig. 4.6: Ammonia production and gelatinase activity by NCDC 400. (a) Bar graph respresenitng the ammonia production; (b) Gelatin liquefaction test showing the absence of gelatinase activity in NCDC 400; (A) NCDC 400; (B) *Serratia marcescens* NCDC 108; (C) *Pseudomonas aeruginosa* NCDC 105; (D) *Bacillus cereus* NCDC 66; (E) *Proteus vulgaris* NCDC 73. Error bars indicate the variations of three determinations in terms of the standard error of mean. Asterisks (****) indicate significant difference at $p < 0.0001$ when tested by t-test for comparing two means.

4.4.5. Gelatinase activity

As gelatinase is one of the pathogenic determinants by which bacteria invade the host tissue, the gelatin liquefaction test was conducted as a prime *in vitro* biosafety assay. In response, NCDC 400 failed to liquefy the gelatin and thereby suggesting the absence of gelatinase activity **(Fig. 4.6b)**. In contrast, other pathogenic cultures, used as positive controls, displayed the gelatin liquefaction phenotype. These results are similar to previous findings by Rastogi *et al*. (2020), wherein they have shown the absence of gelatin hydrolysis by probiotic *Lactobacillus* strains. In contrast, several enterococci isolates have shown a positive gelatinase reaction (Muñoz-Atienza *et al*., 2013).

4.4.6. Urease test

As evidenced by **Fig 4.7A**, NCDC 400 was devoid of urease activity in contrast to positive controls (*Proteus vulgaris* NCDC 73 and faecal flora) that showed a positive reaction on Christenson urea agar by changing the color of the medium from pale yellow

to deep pink. This result is similar to the findings of Kang *et al*. (2019) who noted urease negative phenotype among probiotic *Weissella cibaria* CMU and CMS1 strains. Although urease offers an adaptative phenotype to survive under acidic conditions by neutralizing the pH of the vicinity by producing ammonia, it is mostly considered a harmful enzyme and virulent phenotype. It is because the end product of urease action i.e., ammonia, a toxic nitrogenous metabolite, has been associated with liver toxicity and mucosal injury. Thus formed ammonia has been involved in fostering various debilitating pathophysiologies like urolithiasis, pyelonephritis, ammonia-induced hepatic encephalopathy, hepatic coma, and gastroduodenal infections (Mora and Arioli, 2014)

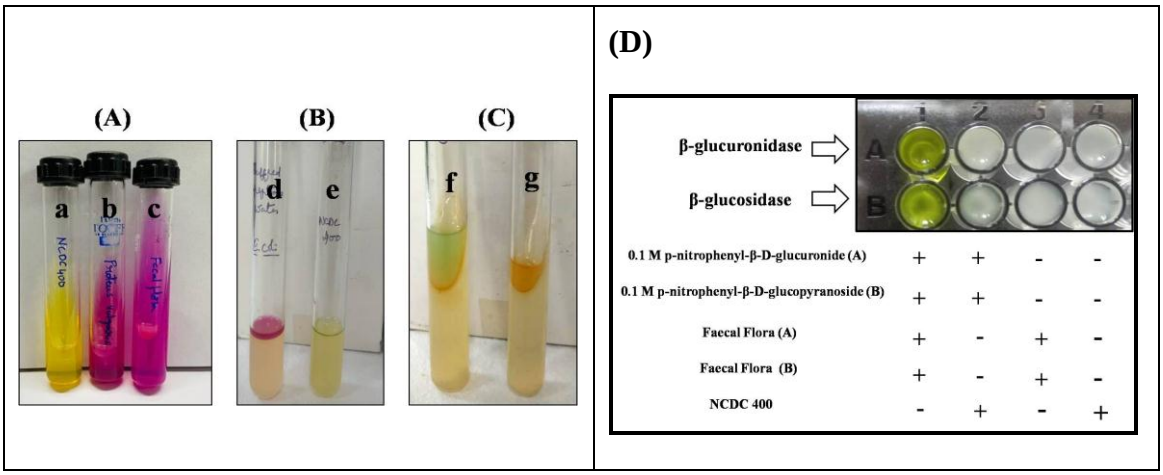

Fig. 4.7: Qualitative approaches for assaying urease action (A), indole production (B), phenylalanine degradation ability, and harmful intestinal enzymes activity (β -glucosidase and β -glucuronidase activity) (D) in NCDC 400. The labeling of test tubes is as here; a, e, g: NCDC 400; b, f: *Proteus vulgaris* NCDC 73; c: Faecal flora; d: *E. coli* NCDC 134

4.4.7. Indole test

NCDC 400 did not produce indole as it fails to produce a pink ring after the addition of Kovac's reagent. However, *E. coli* NCDC 134 (positive control) showed a pink ring suggesting a positive response for the test (**Fig. 4.7B**). This result aligns closely with the earlier findings reporting the absence of indole production by candidate probiotic strains of *Limosilactobacillus reuteri* (Lee *et al*., 2009). Another report by Li *et al*. (2018) also underpins the negative reaction of enterococci probiotic strains toward indole production. Indole is an important nitrogen-derived harmful metabolite that may be produced by microbes upon protein or peptide degradation in the intestinal milieu (Ishibashi and Yamazaki, 2001). The activity of tryptophanase converts the tryptophan to indole. The overproduction of indole is associated with neurotoxic effects with reduced

motor activity and increased anxiety (Jaglin *et al*., 2018). Additionally, skatol and phenols are considered potential biomarkers of colorectal cancer. Hence, potential probiotic strains must be evaluated for indole overproduction as these microbes are generally ingested in relatively higher doses.

4.4.8. Phenylalanine degradation test

The phenolic compounds from the aromatic amino acids (tyrosine and phenylalanine) derived from the metabolic action of intestinal microbes are known to cause gastroesophageal cancer (Wiggins *et al*., 2015). Owing to this fact, the production of phenylpyruvate with the action of phenylalaninase was investigated. The phenylpyruvic acid, if present in the medium, turns to green color upon reaction with 10% ferric chloride. In this study, the positive control *P. vulgaris* NCDC 73 displayed a green color reaction between phenylpyruvic acid and 10% ferric chloride. However, the NCDC 400 did not show green color at the end (**Fig. 4.7C**), suggesting that it will not produce phenylpyruvic acid. The results are in agreement with Kang *et al*. (2019) who also reported the absence of phenylalanine degradation capability among lactic strains.

4.4.9. Harmful intestinal enzymes

The activities of two harmful intestinal enzymes such as beta-glucosidase and beta-glucuronidase were evaluated in NCDC 400. As evident from **Fig. 4.7D**, NCDC 400 fails to interact with the specific substrate for beta-glucosidase and beta-glucuronidase which results in no color formation. Whereas, the positive culture (faecal flora) produced specific enzymes that can in turn hydrolyze the p-nitrophenyl-β-D-glucopyranoside and p-nitrophenyl-β-D-glucuronide substrates to nitrophenol which contributes to yellow color development. This evidence suggests that NCDC 400 does not show the activity of beta-glucosidase and beta-glucuronidase. These results are in harmony with the report of Kang *et al*. (2019) who also suggest the lack of these harmful enzymes activity in a few lactic strains of probiotic candidature. Beta-glucosidase and beta-glucuronidase are the major enzymes considered to be carcinogenic factors for colorectal cancer and have been associated with the generation of potential carcinogenic metabolites by converting procarcinogens into carcinogens (O'Bryan *et al*., 2013)

4.4.10. D-/ L- lactic acid production

Although rare in healthy individuals, D-lactic acid may cause acidosis among patients with short bowel syndrome. Hence, the ability of NCDC 400 to produce D-/ L-

lactic acid was quantified in contrast to L- and D- isomers producer strains like *E. faecalis* and *Leuconostoc* spp., respectively. It was found that NCDC 400 notably produces L-lactic acid (0.71 ± 0.04 g/ L) corresponding to nearly about 77.52% (**Table 4.1**). The level of D-lactate produced by NCDC 400 corresponds to relatively a lower proportion (0.21 ± 0.02 g/ L). This suggests that NCDC 400 may have least potential to cause D-lactic acid-related toxicity. However, it should be considered that currently there are no recommended higher limits for D-lactic acid levels for probiotics/ probiotics derived fermented foods. Hence, a comparison with commercial reference strains or published literature would serve as a better indication to substantiate the safety of new probiotic strains. Accordingly, *L. rhamnonss* GG, a well-studied probiotic has also been reported to produce D-lactic acid (Gorbach *et al*., 2017). Similarly, our results are in close agreement with Meleh *et al*. (2020) and Lee *et al*. (2022) who also observed the production of a relatively lower amount of D-lactic acid by potential probiotic *Limosilactobacillus* isolates. Different strains of lactobacilli create these lactic acid isomers in idiosyncratic ratios depending on the genome fingerprints as well as environmental factors. No strain creates 100% one isomer alone but there is wide variability in the ratio of D-/L- forms across the lactobacilli (Gorbach *et al*., 2017).

Table 4.1: Idiosyncratic proportion of isomers of lactic acid produced by NCDC 400

Cultures	D–lactate (g/ L)	L-lactate (g/ L)
E. faecalis	0.04 ± 0.03 (5.70%)	0.77 ± 0.05 (94.30%)
Leuconostoc spp.	0.81 ± 0.01 (99.85%)	0.0012 ± 0.01 (0.14%)
NCDC 400	0.21 ± 0.02 (22.70%)	0.71 ± 0.04 (77.52%)

Note: Values are presented as the mean ± SEM (n = 3)

4.4.11. Resistance to human serum

In comparison to community-type microbes isolated from human faeces (faecal flora), NCDC 400 was relatively sensitive to the bactericidal effect of human serum. It was noticed that 3 h of exposure of human serum to NCDC 400 resulted in the logarithmic reduction in bacterial viability by 3.36 ± 0.23 (**Fig. 4.8A**). In contrast, faecal flora was quite resistant to the antagonistic activity of serum as evidenced by only 1.39 ± 0.33 $\log_{10}$ reductions in their viability even after serum exposure for 3 h, suggesting their survival during the bloodstream infections. However, there was no considerable loss of

bacterial viability in the buffer system was observed among both cultures. Humans have several barriers to protect from various infections. Even if the gut bacteria cross the epithelial as well as immunological barriers and enter the bloodstream, the complement systems in the blood opsonize bacteria and facilitate their phagocytosis. Thus, the activated complement system can also form a membrane-active complex that kills bacteria (Vesterlund *et al*., 2007). But the serum-resistant bacteria proliferate and colonize the system and aggravate the life-threatening broad spectrum of pathologies like bacteremia, sepsis, infective endocarditis, pyelonephritis, reactive arthritis, carotid arterial plaques, coronary thrombosis, atherosclerosis, etc. (Minasyan, 2019). Hence, serum resistance is considered an undesirable phenotype of any food-grade bacteria. In this regard, approximately 99.9% (> 3 log reduction) decrease in the viability of NCDC 400 suggests the incapability to grow and proliferate in serum. This result is analogous to the findings of Baumgartner *et al*. (1998) who noticed that *Lactobacillus* strains of non-human origin, in contrast to the clinical origin, were more sensitive to the bactericidal effect of human serum.

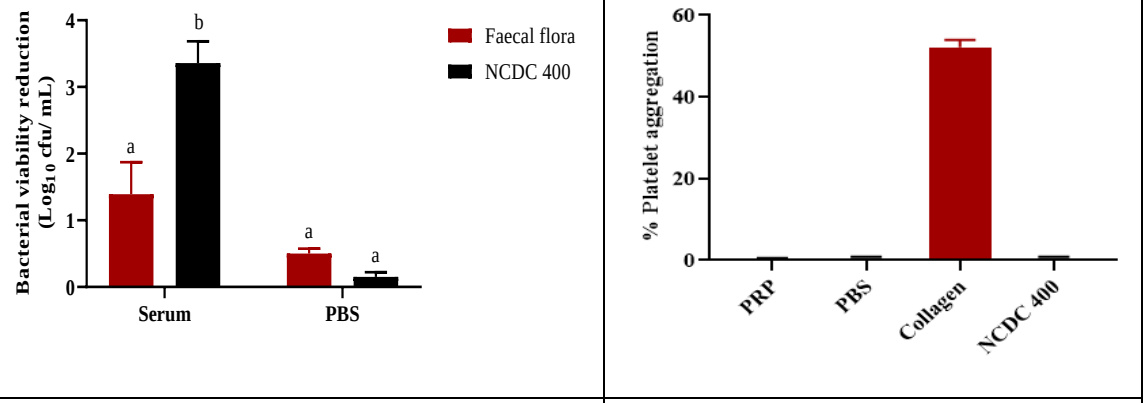

A. Serum resistance | **B. Platelet aggregation**

Fig. 4.8: Bar-graph representing the serum sensitivity and platelet aggregation ability of NCDC 400. Error bars indicate the variations of three determinations in terms of the standard error of mean. Lowercase superscripts (a and b) in serum resistance test indicate the significant differences ($p < 0.05$) between the faecal flora and NCDC when tested by t-test for comparison of two means.

4.4.12. Platelet aggregation test

In contrast to collagen, a known platelet aggregation agonist, NCDC 400 was incapable of aggregating the platelets under *in vitro* conditions (**Fig. 4.8B**). On the other

hand, collagen showed 52.14 ± 1.03% platelet aggregation. Our results are in agreement with the previous work that reports the absence of platelet aggregation ability of two potential probiotic strains (*L. plantarum* and *L. fermentum* strains) of human gut origin (Pradhan *et al*., 2019a). In contrast, bacteremia-associated *Lactobacillus* cultures have been shown to aggregate the platelet *in vitro (*Kirjavainen *et al*., 1999). This clearly suggests that the source of origin of bacteria plays a pivotal role before their food or pharma applications. Hence, safety evaluation of probiotic bacteria before food applications is imperative to evade avoidable health concerns. Of them, platelet adhesion, also known as platelet aggregation, is an essential test to be acknowledged because bacterial-mediated platelet aggregation has been linked with the progression of infective endocarditis (Ishibashi and Yamazaki, 2001). The bacterial mediated aggregation is believed to be associated with the various cell surface-associated proteins and aggregation substances (*agg*) (Gueimonde *et al*., 2004).

4.4.13. Biogenic amines production test

The ability to produce biogenic amines (tyramine, cadaverine, histamine, and putrescine) from decarboxylation of respective amino acids *viz*. tyrosine, lysine, histidine, and arginine was tested in three different stages. Firstly, NCDC 400 was sub-cultured four times in decarboxylase broth containing specific amino acids. In response, there was no color change in the medium to which NCDC 400 was inoculated suggesting that the pH of the medium remained acid. However, the medium inoculated with the positive cultures showed purple coloration thereby indicating that the production of alkaline biogenic amines might have turned the medium pH towards the basic side (pH > 6.0). This provides a presumptive confirmation that NCDC 400 does not produce biogenic amines. In comparison with NCDC 400, there was a significant ($p < 0.05$) increase in pH of the medium inoculated with positive cultures that are known to produce specific biogenic amines (**Fig. 4.9A**). Secondly, the bacterial cultures subcultured in decarboxylase broth were streaked on decarboxylase agar supplemented with specific amino acid. An analogy with the previous results, in contrast to the purple coloration in the positive culture straked area on decarboxylase agar, there was no such color change observed in the vicinity of the NCDC 400 streaked area (**Fig. 4.9B**). This qualitatively clarifies that NCDC 400 does not have metabolic capabilities to produce biogenic amines.

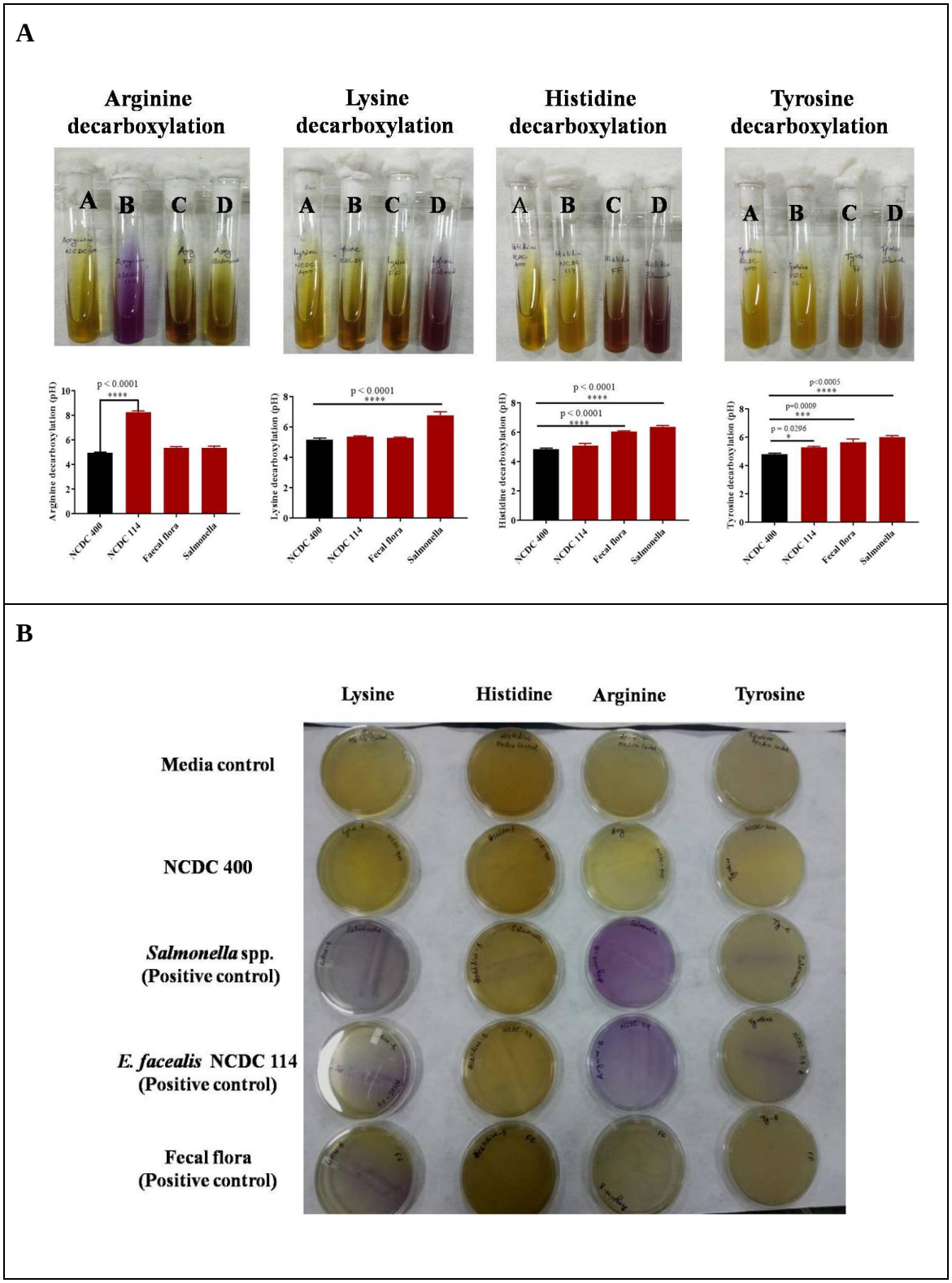

Fig. 4.9: Decarboxylase broth (A) and agar plates (B) demonstrating the qualitative estimation of biogenic amines production by NCDC 400 by the change in color and pH of the media. Error bars indicate the variations of three determinations in terms of the standard error of mean. Asterisks indicate significant difference between the groups at $p < 0.05$ when tested by one-way ANOVA following Duncan test.

Further, an attempt was made to detect cadaverine, putrescine, and tyramine in the MRS medium supplemented with specific amino acids after four times repeated subculturing of NCDC 400. However, none of the biogenic amines were detected in the medium, as shown in the HPLC chromatogram (**Fig. 4.10**). These results commemorate the findings of Ku *et al*. (2020) who also validated the inability to produce biogenic amines by potential probiotic strains through HPLC. Yet another similar study reported exactly opposite findings underscoring the high levels of biogenic amines production by food-grade LAB (Deepika *et al*., 2011). However, it should be considered the metabolic capacity to produce toxic amines is a strain-specific property and is purely guided by the genome. High levels of biogenic amines have been affiliated to cause various adverse health effects including allergies, neurological and cardiac disorders, nausea, and hypotension. Nevertheless, there is no well-described upper limit for the biogenic amines that cause acute side effects in the human body. Overall, our results suggest the likeness of industrial applicability of NCDC 400 for future food or probiotic use without significant adverse effects from biogenic amines.

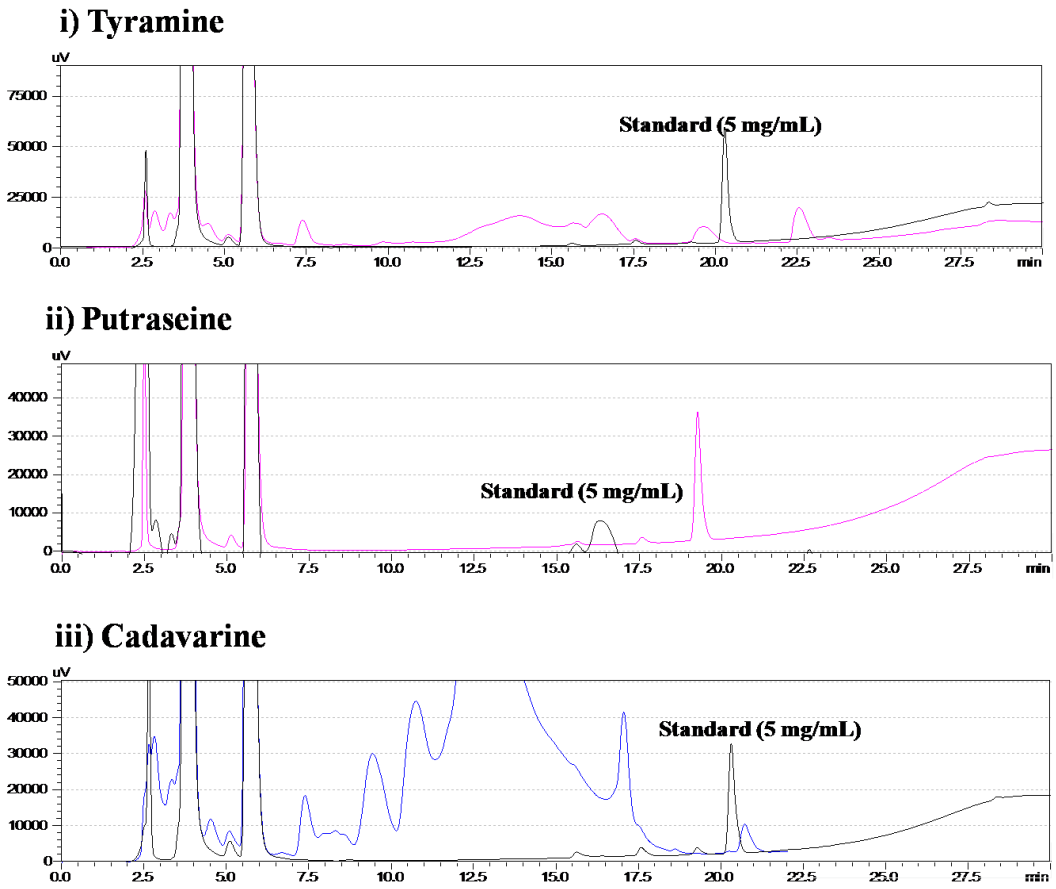

Fig. 4.10: HPLC chromatograms for detection of biogenic amines production by NCDC 400

4.4.14. Mucin degradation test

Mucin degradation in the gut allows commensal or pathogenic microbes to access the bloodstream through the mucosal surface. The probiotics are generally applied to tissues where mucin is secreted. Therefore, probiotic bacteria mustn't degrade the mucin layer which provides a barrier function against opportunistic gut pathogens (Byakika *et al*., 2019). Henceforth, the mucin-degrading ability of NCDC 400 was tested by different methods. When assayed through the Petri dish method by supplementing only mucin (0.5 and 0.1%) as a carbon source, the growth of NCDC 400 was not actively induced and the colony formed on the medium was not dense and intense (**Fig. 4.11**). But faecal flora formed intense colonies on mucin-rich media by exhibiting a clear lysis zone around the colony. On the other hand, NCDC 400 showed luxurious growth and distinct colony on basal media containing 1% glucose. This observation is a clear indication that NCDC 400 does not utilize mucin as the sole carbon source as it may lack the typical enzyme required for mucin degradation. This finding is in accordance with Rastogi *et al*. (2020), who also found the probiotic *Lactobacillus* strains are non-mucolytic.

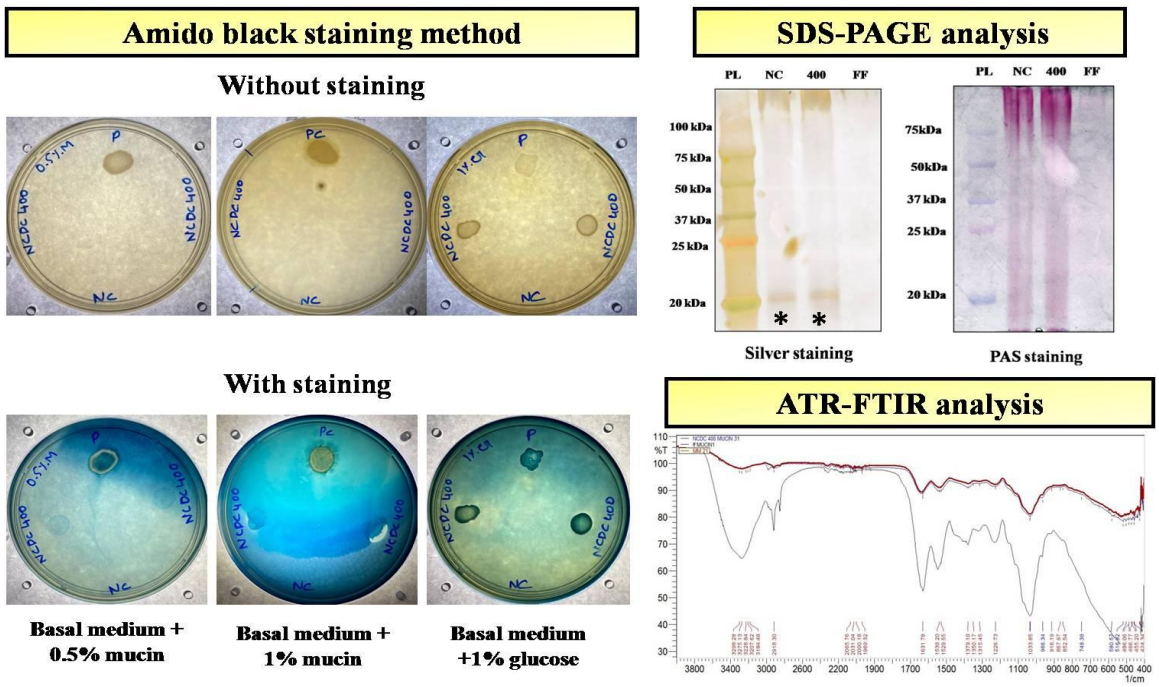

Fig. 4.11: Pictorial representation showing the absence of mucolytic activity of NCDC 400 through *in vitro* experiments. The labeling on Petri plates is as here; P: positive control (faecal flora), NC: negative control (only MRS medium in which culture has been grown). Asterisk (*) indicates the position of mucin bands upon silver staining of SDS-PAGE gel. The labeling on SDS-PAGE gels is provided here; PL: protein ladder; NC negative control (only mucin media); 400: NCDC 400 strain; FF: faecal flora (positive control). The FTIR spectra drawn in red, blue, and black lines belong to mucin media, NCDC 400, and only hog mucin, respectively.

The mucin residues after culturing NCDC 400 in basal medium supplemented with 1% mucin were analyzed by SDS-PAGE with silver and PAS staining for protein and glycoprotein residues, respectively. The silver staining of SDS-PAGE gel revealed one intact mucin band in NCDC 400 lane (indicated as *; **Fig. 4.11**) while the same band faded out after the treatment with faecal flora suggesting the inability to degrade mucin by NCDC 400. Similarly, PAS staining of SDS-PAGE gel also showed the mucin degrading ability of facial flora as there was a clear missing pink glycoprotein band relative to that of NCDC 400 or negative control that showed no degraded patterns of mucin (faint pink color)

ATR-FTIR spectroscopy is a useful tool for characterizing functional groups and the exhibiting bonds. It is widely used in probing the molecular structure of a substance. Considering this, the mucin residues after culturing NCDC 400 in basal medium supplemented with 1% mucin were lyophilized and subjected to FTIR analysis. As expected, the FTIR spectra of mucin media treated with NCDC 400, negative control (only mucin media), and pure mucin (hog mucin) were identical with no changes in the peak absorption intensity (**Fig. 4.11**). This indicates that NCDC 400 does not alter the molecular structure of mucin and thereby reconfirmed its inability to degrade the mucin. The absorption peaks at 1500-1650 cm^{-1} are attributable to the Amide I of beta-helices of proteins. The starching vibrations at 1300-1400 cm^{-1} can be affiliated with the symmetric stretching of C-O belonging to COO^{-} groups as well as Amide III of proteins. Further, the typical peaks at 900-1230 cm^{-1} could be linked to the C-O-C and C-O dominated by ring vibrations of carbohydrates. The broad band (3500 to 3100 cm^{-1}) of O-H stretching vibrations in all the samples can be assigned to the alcohol functional groups in oligosaccharides. One peak at 2918 cm^{-1} can be affiliated with C-H asymmetric stretching vibrations of CH and CH_2 groups in mucin (Gavriely *et al*., 2022). In nutshell, these peaks indicate, beta-sheet and beta-turn secondary structures for mucin with well-persevered carbohydrate and amino acid moieties intact. These results are in close alliance with Lewis *et al*. (2013) who also noticed similar absorption peaks in FTIR spectra during ATR-FTIR-assisted prediction of mucin structure.

Further, the growth of NCDC 400 in basal medium (no carbon source), basal medium with mucin (0.5 and 1%) as the only carbon source, and basal medium with glucose (0.5 and 1%) as carbon source was checked by recording the absorbance at 600 nm. In response, the growth of NCDC 400 and faecal flora was hindered in the basal

medium although it consists of most nutrients except carbon source. Likewise, the growth of NCDC 400 was also not triggered upon adding the mucin either at 0.5 or 1% in contrast to a constant rise in the growth of faecal flora in a time-dependent fashion. Nevertheless, the growth NCDC 400 was actively triggered upon the addition of glucose at 0.5 and 0.1%. In fact, the growth of NCDC was significantly ($p < 0.05$) higher than the faecal flora in the glucose-enriched media after 12 h of incubation at 37˚C (**Fig. 4.12**). Overall, the laagered growth of NCDC 400 in mucin media provides us with a clear understanding that the test culture lacks the cellular machinery or enzymes to degrade the mucin and utilize it as a carbon source.

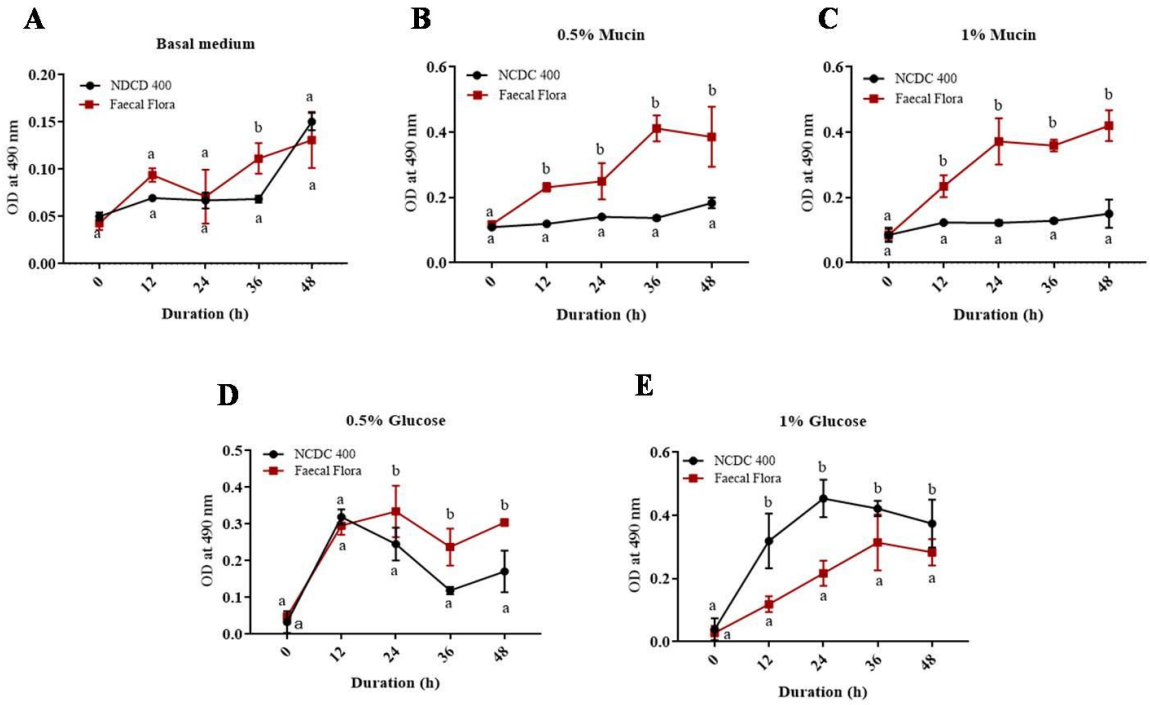

Fig. 4.12: Line graph illustrating the growth of NCDC 400 in culture medium containing glucose and mucin as carbon sources. Error bars indicate the variations of three determinations in terms of the standard error of mean. Lowercase superscripts (a and b) represent the significant differences ($p < 0.05$) between the NCDC 400 and faecal flora at different duration when analyzed by t-test.

4.4.15. Evaluation of *in vitro* adhesion and cytotoxic activity of NCDC 400 on eukaryotic cell line

Caco-2 cells, received from the NCCS, were immediately passaged and propagated in the fresh DMEM at 37 ˚C for 15-20 days in 5% CO_2 incubator. The cells reached almost 60-80% confluence after 15 days of culturing in DMEM. The cell

morphology was evaluated routinely. The cells appeared to be round to irregular morphology when they reach a completely polarized and differentiated state as shown in **Fig. 4.13.** The moment cells reached 60% confluence; the cells were detached from the surface of the culture flask by trypsin digestion and seeded to the 96 and 6 well tissue culture plates for further adhesion and cytotoxicity experiments.

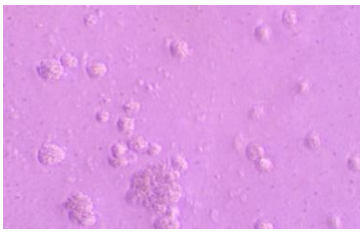	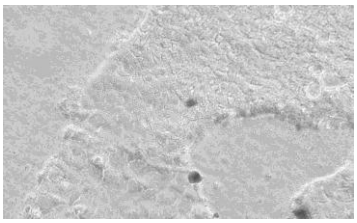	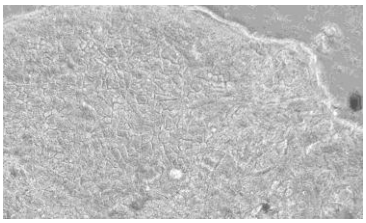
Day 2	**Day 7**	**Day 15**

Fig. 4.13. Microphotographs (100 X) of Caco-2 cells at different stages of confluence

4.4.15.1. Adhesion assays

Adhesion to gut enterocytes that express mucin is a prerequisite for a potential probiotic in order to exhibit effective colonization in the host intestinal milieu. Considering the fact that Caco-2 cells do not express mucin (Cai *et al*., 2022), the adhesion to both Caco-2 cells as well as mucin was independently assessed for NCDC 400. As presented in **Fig 4.14A**, NCDC 400 showed excellent adhesion to Caco-2 cells and mucin corresponding to 15.60 ± 2.88 and 14.40 ± 0.83% relative adhesion, respectively. However, there was no significant difference in the adhesion of NCDC 400 to either Caco-2 cells or mucin *in vitro* suggesting that NCDC 400 can colonize and thrive in a mucin-rich environment like the human gut. It is noteworthy to mention here that the adhesion knack of NCDC 400 was much higher than the previously reported *L. fermentum* strain MTCC 8711 evidencing only ~7 $\log_{10}$ cells adhesion to Caco-2 cells (Jayashree *et al*., 2018). However, the adhesion ability of probiotics is a strain-specific behavior and depends on several factors like cell surface hydrophobicity, bacteria extracellular appendages like cell surface proteins, moon-light proteins, extracellular matrix binding proteins, exopolysaccharides (EPS), etc. (Dhanani and Bagchi, 2013). This excellent gut enterocyte adhesion ability of NCDC 400 could be attributed to its profound ability to produce EPS. Our results are in agreement with Celebioglu *et al*. (2017) who have reported almost >10% of relative adhesion of *Lactobacillus* strains to porcine gastric mucin.

4.4.15.2. Cytotoxicity assays

The *in vitro* cytotoxicity of NCDC 400 was assessed by three different methods. When the cell metabolic activity we assessed by MTT assay, there was no significant reduction in the viability of Caco-2 cells exposed to the lowest (10^8 CFU/ mL) to highest (10^{11} CFU/ mL) doses of NCDC 400 after 24 h (**Fig. 4.14B**). Similarly, none of the NCDC 400 doses were found to be cytotoxic to Caco-2, as witnessed by no loss of cellular viability, assessed using the neutral red assay (**Fig. 4.14C)**. As neutral red is a weak cationic dye, it accumulates in the lysosome of the viable cell by passively diffusing through the cell membrane of viable cells. Upon testing by trypan blue exclusion assay (a direct cell toxicity assay), Caco-2 cells significantly maintained viability (no loss of membrane integrity) upon treatment with different doses of NCDC 400. In comparison with control (untreated cells), Caco-2 cells maintained nearly about 94-95% viability after exposure to NCDC 400 even at a higher dose (10^{11} CFU/ mL) (**Fig. 4.14D)**.

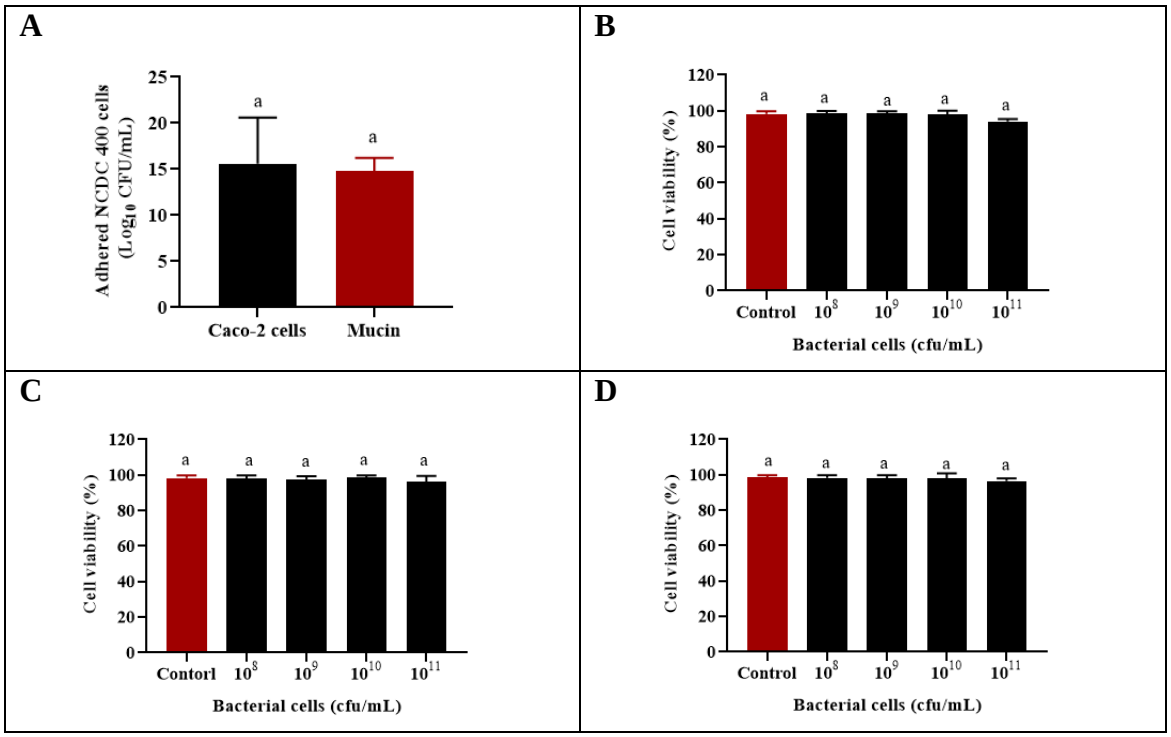

Fig. 4.14: Bargraphs representing the adhesion ability and non-cytotoxic nature of *L. fermentum* NCDC 400 at different doses on Caco-2 cells. Adhesion to Caco-2 cells and mucin (A), MTT reduction (B), Neutral red uptake (C), and Trypan blue exclusion (D) assays. Error bars indicate the variations of three determinations in terms of the standard error of mean. Lowercase (a) represents no significant differences ($p < 0.05$) between the groups when analyzed by t-test for adhesion assay and one-way ANOVA following Duncan test for cytotoxicity assays.

These results suggest that NCDC 400 was non-toxic *in vitro* and may be suitably applied to unravel the various toxicological aspects *in vivo*. These results are in conformity with previous reports suggesting that treatment with various *Lactobacillus* strains at various doses has no major cytotoxicity issues on various cell lines like Caco-2, HT-29, and Vero (Bhat *et al*., 2019; Fochesato *et al*., 2020; Rokana *et al*., 2017). *In vitro* toxicology offers more advantages by means of time and cost-effectiveness than *in vivo* studies. These assays are useful to elucidate the basal cytotoxicity levels to determine the intrinsic ability of a test compound that damages cellular functions to cause cell death. Considering this, a safer dose can be chosen for *in vivo* trials (Visk, 2015).

4.4.16. Effect of NCDC 400 on cellular barrier integrity of Caco-2 cells

The effect of NCDC 400 on gut barrier integrity was tested in terms of measuring the phenol red transflux across the Caco-2 cell monolayer. The cell culture inserts exhibiting < 2% phenol red transflux were selected for this assay and challenged with different doses of NCDC 400 (10^8-10^{11} CFU/ mL). Upon exposure to NCDC 400 at different doses for 24 h, there was no significant ($p < 0.05$) change in paracellular phenol permeability across the Caco-2 monolayer suggesting that NCDC 400 may not impair the gut barrier integrity (**Fig. 4.15**). In congruent with this observation, *Lactobacillus* probiotic strains showed protective effects on the pathogen-induced aberration in gut barrier intactness (Bhat *et al*., 2020). On the other hand, treatment with *E. coli* NCDC 135 significantly ($p < 0.05$) increased the phenol red transflux to 12.94 ± 1.56% and thereby indicating that *E. coli* NCDC 135, even at a lower dose of 10^8 CFU/mL, may disrupt the epithelial integrity. *E. coli* is a Gram-negative pathogen and therefore the loss of epithelial tightness can be attributed to the toxins or lipopolysaccharides (LPS)-mediated distortive effect on the tight junction proteins expression. This result concurs with the Bhat *et al*. (2019b) who noticed a significant loss of epithelial coherence upon treatment with the *E. coli* strain (as low as 10^3 CFU/ mL) in the Caco-2 cells. Overall, the role of microbiota in the context of maintaining gut tightness is significant, as it affects the barrier, leading to the entry of lumen bacteria into the bloodstream. Few bacteria are known to fortify the gut barrier function while opportunistic commensal or gut pathogens or their toxic compounds ruin the integrity. Hence, it is pertinent to evaluate the effect of test probiotic strain on gut barrier intactness before human/ animal intervention studies.

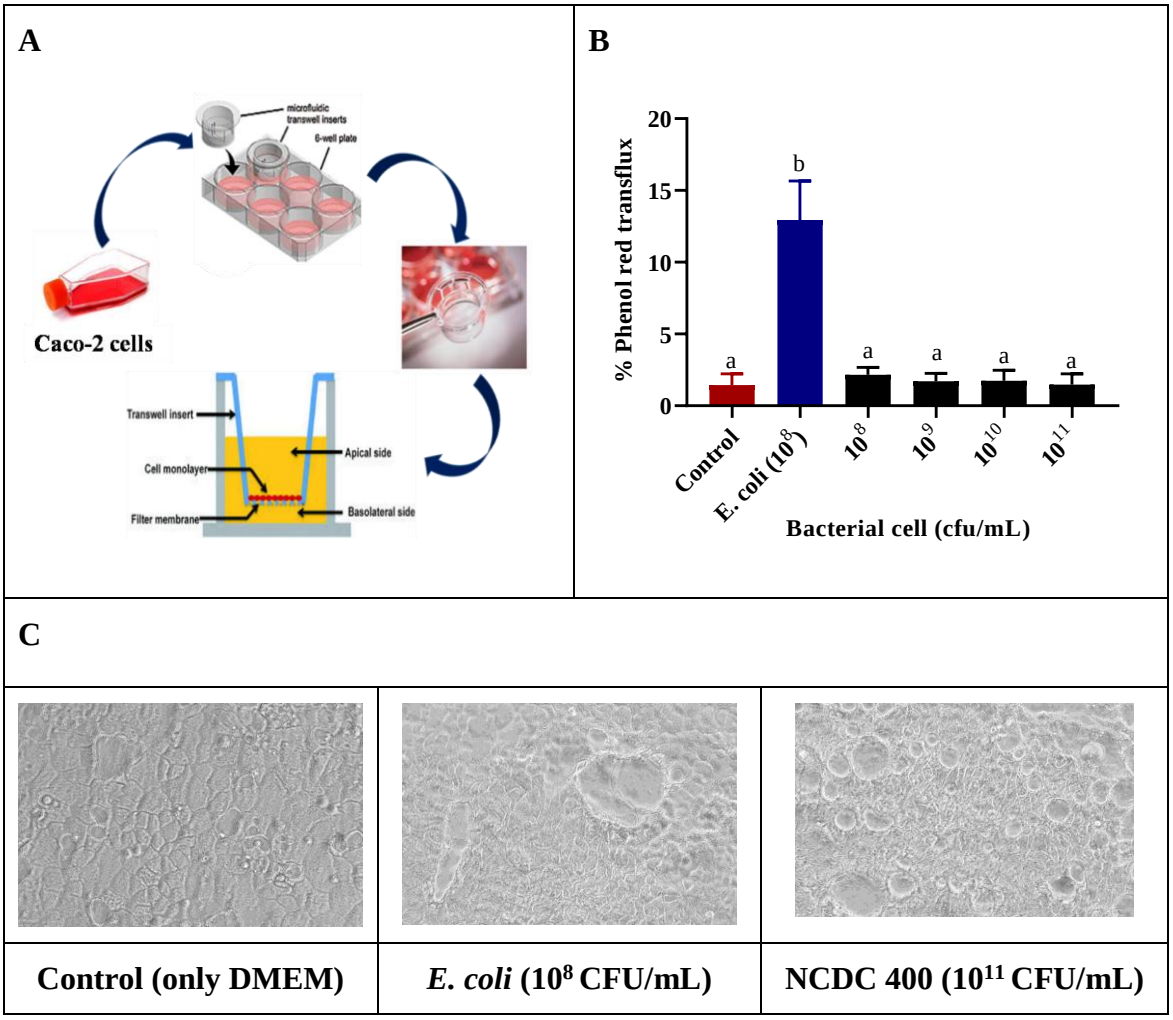

Fig. 4.15: Effect of NCDC 400 on transwell permeability of phenol red across the Caco-2 cell monolayer. (A) Pictorial representation of transwell permeability assay; (B) Bar-graph showing the phenol red transflux across the Caco-2 cell monolayer upon exposure to different doses of NCDC 400; (C) Microphotograph of completely differentiated and polarized Caco-2 cells on transwell inserts treated with either *E. coli* or NCDC 400. Error bars indicate the variations of three determinations in terms of the standard error of mean. Lowercase superscripts (a and b) represent the significant differences ($p < 0.05$) between the groups when analyzed by one-way ANOVA following Duncan test.

4.4.17. Antibiotic resistance profiling of *L. fermentum* NCDC 400

4.4.17.1 Antibiotic susceptibility test

A total of 27 antibiotics were used either singly or in combinations to decipher the drug-resistant pattern of NCDC 400. The zone of inhibition toward different antibiotics and their corresponding interpretation of sensitivity profile based on the published literature are presented in **Table 4.2**.

Table 4.2: Antibiotic susceptibility profile of NCDC 400

Antibiotics	Symbol	Inhibition zone diameter (mm)	Interpretation	References for interpretation
Kanamycin	K (30 mcg)	29.0± 1.0	S	Radulovic *et al.* (2010)
Ofloxacin	OF (5 mcg)	33.5±1.5	S	Thakur *et al*. (2018)
Linezolid	LZ (30 mcg)	40.0±0.0	S	Sharma *et al*. (2015)
Clindamycin	CD (2 mcg)	51.0±1.0	S	Bhat *et al*. (2019a)
Tetracycline	TE (30 mcg)	41.0±1.0	S	
Chloramphenicol	C (30 mcg)	42.5±2.5	S	
Oxacillin	OX (1 mcg)	42.5±0.5	S	
Teicoplanin	TEI (10 mcg)	24.0±1.0	S	Thakur *et al*. (2018)
Vancomycin	VA (30 mcg)	15.0±0.0	IR	Bhat *et al*. (2019a)
Penicillin	P (10 Units)	52.5±2.5	S	
Amikacin	AK (30 mcg)	29.5±0.5	S	
Gentamicin	GEN (10 mcg)	29.5±0.5	S	
Clarithromycin	CLR (15 mcg)	39.5±2.5	S	Singh *et al*. (2021)
Co-Trimoxazole	COT (25 mcg)	20.0±0.0	S	Thakur *et al*. (2018)
Netillin	NET (30 mcg)	34.0±4.0	S	Bhat *et al*. (2019)
Cefaclor	CF (30 mcg)	37.5±2.5	S	Sharma *et al*. (2015)
Cefotaxime	CTX (30 mcg)	43.5±1.5	S	Thakur *et al*. (2018)
Azithromycin	AZM (5 mcg)	31.5±1.5	S	Thakur *et al*. (2018)
Ampicillin/ Cloxacillin	AX (10/10 mcg)	42.5±2.5	S	Singh *et al*. (2021); Sharma *et al*. (2015)
Ampicillin/ Sulbactam	A/S (10/10 mcg)	39.0±1.0	S	
Ciprofloxacin	CIP (5 mcg)	37.5±0.5	S	Bhat *et al*. (2019a); Thakur *et al*. (2018)
Amoxyclav	AMC (30 mcg)	23.0±1.0	S	Thakur *et al*. (2018)
Novobiocin	NV (5 mcg)	35.0±0.0	S	Zhou *et al*. (2005)
Erythromycin	E (15 mcg)	39.0±1.0	S	Bhat *et al*. (2019a)
Cefadroxil	CFR (30 mcg)	25.0±0.0	S	Thakur *et al*. (2018)
Ampicillin	AMP (30 mcg)	40.5±0.5	S	Bhat *et al*. (2019a)
Cephalothin	CEP (30 mcg)	35.0±0.0	S	Thakur *et al*. (2018)

Note: Values are presented as the mean ± SEM (n = 3)

It was found that NCDC 400 was sensitive to nearly all tested antibiotics except for vancomycin exhibiting the least inhibition zone (15.0 ± 0.0 mm). NCDC 400 revealed intermediate resistance to vancomycin, a glycopeptide antibiotic that acts on the bacterial cell wall. Nevertheless, the vancomycin resistance among LAB is not a concern of resistance as most of the LAB are intrinsically resistant to vancomycin due to the structural alterations in their cell wall (Mathur and Singh, 2005). Similarly, resistance to aminoglycoside antibiotics is another intrinsic resistance property that was unnoticed in NCDC 400. A similar observation has been reported by Mann *et al*. (2021a). These researchers could not find the aminoglycoside resistance phenotype in an oral probiotic *L. fermentum* OK. The concern of antibiotic resistance among food-grade LAB, including probiotics, is amplifying every day. The resistance to unusual antibiotics is generally acquired and such resistance is corroborated to be associated with the mobile genetic elements. The acquired resistance has the plausibility to get transfer the resistance genes to other gut commensal bacteria through the horizontal gene transfer episodes. Hence, the prospective probiotic strain should not contain laterally transferable extrinsic resistance.

4.4.17.2 Determination of MICs

As presented in **Table 4.3**, the MIC values for different antibiotics toward *L. fermentum* NCDC 400 were less than the EFSA cut-off values for antibiotics to distinguish microbes with antibiotic resistance from sensitive patterns for food applications. The MICs values for EFSA-directed antibiotics against NCDC 400 ranged from 0.01-4 mcg/ mL. The test strain was sensitive to all EFSA enlisted antibiotics (Kanamycin, Ampicillin, Gentamicin, Streptomycin, Clindamycin, Tetracycline, Erythromycin, and Chloramphenicol) for heterofermentative lactobacilli for food applications. This suggests that its subsequent food applications may not create a threat to the environment and human health. There was a general resistance to nalidixic acid, vancomycin, and teicoplanin antibiotics whose MIC values were found to be > 20 mcg/ mL. However, the resistance to aminoglycosides (neomycin, kanamycin, streptomycin) or quinolones (ciprofloxacin, norfloxacin, nalidixic acid) among LAB is considered intrinsic property, which has minimal concern on transferability. More specifically, lactobacilli have been reported to have a high level of natural intrinsic resistance to vancomycin, bacitracin, cefoxitin, metronidazole, nitrofurantoin, and sulfadiazine, as well as protein systems inhibitors like chloramphenicol, erythromycin, clindamycin, lincomycin and tetracyclines (Álvarez-Cisneros *et al*., 2018). The results are in

alignment with de Souza *et al*. (2019) who also reported that the other strains of *L. fermentum* isolated from dairy origin were resistant to similar antibiotics.

Table 4.3: MIC values of different antibiotics against NCDC 400

Antibiotics	Symbol	MIC	EFSA Cut-off	Range tested (mcg/ mL)
Cephalotin	CE	0.19		0.016-256
Azithromycin	AZ	0.94		0.016-256
Amoxicillin	AC	0.1		0.016-256
Levofloxacin	LE	8		0.002-32
Ceftriaxone	CTR	0.19		0.016-256
Nitrofurantoin	NIT	2		0.032-512
Kanamycin	KAN	4	64	0.016-256
Cefotaxime	CTX	0.19		0.016-256
Cefuroxime	CXM	1.5		0.016-256
Ampicillin	AMP	0.5	2	0.016-256
Gentamicin	HLG	1	16	0.064-1024
Nalidixic acid	NAL	20		0.016-256
Clarithromycin	CH	0.125		0.016-256
Penicillin	PEN	0.25		0.002-32
Amoxyclav	AMC	0.25		0.016-256
Cefoperazone	CFP	0.75		0.016-256
Ampicillin	AB	0.032		0.016-256
Teicoplanin	TEI	66		0.016-256
Doxycycline	DOX	0.32		0.016-256
Oxacillin	OXA	1.5		0.016-256
Amoxicillin	AMX	0.38		0.016-256
Streptomycin	SM	2	64	0.064-1024
Ciprofloxacin	CI	0.25		0.002-32
Clindamycin	CLN	1.5	4	0.016-256
Cefepime	CPM	0.75		0.016-256
Vancomycin	VAN	55	n.r.	0.016-256
Tetracycline	TET	4	8	0.016-256
Norfloxacin	NEX	0.47		0.016-256
Erythromycin	E	0.01	1	0.001-32
Chloramphenicol	C	1	4	0.016-256

Note: n.r: not required; mcg: microgram

4.4.18. PCR-based identification of antibiotic resistance and virulence genes

Although NCDC 400 was not phenotypically resistant to concerning antibiotics, targeted PCR was used to confirm the presence or absence of ARGs. It is because, in many instances, bacteria carry the resistance genes but they fail to express their phenotype because of non-functional/ pseudo-genes. A total of 14 ARGs confirming resistance towards tetracycline (*TetO* and *TetM*), erythromycin (*ermA*, *ermB*, *ermC*, *msrA*, and *ermf*), aminoglycoside-modifying-enzyme genes (*ant(6')-Ia*, *aph(3')-IIIa*, and *aac(6')-le-apha (2'')-Ia*), chloramphenicol (*CatA8*), multidrug resistance efflux (*emeA*), beta-lactam (*blaTEM*), and *Int-Tn* (*Tn916/Tn1545*) encoding *TetM* were tested based on their high prevalence in LAB. However, none of them were detected in the NCDC 400 either in chromosomal or plasmid DNA (**Fig. 4.16**) thereby signifying the safe use of this culture without any major issue of AMR. Similarly, the virulence genes that encode coagulase (*Coa*), nuclease (*nucA*), and gelatinase (*gelE*) were not detected in NCDC 400. These results are in agreement with de Souza *et al*. (2019) who also disclosed the absence of virulent and resistance genes except for *ermB* in *L.* casei and *L. fermentum* probiotic strains. However, the authors found that *ermB* gene was silent as it was not phenotypically expressed.

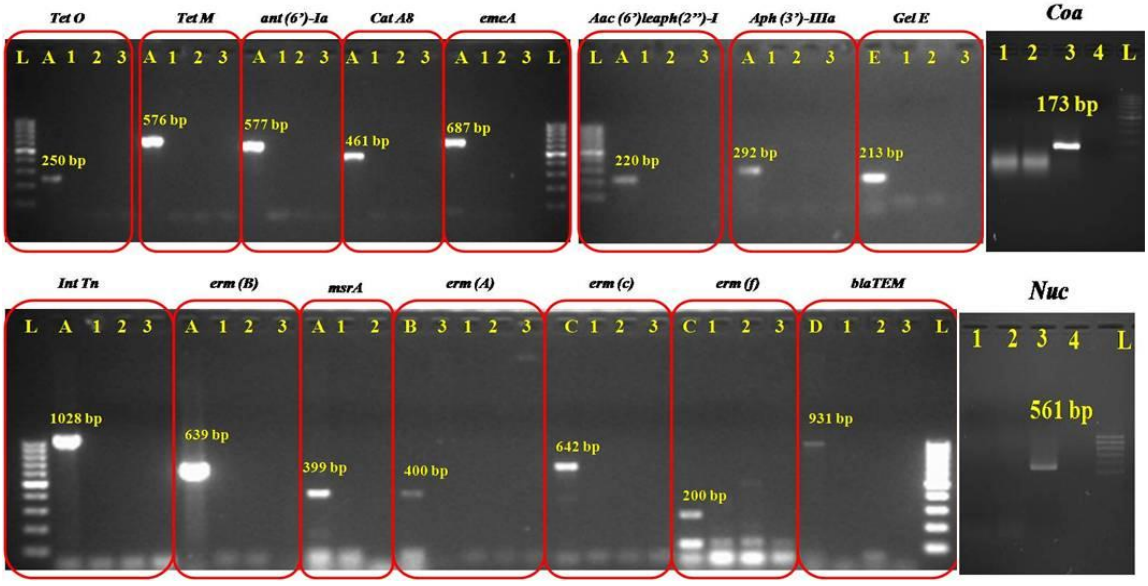

Fig. 4.16. Agarose gel showing the absence of tested antibiotic resistance and virulence genes in NCDC 400. The description of lanes are as here; L:100 bp DNA ladder; A: B1(F) Enterococci; B: KnX (D) Enterococci; C: Km (H) Enterococci; D: Ar (D) Enterococci; E: G2 (H) Enterococci; 1: NCDC 400 genomic DNA; 2: NCDC 400 plasmid DNA; 3: NTC (Non-template control). The description of lanes for *Coa* and *NucA* genes are as here: 1: NCDC 400 genomic DNA; 2: NCDC 400 plasmid DNA; 3: *S. aureus*; 4: NTC; L: 100 bp ladder.

4.4.19. *In silico* prediction of virulence and antibiotic resistance genes

The size of the whole genome of *L. fermentum* NCDC 400 was found to be 1,895,978 bp (1.89 Mb), which was comparable to the genome size of type strain *L. fermentum* ATCC 14931 (**Fig. 4.17**). The assembled sequence had 185 contigs joined into 138 scaffolds. Prokka predicted 1841 protein-coding genes in the total scaffolds involved in various metabolism and cellular processes. Further, a total of 56 tRNA and 1 tmRNA gene in the genome were predicted by Prokka. Similarly, a total of 9 rRNA genes were predicted by Prokka in contrast to 15 rRNA genes (5 5S rRNAs, 4 16S rRNA, and 6 23S rRNAs) found by BLASTn. However, such variations in the gene calling among various genome annotation pipelines have been previously reported in a comparative study. The study indicated that few of the platforms are curated but fast while some can take time but use several databases for comprehensive annotations at the expense of increased computational resources. In addition, the accuracies of annotations may also differ between the reference databases to which the pipelines are connected (Ruiz-Perez *et al*., 2021).

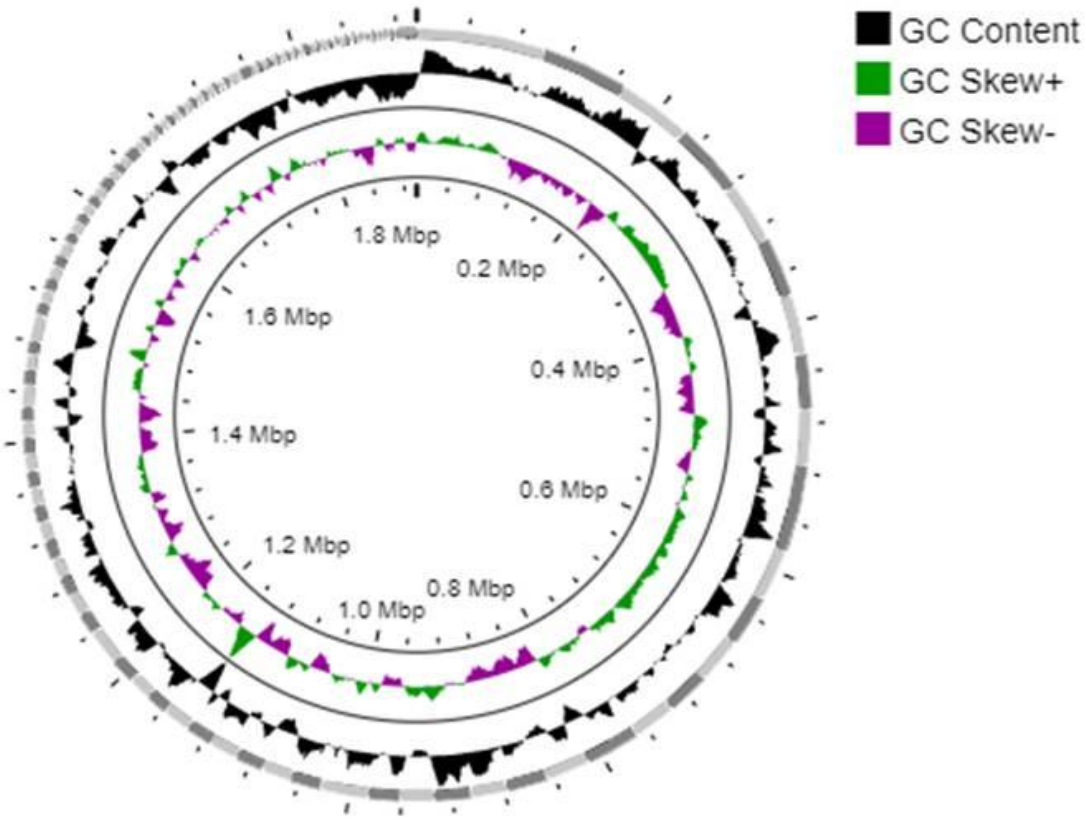

Fig. 4.17. Genome map of NCDC 400 (developed using Proksee genome visualization tool)

4.4.19.1. Identification of virulent genes

None of the virulence genes were predicted in the whole genome sequence of NCDC 400 upon prediction through the VirulenceFinder tool. An alignment of the whole genome of NCDC 400 against the BLASTp VFDB program (> 60% against the pair-wise sequence similarly search when the e-value set at 0.000010) returned no hits suggesting the absence of virulent genes. Further inquiry on the pathogenicity of the strain using the PathogenFinder tool indicated that the calculated matched pathogenic families for *L. fermentum* NCDC 400 was zero; the matched not pathogenic families was 2, and the probability of the strain being a human pathogen was 0.195 (**Fig. 4.18**). Therefore, the strain was predicted as a non- pathogenic to humans and can be considered safe for human consumption after subsequent *in vivo* trials. These results are in accordance with the findings of Alayande *et al*. (2020) who found that *Limosilactobacillus reuteri* PNW1 was also regarded non-pathogenic strain, however, the probability of the strain being a human pathogen was 0.217 which was quite higher than NCDC 400.

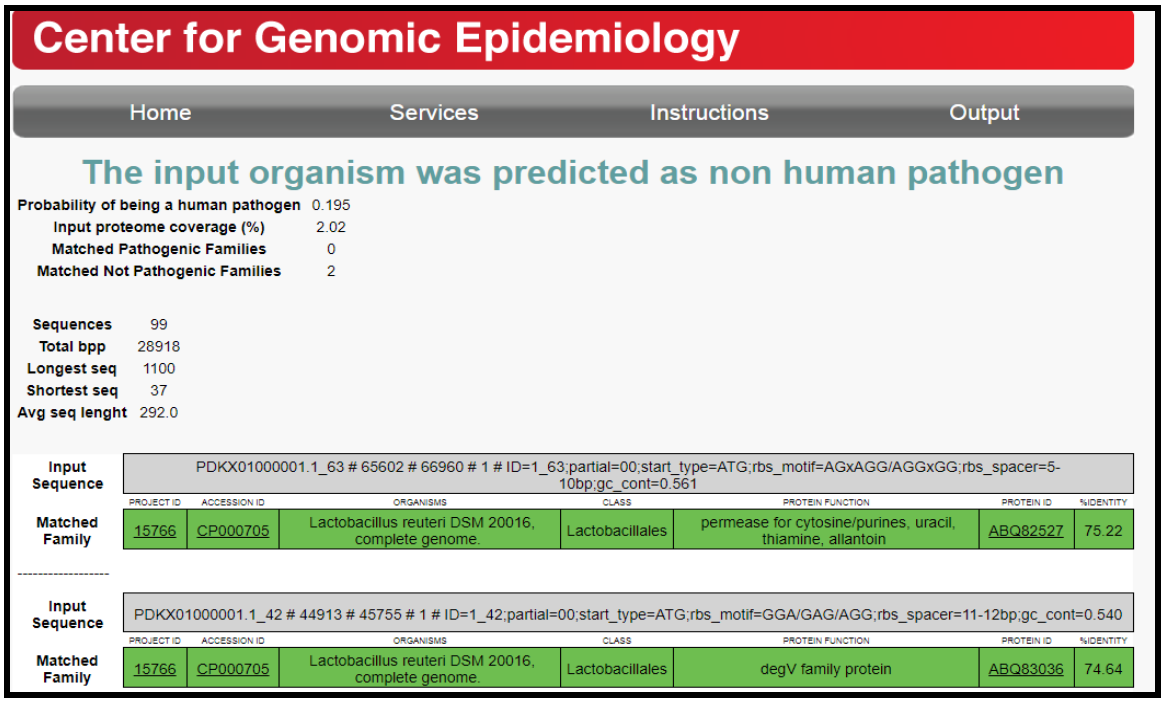

Fig. 4.18. Center for Genomic Epidemiology (CGE) hosted PathogenFinder publically available server predicting the non-pathogenicity of NCDC 400

4.4.19.2. Identification of antibiotic resistance genes

The analysis of genome sequences of NCDC 400 through the CGE-hosted ResFinder tool (Selected threshold for %ID: 90%; Selected minimum length: 60%)

revealed the absence of antibiotic resistance genes confirming the acquired resistance. This indicates that NCDC 400 is devoid of acquired or extrinsic resistance which has a greater potential for lateral transferability. ResFinder database has been sufficiently equipped to predict the bacterial acquired resistance to various antibiotics *viz*. aminoglycoside, beta-lactam, colistin, disinfectant, fluoroquinolone, fosfomycin, fusidic acid, glycopeptide, MLS: macrolide, lincosamide, streptomycin, nitroimidazole, oxazolidinone, phenicol, pseudomonic acid, rifampicin, tetracycline, trimethoprim. In this regard, Terai *et al*. (2020) have also predicted no acquired resistance genes in the whole genome sequences of probiotic *Lactobacillus crispatus* YIT 12319 isolated from the oral cavity. ARG-ANNOT, a new bioinformatic tool that can detect ARGs in bacterial genomes and easily discover putative new ARG determinants (if any), also indicated no resistance genes in the NCDC 400 whole genome. This database is equipped to predict the existing and novel resistance determinants based on the detection of point mutations in chromosomal target genes (Zankari, 2014). Another pipeline, command-line interface ABRicate (Galaxy Version 1.0.1 linked to ARG-ANNOT, CARD, EcOH, MEGARes, NCBI, Plasmidfinder, ResFinder, and VFDB) also ended with no resistance as well as virulence confirming genes in the genome sequences of NCDC 400.

On the other hand, the genome analysis using the RGI predicted one strict hit corresponding to *VanT* gene in the *VanG* cluster (**Fig. 4.19A**). The E-value, Bit score and percentage identity are as here; 2.6e-51, 197.2, and 34.69. The forecasted gene has been presumed to be involved in conferring resistance toward glycopeptide antibiotics through antibiotic target alteration. Further, UniProt BLAST analysis of the predicted amino acid sequence revealed sequence homology with Alanine racemase (EC: 5.1.1.1) that catalyzes the conversion of L-alanine to D-alanine (D-Ala) which is the essential substrate for the D-Ala-D-Ser based resistance mechanism (**Fig. 4.19B)**. Vancomycin interacts with the D-Ala-D-Ala region of Lipid II by hydrogen bonds and thereby inhibits the peptidoglycan layer synthesis. But the resistance to vancomycin involves the replacement with DAla-D-lac or D-Ala-D-Ser alternative to which vancomycin has a relatively low affinity (Stogios and Savchenko, 2020). Nevertheless, the vancomycin resistance and its associated genes in lactobacilli is an intrinsic resistance linked with chromosomes and has the least possibility of transferability via horizontal gene transfer.

The presence of vancomycin resistance genes specifically *VanT* has been reported in several LAB of probiotic candidature (De Vries *et al*., 2006; Jiang *et al*., 2021).

A

B

```
Length=373

                                                                    Score     E
Sequences producing significant alignments:                        (Bits)  Value

SP:B2GA65ALR_LIMF3 Alanine racemase OS=Limosilactobacillus fermen...  730     0.0
TR:A0A0F4HC03A0A0F4HC03_LIMFE Alanine racemase OS=Limosilactobaci...  730     0.0
TR:C7XXD3C7XXD3_9LACO Alanine racemase OS=Limosilactobacillus col...  500     4e-175
SP:B2G5M9ALR_LIMRJ Alanine racemase OS=Limosilactobacillus reuter...  478     2e-166
SP:A5VI51ALR_LIMRD Alanine racemase OS=Limosilactobacillus reuter...  478     2e-166
```

Fig. 4.19: CARD-RGI-based identification of vancomycin resistance gene in NCDC 400. (A) Ring wheel depicting RGI strict hit corresponding to the *VanT* gene in the NCDC 400 genome. B) UniProt BLAST view displaying the sequence similarity of *VanT* sequence with alanine racemase enzyme.

On the other hand, the putative ARGs were identified using the ideal and strict algorithms of the CARD-BLASTn with an identity > 80%, and E-value > e−6. Not surprisingly, the genome of NCDC 400 showed the presence of a total of 20 putative resistance genes towards aminoglycosides, linezolid, fluoroquinolone, chloramphenicol, and macrolide antibiotics (**Table 4.4)**. It is well known that lactobacilli intrinsically/ naturally demonstrate high resistance to vancomycin, aminoglycosides, bacitracin, and cefoxitin, as well as, protein synthesis inhibitors such as chloramphenicol, erythromycin,

lincomycin, clindamycin, and tetracyclines (Álvarez-Cisneros *et al*., 2018). Since the resistance to these antibiotics is dealt with intrinsic resistance of lactobacilli, it is reported to have minimal propagation among the bacteria, as these genes are loaded on the chromosomal DNA causing limited transference to other microbes. These results show close similarity with Mann *et al*. (2021a) and Mann *et al*. (2021b), who also identified the 16 genes affiliated with resistance conferring towards beta-lactams, bacitracin, aminoglycoside, aminocoumarin, lincomycin, polymyxin, macrolide, and multi-antibiotics in two probiotic strains *L. fermentum* OK and *L. gasseri*. Researchers stated that these genes are inherent or may be involved in several other functioning of the cells. For example, *GyrA* is involved in DNA replication, efflux pumps in detoxification, PBP2a in cell wall synthesis, etc. But considering the fact that any gene responsible for intrinsic resistance may be disseminated and transferred to other microbes when it is flanked by IS elements that could encourage the mobilization, the IS elements were searched in the contigs where these genes were identified, and surprisingly none of them were flanked between the insertion sequences (described under **section 4.4.19.3**).

However, it is worth highlighting that the criteria used to identify the resistance genes at the first level were >80% identity and E-value > e−6 which may facilitate identifying off-target genes. Since nucleic-acid-based BLAST searches are highly specific, they generally relay and are considered valid when nucleotide sequence similarity > 98%. Therefore, the stringency of the CARD search was further increased (identity > 90%, and E-value > e−6). This resulted in the identification of no resistance genes suggesting that NCDC 400 may not exhibit the resistance genes with high sequence similarities with the CARD database, a complete and up-to-date global AMR database. These findings are analogous to the phenotypic test wherein the strain showcased no resistance to respective antibiotics against the annotated genes. This indicates that the strain neither has phenotypic nor genotypic resistance against concerning antibiotics. The absence of aminoglycoside resistance phenotype in NCDC 400, which is most commonly demonstrated by most LAB (Gueimonde *et al*., 2013), can be correlated with the presence of cytochrome bd-I ubiquinol oxidase subunit 1 (EC: 1.10.3, *cydA*) and cytochrome bd-I ubiquinol oxidase subunit 2 (7.1.1.7, *cydB*) in the NCDC 400 whole genome. Besides being involved in the electron transport chain (ETC), *cydA* and *cydB* are reported to show cytochrome-mediated drug transport (Duc *et al*., 2020).

Table 4.4: Results of CARD analysis of NCDC 400 genome with liberal search criterion (identity > 80%, and E-value > e−6)

Sl. No.	Accession	Name	E-value	Identity	Score
1	3004853	16S rRNA mutation conferring resistance to capreomycin	0	80	953
2	3003436	16S rRNA mutation conferring resistance to kanamycin	0	80	953
3	3003437	16S rRNA mutation conferring resistance to viomycin	0	80	953
4	3003480	16S rRNA mutation conferring resistance to streptomycin	0	80	953
5	3003481	16S rRNA mutation conferring resistance to amikacin	0	80	953
6	3003495	16S rRNA mutation conferring resistance to spectinomycin	0	80	950
7	3003405	16S rRNA (rrsB) mutation conferring resistance to streptomycin	2.03E-86	81	318
8	3003399	16S rRNA (rrsB) mutation conferring resistance to kanamycin A	2.03E-86	81	318
9	3003376	16S rRNA (rrsB) mutation conferring resistance to spectinomycin	2.03E-86	81	318
10	3004058	23S rRNA with mutation conferring resistance to linezolid	9.50E-80	84	296
11	3003515	16S rRNA mutation conferring resistance to kanamycin A	7.40E-76	82	283
12	3003518	16S rRNA mutation conferring resistance to neomycin	7.40E-76	82	283
13	3003516	16S rRNA mutation conferring resistance to tobramycin	7.40E-76	82	283
14	3003514	16S rRNA mutation conferring resistance to amikacin	7.40E-76	82	283
15	3003517	16S rRNA mutation conferring resistance to gentamicin C	7.40E-76	82	283
16	3003540	16S rRNA (rrsB) mutation conferring resistance to hygromycin B	9.50E-80	81	296
17	3004058	23S rRNA with mutation conferring resistance to linezolid	0	90	922
18	3004170	23S rRNA with mutation conferring resistance to macrolide antibiotics	0	91	922
19	3004616	23S rRNA mutations confers resistance to fluoroquinolone and macrolide antibiotics	1.30E-112	81	405
20	3004150	23S rRNA with mutation conferring resistance to chloramphenicol	2.12E-125	80	448

4.4.19.3. Insertion Elements, Prophages, CRISPR‑Cas System, and Origin of Transfer

4.4.19.3.a. Insertion elements

Unraveling the putative insertion sequences (IS) and their possible transferability within the NCDC 400 genome by the IS-finder tool revealed a total of 54 IS of different families wherein none were found to be transferable except for IS 19 (**Table 4.5**). Fifty-four IS elements were disturbed among 5 different IS families *viz*. IS 30, IS 3, IS 982, IS L3, and IS5. Amongst, 43% and 48% of IS elements belonged to IS 30 and IS 3 families, respectively (**Fig. 4.20A**). In accordance with this prediction, Alayande *et al*. (2020) has also reported a higher abundance of IS 30 and IS 3 families IS elements in the *Lactobacillus reuteri* PNW1. Furthermore, the prevalence of ISLhe30 in the NCDC 400 was notably higher followed by ISLp2. It is important to note that the IS elements belonging to these families were contemplated to be originated from *L. helveticus*, *L. plantarum*, *Pediococcus pentosaceus* (IS30 family); *L. plantarum*; *L. sanfrancisensis*, *L. salivarius*, *L. casei* (IS3 family); *Enterococcus faecium*, *Lactococcus lactis* (IS982 family); *Leuconostoc mesenteroids* (ISL3 family), and *L. plantarum* (IS 5 family). This evidence perhaps suggests the role of genome shuffling among the closely related microbes during the course of bacterial evolution. Moreover, the occurrence of multiple copies of IS elements indicates that bacteria might have undergone specific DNA rearrangements, which leads to an increase in genetic diversity.

It was envisaged that most of the IS elements identified in the NCDC 400 were non-transferable. But IS19 of IS 982 family (origin *Lactococcus lactis*) was predicted to be transferable. The transferability may be due to the presence of ORF 1 region that codes for transposase, analyzed by NCBI ORF finder, as well as previously reported in *L. lactis* by Magni *et al*. (1996). However, it is conceivable that the conspicuous genetic fluidity in the NCDC 400 could be relatively low as it carries only one transferable IS element. In fact, the scarcity of complete and transferable IS element is instrumental in determining genome stability (Wei *et al*., 2012). There is every possibility that this IS element carries one or more resistance genes. Hence, the predicted complete or transferable IS sequence (IS 19) was analyzed by the CARD-BLASTn tool and found to have no resistance gene embedded in the ORF of IS 19. This confirms that the presence of IS 19 may not promote the dissemination of ARGs.

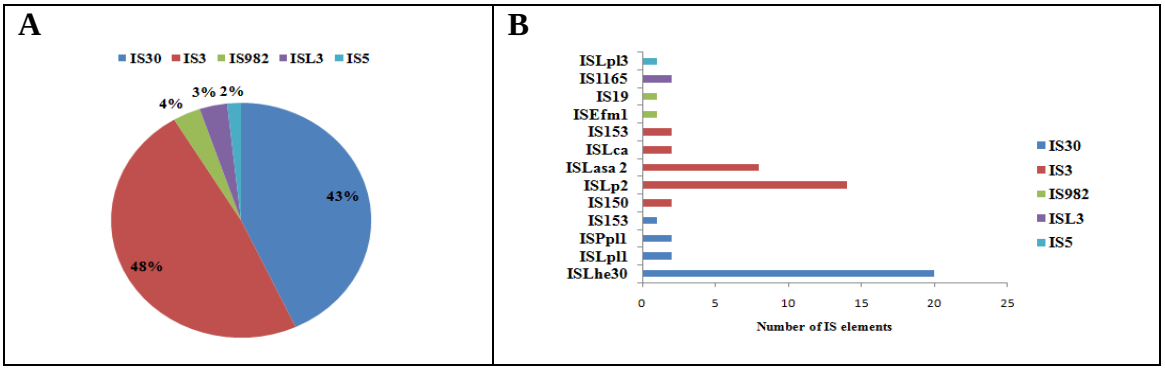

Fig. 4.20: Distribution and abundance of insertion sequences in the NCDC 400 genome. (A) Pi-chart displaying the abundance of different IS families in the NCDC 400 genome. (B) Bar chart showing the number of IS and their classification.

4.4.19.3.b. Prophage regions

Two incomplete prophage regions were identified within the genome of the NCDC 400 strain and their localization in the whole genome has been presented in **Fig. 4.21**. One putative incomplete prophage on scaffold 9 was identified in the genome. The prophage sequence on scaffold 9 had 9 coding sequences (CDS) encoding for proteins similar to a tail shaft, attachment site, and phage-like proteins. Similarly, another incomplete prophage on scaffold 64 had the proteins like transposase, attachment site, and phage-like proteins (**Fig. 4.22**). However, it is worth noting that both the prophage sequences failed to have an integrase protein, a key protein for prophage induction. Other important proteins for phage infection and lysis were lacking in both the predicted prophage sequences. This evidence indicates the absence of phage mediated lateral transmissibility of genes. The presence of prophage remnants rather than a complete prophage is an indication of the evolution of bacterial strain toward a stable genome by inactivation or elimination of integrated prophages (Senan *et al*., 2015).

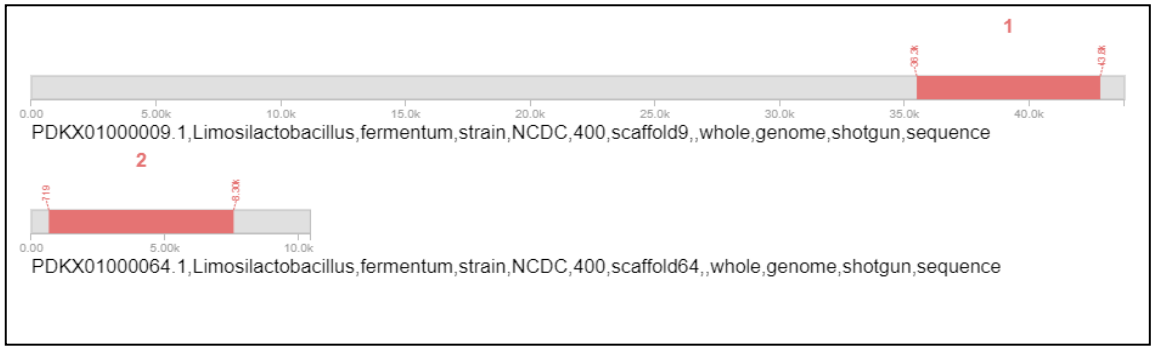

Fig. 4.21. Localization of two incomplete prophage sequences in the NCDC 400 genome

Fig. 4.22. Organization of two incomplete prophage sequences in the NCDC 400 genome

In order to further validate the CDS predicted by the PHASTER tool, an alignment of CDS against the BLASTp RefSeq data based resulted in no complete match in the prediction. Upon BLAST analysis, complement sequences (CDS: 43707..43838; CDS: 1659..1802) were identified as transposon on prophages 1 and 2 (**Tables 4.6 and 4.7**). BLAST search of complement sequences under the strict algorithm of CARD did not reveal the presence of any ARG. Further, upstream and downstream sequences of these CDS were analyzed by CARD and RGI analysis, and the results indicated that the absence of any ARGs that would otherwise transfer during transposition (if exist). In fact, no invert repeats were found in upstream or downstream sequences where transposons are located suggesting the lack of mobility of predicted transposase. Genome stability is affected by many transition elements, such as mobilizable plasmids, insertion sequence (IS), and prophages. However, NCDC 400 lacks the complete prophage sequences that lack a lysogenic cycle. Therefore, it can be stated that the NCDC 400 has quite a stable genome and may lack genome shuffling. In contrast to this, the genomes of several other potential probiotic strains were reported to have at least one complete prophage sequence (Alayande *et al*., 2020; Fu *et al*., 2022). In such cases, genome

stability is a big challenge to researchers. The genomic stability of all probiotics is corroborated by the fact that their techno-functional properties are not affected during production and long-term preservation. In this regard, NCDC 400 has shown a stable technological performance (EPS production and milk acidification) over 2 decades without changes in the whole-genome order. This provides conclusive evidence that more IS as well as prophage remnants (non-transferable) did not cause genetic instability.

4.4.19.3.c Origin of Transfer (OriT) regions

No OriT regions that can be recognized by relaxases were detected in the NCDC 400 whole genome (**Fig. 4.23**). The virulence factors like the type IV coupling protein (T4CP) gene and gene cluster for the bacterial type IV secretion system (T4SS) apparatus were not identified in NCDC 400 whole genome suggesting that the genome does not demonstrate a classical conjugal DNA transfer. Conjugation-mediated chromosomal DNA in bacteria requires the presence of OriT (a cis-acting site) in the chromosome. Although gaining of an oriT region by chromosomal DNA is rare, but occurs if a conjugative plasmid integrates into the chromosome to form high-frequency recombination (Hfr) donor strain, which can transfer widespread regions of chromosomal DNA (Wang *et al*., 2005).

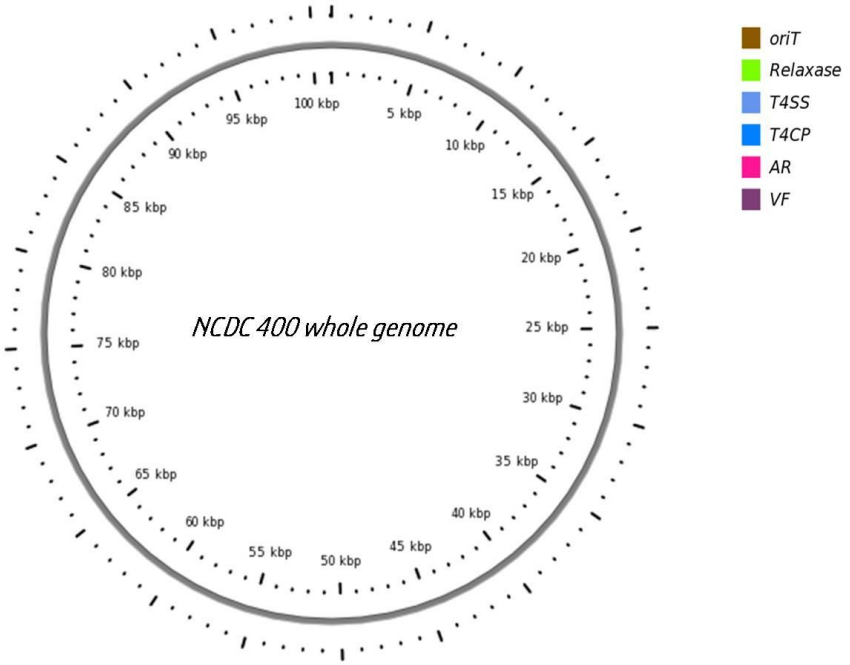

Fig. 4.23: Circular genome map showing no OriT regions in NCDC 400 genome

Table 4.5: Details of IS elements present in NCDC 400 (IR: Inverted Repeats; IS: Insertion; ND: Not Determined; Y: Yes)

Sr. No.	IS Element	IS Family	Group	IS length	IR length	Transposition	% Identity	E value	Origin	Accession number
1	ISLhe30	IS30		1025 bp	23/34	ND	81	1.00E-20	*Lactobacillus helveticus*	CBUL010000181
2	ISLhe30	IS30		1025 bp	23/34	ND	94	0	*Lactobacillus helveticus*	CBUL010000181
3	IS153	IS3		1127 bp	27/37	ND	96	0	*Lactobacillus sanfranciscensis*	AJ239042
4	ISLpl1	IS30		1043 bp	22/24	ND	92	0	*Lactobacillus plantarum*	AF459445
5	ISPp1	IS30		1039 bp	21/23	ND	92	0	*Pediococcus pentosaceus*	Z32771
6	ISLhe30	IS30		1025 bp	23/34	ND	94	0	*Lactobacillus helveticus*	CBUL010000181
7	ISLpl2	IS3	IS150	1491 bp	24/27	ND	97	6.00E-135	*Lactobacillus plantarum*	CP024414
8	ISLpl2	IS3	IS150	1491 bp	24/27	ND	95	0	*Lactobacillus plantarum*	CP024414
9	ISEfm1	IS982		1041 bp	22	ND	99	0	*Enterococcus faecium*	AF138282
10	IS19	IS982		1038 bp	21	Y	99	3.00E-87	*Lactococcus lactis*	AF169285
11	ISLasa	IS3	IS150	1619 bp	19/22	ND	89	1.00E-20	*Lactobacillus salivarius*	CP089850
12	ISLhe30	IS30		1025 bp	23/34	ND	96	2.00E-46	*Lactobacillus helveticus*	CBUL010000181
13	ISLhe30	IS30		1025 bp	23/34	ND	94	5.00E-179	*Lactobacillus helveticus*	CBUL010000181
14	ISLhe30	IS30		1025 bp	23/34	ND	95	0.00E+00	*Lactobacillus helveticus*	CBUL010000181
15	ISLpl2	IS3	IS150	1491 bp	24/27	ND	96	5.00E-179	*Lactobacillus plantarum*	CP024414
16	ISLasa2	IS3	IS150	1619 bp	19/22	ND	89	6.00E-12	*Lactobacillus salivarius*	CP089850
17	ISLpl2	IS3	IS150	1491 bp	24/27	ND	95	0.00E+00	*Lactobacillus plantarum*	CP024414
18	ISLpl2	IS3	IS150	1491 bp	24/27	ND	96	0.00E+00	*Lactobacillus plantarum*	CP024414
19	ISLca1	IS3	IS150	1613 bp	29/47	ND	86	0.00E+00	*Lactobacillus casei*	NC_008526

Sr. No.	IS Element	IS Family	Group	IS length	IR length	Transposition	% Identity	E value	Origin	Accession number
20	IS1165	ISL3		1553 bp	20/39	ND	98	5.00E-26	*Leuconostoc mesenteroides*	X62617
21	ISLpl2	IS3	IS150	1491 bp	24/27	ND	95	0.00E+00	*Lactobacillus plantarum*	CP024414
22	ISLpl2	IS3	IS150	1491 bp	24/27	ND	97	8.00E-131	*Lactobacillus plantarum*	CP024414
23	ISLhe30	IS30		1025 bp	23/34	ND	94	0.00E+00	*Lactobacillus helveticus*	CBUL010000181
24	ISLasa2	IS3	IS150	1619 bp	19/22	ND	89	9.00E-14	*Lactobacillus salivarius*	CP089850
25	ISLpl2	IS3	IS150	1491 bp	24/27	ND	97	2.00E-53	*Lactobacillus plantarum*	CP024414
26	ISLpl2	IS3	IS150	1491 bp	24/27	ND	98	1.00E-23	*Lactobacillus plantarum*	CP024414
27	IS153	IS3	IS3	1127 bp	27/37	ND	97	0.00E+00	*Lactobacillus sanfranciscensis*	AJ239042
28	ISLasa2	IS3	IS150	1619 bp	19/22	ND	90	2.00E-16	*Lactobacillus salivarius*	CP089850
29	ISLhe30	IS30		1025 bp	23/34	ND	94	0.00E+00	*Lactobacillus helveticus*	CBUL010000181
30	ISLasa2	IS3	IS150	1619 bp	19/22	ND	90	2.00E-16	*Lactobacillus salivarius*	CP089850
31	ISLhe30	IS30		1025 bp	23/34	ND	95	0.00E+00	*Lactobacillus helveticus*	CBUL010000181
32	ISLhe30	IS30		1025 bp	23/34	ND	95	0.00E+00	*Lactobacillus helveticus*	CBUL010000181
33	ISLpl2	IS3	IS150	1491 bp	24/27	ND	97	2.00E-43	*Lactobacillus plantarum*	CP024414
34	ISLasa2	IS3	IS150	1619 bp	19/22	ND	90	1.00E-16	*Lactobacillus salivarius*	CP089850
35	IS1165	ISL3		1553 bp	20/39	ND	98	0.00E+00	*Leuconostoc mesenteroides*	X62617
36	ISLpl3	IS5	IS427	852 bp	16/18	ND	99	8.00E-98	*Lactobacillus plantarum*	NC_004567
37	ISLpl1	IS30		1043 bp	22/24	ND	100	3.00E-54	*Lactobacillus plantarum*	AF459445
38	ISPp1	IS30		1039 bp	21/23	ND	97	6.00E-40	*Pediococcus pentosaceus*	Z32771
39	ISLasa2	IS3	IS150	1619 bp	19/22	ND	89	5.00E-14	*Lactobacillus salivarius*	CP089850

Sr. No.	IS Element	IS Family	Group	IS length	IR length	Transposition	% Identity	E value	Origin	Accession number
40	ISLca1	IS3	IS150	1613 bp	29/47	ND	85	6.00E-157	*Lactobacillus casei*	NC_008526
41	ISLpl2	IS3	IS150	1491 bp	24/27	ND	98	8.00E-67	*Lactobacillus plantarum*	CP024414
42	ISLpl2	IS3	IS150	1491 bp	24/27	ND	97	2.00E-53	*Lactobacillus plantarum*	CP024414
43	ISLhe30	IS30		1025 bp	23/34	ND	95	0.00E+00	*Lactobacillus helveticus*	CBUL010000181
44	IS153	IS3	IS3	1127 bp	27/37	ND	97	0.00E+00	*Lactobacillus sanfranciscensis*	AJ239042
45	ISLpl2	IS3	IS150	1491 bp	24/27	ND	96	3.00E-180	*Lactobacillus plantarum*	CP024414
46	ISLasa2	IS3	IS150	1619 bp	19/22	ND	90	1.00E-16	*Lactobacillus salivarius*	CP089850
47	ISLhe30	IS30		1025 bp	23/34	ND	92	4.00E-81	*Lactobacillus helveticus*	CBUL010000181
48	IS153	IS3	IS3	1127 bp	27/37	ND	97	5.00E-49	*Lactobacillus sanfranciscensis*	AJ239042
49	ISLhe30	IS30		1025 bp	23/34	ND	93	0.00E+00	*Lactobacillus helveticus*	CBUL010000181
50	ISLhe30	IS30		1025 bp	23/34	ND	94	0.00E+00	*Lactobacillus helveticus*	CBUL010000181
51	ISLhe30	IS30		1025 bp	23/34	ND	90	3.00E-173	*Lactobacillus helveticus*	CBUL010000181
52	ISLhe30	IS30		1025 bp	23/34	ND	91	7.00E-57	*Lactobacillus helveticus*	CBUL010000181
53	ISLpl2	IS3	IS150	1491 bp	24/27	ND	98	4.00E-12	*Lactobacillus plantarum*	CP024414
54	ISLhe30	IS30		1025 bp	23/34	ND	90	3.00E-87	*Lactobacillus helveticus*	CBUL010000181
55	ISLhe30	IS30		1025 bp	23/34	ND	90	8.00E-55	*Lactobacillus helveticus*	CBUL010000181
56	ISLhe30	IS30		1025 bp	23/34	ND	96	0.00E+00	*Lactobacillus helveticus*	CBUL010000181
57	ISLasa2	IS3	IS150	1619 bp	19/22	ND	91	8.00E-27	*Lactobacillus salivarius*	CP089850
58	ISLhe30	IS30		1025 bp	23/34	ND	92	2.00E-163	*Lactobacillus helveticus*	CBUL010000181

Table 4.6: BLAST search results of CDS in prophage sequence 1 (scaffold 9)

CDS position	Description	Query cover	E-value	Percentage identity	Accession number
36312..37892	Single recognition particle –docking protein FtsY (*Limosilactobacillus fermentum*)	100%	0.0	100%	WP_100351566.1
38437..39867	Signal recognition particle protein (Lactobacillaceae)	100%	0.0	100%	WP_003683870.1
40430..41146	NUDIX domain containing protein (*Limosilactobacillus fermentum*)	100%	1e-175	100%	WP_100351567.1
41273..41725	Nicotinate phosphoribosyltransferase (Limosilactobacillus)	100%	3e-105	98%	WP_139561488.1
41834..42679	Nicotinate phosphoribosyltransferase (Lactobacillaceae)	100%	0.0	98.21	WP_003645597.1
42690..43235	Cysteine hydrolase (Limosilactobacillus fermentum)	100%	6e-134	100%	WP_021816750.1
Complement (43707..43838)	IS-30 family transpoases (*Limosilactobacillus fermentum*)	100%	4e-23	100%	WP_024500932.1

Table 4.7: BLAST search results of CDS in prophage sequence 2 (scaffold 64)

CDS position	Description	Query cover	E-value	Percent identity	Accession number
719..1450	RNA-guided endonuclease TnpB family protein (*Limosilactobacillus fermentum*)	89%	4e-160	99.08%	WP_205304220.1
Complement (1659..1802)	IS200/IS605 family transposase (*Limosilactobacillus fermentum*)	100%	4e-26	97.87%	WP_213491331.1
1876..2778	RNA-guided endonuclease TnpB family protein (*Limosilactobacillus fermentum*)	97%	0.0	99.66%	WP_154244371.1
2805..3848	RNA-guided endonuclease TnpB family protein (*Limosilactobacillus fermentum*)	100%	0.0	100%	WP_100352081.1
4063..5196	Endonuclease SbcCD subunit D (*Limosilactobacillus fermentum*)	100%	0.0	100%	WP_100352082.1
5214..8297	SMC family ATPase (*Limosilactobacillus fermentum*)	100%	0.0	100%	WP_100352083.1

4.4.19.3.d CRISPR-Cas system

When the genome of NCDC 400 was searched for CRISPR-related sequences, a total of three CRISPR sequences were predicted (**Table 4.8**). Amongst, two were questionable (located on contigs 3 and 10) and one was confirmed (present on contig 28). CRISPR-Cas system provides general defense systems that protect cells from invading DNA. Further CRISPRCasFinder predicted 9 putative Cas-related enzymes in the CRISPR array 1 and 4 in CRISPR array 3 (**Table 4.9**), and their location has been predicted by the CRISPRone tool (**Fig. 4.24**). Similar results were obtained for *Enterococcus lactis* wherein, two incomplete CRISPR motifs were identified (Fu *et al*., 2022). *L. reuteri* PNW1 showed five CRISPR sequences in the genome (Alayande *et al*., 2020). On the other hand, although *L. plantarum* MTCC 5463 did not possess any CRISPR sequences, the authors reported that the strain is stable over 25 years (Senan *et al*., 2015).

Table 4.8: Putative CRISPR-Cas sequences found within NCDC 400 genome

Contigs No.	Fragment position	Spacer count	Spacer sequence	Repeat consensus (DR)
3	38179-38329	2	>spacer1 CCATTGACATGGCCACCAGGGACTACTATCAA >spacer2 CCCGAAAGTCCCCGTTGTCGGCAATTTCCGTG	1
10	1319-1430	1	>spacer1 CCTGTAAGCGCTTATGGTAACGGTTAATCCCGTA	1
28	7909-8538	9	>spacer1 TACGTCGACGTATCTTGACGATGAATTAGG >spacer2 CTCTATCCGCAACTAGAGGAATCGAACCTC >spacer3 ATACATCATCGCCAACTGCACCGATAACAA >spacer4 CCGCCACTTTCGAGATTGCGCGCTTTTATG >spacer5 TCCTTGGCTTCAAAATAATTGTTTTTATTT >spacer6 TACCCACTTACCGGGTTGCCACGTGCAGCG >spacer7 AACGGGTACGTTACAACCTTGTCAAGCTTT >spacer8 TAGAGTGGATAACCTTAACCGTGCGGAAGA >spacer9 CATCGTCATTTCAAGGTTGCTCGTAACTGG	1

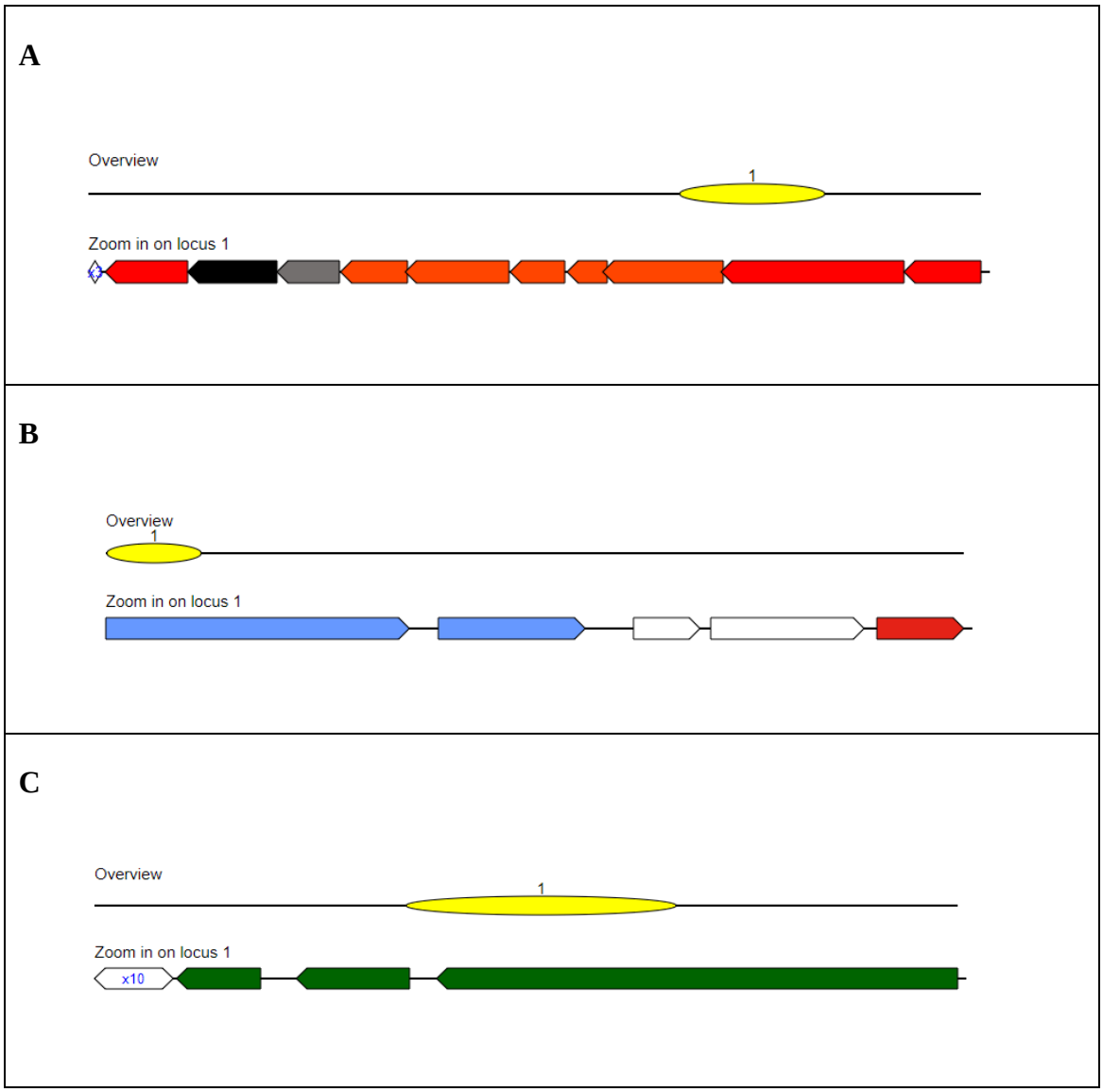

Fig. 4.24: CRISPR- Cas system visualization on the assembled genome predicted using CRISPRone tool. The colored regions are the Cas-predicted genes in two loci. The CRISPR-Cas prediction in locus1 is shown as yellow markings on the first track. The white box is the predicted CRISPR repeat region.

Table 4.9: Cas-related enzymes coded by CRISPR arrays in NCDC 400

Gene name	Start	End	Orientation
CRISPR sequence 1 (contig 3)			
Cas2_Type IE	32,359	39,237	-
Cas3_Type I	44,884	46,821	-
Cas3_Type I	44,884	46,821	-
Cas3a_Type I	46,822	47,625	-
Cas3a_Type I	46,822	47,625	-
Cas5_Type IE	40,851	41,561	-
Cas6_Type IE	40,182	40,838	-
Cas7_Type IE	41,539	42,626	-
Cse2_Type IE	42,654	43,232	-
CRISPR sequence 3 (contig 28)			
Cas_Type I-II-III	9,235	9,555	-
Cas1_Type II	9,518	10,423	-
Cas9_Type II	10,631	14,767	-
Csn2-Type IIA	8,567	9,238	-

4.4.19.3.e. Functional annotation of NCDC 400 using RAST and Prokka and prediction of ARGs and virulent genes

The previously sequenced whole genome of NCDC 400 was annotated for functional coordinates. The RASTtk server predicted genome size of 1.89 Mb with a GC content of 51.6%. RAST server indicated the total number of 2082 predicted protein-coding sequences (CDSs), distributed in 207 SEED subsystems. In addition, the RAST analysis showed 66 structural RNAs in the genome. Similarly, the genome annotation using Prokka showed 1841 CDS, a total of 66 functional RNA comprising 9 rRNA, 56 tRNA, and 1 tmRNA. Although both the pipelines predicted the same number of RNA, the number of CDS was different because the RASTtk server is not equipped to predict

the hypothetical proteins while the same is not true with Prokka. Amongst the various subsystems, the present study was interested in two subsystem features; i) mobile genetic elements and ii) virulence, disease, and defense (**Fig. 4.25**). Among the mobile genetic elements, the genome portrayed one remnant of phage minor capsid protein (*Min*). The incompleteness of complete prophage sequences underpins the genome stability of this strain. It is interesting to note that this genome was free from pathogenicity islands, gene transfer agents, and transposable elements suggesting excellent genome stability and the non-virulent nature of NCDC 400.

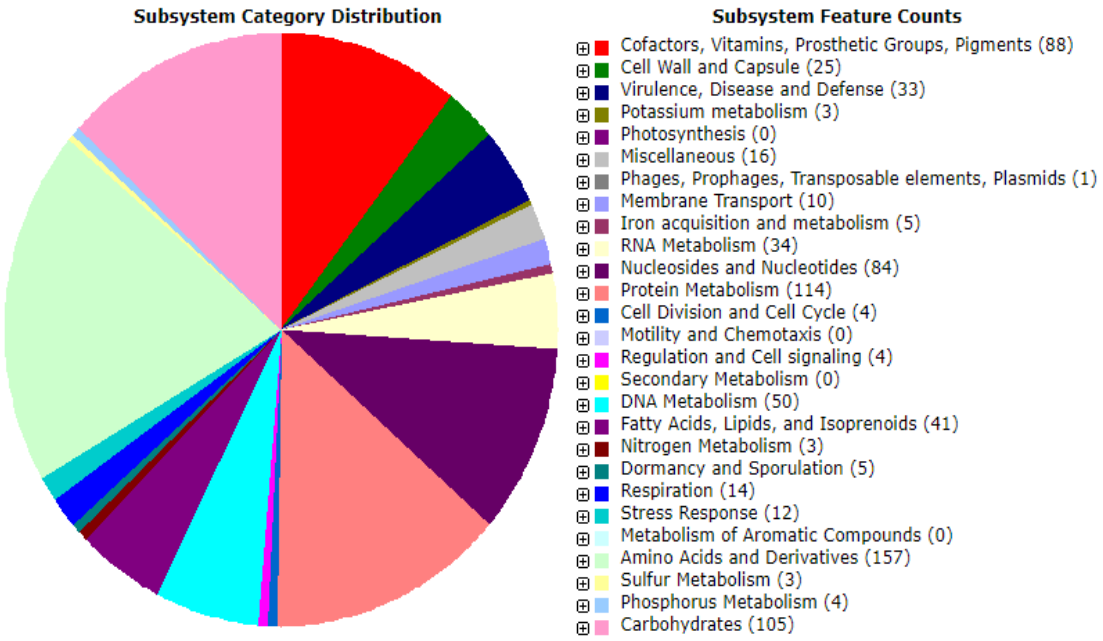

Fig. 4.25: An overview of the RAST annotation and subsystems for the NCDC 400 genome

Secondly, the subsystems under the category of "virulence, disease, and defense" showed 8 coordinates conferring antibiotic resistance. Amongst, two genes (*EF_G* and *Tet_like 2*) for tetracycline resistance, two genes for fluoroquinolones resistance (*gyrA* and *gyrB*), and one multidrug efflux pump (*MATE_family_MDR_Pump*) were found in the NCDC 400 genome (**Table 4.10**). In order to further confirm this annotation accuracy through a valid and updated AMR database, the aforementioned gene sequences were analyzed by CARD-BLASTn and RGI and found no hits with any resistance genes. On the other hand, the annotation with Prokka demonstrated the presence of resistance genes towards tetracycline (*TetO* and *Tetracycline resistance protein, class B*), multidrug resistance (*mdtD_1*, *mdtG_1 mdtG_2*, *mdtD_3*, and *emrY*)

and Fosmidomycin (*fsr*), which was not predicted by RAST. Further analysis of Prokka-predicted genes by CARD-BLASTn and RGI indicated no hits against the corresponding to these gene sequences. This suggests that the genome predition by RAST and Prokka with respect to ARGs may be inappropriate/ invalid. Moreover, it is worth dragging attention here that there was no analogy between the genotype and phenotype because this strain did not show phenotypic resistance to corresponding antibiotics. The multiple antibiotic resistance index (MAR index) of this strain was almost negligible (0.03; calculated by dividing the number of antibiotics to which the strain showed resistance by total tested antibiotics) suggesting no resistance phenotype toward multiple antibiotics. This indicates that these genes may exist as non-functional pseudogenes in the bacterium or they may be assigned to several other roles in bacterial physiology. For example, *GyrA* is required for DNA replication. Several multidrug resistance proteins and efflux pumps are reported to be involved in the detoxification process (commonly spread across several types of *Lactobacillus* spp.) as well as conferring resistance to other toxic compounds in the environment (Mann *et al*. 2021a). These results are similar to the finding of Mann *et al*. (2021a) who also reported similar genes in *L. fermentum* OK upon CARD-based annotation. Goyal (2018) also deciphered the whole genome of another probiotic species of *Limosilactobacillus* genera (*L. reuteri* LR6) and reported similar tetracycline and fluoroquinolones resistance genes (Goyal, 2018). This confirms that these genes may exist in bacteria as pseudogenes and are found ubiquitously in the genus *Limisolilactobacillus* (Goyal, 2018). In agreement with this bioinformatics prediction, Senan *et al*. (2015) have also reported tetracycline resistance confirming ribosomal protection proteins having homology to elongation factors were identified in *L. helveticus* MTCC 5463, a well-studied and applied Indian probiotic with stable features. The author states that *Lactobacilli* possess intrinsic resistances to quinolones and vancomycin as well as protein-binding antibiotics like tetracycline and erythromycin. These reports support the safety and the ongoing use NCDC 400 strain.

Table 4.10: Validation of RAST and Prokka annotated ARGs using globally accepted CARD and RGI database

Sr. No.	AMR gene	Function	Antibiotics class	Annotation platform	CARD and RGI	Phenotypic resistance
1	*EF_G*	Translation elongation factor G	Tetracycline	RAST	No hit found	No
2	*Tet_like2*	Ribosome protection-type tetracycline resistance related proteins, group 2				
3	*gyrA*	DNA gyrase subunit A (EC 5.99.1.3)	Fluoroquinolones			
4	*gyrB*	DNA gyrase subunit B (EC 5.99.1.3)				
5	*MATE_family_MDR_Pump*	Multi antimicrobial extrusion protein (Na(+)/drug antiporter), MATE family of MDR efflux pumps	Multiple drugs			
6	*Tet* O	Tetracycline resistance	Tetracycline	Galaxy Prokka		No
7	Tetracycline resistance protein, class B	Tetracycline resistance				
8	*mdtG_1*	Multidrug resistance	Multiple drugs			
9	*mdtD_1*	Multidrug resistance				
10	*mdtG_2*	Multidrug resistance				
11	*fsr*	Fosmidomycin resistance	Phosphonic antibiotics			Not Tested
12	*mdtD_3*	Multidrug resistance	Multiple drugs			No
13	*emrY*	Putative multidrug resistance protein	Multiple drugs			

Virulence, Disease, and Defense subsystem under the invasion and intracellular resistance category demonstrated the *Mycobacterium* virulence operon involved in protein synthesis, DNA transcription, and an operon possibly involved in the quinolinate biosynthesis (**Table 4.11**). However, when the RAST predicted nucleotide sequences were further verified by BLAST analysis in VFDB and PathogenFinder resulted in no hits or matches suggesting that these genes may be not involved in the causing pathogenesis or invasion. In addition, these genes were also not predicted in the Prokka pipeline. This suggests that these genes may play multifunctional roles in bacterial biology involving transcription and translation processes, but not virulence. It is worth mentioning that these sequences showed 100% identity (E-value 0.0) with several other similar sequences of *L. fermentum, L. mucosae,* and *L. reuteri* complete genome (Accession number: CP044354.1; CP050919.1; CP045034.1; CP062966.1, etc) upon NCBI-BLASTn analysis. This provides a hint that these sequences are highly conserved among *L. fermentum* and *L. reuteri*. These results are in close analogy with Goyal (2018) who reported complete gene set involved in transcription, translation as well their transportation in potential probiotic *L. reuteri* LR6.

Although not frequently reported in LAB, the RAST predicted the genes for quinolinate biosynthesis in NCDC 400 genome; however, such genes were not identified by Prokka. Quinolinate is a biochemical that is reported to act as a double-edged sword. It is because this metabolite is essential as well as non-essential (acts as a neurotoxin). The quinolinate is synthesized from L-aspartate in presence of two enzymes *viz.* L-aspartate oxidase (*NadB*) and quinolinate synthetase (*NadA*). The beneficial aspect of quinolinic acid is that Nicotinamide Adenine Dinucleotide (NAD), a cofactor in biochemical redox reactions, is synthesized from quinolinic acid *de novo* in presence of quinolinate phosphoribosyltransferase (Ollagnier-de *et al*., 2005). NCDC 400 had both subsystems (*NadB* and *NadA*) to synthesize the quinolinate and subsequently the quinolinate phosphoribosyltransferase for the conversion of quinolinate to NAD. Therefore, it is obvious that cellular stockpiling of quinolinate may not be seen in NCDC 400 because of quinolinate phosphoribosyltransferase. However, the irony lies in quinolinate, if produced in this strain, will be utilized to provide NAD or it stockpiles and secretes into the medium. A clear conclusion to this dilemma can be drawn only upon subjecting these genes to expression studies or conducting the *in vivo* trials of the strain. Gross pathological changes along with a detailed clinical pathology of brain tissue

of animals fed with this strain could answer this question. However, a recent previous study on quinolinate indicates that the accumulation of quinolinate is very less in the brain even upon its co-administration with LPS in rodent models suggesting the non-toxic nature of quinolinate (Moffett *et al*., 2020). Similar to this study, many food-grade *L. fermentum* strains (ING8, MTCC 25067) and *Lactiplantibacillus plantarum* strains (Lp-6 and RI113) have shown the aforementioned gene set to produce quinolinate (NCBI Accession: CP034193.1; CP017408.1; AP017973.1; CP060184.1). This suggests that quinolinate biosynthetic genome fingerprints are not novel in LAB.

Table 4.11: Invasion and intracellular resistance subsystem of NCDC 400 genome annotated by RAST and their validation by Prokka / VFDB/ VirulenceFinder search

Subsystem	Role	Prokka / VFDB/ VirulenceFinder
Mycobacterium virulence operon involved in protein synthesis (SSU ribosomal proteins)	SSU ribosomal protein S7p (S5e)	-
Mycobacterium virulence operon involved in protein synthesis (SSU ribosomal proteins)	Translation elongation factor G	-
Mycobacterium virulence operon involved in protein synthesis (SSU ribosomal proteins)	Translation elongation factor Tu	-
Mycobacterium virulence operon involved in protein synthesis (SSU ribosomal proteins)	SSU ribosomal protein S12p (S23e)	-
Mycobacterium virulence operon involved in DNA transcription	DNA-directed RNA polymerase beta' subunit (EC 2.7.7.6)	-
Mycobacterium virulence operon involved in DNA transcription	DNA-directed RNA polymerase beta subunit (EC 2.7.7.6)	-
Mycobacterium virulence operon possibly involved in quinolinate biosynthesis	Quinolinate synthetase (EC 2.5.1.72)	-
Mycobacterium virulence operon possibly involved in quinolinate biosynthesis	Quinolinate phosphoribosyltransferase [decarboxylating] (EC 2.4.2.19)	-
Mycobacterium virulence operon possibly involved in quinolinate biosynthesis	L-aspartate oxidase (EC 1.4.3.16)	-
Mycobacterium virulence operon involved in protein synthesis (LSU ribosomal proteins)	LSU ribosomal protein L35p	-
Mycobacterium virulence operon involved in protein synthesis (LSU ribosomal proteins)	Translation initiation factor 3	-
Mycobacterium virulence operon involved in protein synthesis (LSU ribosomal proteins)	LSU ribosomal protein L20p	-

4.4.19.3.f. Identification of harmful enzymes and metabolite-associated genes by manual search

After functional annotation of NCDC 400, the annotated files were searched for various virulence factors as well as genes encoding undesirable factors (enzymes or metabolites) based on the published literature on probiogenomics. Accordingly, NCDC 400 did not reveal the genes to express mucin degradation enzymes (glycoside hydrolase, alpha-galactosidases, β-galactosidases, and β-glucosidases) (**Table 4.12**). Moreover, such mucolytic enzymes were also not identified in this strain upon analyses in the Carbohydrate-Active enZYmes (CAZy) database. The genes encoding gelatinase and harmful intestinal enzymes (β-glucuronidase, β-glucosidase, nitrate reductase, arylsulphatase, azoreductase, urease, and tryptophanase) that are collated with the pathophysiology of cancer were also absent. Additionally, the genes encoding for deconjugation of bile acids (hydroxysteroid dehydrogenases (α and β) and bile-acid 7alpha-dehydroxylase) were also not found in the NCDC 400 genome. Similarly, the genome was also devoid of various frequently reported virulence factors like endocarditis antigen, cytolysin, hyaluronidase, aggregation substance, enterococcal surface protein, sex pheromones, endocarditis antigen, and integration factors. These results are in line with the previous findings reporting no evidence of such harmful or pathogenicity-inducing genes in *Lactobacillus* probiotic strains (Alayande *et al*., 2020; Mann *et al*., 2021a, Mann *et al*., 2021b, Senan *et al*., 2015).

On the contrary, Prokka predicted the two virulence factors in the NCDC 400 genome which were not predicted by RAST. Hemolysis A predicted by Prokka was verified by aligning the annotated sequence in BLAST against the UniProt database. The sequence showed perfect alignment with FtsJ (cell division protein) (E value 0 and Bitscore 531) (**Fig. 4.26**). Moreover, FtsJ protein did not show any interaction with the hemolysin A. Nevertheless, even if this hemolysin A gene (*tylA*) exists in NCDC 400, it failed to express since NCDC 400 did not show hemolytic activity phenotypically. Likewise, another virulence determinant, conserved virulence protein B, was also identified in the NCDC 400 genome by Prokka. This protein has been reported to influence the expression of virulence factors and pathogenicity via agr-dependent and agr-independent routes in *S. aureus*. Also, it has been involved in the production of hemolysin, DNase, protease, and protein A (https://www.uniprot.org/uniprotkb/Q2FYP3/entry).

Table 4.12: Harmful enzymes and other virulence factors identified by manual search in the RAST and Prokka annotated files of NCDC 400

Virulence gene	Function	RAST	Prokka	VFDB	UniProt match	Bitscore	E-value
Hemolysin A (*tylA*)	Hemolytic activity	-	+	-	FtsJ (cell division protein)	531	0.0
Glycoside hydrolase	Mucin degradation	-	-				
β-Glucosidases							
Gelatinase	Gelatin hydrolysis	-	-				
Conserved virulence factor B	Production of hemolysin, DNase, protease, and protein A	-	+ (*cvfB*)		IF-3 (Translation initiation factor)	570	0.0
β-Glucuronidase	Induction of cancer	-	-				
β-Glucosidase		-					
alpha-Galactosidases	Mucin degradation	-	-				
Beta-Galactosidases		-	-				
Nitrate reductase	Induction of cancer/ tumor	-	-				
Arylsulphatase		-	-				
Azoreductase		-	-				
Urease and tryptophanase	Ammonia and indole cause spread of systemic infection and mood swings	-	-				
Endocarditis antigen	Sepsis	-	-				
Hydroxysteroid dehydrogenases (α-HSD and beta)	Secondary bile acid metabolism end product	-	-				
Bile-acid 7alpha-dehydroxylase	Secondary bile acid metabolism end product	-	-				

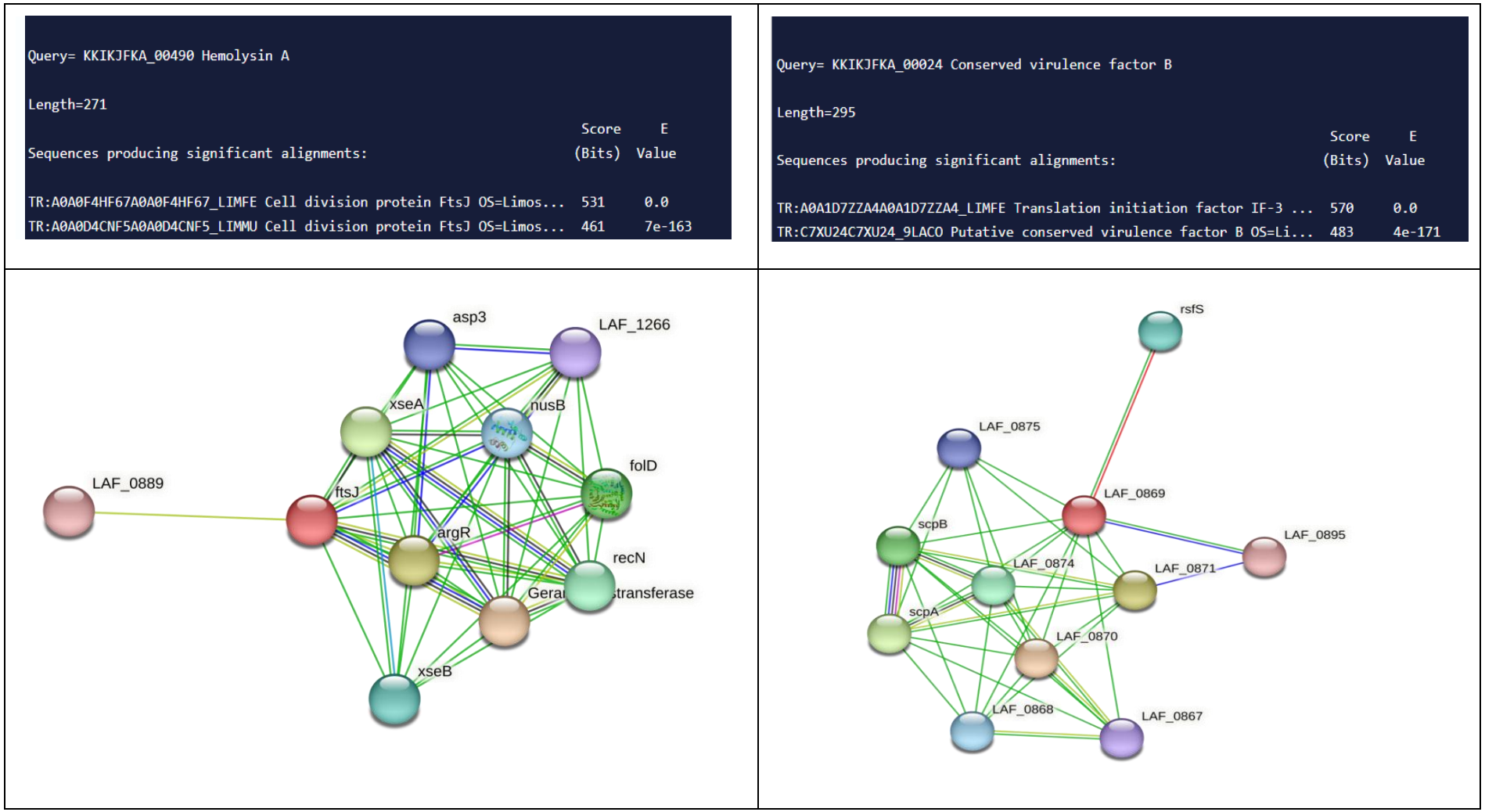

Fig. 4.26: UniProt BLAST search against hemolysin A and conserved virulence factor B identified in NCDC 400 by Prokka and its interactions with other proteins.

Further BLAST analysis using UniProt database suggested it as initiation factor 3 (IF-3) involved in translation (Bit score 573 and E value 0.0). IF-3 did not display any interaction with the conserved virulence protein B (**Fig. 4.26**). However, there was no resemblance between the genotype and phenotype of the strain. It is because the strain did not show hemolytic activity as well as DNAase activity *in vitro*. Therefore, these genes may be considered silent regarding the safety issue. This result is congruent with Fu *et al*. (2022) who also reported hemolysin A and as well as conserved virulence protein B in the *Enterococcus lactis* probiotic strain but failed to express phenotypically. Considering this, it can be inferred that the risk-to-benefit ratio of NCDC 400 is very less and hence strain may hold great potential to be commercialized as a safe probiotic after the animal and human trials thereof.

4.4.19.3.g Platelet aggregation

No genes related to direct platelet aggregation have been identified in the NCDC 400 genome. The well-established microbial platelet aggregation factors like clumping factors A & B (*ClfA* and *ClfB*), protein A (*SpA*), platelet adhesion protein A (*PadA*), iron-regulated surface determinate B, serine aspartate repeat G (*sdrG*), haemagglutinin salivary antigen (*Hsa*), glycosylated streptococcal protein A (*GspB*), and serine-rich protein A (*SrpA*) were missing in the genome. On the other hand, the proteins involved in triggering the platelet aggregation by indirect mode (fibrinogen binding protein, collagen binding protein, mucin binding protein), especially through interaction with bridging proteins (mucin, fibrinogen, collagen) were also not detected. Similarly, no genes involved in triggering the TLR-4 expressed on platelets (for example lipopolysaccharides) were identified. Shiga-like toxins as well as alpha-toxins present in most of the pathogens that promote the platelet aggregation phenomena were also unseen in this whole genome. Rather, the genes coding for teichoic acid that has been reported to inhibit platelet aggregation via interaction with collagen (platelet aggregation agonist) were detected. These microbial platelet aggregation factors used for whole genome search were referenced from Kerrigan (2015).

Likewise, NCDC 400 has no genes related to the metabolic pathway that produces phosphatidylserine, a known blood clotting and platelet aggregation factor. Only incomplete or partial genes involved in the glycine, serine, and threonine metabolism were found in NCDC 400 genome. Through the glycolysis process, the 3-Phospho-glycerate can be formed and it can be converted into 3-Phospho-

hydroxypyruvate and phosphoserine through the action of *serA* (D-3-phosphoglycerate dehydrogenase) and *serC* (Phosphoserin aminotransferase). The phosphoserine can be converted into serine and subsequently to glycine through the action of *GlyA* (Serine hydroxymethyltransferase). But the strain has no genes to carry out the downstream reactions to form O-phosphatidyl L-serine (**Fig. 4.27**) The genes (*CHO1*/*pssA*) coding for CDP-diacylglycerol–-serine O-phosphatidyltransferase were also missing and hence, it cannot even directly produce O-phosphatidyltransferase from serine. All these evidence conclusively suggests that the likeliness of this strain to demonstrate platelet aggregation knack is hardy less or even nil. An analogy with this, NCDC 400 did not demonstrate the platelet aggregation phenotype *in vitro*. These results are in close alignment with Mann *et al*. (2021a), wherein the authors found an incomplete pathway involved in the metabolism of serine and threonine during the whole genome analysis of *L. fermentum* OK.

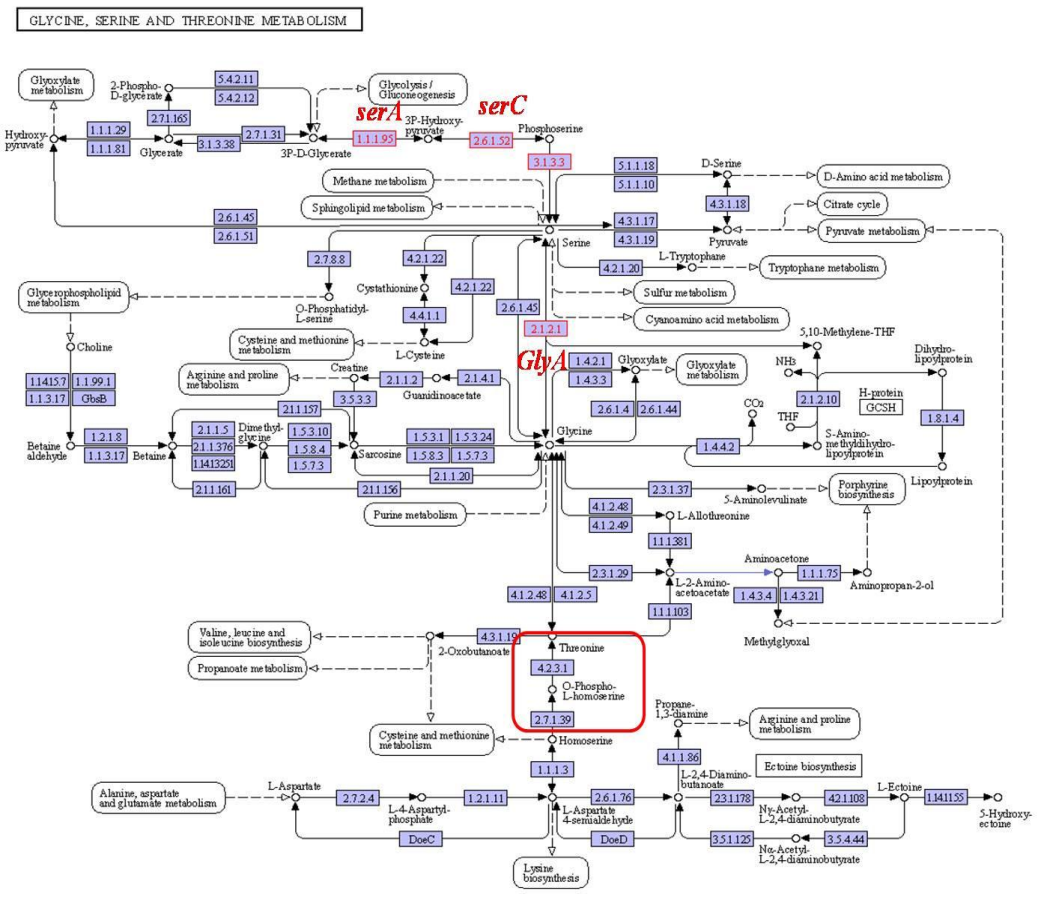

Fig. 4.27: Serine, threonine, and glycine metabolism pathways in *L. fermentum* NCDC 400. *SerA*, *SerC*, and *GlyA* were found in the NCDC 400 genome. The biosynthetic pathways of glycine, serine, and threonine are incomplete in the genome of NCDC 400, analyzed by matching with the KEGG pathway.

4.4.19.3.h. Biogenic amines production

The genes related to the production of biogenic amines either by direct amino acid decarboxylation or indirectly through auxiliary pathways were not detected in the NCDC 400 whole genome sequences. Amongst specific amino acid decarboxylase reactions, no genes that produce tyrosine decarboxylase (which generates tyramine from tyrosine), L-tryptophan decarboxylase (which synthesizes tyramine from tyrosine, histamine from histidine, tryptamine from tryptophan, and phenylethylamine from phenylalanine), lysine decarboxylase (which produces cadaverine from lysine), histidine decarboxylase (which forms histamine from histidine), ornithine decarboxylase (which generates putrescine from ornithine) were identified. However, incomplete gene sets for arginine and ornithine degradation pathways were found in the NCDC 400 (**Table 4.13)**. In the biology of NCDC 400, the glutamate may be converted into carbamoyl phosphate which can be subsequently converted into arginine. Similarly, the ornithine may be converted into citrulline and further to arginine. But no genes to transform ornithine to putrescine and arginine to putrescine were detected (**Fig. 4.28)**. This indicates that NCDC 400, despite the partial existence of arginine and ornithine degradation pathways, does not produce putrescine. In fact, there was a complete match between the phenotype and genotype was observed since putrescine was also not detected in HPLC. These results are consistent with Alayande *et al*. (2020) who also reported the inability of *L. reuteri* PNW1 to produce putrescine even if the genome had an arginine deiminase pathway.

Table 4.13: RAST-based prediction of completeness of arginine and ornithine degradation pathways in NCDC 400 whole genome

Scenario	Input Compounds	Output Compounds	Paint on Map	Status in 6666666.890024
Arginine to Glutamate	L-Arginine	L-Glutamate, Urea L-Glutamate, NH3, CO2	☐	incomplete
Arginine to Proline	L-Arginine	L-Proline, Urea L-Proline, NH3, CO2	☐	incomplete
Arginine to Putrescine	L-Arginine	Putrescine, Urea Putrescine, NH3, CO2	☐	incomplete
Glutamate to Oxoglutarate	L-Glutamate	2-Oxoglutarate, NH3	☐	incomplete
Putrescine to Glutamate and Aminobutanal	Putrescine	L-Glutamate, 4-Aminobutanal	☐	incomplete

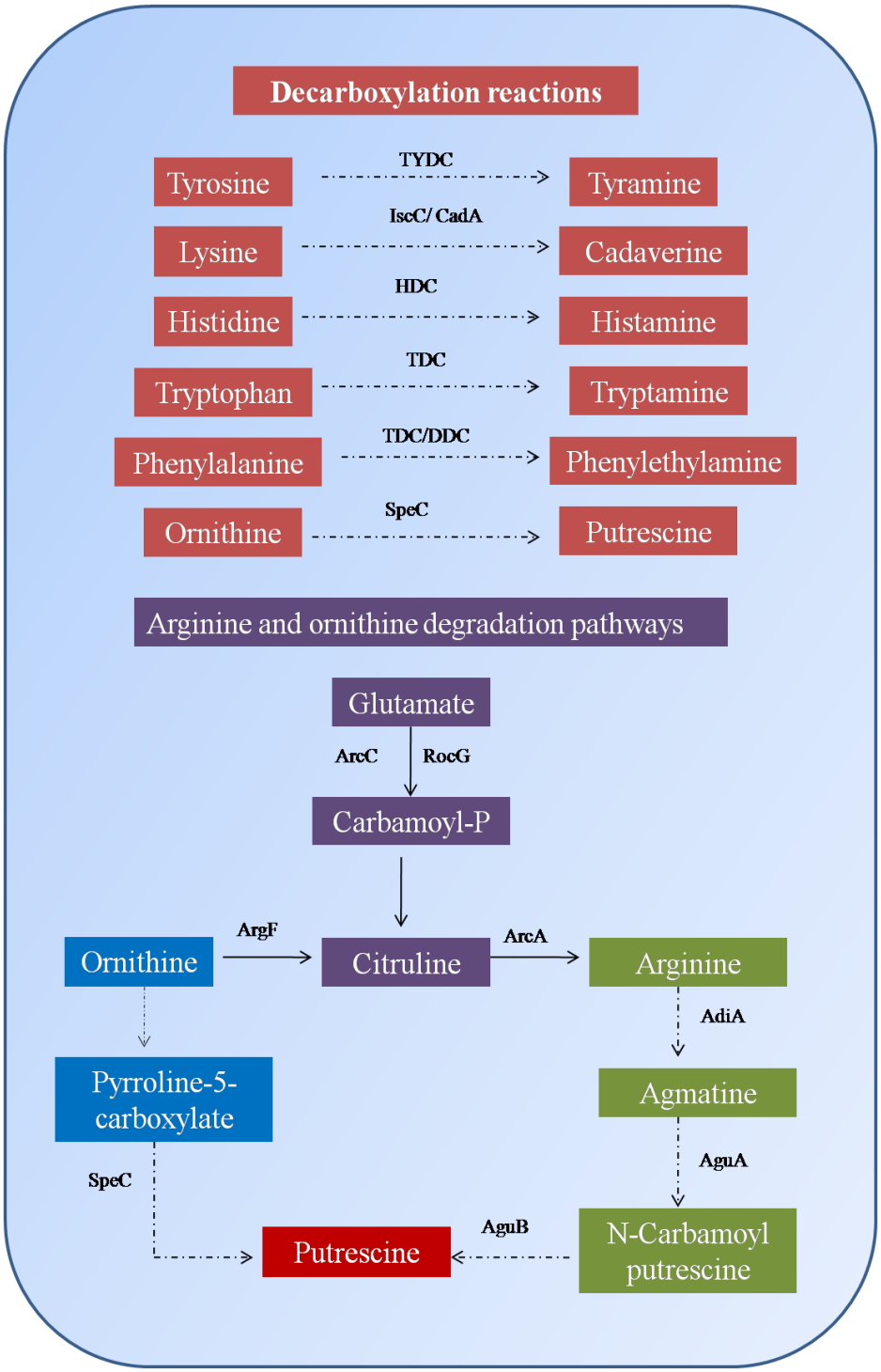

Fig. 4.28: Biosynthetic pathways for biogenic amines production by *L. fermentum* NCDC 400. Solid arrows indicate that the biosynthetic pathways of biogenic amine are effective and dashed arrows indicate invalid pathways. TYDC: Tyrosine decarboxylase; IscC: Lysine decarboxylase; HDC: Histidine decarboxylase; TDC/DDC: Tryptophan decarboxylase; SepC: Ornithine decarboxylase; RocG: NADP specific glutamate dehydrogenase; ArcC: Carbamate kinase; ArgF: Ornithine carbamyltransferase; ArcA: Arginine deiminase; AdiA: Arginine decarboxylase; AguA: Agmatine deiminase; AguB: N-Carbamoylputrescine amidase.

4.4.19.3.i. D-/L-lactate production

The genome of NCDC 400 had 7 sets or homologs of a gene encoding for L-LDH and only 3 homologs of D-LDH, and thereby providing a hint that why the proportion of L-isomer was dominated over D-isomer of lactic acid when assayed through the kit method *in vitro*. Hence, knowing the basic genome footprints of a bacterium can better help in understanding the phenotype. It is pertinent to note that this genome lacks gene coding for lactate racemase (E.C 5.1.2.1). This trait is very important for the probiotic bacterium since it reduces the plausibility of the conversation of lactic acid among its 2 isomeric forms. Owing to the absence of lactate racemase, it is clear that the ultimately produced D-/L-isomers of lactic acid by this strain are undoubtedly stable.

Objective 2: Toxicological evaluation of *Limosilactobacillus fermentum* NCDC 400 in the murine model

4.4.20. General health status

Repeated oral supplementation of NCDC 400 (high and low doses) for different durations (14 days for acute, 28 days for subacute, and 90 days for subchronic oral toxicity tests) showed no treatment-related toxicity signs or mortality in animals. None of the mice revealed clinical toxicity signs in their sleep, salivation, diarrhoea, skin, fur, eyes, and behavior. No changes in the physical appearance were observed throughout the study (**Fig. 4.29A**). The changes in the body weight during the experimental period have been presented in **Figs. 4.29-4.31**, and were found to vary insignificantly. No considerable changes in the average daily feed and water intake per mouse were seen during acute and subchronic toxicity studies. However, a trivial increase in the average daily feed and water consumption per mouse in subacute toxicity study was found in the both LD and HD groups compared to CON (**Fig. 4.30**). This could be correlated to the probiotic-mediated improvement in feed conversion rate (FCR). It is obvious that an increase in feed intake by the animals also boosts relative water consumption. These results acknowledge the findings of Kim *et al*. (2022a) wherein the oral administration of probiotic consortium *Lactiplantibacillus plantarum, Bacillus subtilis,* and *Saccharomyces cerevisiae* to rats for 28 days resulted in an improvement in feed consumption rate as well as body weight. Authors stated that bacterial enzymatic conversation of feed may help animals to absorb more nutrients from the diet which ultimately leads to gain in body weight.

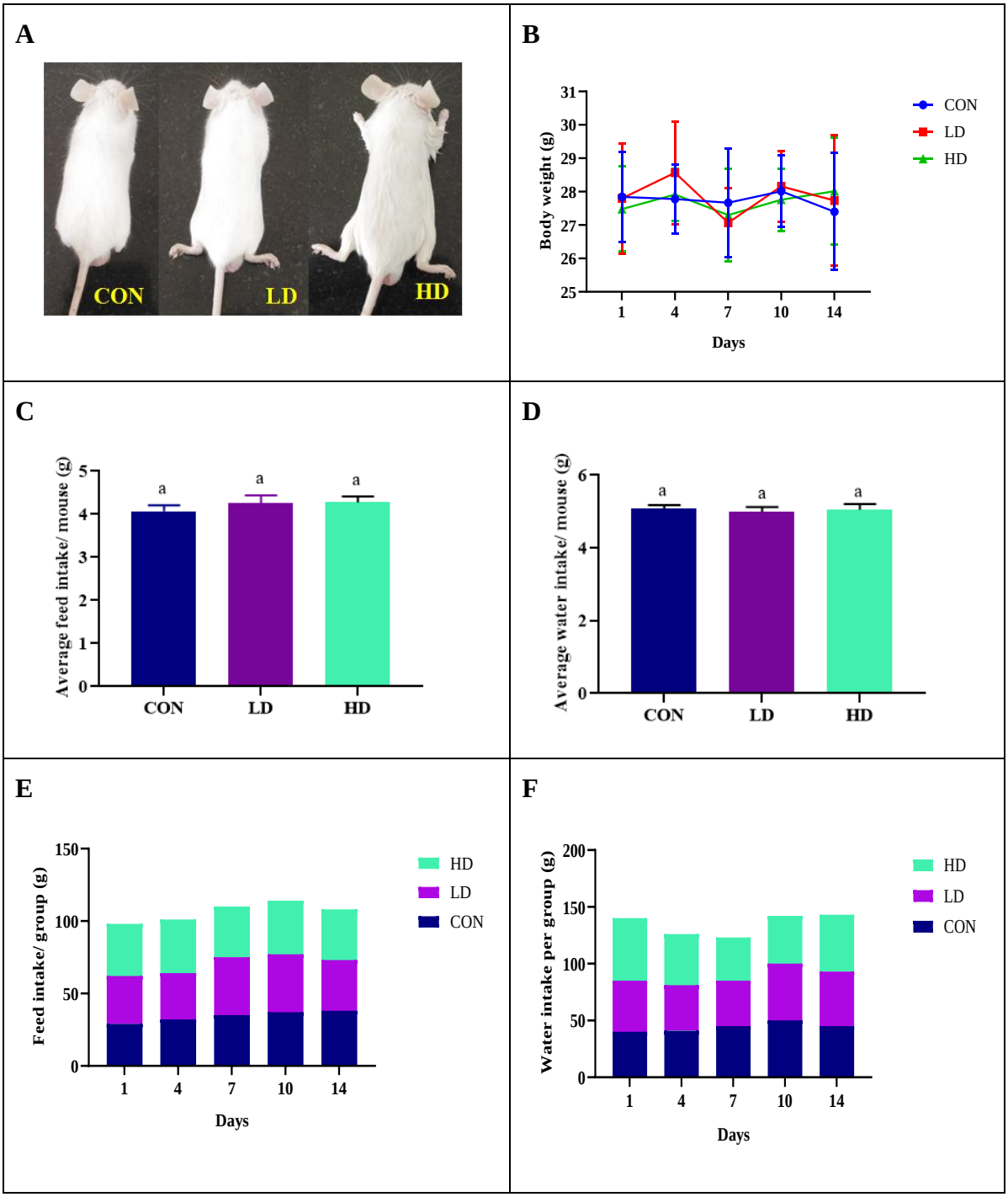

Fig. 4.29: Effect of oral supplementation of NCDC 400 on basic profiles and general health status of mice during acute oral toxicity test. (A) Physical appearance; (B) Changes in body weight; (C) Average daily feed intake/ mouse; (D) Average daily water intake/ mouse; (E) Changes in daily feed intake/ group; (F) Changes in daily water intake/ group. Error bars indicate the variations of nine determinations in terms of the standard error of mean. Lowercase superscript (a) indicates no significant differences ($p > 0.05$) between the groups.

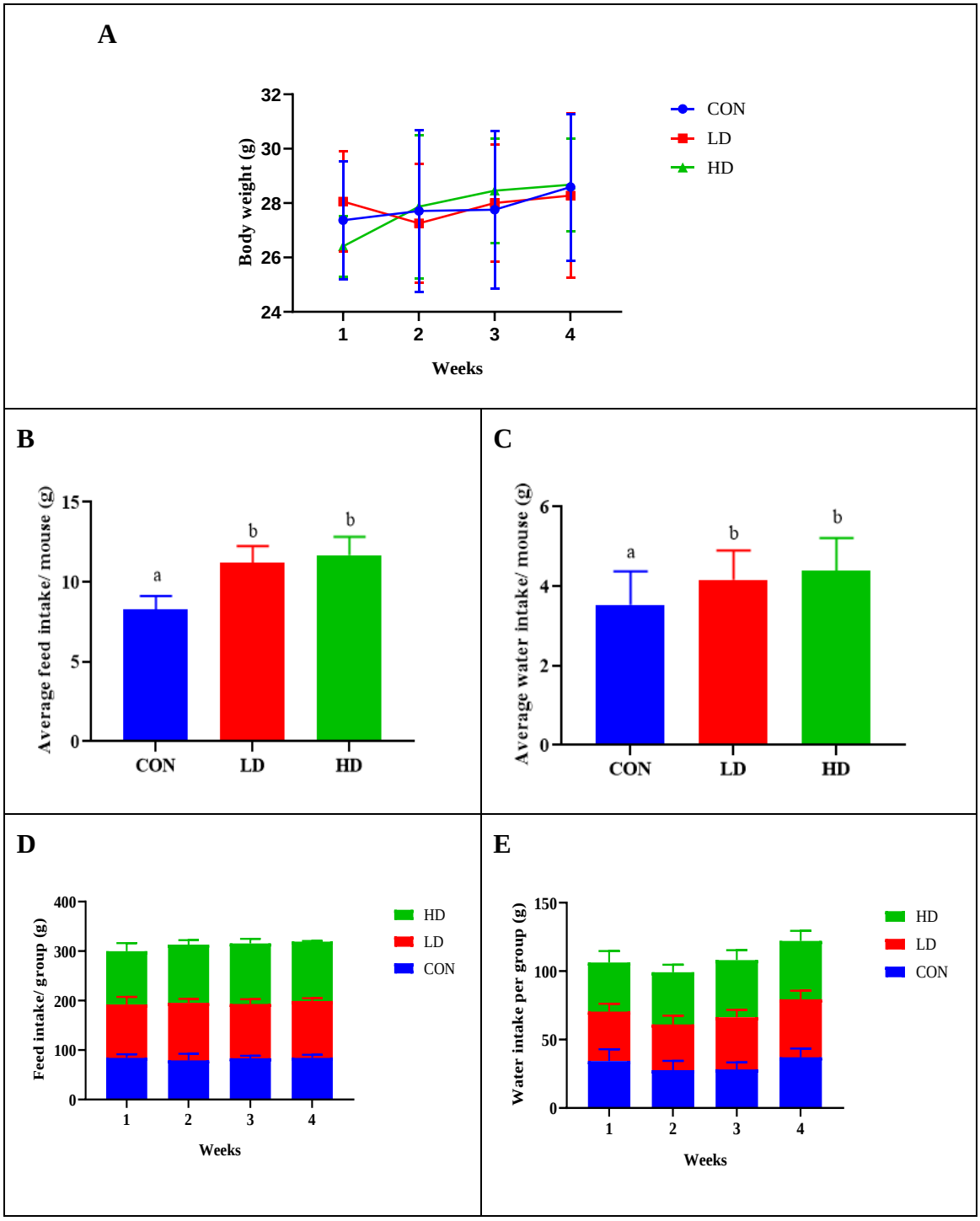

Fig. 4.30: Effect of oral supplementation of NCDC 400 on basic profiles and general health status of mice during sub-acute oral toxicity test. (A) Changes in body weight; (B) Average daily feed intake/ mouse; (C) Average daily water intake/ mouse; (D) Changes in daily feed intake/ group; (E) Changes in daily water intake/ group. Error bars indicate the variations of nine determinations in terms of the standard error of mean. Lowercase superscripts (a and b) indicates significant differences ($p < 0.05$) between the groups.

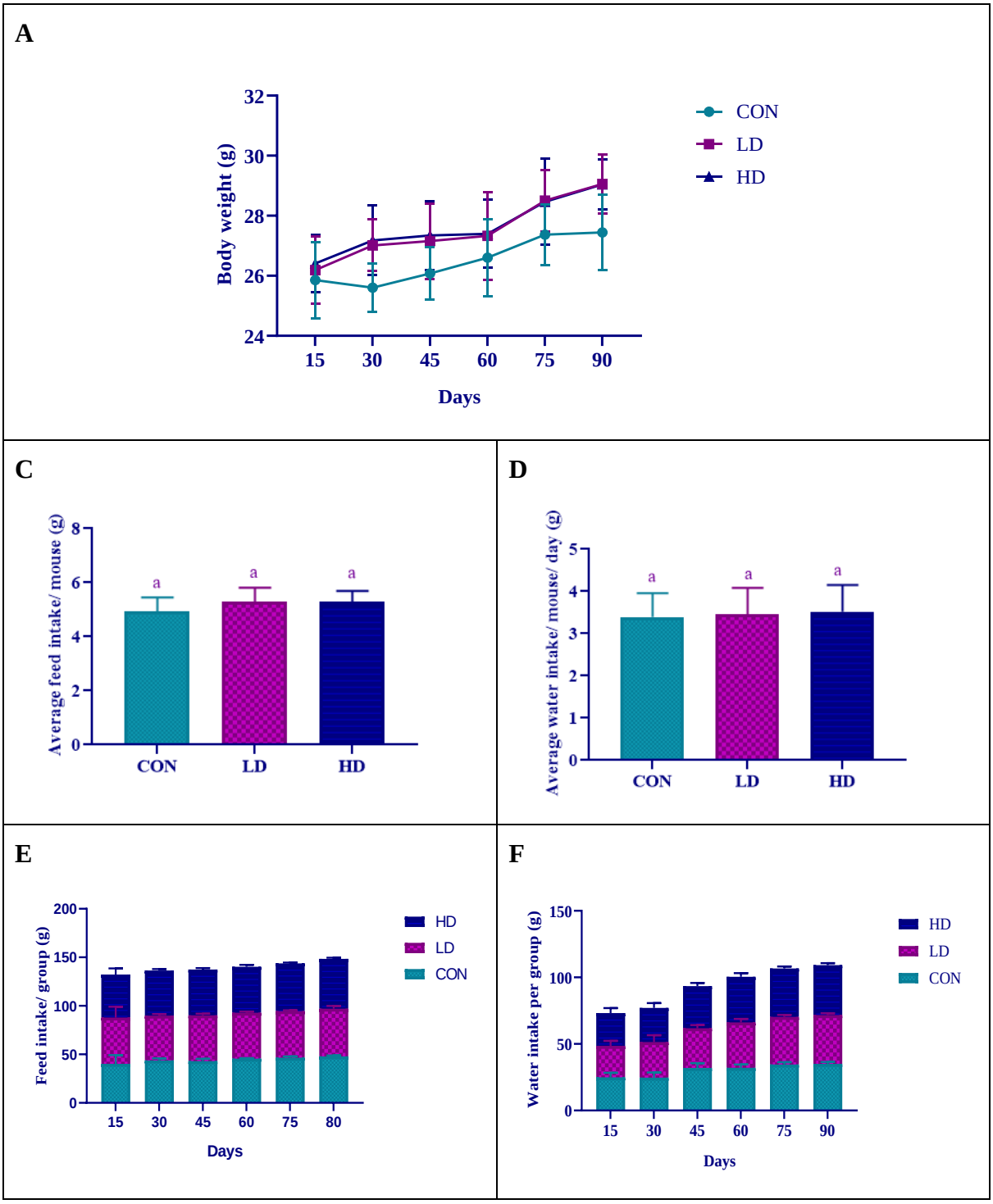

Fig. 4.31: Effect of oral supplementation of NCDC 400 on basic profiles and general health status of mice during sub-chronic oral toxicity test. (A) Changes in body weight; (B) Average daily feed intake/ mouse; (C) Average daily water intake/ mouse; (D) Changes in daily feed intake/ group; (E) Changes in daily water intake/ group. Error bars indicate the variations of nine determinations in terms of the standard error of mean. Lowercase superscript (a) indicates no significant differences ($p > 0.05$) between the groups.

Overall, there was no treatment-related gross weight loss or a decrease in feed and water intake by the experimental animals. The abnormal variations in the weight of experimental animals during toxicological testing indicate the toxic effects of test compounds. Similarly, feed and water consumption are factual indicators of the growth rate of animals, and therefore monitoring these parameters provides insights into treatment effects on appetite and usage of the ingested food (Todić *et al*., 2006). Considerable loss of body weight indicates the debilitating effect of the test substance on animals. Similar to these findings, Shokryazdan *et al*. (2016) have also found that oral dosing of probiotic *L. fermentum* HM3 for 14 and 28 days at 10^{10} CFU/kg BW/day did not influence food and water intake as well as body weight changes of toxicological concern.

4.4.21. Gross pathology

Necropsy is an important act of toxicological research for diagnostic investigations of treatment effects on various organs of experimental animals. At necropsy, there were no observable gross pathological changes in the organs (brain, liver, kidneys, lungs, heart, and spleen) of mice sampled from all three groups during oral toxicity tests. Further, there were no treatment-related visible lesions in all the examined organs (**Fig. 4.32**). These pathological observations are similar to Shokryazdan *et al*. (2016) who also found no gross changes in the vital organs upon acute oral toxicity study of *L. fermentum* HM3.

	CON	**LD**	**HD**
Brain	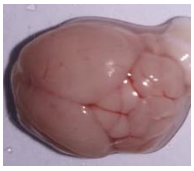		
Liver			
Kidneys			

Lungs	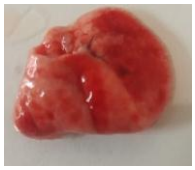	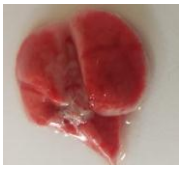	
Heart			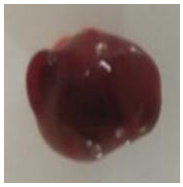
Spleen			

Fig. 4.32: Digital photography of necropsy specimens depicting gross pathological response in relation to the repeated exposure of NCDC 400 (high and low dose) for 14 days

4.4.22. Organ indices

The relative organ weights (also known as organ indices) of major organs *viz.* brain, heart, kidney, spleen, lungs, and liver showed no significant ($p < 0.05$) variations between the control and other two treatment groups (LD and HD) in all three oral toxicity trials (**Figs. 4.33-4.35**). This suggests that oral administration of NCDC 400 for short term (14 days) as well as considerably long term (28 and 90 days) at low and high doses has no adverse effects on various organs. Organ toxicity of test compounds causes changes in organ weight and volume, which in turn can be assessed by determining the organ index. The relative organ index has greater significance in toxicological research as it can be correlated to the development of treatment-related organ hypertrophy. These results are similar to the previous findings of Samtiya *et al*. (2020), who also witnessed no changes in organ indices upon the oral intervention of *L. fermentum* MTCC-5898 (LF) as high as 10^{11} CFU/day/mouse. Li *et al*. (2018) have also reported no changes in the organ indices in rats upon daily feeding of *Entercoccus durans* KLDS6.09030 (1×10^9 CFU/kg BW) for 28 days.

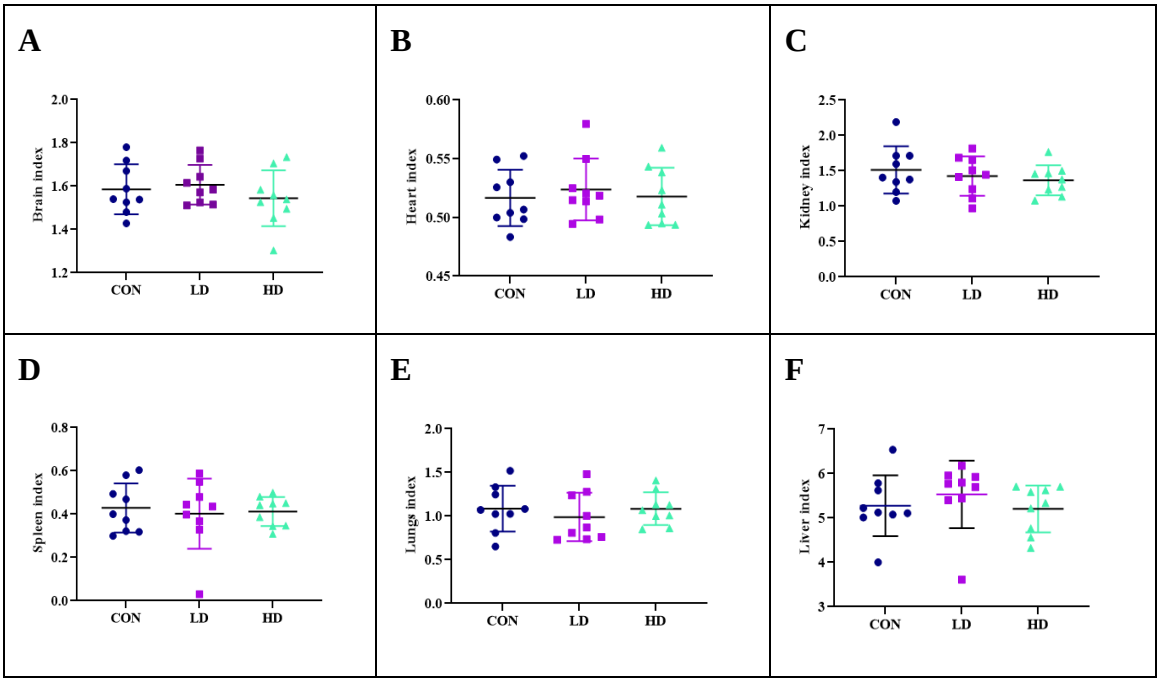

Fig. 4.33: Effect of oral dosing of NCDC 400 on relative organ weights during 14 days repeated dose acute oral toxicity study. (A) Brain index; (B) Heart index; (C) Kidney index; (D) Spleen index; (E) Lungs index; (F) Liver index. No significant difference at $p < 0.05$ was found across the groups (*Analyzed by one-way ANOVA following Duncan test).*

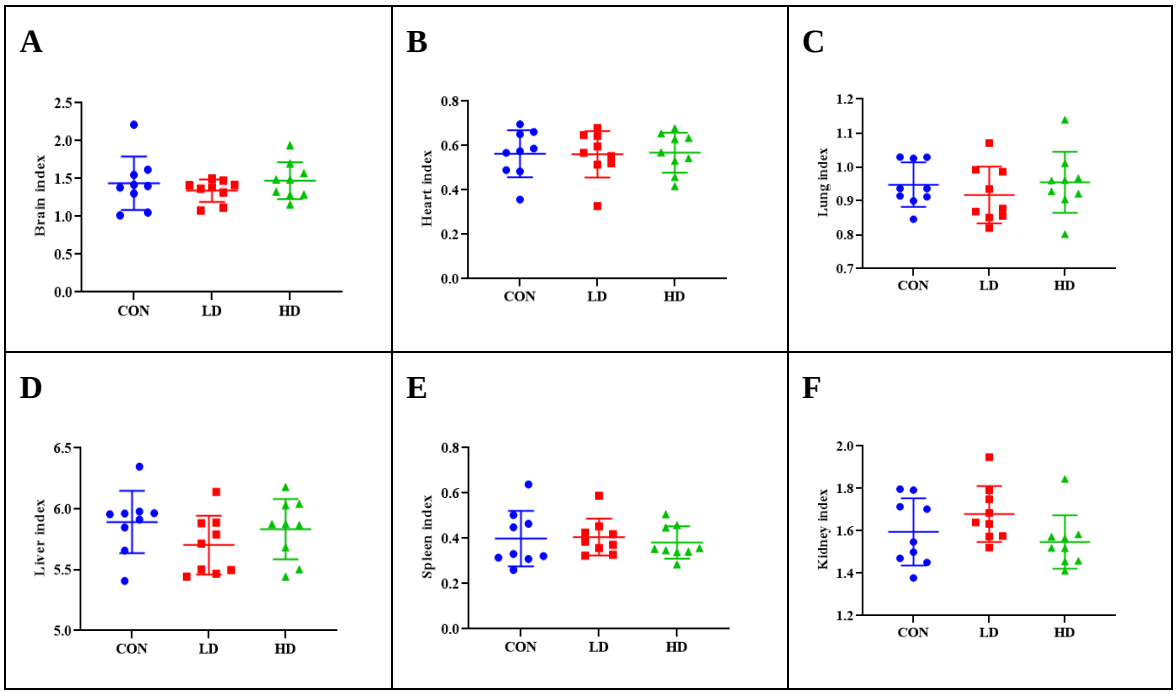

Fig. 4.34: Effect of oral dosing of NCDC 400 on relative organ weights during subacute oral toxicity study. (A) Brain index; (B) Heart index; (C) Kidney index; (D) Spleen index; (E) Lungs index; (F) Liver index. No significant difference at $p < 0.05$ was found across the groups (*Analyzed by one-way ANOVA following Duncan test*)

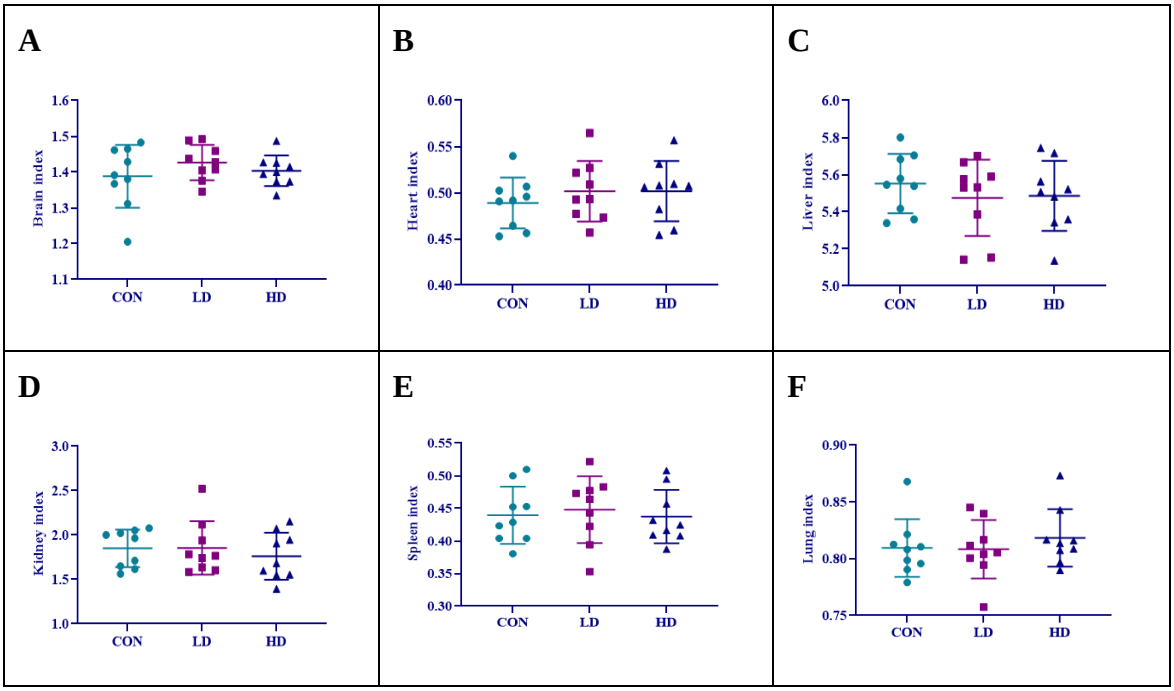

Fig. 4.35: Effect of oral dosing of NCDC 400 on relative organ weights during subchronic oral toxicity study. (A) Brain index; (B) Heart index; (C) Kidney index; (D) Spleen index; (E) Lungs index; (F) Liver index. No significant difference at $p < 0.05$ was found across the groups (*Analyzed by one-way ANOVA following Duncan test*)

4.4.23. Hematology

The effects of acute, subacute, and subchronic administration of NCDC 400 on various hematological parameters are presented in **Tables 4.14**, **4.15, and 4.16**, respectively. In all three oral toxicity studies, orogastric administration of NCDC 400 showed no significant ($p < 0.05$) changes in the hematological parameters like RBC, Hb, HCT, MCV, MCH, MCHC, and MPV. Experimentally determined values for tested blood parameters were within the normal range identified for *Mus musculus* species (Ihedioha *et al*., 2012). There were no abnormalities in the WBC counts as well as differential leukocyte counts (DLC) of animals treated with the low and high doses of NCDC 400. Further, the estimation of fasting blood glucose levels of mice revealed no significant ($p < 0.05$) differences between treatment (LD and HD) and CON groups. Overall, the hematological parameters were comparable between the treatment (LD and HD) and control groups and thereby did not suggest any treatment-related toxic effects.

Hematological parameters are crucial for determining treatment-induced toxicological effects. The hematopoietic system is the most common sensitive target of toxic compounds and an important indicator of the physiological and pathological status of animals. No adverse effect of NCDC 400 on different anemic parameters and RBC

indices (RBC, Hb, HCT, MCV, MCH, and MCHC) is an indication of non-toxic effects on erythropoiesis as well as osmotic fragility of RBC. On the other hand, WBCs are the first line of cellular defense that protect from infectious agents. The neutral effect of NCDC 400 on WBC and related cells suggests that NCDC 400, even at the higher dose, has not exerted a challenge on the immune system, and therefore may be considered immunologically safe. Our results are in-line with Shokryazdan *et al*. (2016), who reported that orally administered *L. buchneri* FD2, *L. fermentum* HM3, or a mixture of them at 10^{10} CFU/kg BW/day for 28 days had no considerable variations in the hematological parameters from the control. In support of our findings, Thumu *et al*. (2020) have also reported no adverse effects on the various hematological parameters of rats after repeated oral supplementation of *L. fermentum* strains FIX and NCMR 2836 at 10^7-10^{10} CFU/rat for 13 weeks. These evidences indicate the blood compatibility of the potential probiotic strains.

Table 4.14: Effect of NCDC 400 on hematological indices of different mice groups during acute oral toxicity study

Parameters	Unit	CON	LD	HD
RBC	10^6/ μL	$8.79^b \pm 0.15$	$9.04^a \pm 0.03$	$8.69^b \pm 0.11$
Hb	g/ dL	$12.73^a \pm 0.13$	$14.03^b \pm 0.34$	$12.23^a \pm 0.17$
HCT	%	$48.33^a \pm 0.60$	$50.16^b \pm 1.47$	$46.86^a \pm 0.71$
MCV	fl	$52.76^a \pm 0.23$	$51.93^a \pm 0.23$	$53.96^a \pm 0.12$
MCH	pg	$14.46^a \pm 0.12$	$13.63^a \pm 0.08$	$14.03^a \pm 0.14$
MCHC	%	$27.40^a \pm 0.10$	$26.36^a \pm 0.08$	$26.03^a \pm 0.28$
MPV	fl	$8.13^a \pm 0.03$	$8.03^a \pm 0.16$	$7.9^a \pm 0.05$
WBC	10^3/ μL	$10.45^a \pm 0.23$	$9.67^a \pm 1.64$	$10.16^a \pm 0.93$
DLC (Lymphocytes)	%	$90.60^a \pm 0.08$	$89.33^a \pm 1.64$	$91.1^a \pm 0.43$
DLC (Neutrophils)	%	$3.26^a \pm 0.24$	$3.16^a \pm 0.74$	$2.6^a \pm 0.27$
DLC (Mix.)	%	$6.06^a \pm 0.21$	$6.5^a \pm 0.90$	$6.23^a \pm 0.26$
Fasting Glucose	mg/ dL	$80.88^a \pm 2.98$	$87.11^a \pm 4.96$	$87.55^a \pm 3.97$

Note: Data are represented as mean ± SEM. Lowercase superscripts a and b indicate the significant differences ($p < 0.05$) between the groups (*Analyzed by one-way ANOVA following the Duncan test*).

Table 4.15: Effect of NCDC 400 on hematological indices of different mice groups during subacute oral toxicity study

Parameters	Unit	CON	LD	HD
RBC	10^6/ µL	8.51 ± 0.53	8.34 ± 0.06	8.73 ± 0.37
Hb	g/ dL	12.4 ± 0.65	12.56 ± 0.03	12.80 ± 0.17
HCT	%	44.76 ± 3.19	45.60 ± 0.20	45.4 ± 1.70
MCV	fl	52.80 ± 0.60	54.66 ± 0.66	54.30 ± 0.87
MCH	pg	14.56 ± 0.17	15.00 ± 0.10	15.23 ± 0.43
MCHC	%	27.73 ± 0.58	27.5 ± 0.20	28.06 ± 1.01
MPV	fl	7.63 ± 0.08	7.73 ± 0.23	7.86 ± 0.17
WBC	10^3/µL	10.97 ± 0.78	12.5 ± 0.26	11.34 ± 0.87
DLC (Lymphocytes)	%	91.90 ± 0.51	89.81 ± 0.30	90.43 ± 0.31
DLC (Neutrophils)	%	1.40 ± 0.15	2.43 ± 0.03	2.1 ± 0.23
DLC (Mix.)	%	7.36 ± 0.21	7.86 ± 0.06	7.36 ± 0.31
Fasting Glucose	mg/ dL	99.11 ± 3.03	95.88 ± 3.56	94.11 ± 3.91

Note: Data are represented as mean ± SEM. No significant variations were found across the groups (*Analyzed by one-way ANOVA following the Duncan test ($p \leq 0.05$)*)

Table 4.16: Effect of NCDC 400 on hematological indices of different mice groups during subchronic oral toxicity study

Parameters	Unit	CON	LD	HD
RBC	10^6/ µL	8.31 ± 0.41	8.40 ± 0.10	8.57 ± 0.24
Hb	g/ dL	11.76 ± 0.29	11.00 ± 0.23	12.13 ± 0.08
HCT	%	45.6 ± 0.95	44.9 ± 0.77	46.83 ± 0.88
MCV	fl	50.76 ± 1.12	52.5 ± 0.25	52.26 ± 0.03
MCH	pg	13.70 ± 0.05	14.46 ± 0.08	14.50 ± 0.10
MCHC	%	27.06 ± 0.57	27.13 ± 0.14	27.26 ± 0.18
MPV	fl	8.1 ± 0.05	8.16 ± 0.14	8.2 ± 0.35
WBC	10^3/µL	12.44 ± 0.71	12.02 ± 0.97	12.26 ± 0.89
DLC (Lymphocytes)	%	80.7 ± 1.11	83.16 ± 0.42	82.3 ± 1.23
DLC (Neutrophils)	%	5.63 ± 0.39	5.10± 0.25	5.3 ± 0.11
DLC (Mix.)	%	13.53 ± 0.75	11.90 ± 0.40	13.11 ± 1.07
Fasting Glucose	mg/dL	91.66 ± 3.58	92.33 ± 2.57	95.77 ± 2.11

Note: Data are represented as mean ± SEM. No significant variations were found across the groups *(Analyzed by one-way ANOVA following the Duncan test ($p \leq 0.05$))*

4.4.24. Clinical biochemistry parameters

The effect of short and long-term exposure to NCDC 400 at two doses on various serum biochemical parameters of mice are presented in **Tables 4.17-4.19**. Repeated dose administration of NCDC 400 at either of the doses had no significant ($p < 0.05$) alterations in the liver functioning markers such as ALT and AST, suggesting its non-hepatotoxic nature. The liver is an important organ in metabolism. It is more susceptible to any toxic insults and therefore, the lesions in the problematic liver cause leaching of important liver enzymes *viz*. AST and ALT into the serum. Therefore, these enzymes become crucial indicators for assessing hepatotoxicity and hepatic cell damage (Porwal *et al*., 2017). Similarly, there were no signs of alterations in the kidney functioning indicators (urea, creatinine, total serum protein, calcium, and phosphorus) in the LD and HD groups in comparison with the CON group, suggesting that no treatment-induced acute nephrotoxicity. Upon comparison with the CON group, no significant ($p < 0.05$) elevation in the serum LDH levels was found in the animals of LD and HD groups. This suggests that NCDC 400 had no unfavorable effects on the liver as well as muscles of the skeletal and cardiac systems. The non-specific uptick in the serum total LDH is an indication of multi-organ toxicity that requires further LDH isoenzymes characterization (Klein *et al*., 2020). Similarly, no significant ($p < 0.05$) changes in the total serum proteins were recorded in all three experimental groups. This indicates the neutral effect of NCDC 400 on fostering liver disease, nephrotic syndrome, acute infection, and immune suppression of animals. Our results concur with the findings of Shokryazdan *et al*. (2016), who also did not witness probiotic-mediated fluctuations in serum biochemistry parameters in rats exposed to *L. buchneri* FD2, *L. fermentum* HM3, or their consortium at 10^{10} CFU/kg BW/day in a subacute oral toxicity study. Similarly, Pradhan *et al*. (2019a) have also reported no significant changes in the serum biochemical parameters (ALT, AST, urea, and creatinine) after repeated administration of *L. fermentum* Lf1 and *L. plantarum* Lp91 strains to mice at $4x10^{10}$ CFU/g of mice body weight for 14 days.

On the other hand, serum lipid profiling is the best method to measure cardiovascular risk and has become almost a routine test in biomedical research. Accordingly, there were no substantial changes ($p < 0.05$) in the serum lipids such as triglycerides, LDL, HDL, and VLDL, as well as total cholesterol recorded upon treatment with NCDC 400 in low and high doses.

Table 4.17: Effect of acute exposure to NCDC 400 on serum biochemical and toxicity parameters of experimental mice

Parameters	Unit	CON	LD	HD
ALT/ SGPT	Unit/ L	37.53 ± 5.16	39.82 ± 1.28	37.50 ± 5.85
AST/ SGOT	Unit/ L	54.12 ± 0.71	57.77 ± 3.59	58.09 ± 3.43
Urea	mg/ dL	54.64 ± 3.35	52.36 ± 4.40	54.08 ± 2.99
Creatinine	mg/ dL	0.49 ± 0.19	0.54 ± 0.21	0.47 ± 0.11
LDH	Unit/ L	271.35 ± 15.66	269.32 ± 13.47	284.23 ± 15.13
Total protein	g/ dL	7.13 ± 0.03	7.11 ± 0.16	7.17 ± 0.17
Calcium	mg/ dL	10.24 ± 0.73	10.98 ± 0.14	11.17 ± 0.32
Phosphorous	mg/ dL	13.79 ± 0.29	13.36 ± 0.50	12.94 ± 0.23
Triglycerides	mg/ dL	94.88 ± 7.80	97.43 ± 6.79	92.77 ± 3.02
Total cholesterol	mg/ dL	108.66 ± 3.06	113.60 ± 5.22	119.5 ± 2.21
LDL-cholesterol	mg/ dL	31.50 ± 2.53	32.67 ± 3.34	35.59 ± 2.22
HDL-cholesterol	mg/ dL	60.24 ± 4.47	63. 90 ± 3.85	60.86 ± 2.53
VLDL-cholesterol	mg/ dL	18.67 ± 1.56	19.48 ± 1.35	18.55 ± 0.60
Atherogenic index	-	0.53 ± 0.04	0.50 ± 0.07	0.59 ± 0.02

Note: Data are presented as mean ± SEM. No significant differences were found across the groups (Analyzed by one-way ANOVA following Duncan test ($p < 0.05$))

Table 4.18: Effect of subacute exposure to NCDC 400 on serum biochemical and toxicity parameters of experimental mice

Parameters	Unit	CON	LD	HD
ALT/ SGPT	Unit/ L	37.72 ± 2.02	31.73 ± 1.45	35.79 ± 5.72
AST/ SGOT	Unit/ L	65.19 ± 2.75	66.86 ± 4.30	65.80 ± 1.84
Urea	mg/ dL	56.45 ± 3.65	50.94 ± 3.71	56.71 ± 2.05
Creatinine	mg/ dL	0.48 ± 0.12	0.41 ± 0.04	0.40 ± 0.07
LDH	Unit/ L	248.07 ± 8.38	245.05 ± 8.98	248.02 ± 6.36
Total protein	g/ dL	7.10 ± 0.12	7.11 ± 0.11	7.04 ± 0.24
Calcium	mg/ dL	10.10 ± 0.72	11.00 ± 0.14	10.59 ± 0.33
Phosphorous	mg/ dL	14.23 ± 0.03	12.97 ± 0.24	13.52 ± 0.38
Triglycerides	mg/ dL	89.66 ± 4.87	89.96 ± 3.40	87.60 ± 2.28
Total cholesterol	mg/ dL	117.68 ± 3.44	112.33 ± 6.03	118.37 ± 5.44
LDL-cholesterol	mg/ dL	38.35 ± 6.17	35.74 ± 6.14	36.93 ± 5.23
HDL-cholesterol	mg/ dL	61.40 ± 6.20	58.59 ± 5.37	60.91 ± 3.77
VLDL-cholesterol	mg/ dL	17.93 ± 0.97	17.09 ± 0.68	18.52 ± 0.45
Atherogenic index	-	0.61 ± 0.19	0.60 ± 0.20	0.62 ± 0.06

Note: Data are presented as mean ± SEM. No significant differences were found across the groups (Analyzed by one way ANOVA following Duncan test ($p < 0.05$))

Table 4.19: Effect of subchronic exposure to NCDC 400 on serum biochemical and toxicity parameters of experimental mice

Parameters	Unit	CON	LD	HD
ALT/ SGPT	Unit/ L	31.80 ± 4.07	33.31 ± 4.91	32.83 ± 6.67
AST/ SGOT	Unit/ L	62.41 ± 6.28	61.24 ± 4.14	62. 46 ± 2.76
Urea	mg/ dL	44.5 ± 3.00	43.83 ± 2.74	44.83 ± 2.23
Creatinine	mg/ dL	0.45 ± 0.19	0.46 ± 0.16	0.41 ± 0.13
LDH	Unit/ L	237.12 ± 13.37	233.12 ± 14.49	239.95 ± 6.04
Total protein	g/ dL	7.11 ± 0.01	7.28 ± 0.09	7.19 ± 0.17
Calcium	mg/ dL	10.83 ± 0.44	10.28 ± 0.10	10.64 ± 0.68
Phosphorous	mg/ dL	13.74 ± 0.31	13.33 ± 0.55	13.47 ± 0.33
Triglycerides	mg/ dL	89.02 ± 2.38	87.19 ± 1.83	88.46 ± 2.43
Total cholesterol	mg/ dL	111.90 ± 2.21	117.2 ± 4.63	115.93 ± 4.53
LDL-cholesterol	mg/ dL	38.13 ± 3.89	36.82 ± 2.90	38.77 ± 2.09
HDL-cholesterol	mg/ dL	63.70 ± 4.77	65.82 ± 1.32	62. 72 ± 2.87
VLDL-cholesterol	mg/ dL	17.80 ± 0.47	17.43 ± 0.36	17.69 ± 0.48
Atherogenic index	-	0.71 ± 0.06	0.69 ± 0.04	0.72 ± 0.05

Note: Data are presented as mean ± SEM. No significant differences were found across the groups (Analyzed by one-way ANOVA following Duncan test ($p < 0.05$))

Most importantly, there was no treatment-assisted considerable ($p < 0.05$) increase in the atherogenic index of experimental mice suggesting no influence of NCDC 400 on the developing cardiovascular risks. Similar to our results, Samtiya *et al*. (2019) have also reported no significant changes in the total serum lipid profile and atherogenic index of mice after subacute exposure to *L. fermentum* MTCC-5898 as high as 10^{11} cells/ animal.

4.4.25. Histopathological examination

There were no test strain (NCDC 400) as well as dose-related histopathological changes in any of the tested organs (brain, heart, lung, liver, spleen, kidney, spleen, small intestine, and large intestine) at various dose levels in all three oral toxicity studies (**Figs. 4.36-4.38**). No loss of normal architecture, necrosis, fibrosis, atrophy, or inflammation was recorded in any of the investigated organs. However, few tissues had lesions like extramedullary hematopoiesis (minimal) in the spleen, unilateral tubular basophilia (minimal) in the kidney, and mononuclear cell infiltration (minimal) in the liver. All

these observed lesions were considered incidental as they were not dose-related and were distributed randomly across the groups (**Tables 4.20-4.25**). Further, all other tested organs were free of lesions and the cellular architecture was found intact.

The microscopic examination of brain tissue of all three groups demonstrated normal architecture revealing glia with the random distribution of oligodendrocytes, astrocytes, neurons, microglia, choroid plexus, and capillaries. Similarly, the lungs showed proper alveoli exhibiting air space with no manifestations of edema or pulmonary alveolar proteinosis (PAP) in all three groups. Alveolar cells are outlined with septa composed of pneumocytes and blood vessels embedded in collagen. No visible signs of sepsis or bacterial infections were revealed in the lungs as evidenced by no acute neutrophil infiltrations, inflammation, or acute bronchopneumonia. Bronchus and bronchovascular bundles often appeared in all the lung tissue with a clear lumen. The histopathology of the liver showed normal hepatic central veins surrounded by hepatocytes but no connective tissue. The hepatic cords and sinusoids originating from the surroundings showed convergence towards the central veins. In contrast, the portal veins were normal and they were surrounded by the connective tissue, bile ducts, and hepatic arteries. The microscopic examination of heart muscles showed a normal striated appearance of myocardium containing eosinophilic cytoplasm and an intact nucleus. The tissue from all three groups also showed smooth muscle with a non-striated appearance composed of sheets of fusiform cells with one nucleus. Histology of the kidney revealed normal morphology exhibiting inner striated medulla and outer granulated cortex area. The inner medulla exhibited nephrons composed of the renal corpuscle and renal tubule. The renal corpuscle had intact and undamaged glomerulus with distinct Bowman's capsule and renal tube. However, rarely, unilateral tubular basophilia (minimal) was seen across all groups. Histopathology of the spleen showed equal distribution of red pulp (containing RBCs and monocytes) and white pulp area (containing lymphocytes). Extramedullary hematopoiesis (EMH) in the red pulp region of the spleen was recorded in all groups. However, EMH minimal in the young mice is considered quite normal and most frequent. The microscopic examination of small intestine (jejunum) showed mucosa, submucosa and muscularis mucosa, muscularis externa, and serosa. The mucosa showed the typical structural features of crypts of Lieberkuhn as well as the extended projection of villi into the lumen. The villi were composed of enterocytes and goblet cells at the outer layer and lamina propria within its core.

	CON	LD	HD
Lungs	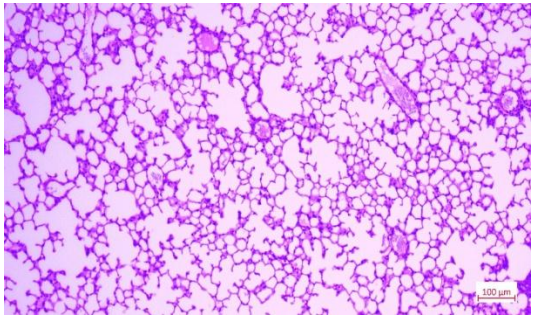	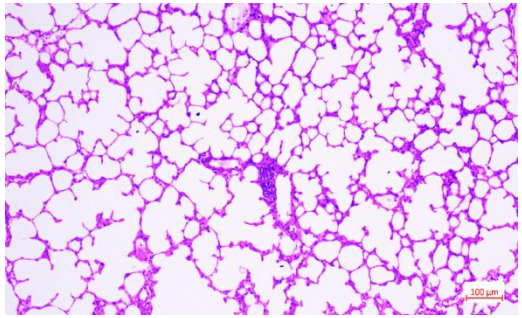	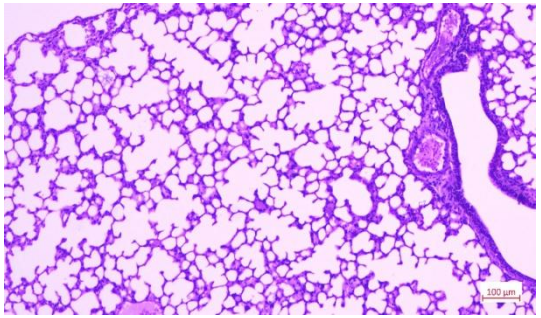
Liver	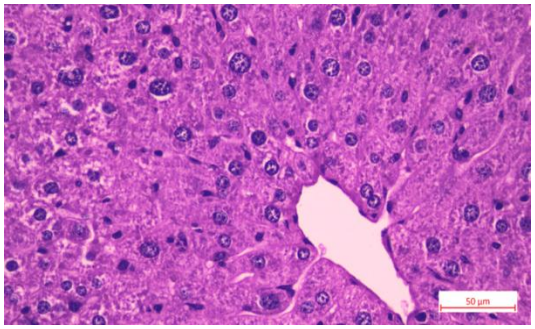	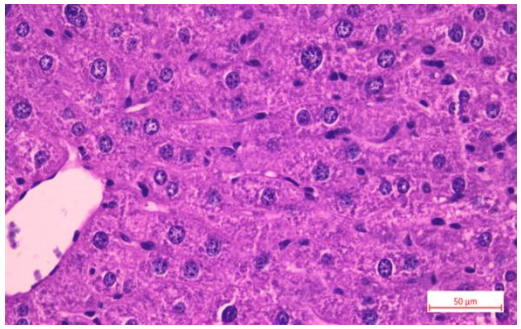	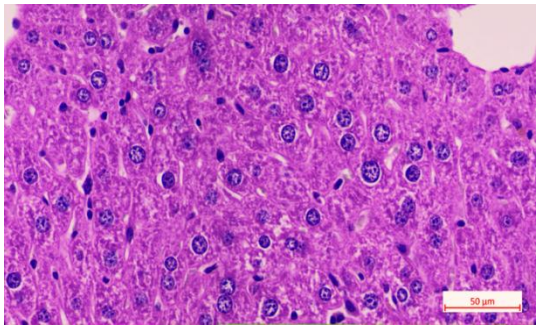
Brain	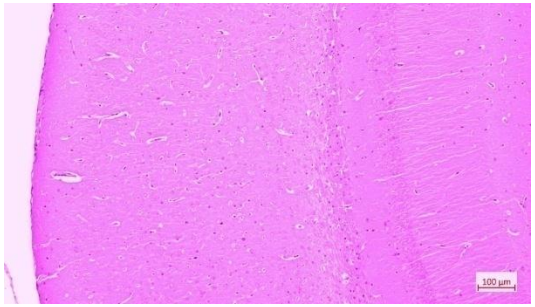	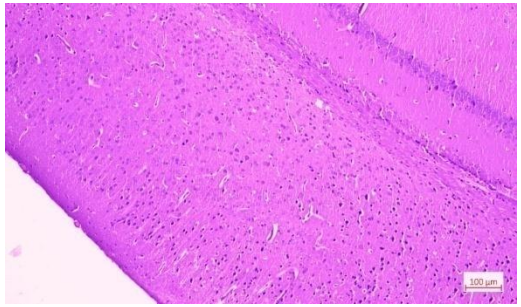	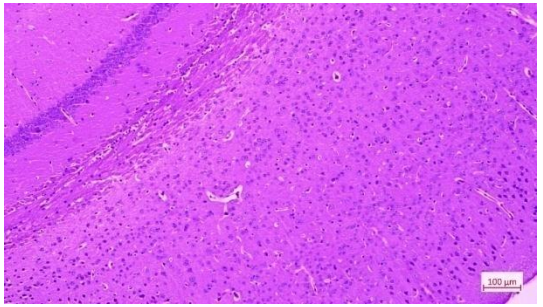

Heart	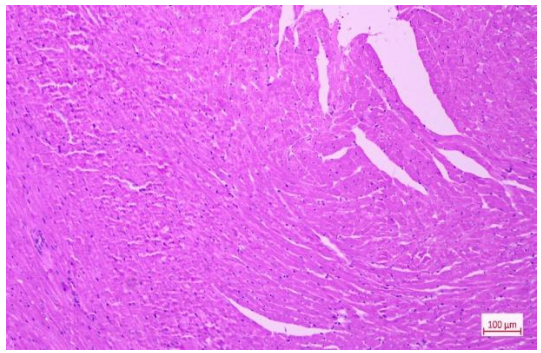	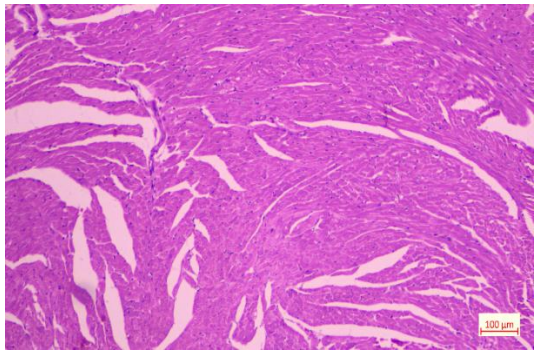	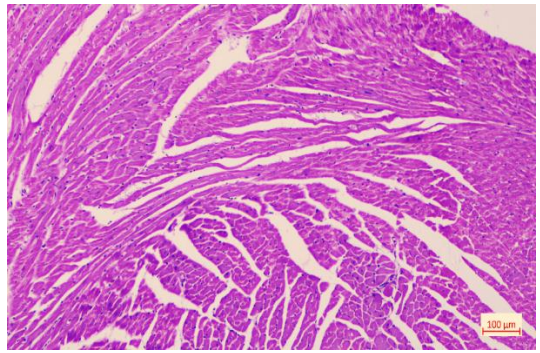
Kidney	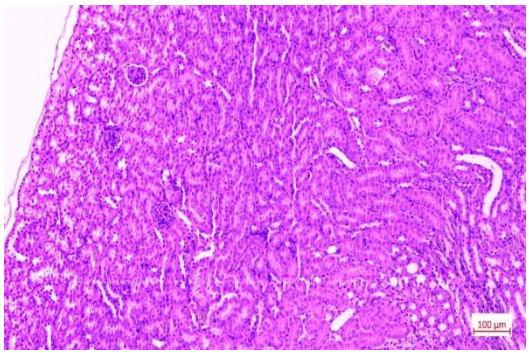	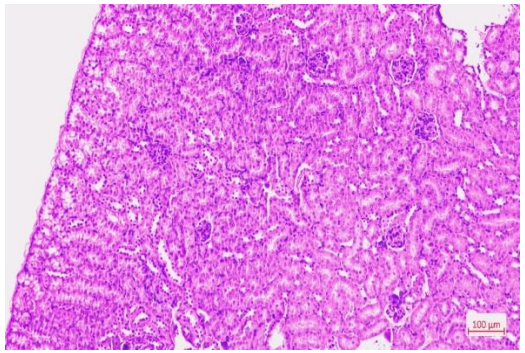	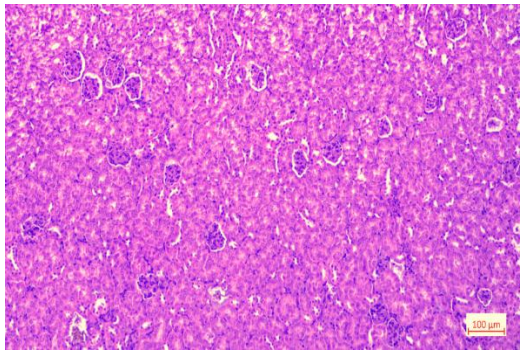
Spleen	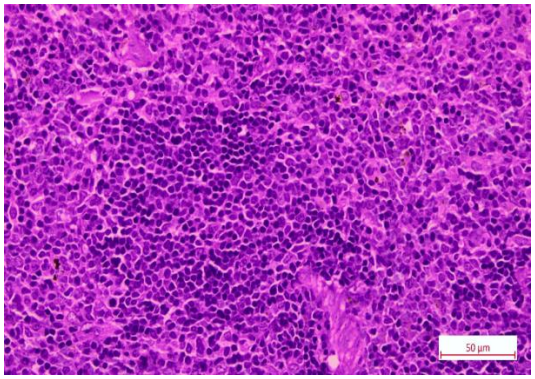	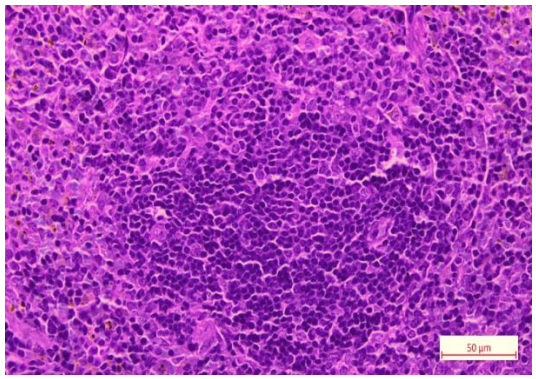	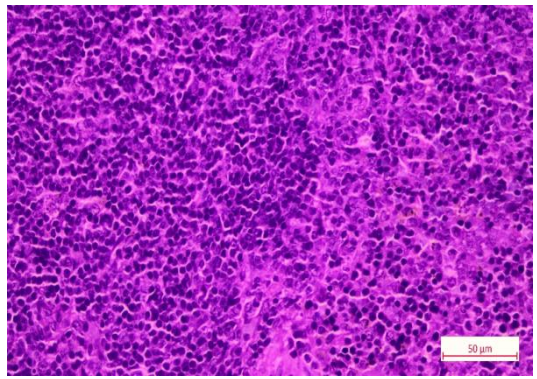

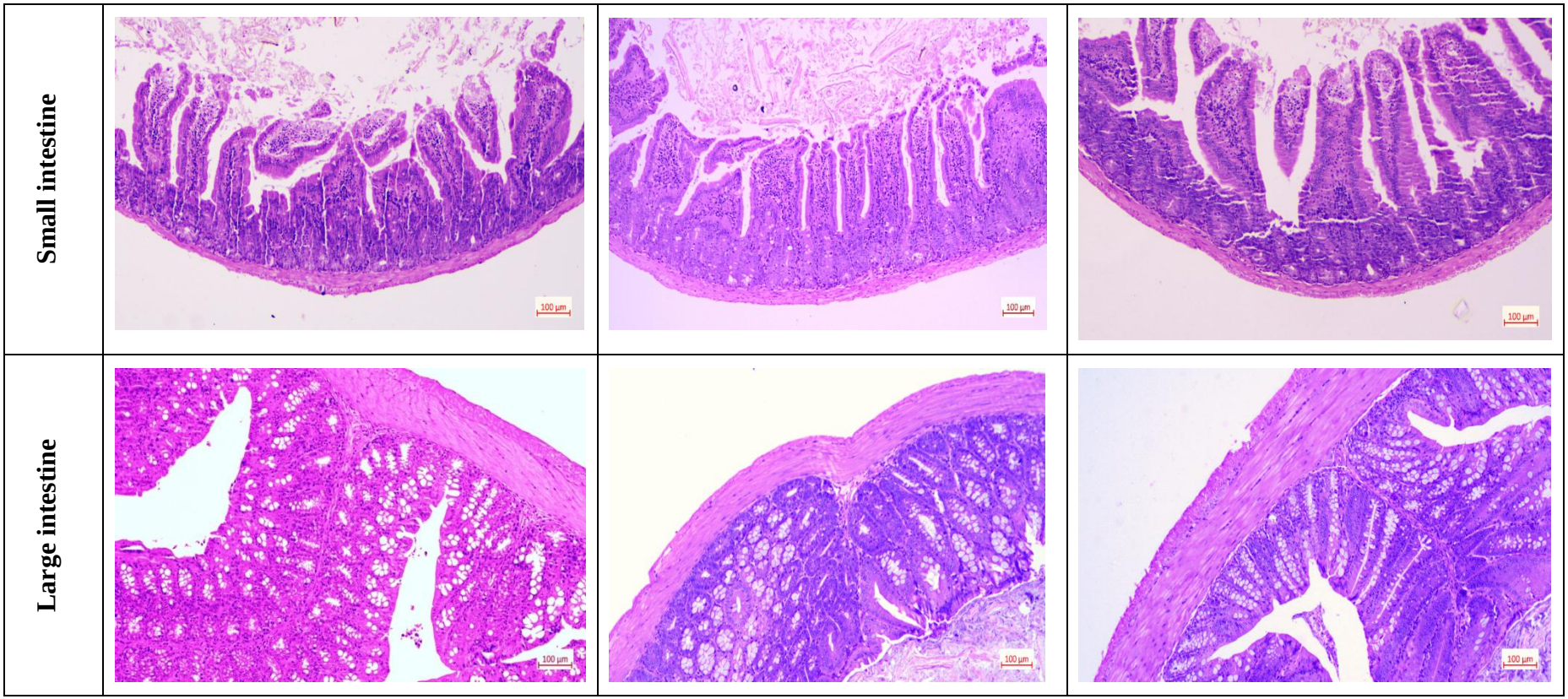

Fig. 4.36: Histopathological photomicrographs (100 X magnification) of various organs or tissues of experimental animals after acute exposure to NCDC 400 at low and high doses.

	CON	LD	HD
Lungs	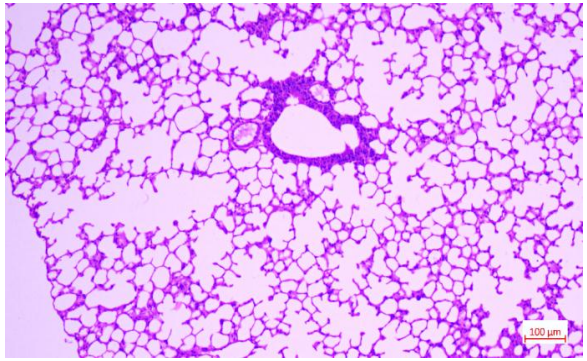	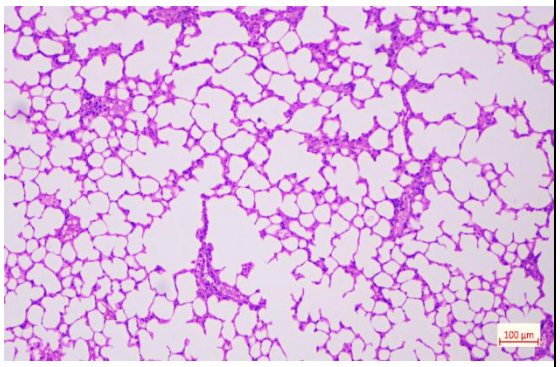	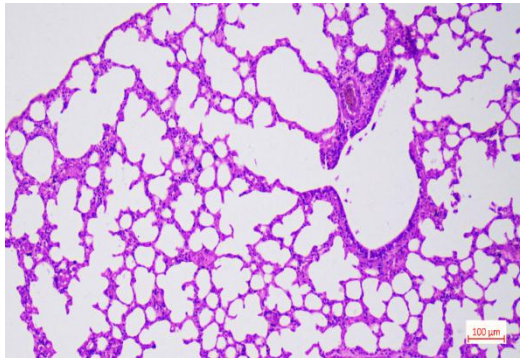
Liver	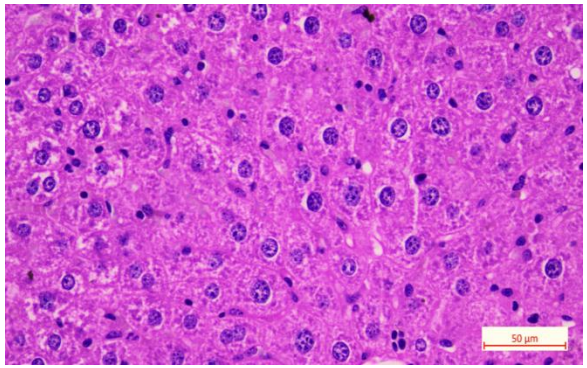	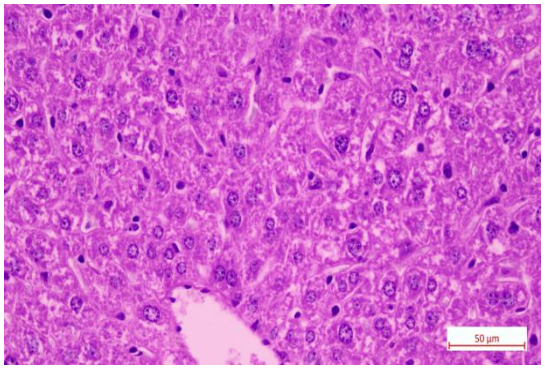	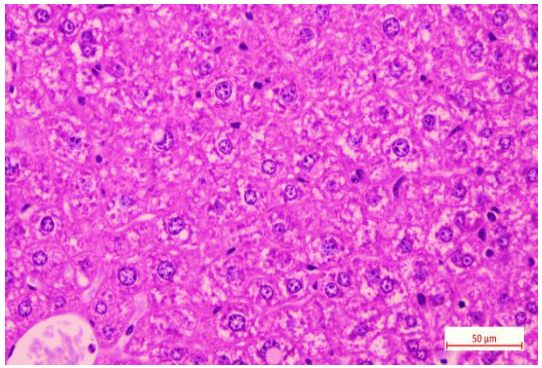
Brain	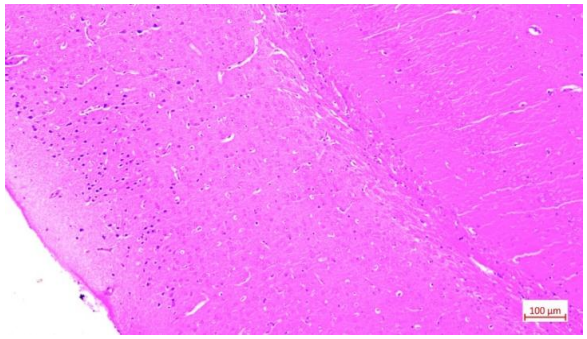	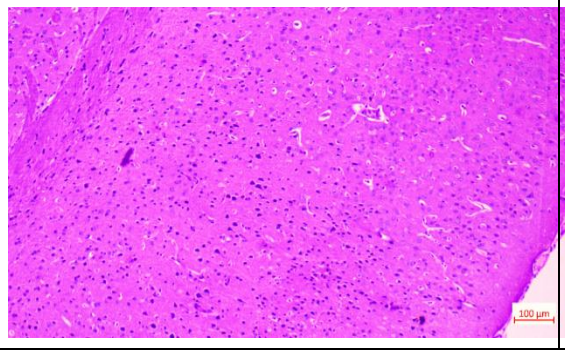	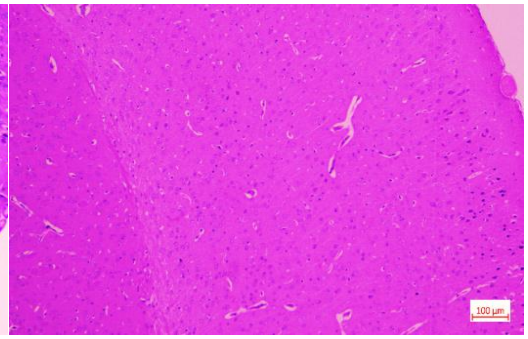

Heart	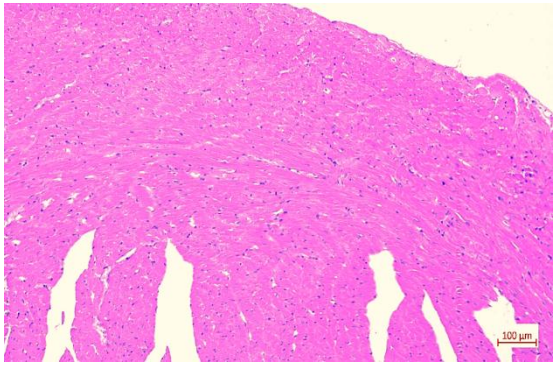	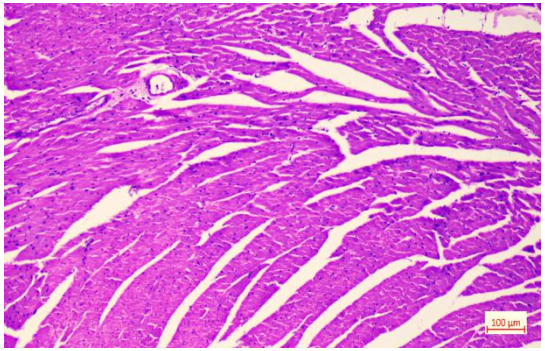	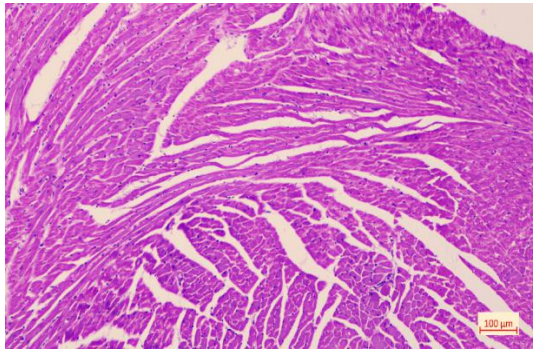
Kidney	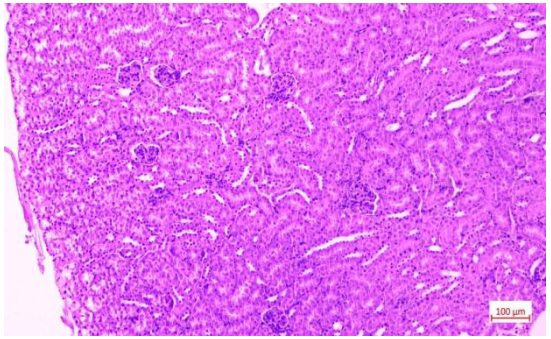	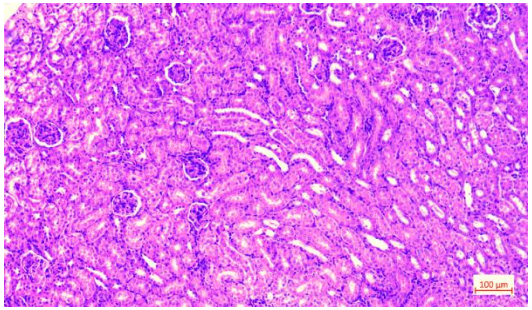	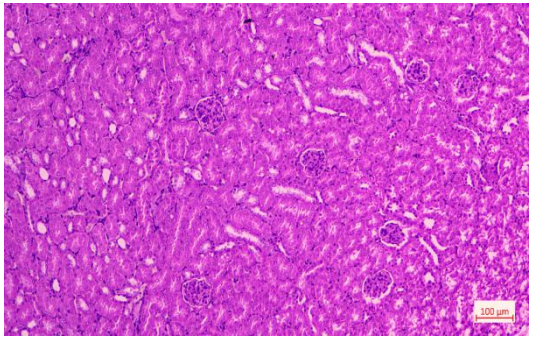
Spleen	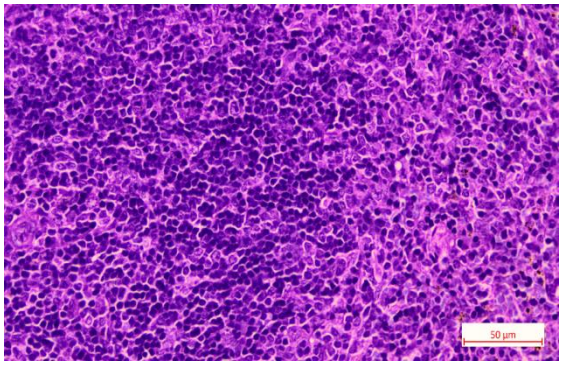	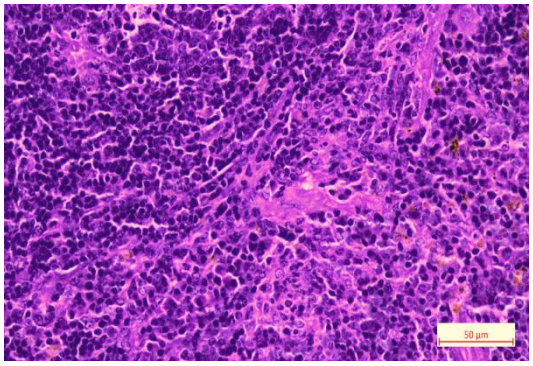	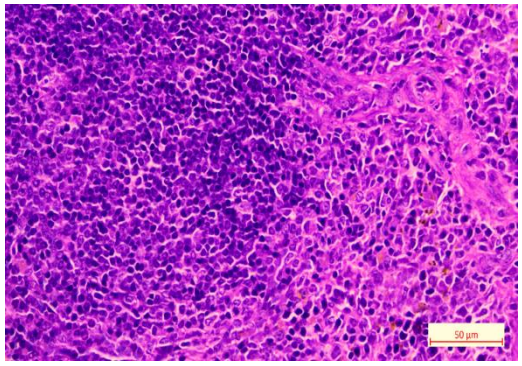

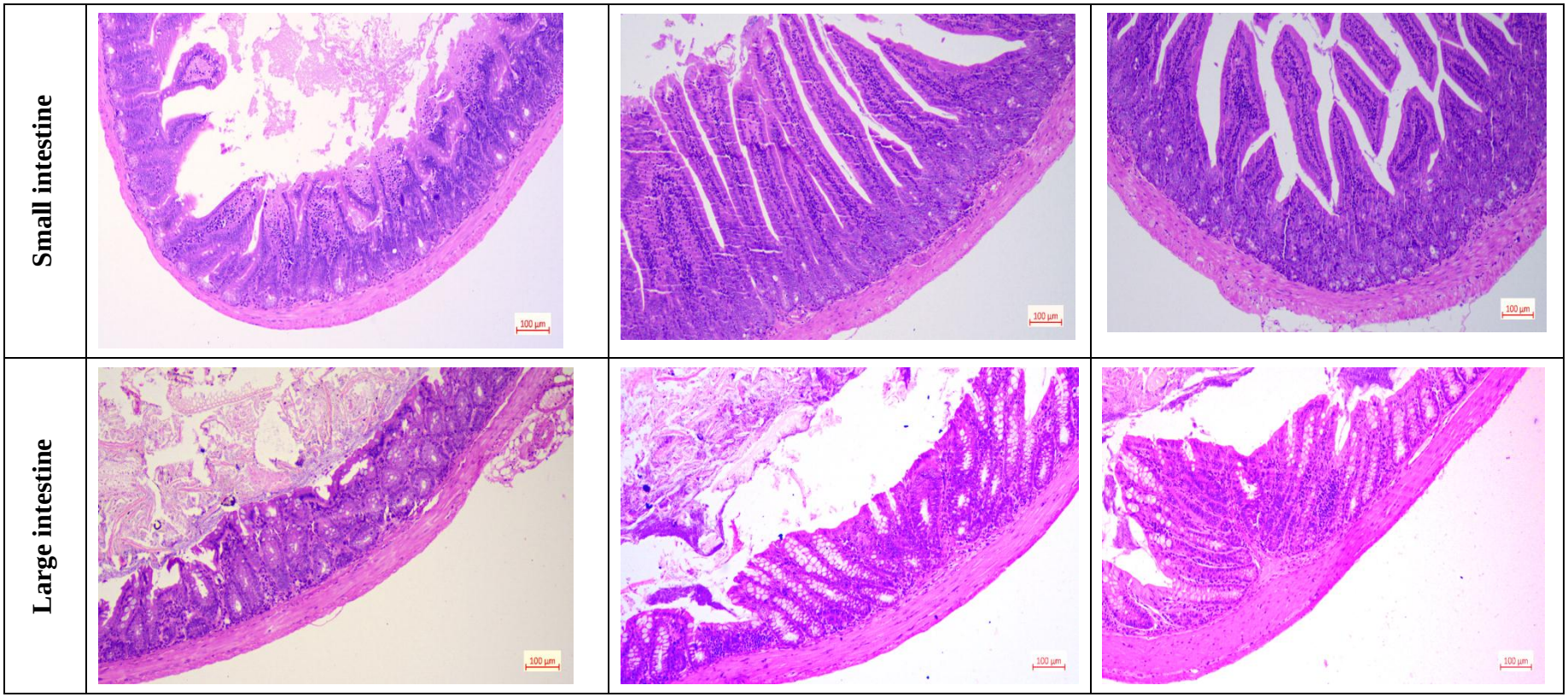

Fig. 4.37: Histopathological photomicrographs (100 X magnification) of various organs or tissues of experimental animals after subacute exposure to NCDC 400 at low and high doses.

	CON	LD	HD
Lungs	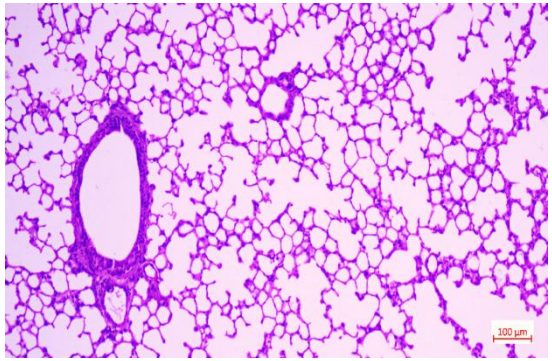	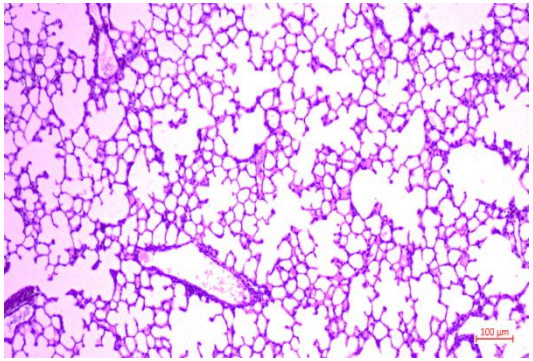	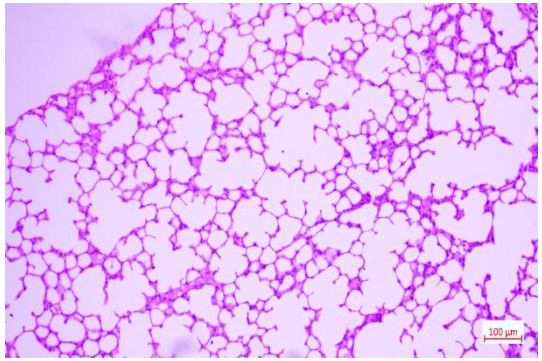
Liver	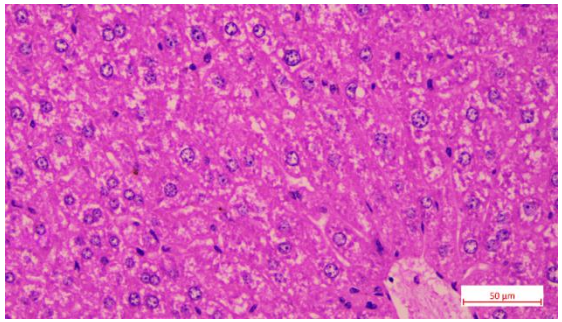	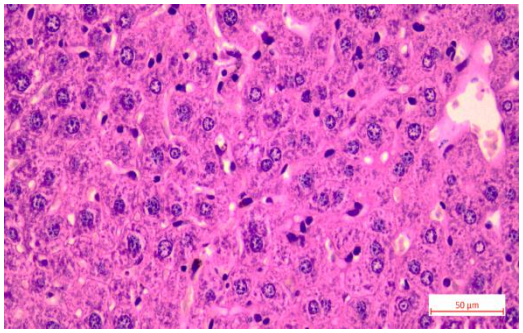	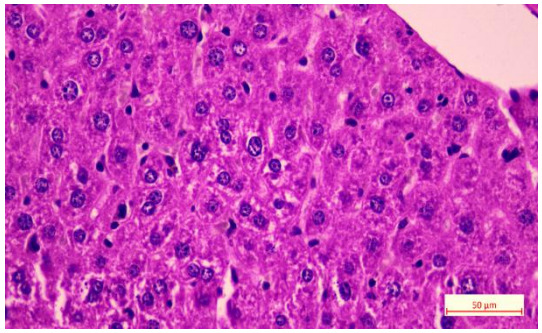
Brain	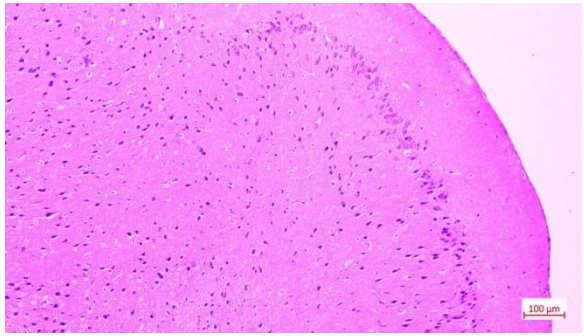	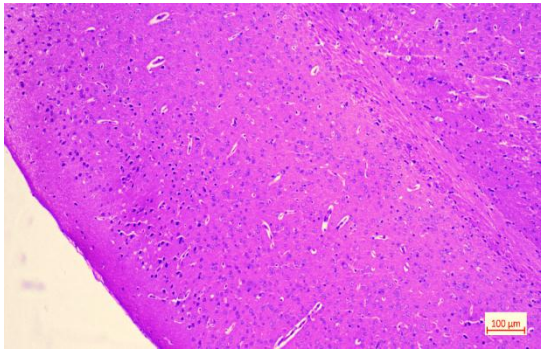	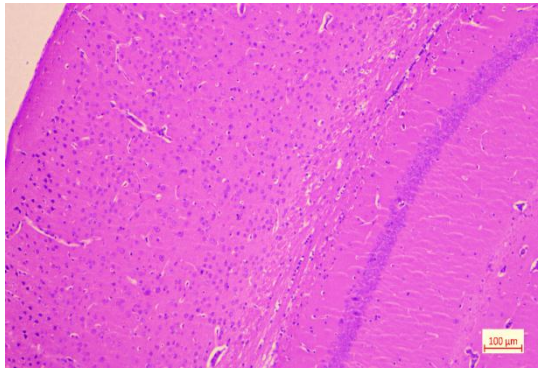

Heart	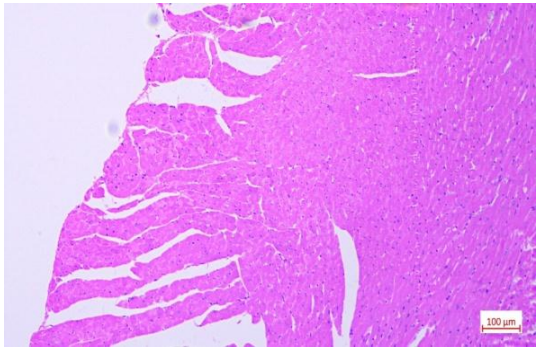	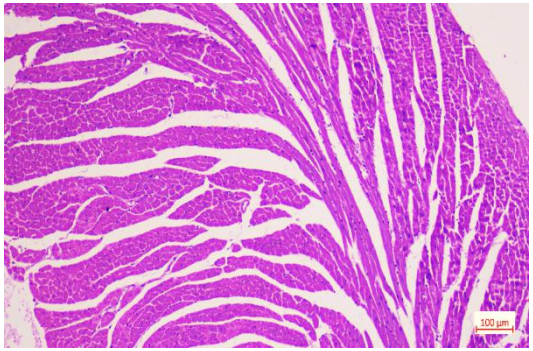	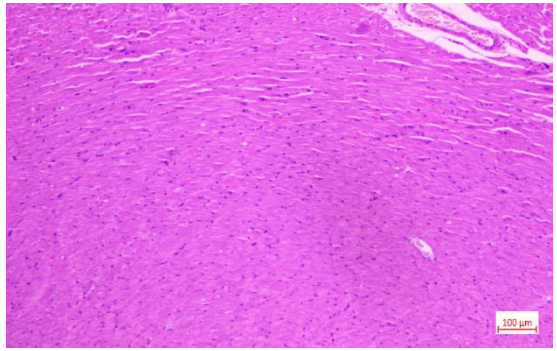
Kidney	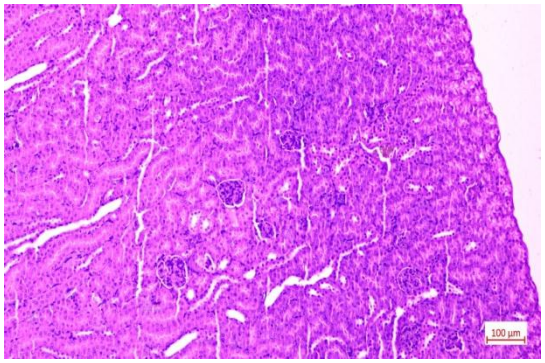	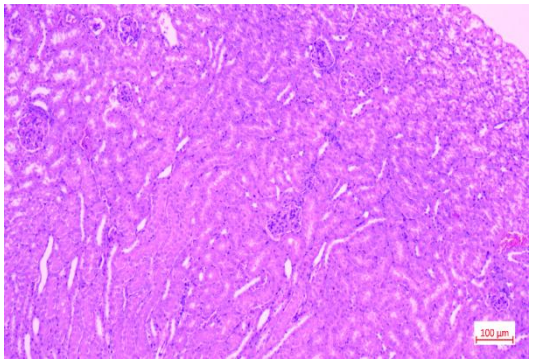	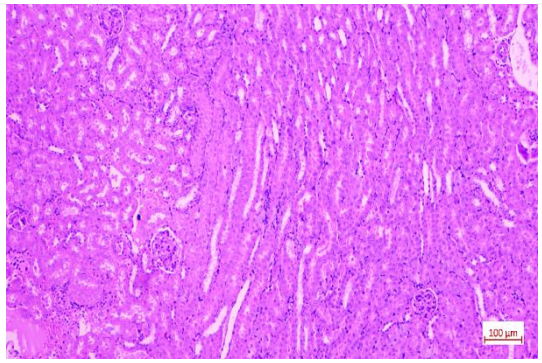
Spleen	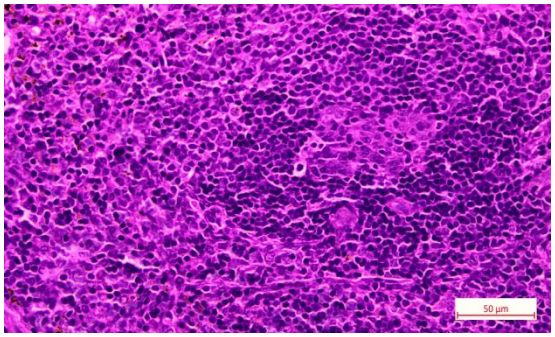	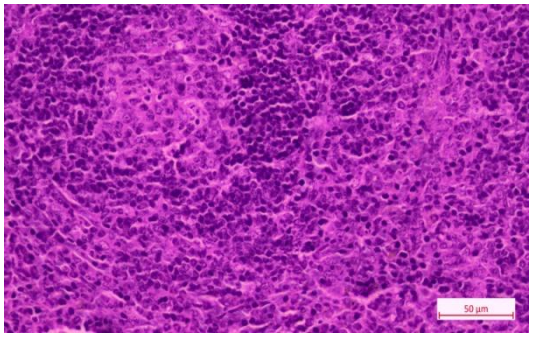	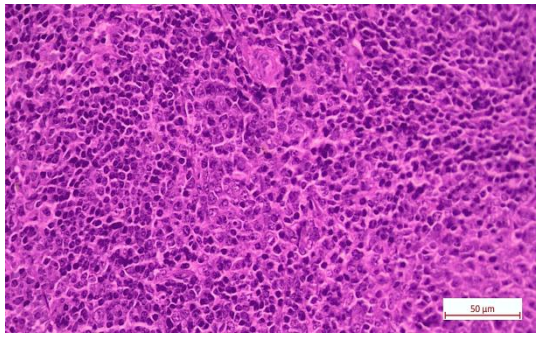

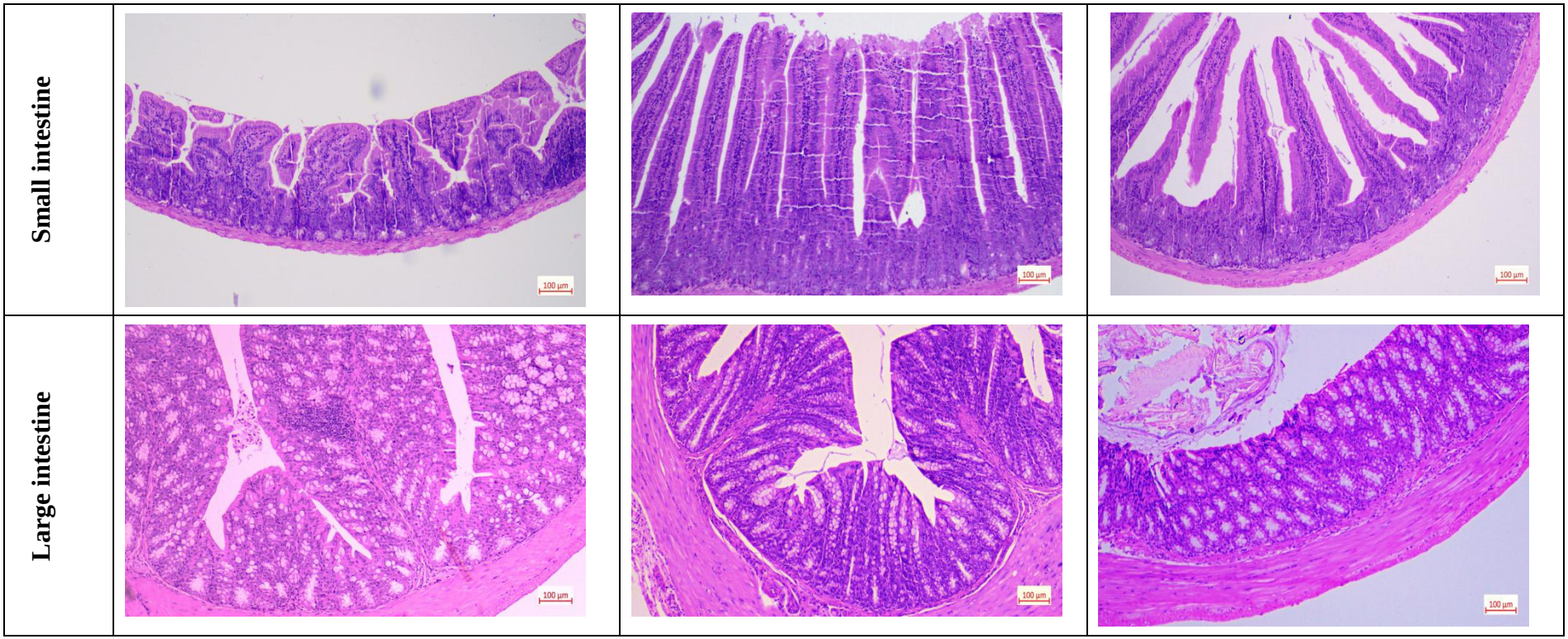

Fig. 4.38: Histopathological photomicrographs (100 X magnification) of various organs or tissues of experimental animals after subchronic exposure to NCDC 400 at low and high doses.

On the contrary, the histology of the colon showed four distinct layers of mucosa, submucosa, muscularis propia, and serosa. Colonic mucosa displayed deep and intact crypts which are composed of the epithelium (made of absorptive enterocytes and goblet cells) and lamina propria filled with various lymphocytes and plasma cells. Overall, these histopathology results matched the clinical findings, hematology, serum biochemistry, organ weights, and other relevant data of the study suggesting the non-toxic nature of NCDC 400. Our results in this regard are in close alignment with Shokryazdan *et al*. (2016), who also found no gross histological changes or distortion in the major tissues (brain, kidney, liver, lungs, intestine, and heart) after repeated oral administration of *L. buchneri* FD2, *L. fermentum* HM3, or a mixture (10^{10} CFU/kg BW/day) for 28 days. Similarly, Samtiya *et al*. (2020) have also found no visual microscopic changes in the tissue histology of mice kidney, liver, and intestine after oral administration of *L. fermentum* MTCC-5898 (>10^8 CFU/mouse/day) for 28 days.

Overall, the daily oral gavage administration of *L. fermentum* NCDC 400 to mice at 10^8 and 10^{10} CFU/day for 14, 28, and 90 days did not reveal any test strain-related changes or gross lesions upon microscopic examination of various organs. Based on the histopathological analysis, a dose of 10^{10} CFU/day/mouse may be considered as No Observed Effect Level (NOEL) of *L. fermentum* NCDC 400.

Table 4.20: Summary of histopathological findings of acute oral toxicity study

Group		**NC**	**LD**	**HD**
No. of mice examined/group		3	3	3
Dose (CFU/mice/day)		0	10^8	10^{10}
Organs / Lesions	Mode of Death	TS	TS	TS
Lungs		N	N	N
Small intestine (Jejunum)		N	N	N
Large intestine (Colon)		N	N	N
Brain		N	N	N
Heart		N	N	N
Spleen		L	N	N
Increased Extramedullary hematopoiesis, minimal		1	-	N
Kidney		N	N	N
Liver		N	N	N

Table 4.21: Individual animal histopathology findings of acute oral toxicity study

Group		NC			LD			HD		
Representative animal no.		1	2	3	1	2	3	1	2	3
Organs / Lesions	Mode of Death	TS	TS	TS	TS	TS	TS	TS	TS	TS
Spleen		L	N	N	N	N	N	N	N	N
Increased Extramedullary hematopoiesis, minimal		1	-	-	-	-	-	-	-	-

Note: TS-Terminal sacrifice; L-Lesion; N-Normal

Table 4.22: Summary of histopathology findings of subacute oral toxicity study

Group		NC	LD	HD
No. of mice examined/group		3	3	3
Dose (CFU/mice/day)		0	10^8	10^{10}
Organs / Lesions	Mode ofDeath	TS	TS	TS
Lungs		N	N	N
Small intestine (Jejunum)		N	N	N
Large intestine (Colon)		N	N	N
Brain		N	N	N
Heart		N	N	N
Spleen		L	L	N
Increased Extramedullary hematopoiesis, minimal		1	1	-
Kidney		L	N	N
Basophilia, tubular, Unilateral, minimal		1	-	-
Liver		N	N	N

Table 4.23: Individual animal histopathology findings of subacute oral toxicity study

Group		NC			LD			HD		
Representative animal no.		1	2	3	1	2	3	1	2	3
Organs / Lesions	Mode of Death	TS	TS	TS	TS	TS	TS	TS	TS	TS
Kidney		N	N	L	N	N	N	N	N	N
Basophilia, tubular, Unilateral, minimal		-	-	1	-	-	-	-	-	-
Spleen		N	N	L	L	N	N	N	L	N
Extramedullary hematopoiesis, minimal		-	-	1	1	-	-	-	1	-

Note: TS-Terminal sacrifice; L-Lesion; N-Normal

Table 4.24: Summary of histopathology findings of subchronic oral toxicity study

Group		CON	LD	HD
No. of mice examined/group		3	3	3
Dose (CFU/mice/day)		0	10^8	10^{10}
Organs / Lesions	Mode ofDeath	TS	TS	TS
Lungs		N	N	N
Small intestine (Jejunum)		N	N	N
Large intestine (Colon)		N	N	N
Brain		N	N	N
Heart		N	N	N
Spleen		L	L	N
Extramedullary hematopoiesis, minimal		1	1	-
Kidney		L	N	N
Basophilia, tubular, Unilateral, minimal		1	-	-
Liver		L	N	N
Infiltration, mononuclear cell, minimal		1	-	-

Table 4.25: Individual animal histopathology findings of subchronic oral toxicity study

Group		CON			LD			HD		
Representative animal no.		1	2	3	1	2	3	1	2	3
Organs / Lesions	Mode of Death	TS	TS	TS	TS	TS	TS	TS	TS	TS
Liver		N	L	N	N	N	N	N	N	N
Infiltration, mononuclear cell, minimal		-	1	-	-	-	-	-	-	-
Kidney		L	N	N	N	N	N	N	N	N
Basophilia, tubular, Unilateral, minimal		1	-	-	-	-	-	-	-	-
Spleen		N	N	L	N	L	N	N	N	N
Extramedullary hematopoiesis, minimal		-	-	1	-	1	-	-	-	-

Note: TS-Terminal sacrifice; L-Lesion; N-Normal

4.4.26. Bacterial translocation and integrity of gut mucosa

Bacterial translocation to extra-intestinal organs is considered as an important indication of probiotic toxicity as the tissue invasion is the first step in microbial pathogenesis. Hence, the effect of NCDC 400 on the gut mucosa was conducted by translocation assay and detailed microscopic examination of intestinal tissues. Agar plating of blood and other extra-intestinal organs like the liver, kidney, spleen, and lungs showed no NCDC 400-related bacterial translocation. The blood collected from the experimental animals was sterile, suggesting the absence of NCDC 400-mediated sepsis or bacteremia. The plating of other organs formed relatively a limited number of colonies on the MRS agar (**Tables 4.26-4.28)**. However, their genotypic identification using the colony PCR approach revealed no amplified bands specific to *L. fermentum* species (**Figs. 4.39-4.41**). Since species-specific PCR confirmed the absence of *L. fermentum* molecular identity, we did not further proceed with RAPD-based characterization of those isolates for strain-level discrimination. Overall, the percentage incidence of NCDC 400 translocation during acute, subacute, and subchronic exposure to mice was zero (**Tables 4.26-4.28**). Nevertheless, the incidence of other bacterial translocation to

visceral tissues but their absence in blood indicates the cross-contamination during animal dissection, handling, and processing. Given the fact that every organ contains its own microflora, the obtained bacterial colonies on the MRS agar could also be considered as indigenous microbes of the mice.

In analogy with these observations, detailed microscopic examination of small and large intestinal tissues of control and treatment groups showed no signs of distortion in epithelial architecture, inflammation, necrosis, and local toxicity. The morphology of villi was normal and there were no remarkable changes in the arrangement of epithelial cells. There were no signs of enterocytes breach in the epithelial lining of the mucosa. No incidences of neutrophil or mononuclear cell infiltration were recorded across the groups. Furthermore, the underlying supporting and connective tissues of the mucosa demonstrated no distortion in the submucosa, muscularis, and serosa suggesting no evidence of test bacterial leaching into the bloodstream via gastrointestinal route. These results, therefore, indicate that NCDC 400 does not exhibit local toxicity and mucosal damage at its primary adhesion site. Our results are in agreement with Meleh *et al*. (2020) wherein after an acute exposure to *L. reuteri* 29B (1×10^{10} CFU/mouse/day), the researchers found few colonies of indigenous microflora in different organs of mice but none of them have matched the molecular identity of test probiotic strain (*L. reuteri* 29B).

Table 4.26: The incidence of NCDC 400 translocation during acute exposure to mice

Sample	**CON**	**LD**	**HD**	**No. of colonies (LD) used for PCR**	**No. of colonies (HD) used for PCR**	**No. of confirmed colonies by PCR**	**% Translocation**
	Colonies on MRS agar			**Colonies used for PCR approach**			
Blood	Nil/3	Nil/3	Nil/3	-	-	0	0
Liver	27/3	18/3	19/3	10	10	0	0
Kidney	16 /3	29 /3	13/3	10	10	0	0
Spleen	12 /3	21/3	09/3	10	09	0	0
Lungs	22 /3	26 /3	03/3	10	03	0	0

Table 4.27: The incidence of NCDC 400 translocation during subacute exposure to mice

Sample	CON	LD	HD	No. of colonies (LD) used for PCR	No. of colonies (HD) used for PCR	No. of confirmed colonies by PCR	% Translocation
	Colonies on MRS agar			Colonies used for PCR approach			
Blood	Nil/3	Nil/3	Nil/3	-	-	0	0
Liver	48/3	17/3	22/3	10	10	0	0
Kidney	18/3	12/3	18/3	10	10	0	0
Spleen	27/3	21/3	15/3	10	10	0	0
Lungs	12/3	19/3	16/3	10	10	0	0

Table 4.28: The incidence of NCDC 400 translocation during subchronic exposure to mice

Sample	CON	LD	HD	No. of colonies (LD) used for PCR	No. of colonies (HD) used for PCR	No. of confirmed colonies by PCR	% Translocation
	Colonies on MRS agar			Colonies used for PCR approach			
Blood	Nil/3	Nil/3	Nil/3	-	-	0	0
Liver	48	17	22	10	10	0	0
Kidney	18	12	18	10	10	0	0
Spleen	27	21	15	10	09	0	0
Lungs	12	19	16	10	03	0	0

Note: Values of colonies on MRS agar are presented as the sum of total number of colonies on MRS agar from each organ (n=3) / total number of animals tested per group.

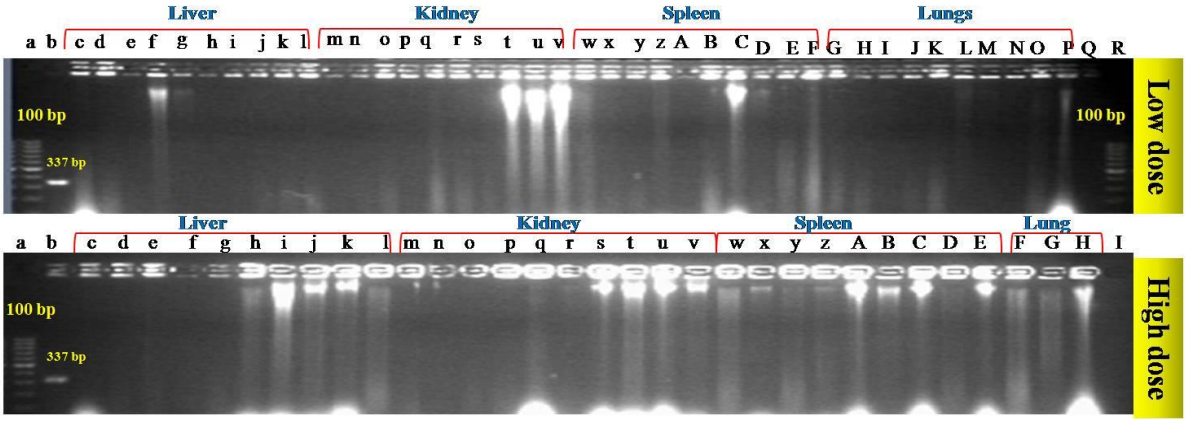

Fig. 4.39. Gel image showing the absence of confirmed *L. fermentum* isolates recovered from mice tissues from LD and HD groups during acute toxicity study. a, R: 100 bp DNA ladder; b: Positive control (NCDC 400); Q, I: Non-template control.

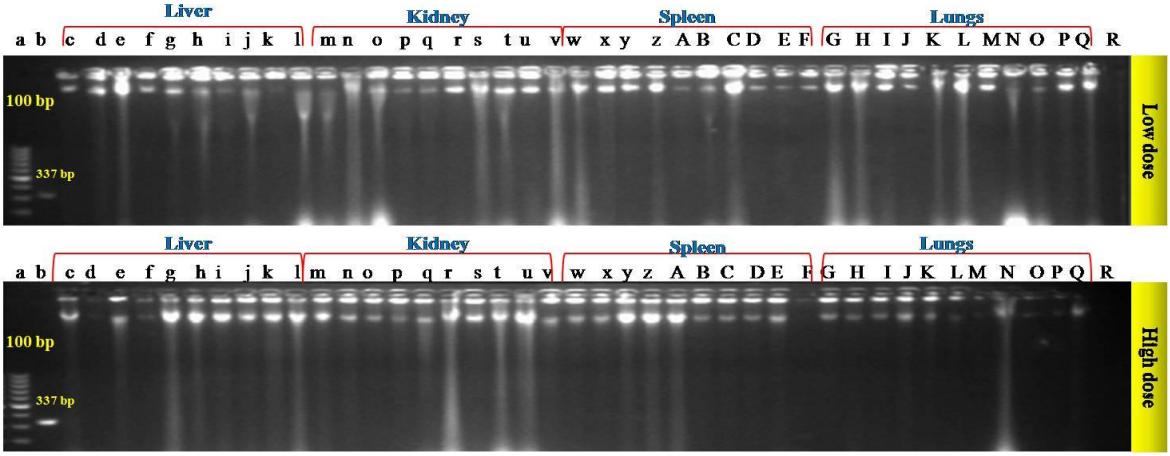

Fig. 4.40: Gel image showing the absence of confirmed *L. fermentum* isolates recovered from mice tissues from LD and HD groups during subacute toxicity study. a: 100 bp DNA ladder; b: Positive control (NCDC 400); R: Non-template control.

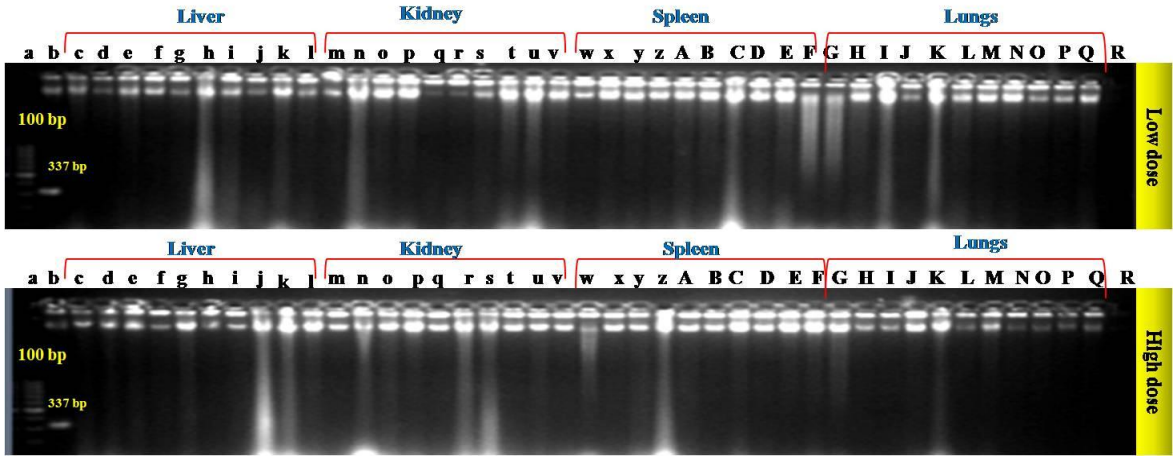

Fig. 4.41: Gel image showing the absence of confirmed *L. fermentum* isolates recovered from mice tissues from LD and HD groups during subchronic toxicity study. a: 100 bp DNA ladder; b: Positive control (NCDC 400); R: Non-template control.

4.4.27. Gut health indices and harmful caecal bacterial enzymes

The effects of intragastric administration of NCDC 400 on faecal biochemical attributes have been assessed at the end of the feeding trials. In all three oral toxicity tests, the orogastric administration of NCDC 400 significantly ($p < 0.05$) reduced the faecal pH compared to the control **(Figs. 4.42-4.44)**. In comparison with CON, an increase in the faecal pH of LD and HD groups can be justified by a parallel increase in the faecal lactate content to a significant ($p < 0.05$) level **(Figs. 4.42-4.44)**. Further, there was a notable reduction ($p < 0.05$) in the faecal ammonia in the LD and HD groups in a dose-specific manner **(Figs. 4.42-4.44)**. An elevation in the faecal lactate and reduction in the pH could be attributed to the fermentation of carbohydrates and formation of acidic end products by NCDC 400 alone or the other beneficial microbes that flourished after its administration (gut microbiota modulation). Similarly, the reduction in faecal ammonia may be corroborated by the test strain-mediated probable exclusion or elimination of pathogenic bacteria that would otherwise produce alkaline products like ammonia, indole, *skatole, and* p-cresol in the gut. Similar to our findings, Ara *et al*. (2002) have also reported an increase in the faecal lactate content and a decrease in the faecal pH and ammonia upon administration of *B. coagulans* SANK 70258 (1×10^5 CFU/day) to rats for 14 days. A similar study by Gupta *et al*. (2021a) has also evidenced a reduction in the pH and ammonia as well as an increase in the lactate of rat faeces fed with probiotic *L. salivarius* CPN60 for 21 days. The authors justified that the shedding of harmful pathogens that produce ammonia could be the underlying mechanism behind the reduction in ammonia. Likewise, the pH reduction in the stool was correlated with the formation of lactic acid and other short-chain fatty acids by test strain.

On the other hand, acute, subacute, and subchronic exposure to NCDC 400 showed a dose-specific reduction in the activity of harmful bacterial enzymes *viz*. β-glucosidase, β-glucuronidase, and tryptophanse in the caecal content of mice **(Figs. 4.42-4.44)**. However, in a few instances, the reduction in the enzyme activity was almost uniform and found insignificant between LD and HD but both showed significant ($p < 0.05$) differences with CON. This suggests that irrespective of the NCDC 400 doses administrated, there was no further reduction in the concentration of these enzymes at the end of experimental trials. In this study, the reduction in the concentration of caecal harmful enzymes could explain the evolution toward the formation of healthy and stable gut microbiota by the exclusion of pathogenic bacteria. It is well established that these

enzymes are generally produced by Gram-negative commensal gut pathogens and therefore, reduction in such enzyme activities indirectly suggests the NCDC 400 mediated elimination of harmful pathogens from gut. The pathogen exclusion mechanisms in probiotics are well established and are executed by fostering an antagonistic environment in the gut eco-niche as well as creating the competition for nutrition and adhesion sites in the colon. Our results are in agreement with Shokryazdan *et al.* (2016), who also noticed a reduction in the caecal β-glucuronidase and β-glucosidase activities after feeding *L. buchneri* FD2, *L. fermentum* HM3, or a mixture at 10^{10} CFU/kg BW/day for 28 days through oral route. Likewise, oral gavaging of *Bacillus coagulans* SANK 70258 to rats at a concentration of 1×10^5 CFU/day for 14 days significantly reduced the beta-glucuronidase and tryptophanase activities in the intestine with a concomitant decrease in the intestinal *Clostridium perfringens* pathogen (Ara *et al*., 2002). Overall, these shreds of evidence suggest that, besides being safe in healthy animals, NCDC 400 also play a key role in shaping gut health by demonstrating the antagonizing effect on harmful pathogens and shifting the gut microflora towards the beneficial wing.

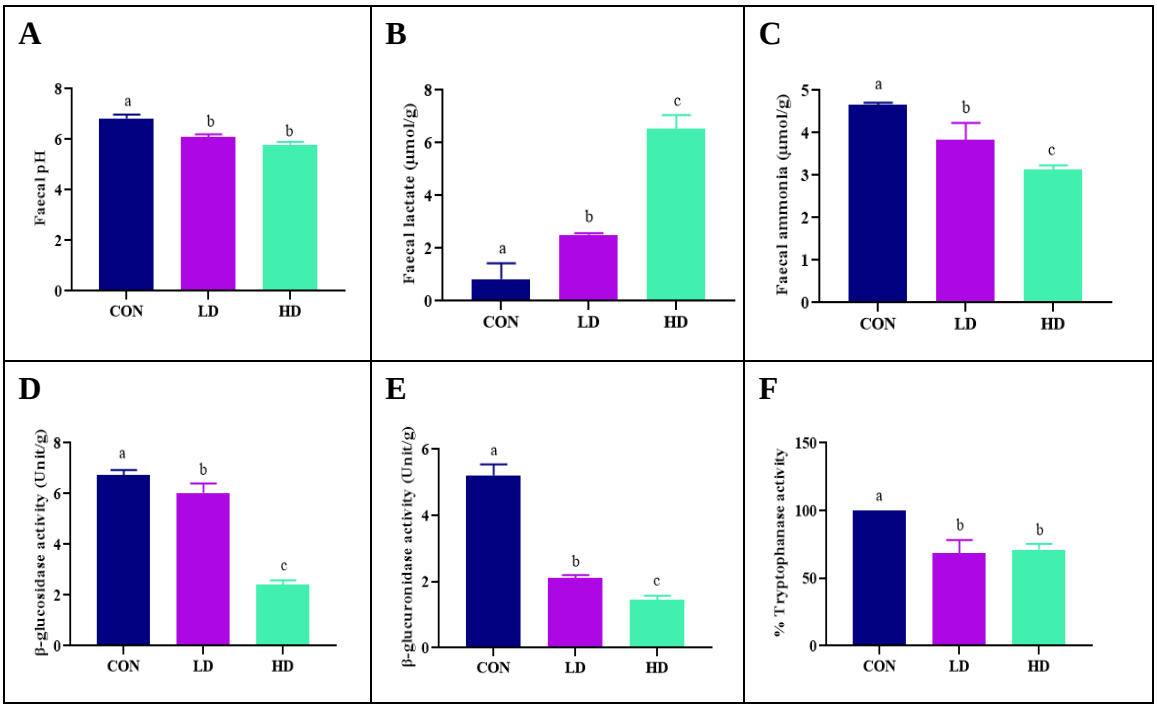

Fig. 4.42: Effect of acute exposure to NCDC 400 on faecal indices and harmful intestinal enzymes of mice. (A) Faecal pH; (B) Faecal lactate; (C) Faecal ammonia; (D) Beta-glucosidase; (E) Beta-glucuronidase; (F) Tryptophanase. Lowercase superscripts a, b, and c indicate the significant differences ($p < 0.05$) between the groups (analyzed by one-way ANOVA following Duncan test).

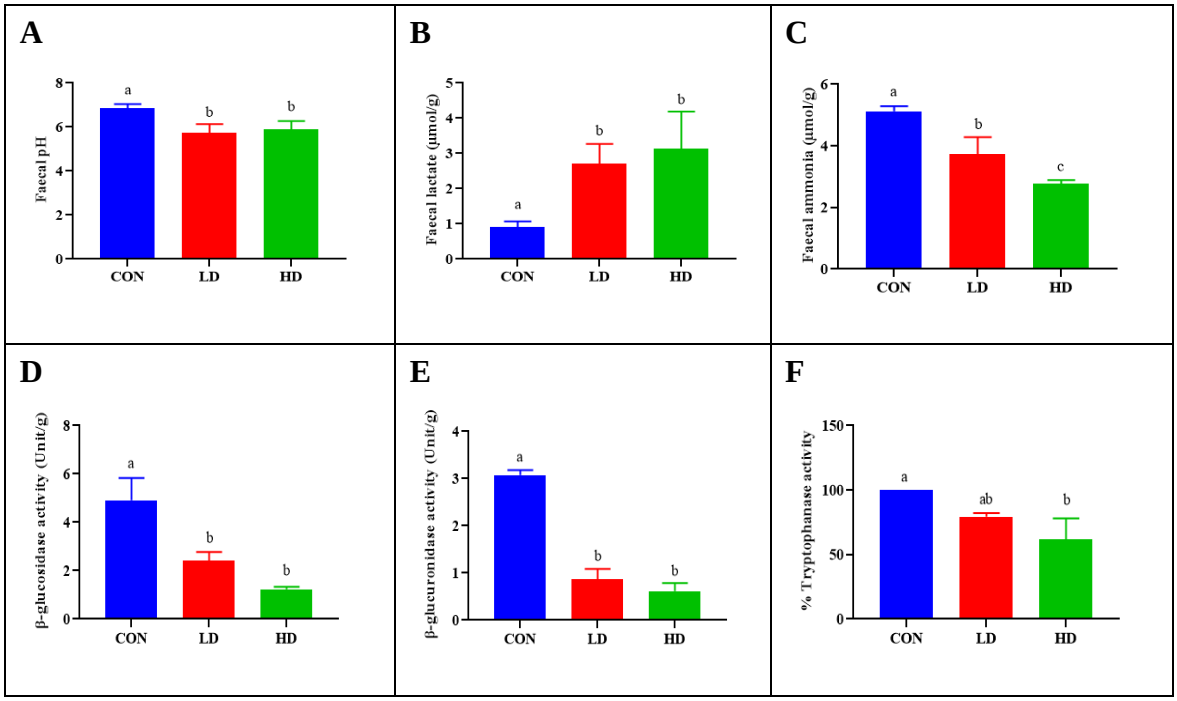

Fig. 4.43: Effect of subacute exposure to NCDC 400 on faecal indices and harmful intestinal enzymes of mice. (A) Faecal pH; (B) Faecal lactate; (C) Faecal ammonia; (D) Beta-glucosidase; (E) Beta-glucuronidase; (F) Tryptophanase. Lowercase superscripts a, b, and c indicate the significant differences ($p < 0.05$) between the groups (analyzed by one-way ANOVA following Duncan test).

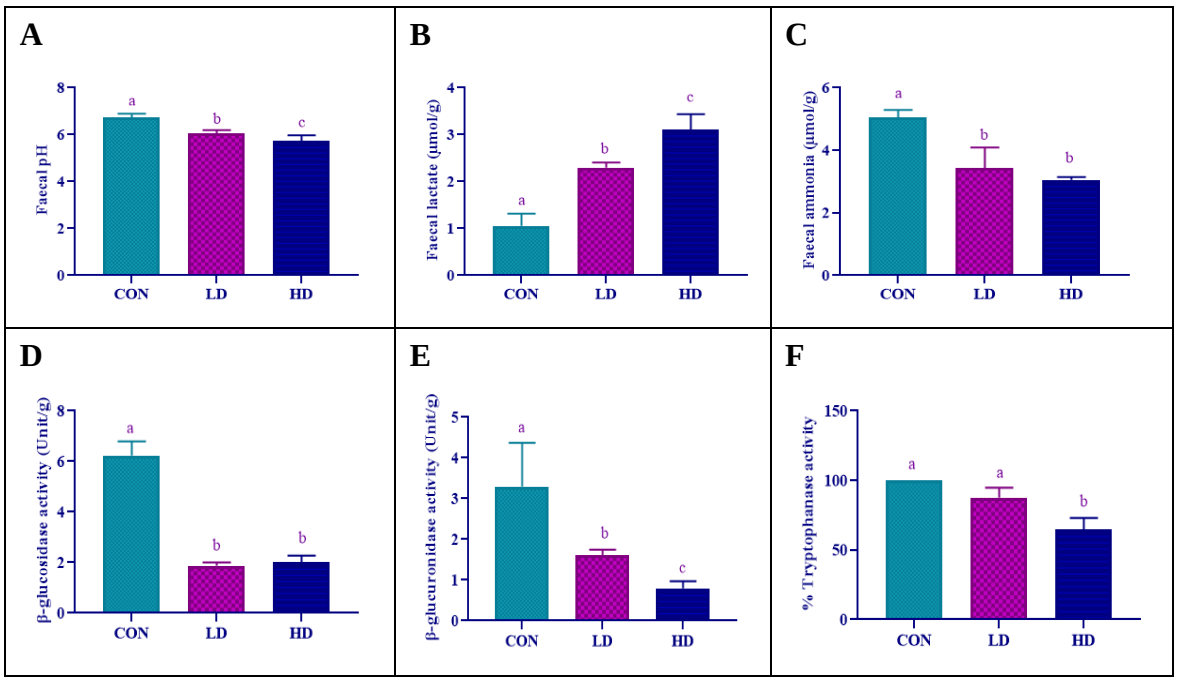

Fig. 4.44: Effect of subchronic exposure to NCDC 400 on faecal indices and harmful intestinal enzymes of mice. (A) Faecal pH; (B) Faecal lactate; (C) Faecal ammonia; (D) Beta-glucosidase; (E) Beta-glucuronidase; (F) Tryptophanase. Lowercase superscripts a, b, and c indicate the significant differences ($p < 0.05$) between the groups (analyzed by one-way ANOVA following Duncan test).

4.4.28. Caecal short-chain fatty acids

The caecal acetate, propionate and butyrate were assessed after the end of all three oral toxicity trials. In the acute toxicity test, the concentrations of acetate, propionate and butyrate and subsequently the total-SCFAs in LD and HD groups were significantly ($p < 0.05$) increased compared to CON but showed no significant difference between the doses (LD and HD) (**Fig. 4.45**). In the subacute toxicity study, the oral administration of *L. fermentum* NCDC 400 at HD significantly ($p < 0.05$) enhanced the production of acetate, propionate and butyrate with a concomitant increase in total SCFA and acetate to propionate ratio (**Fig. 4.46)**. In the subchronic toxicity trial, the oral administration of NCDC 400 for 90 days to mice showed a considerable ($p < 0.05$) upsurge in caecal acetate and propionate and total SCFA (**Fig. 4.47)**. Butyrate was found to be least influenced by the long-term administration of NCDC 400 as there was no increase in the faecal butyrate concentration (**Fig. 4.47C)**. An increase in the caecal SCFA levels after oral gavaging of NCDC 400 indicates better performance in stimulating microbial fermentation of complex carbohydrates in the large intestinal of the mice. Another reason why NCDC 400 administration elevated the caecal SCFAs could be due to gut microbiota modulation. These results are constant with the Gupta *et al*. (2021b), who also witnessed an increase in the faecal SCFAs levels after *L. salivarius* CPN60 administration in healthy rats. Our results are further supported by Nagpal *et al*. (2018), wherein, researchers found an increased SCFAs production (particularly propionate and butyrate) upon oral dosing of a 10-strain probiotic cocktail in a single dose (oral gavage) as well as 5 consecutive doses in mice.

Probiotic bacteria, once engraft in the host gut, ferment food-derived indigestible carbohydrates to produce SCFA. It has been reported that heterofermentative lactobacilli synthesize SCFAs from phosphoketolase pathway (Nataraj *et al*., 2020). In this regard, NCDC 400 genome had the complete gene sets to demonstrate the phosphoketolase pathway (verified by RAST annotation). These SCFAs have been believed to have several health benefits. It has been reported that SCFAs act as an energy source for liver cells and colonocytes. Amongst, butyrate acts as the chief energy source for the colonocytes and also regulates the colonic microbiome, cellular proliferation, and differentiation of gut enterocytes (Nataraj *et al*., 2020). Taken together, the results that emerged from this study further consolidate the gut health-augmenting effects of the probiotic in healthy conditions as well.

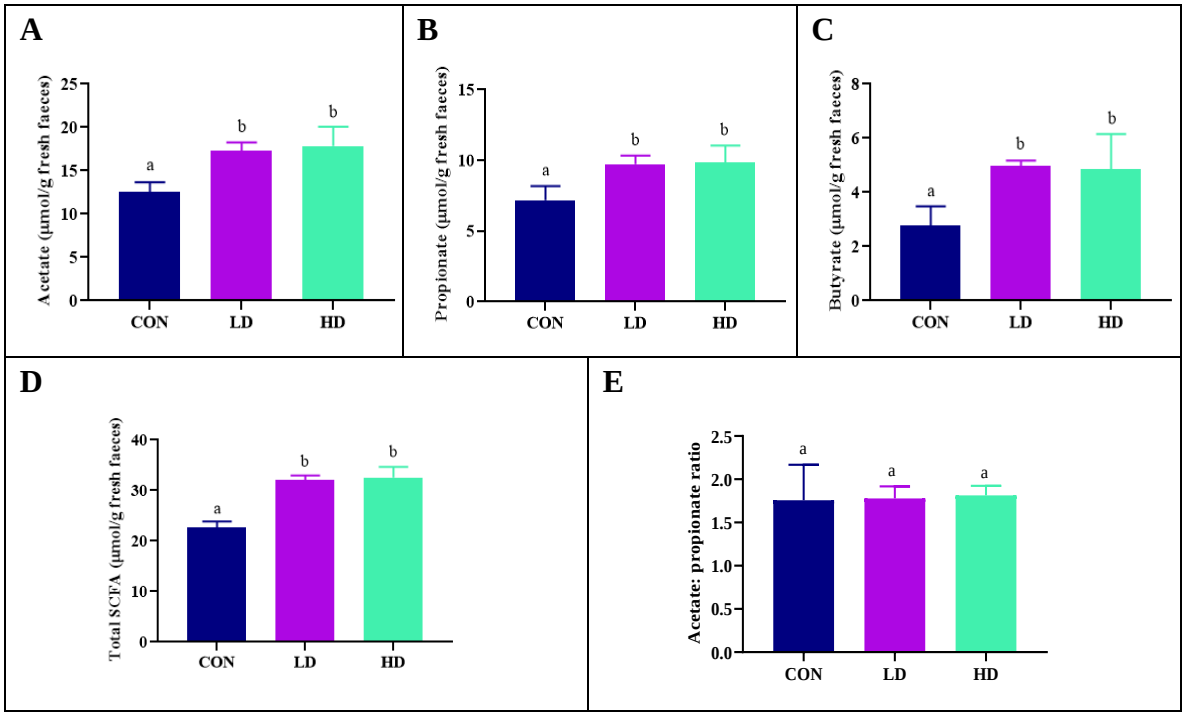

Fig. 4.45: Effect of NCDC 400 on mice caecal SCFAs content in acute oral toxicity study. (A) Acetate; (B) Propionate; (C) Butyrate; (D) Total SCFAs; (E) Acetate to propionate ratio. Lowercase superscripts a and b indicate the significant differences ($p < 0.05$) between the groups *(analyzed by one-way ANOVA following Duncan test).*

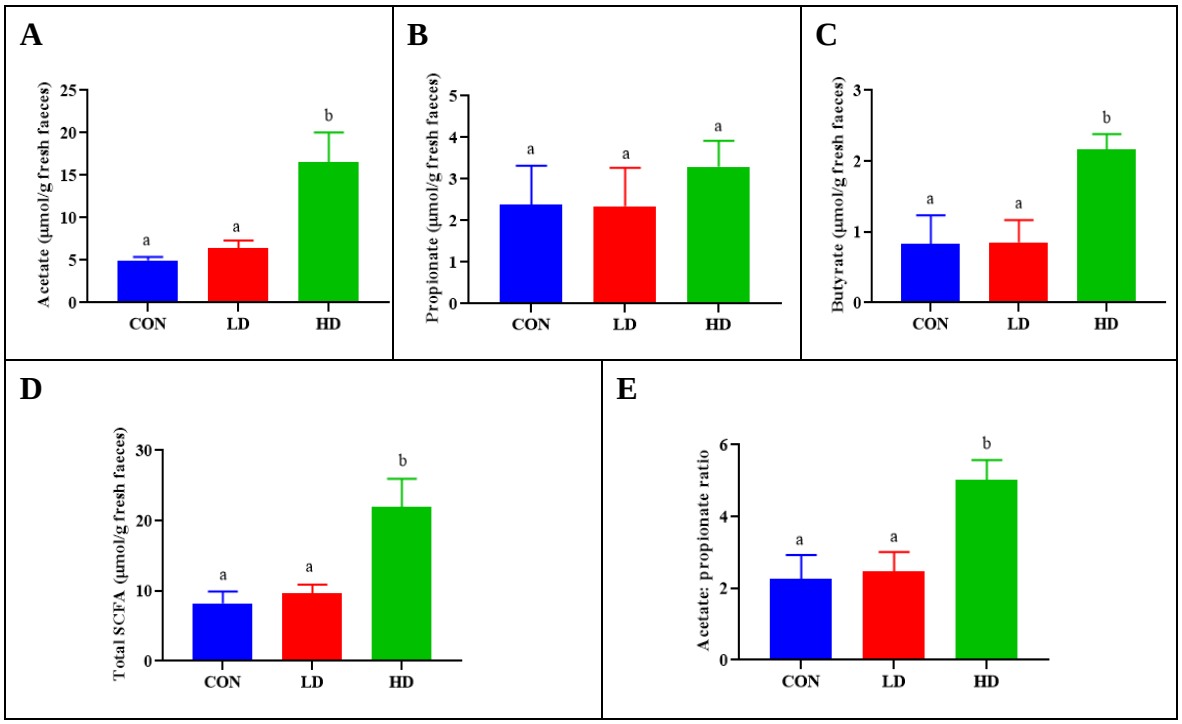

Fig. 4.46: Effect of NCDC 400 on mice caecal SCFAs content in subacute oral toxicity study. (A) Acetate; (B) Propionate; (C) Butyrate; (D) Total SCFAs; (E) Acetate to propionate ratio. Lowercase superscripts a and b indicate the significant differences ($p < 0.05$) between the groups *(analyzed by one-way ANOVA following Duncan test).*

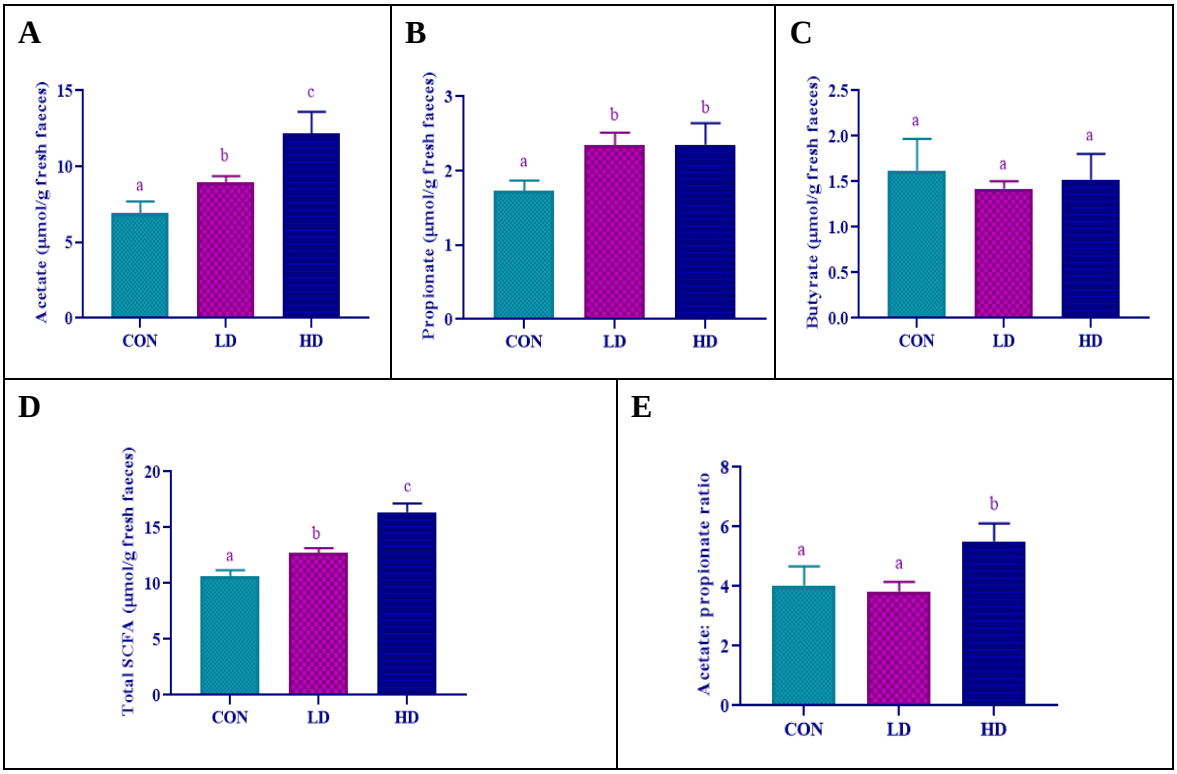

Fig. 4.47: Effect of NCDC 400 on mice caecal SCFAs content in subchronic oral toxicity study. (A) Acetate; (B) Propionate; (C) Butyrate; (D) Total SCFAs; (E) Acetate to propionate ratio. Lowercase superscripts a, b & c indicate the significant differences ($p < 0.05$) between the groups *(analyzed by one-way ANOVA following Duncan test).*

4.4.29. Immune markers in serum

The effect of NCDC 400 on the levels are serum immunoglobulins are presented in **Figs. 4.48-4.50** and their concentrations in mice serum revealed varying degrees of changes upon orogastric administration of NCDC 400 for various durations. As shown in **Fig. 4.48**, the level of IgA and IgG improved significantly ($p < 0.05$) in the HD compared to the CON group during the acute toxicity study. Likewise, subacute exposure to NCDC 400 at a high dose showed an elevation in the serum IgA and IgG levels (**Fig. 4.49)**. In the subchronic toxicity study, only HD was effective in improving the IgA significantly ($p < 0.05$) while both HD and LD were effective in augmenting the serum IgG level compared to the CON group (**Fig. 4.50)**. Immunoglobulins play important role in the host's immune defense by neutralizing the effect of antigens. IgG reflects the systemic immune status and is the most abundantly present in serum. IgA is the second most abundant immunoglobulin in the circulating system. Amongst, sIgA represents mucosal immunity and protects against mucosal-invading pathogens. It has been reported that serum IgA down-regulates the release of pro-inflammatory cytokines

while upregulating the expression of the anti-inflammatory cytokine from immune cells. Moreover, IgA has been also reported to bind complement components to enhance chemotaxis or phagocytosis of immune cells (Leong and Ding, 2014.). Our results are in agreement with previous works of Shu and Gill (2001) and Li *et al*. (2019) who reported that administration of probiotic *Bacillus subtilis*, *Bifidobacterium lactis*, and *Bifidobacterium infantis* and *Bacillus velezensis* at 1×10^9 CFU/day for 21 consecutive days enhanced serum IgG, IgM, and IgA levels in mice.

Regarding serum cytokines levels, in the acute toxicity study, we observed that the mice in the HD group had considerably ($p < 0.05$) higher IL-10 levels than the CON group. In comparison with CON, the levels of IL-6 and TNF-alpha reduced in the HD group while exhibiting no influence of serum TGF-beta and MCP-1 **(Fig. 4.48)**. Similarly, after 28 days of NCDC 400 feeding trial in the subacute toxicity study, the animals in the LD and HD groups showed a significant ($p < 0.05$) increase in the serum IL-10 compared to the CON; while not affecting statistical significance between the test groups (LD and HD) suggesting that long-term exposure of even a low dose of NCDC 400 is also enough to stimulate the production of IL-10. Further, experimental groups had profound ($p < 0.05$) increase in TGF-beta compared to the CON group. On the other hand, LD and HD groups showed a significant ($p < 0.05$) reduction in the serum TNF-alpha level while having a neutral effect on IL-6 and MCP-1 markers (**Fig. 4.49)**. Upon subchronic exposure to test strain, there was no significant variation in the serum IL-10 level in the mice administered with either LD or HD but showed a significant ($p < 0.05$) increase in the TGF-beta in both LD and HD groups. On the other side, the serum of mice under LD and HD groups showed a significant ($p < 0.05$) reduction in IL-6 level with no effect on TNF-alpha and MCP-1 **(Fig. 4.50)**. These results are in agreement with the previous work that evidenced a momentous reduction in TNF-alpha upon oral gavaging of *L. casei* Zhang to mice (Núñez *et al*., 2014). Earlier, Samtiya *et al*. (2019), have observed elevation in the serum TGF-beta upon oral administration of *L. fermentum* MTCC-5898 to mice for 28 days. Likewise, probiotic-mediated reduction in the serum pro-inflammatory factors (TNF-α and IL-6) and an increase in an anti-inflammatory cytokine (IL-10) in mice were witnessed by Li *et al*. (2019).

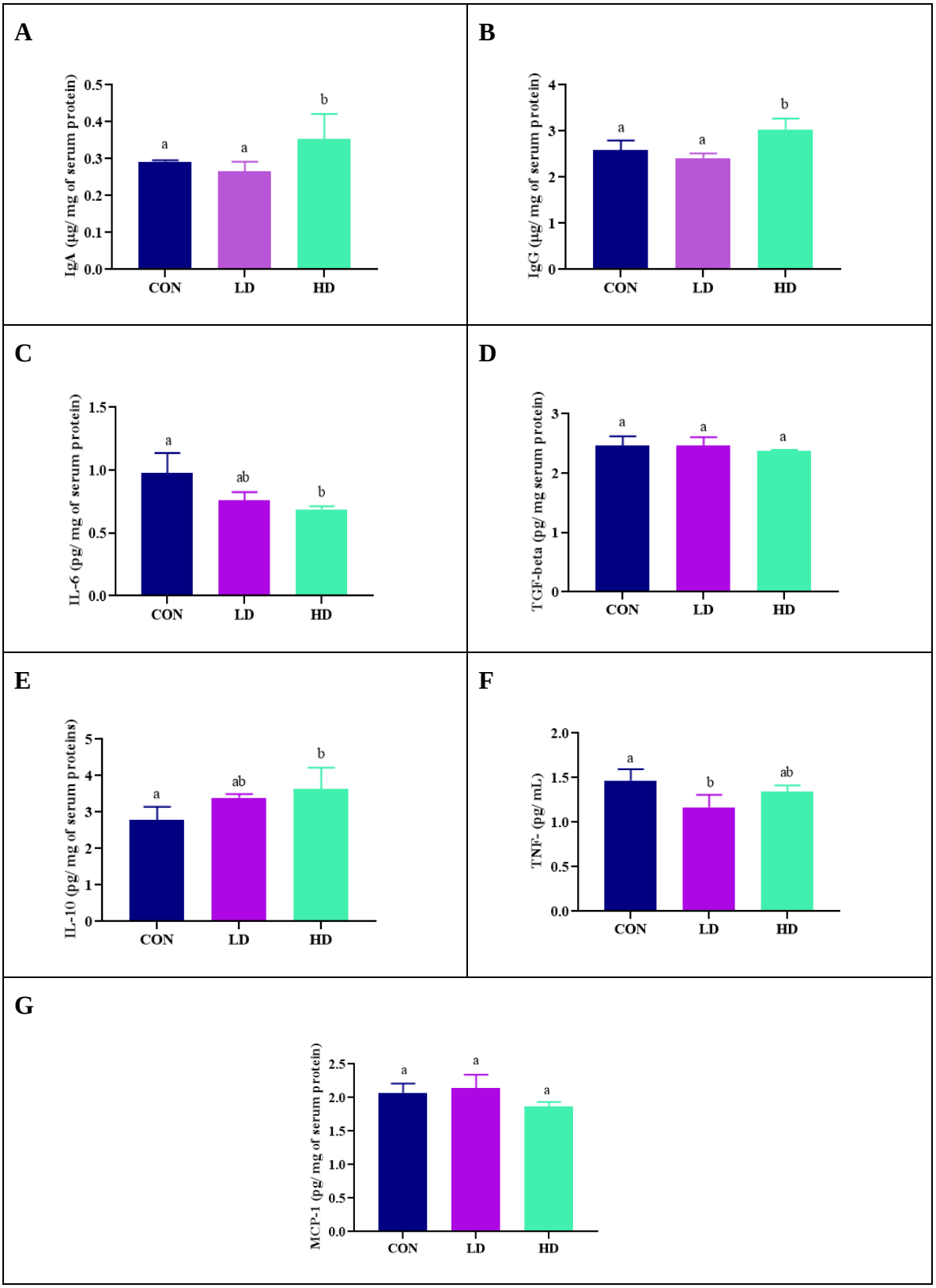

Fig. 4.48: Effect of acute exposure of NCDC 400 on immunoglobulins, cytokines, and chemokine levels in mice serum. (A) IgA; (B) IgG; (C) IL-6; (D) TGF-β (E) IL-10; (F) TNF-alpha; (G) MCP-1. Lowercase superscripts a and b indicate the significant differences ($p < 0.05$) between the groups *(analyzed by one-way ANOVA following Duncan test).*

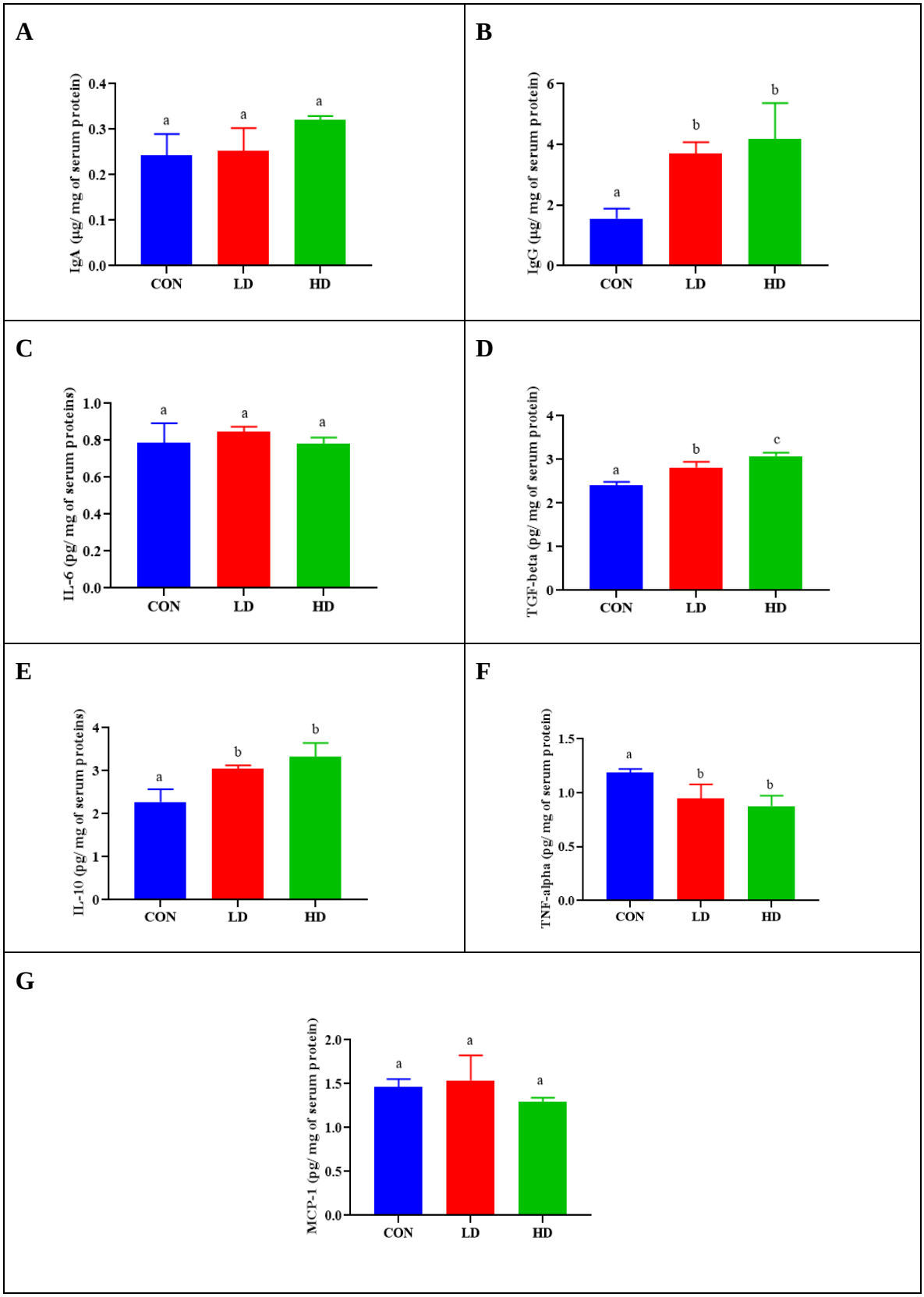

Fig. 4.49: Effect of subacute exposure of NCDC 400 on immunoglobulins, cytokines, and chemokine levels in mice serum. (A) IgA; (B) IgG; (C) IL-6; (D) TGF-β (E) IL-10; (F) TNF-alpha; (G) MCP-1. . Lowercase superscripts a, b, and c indicate the significant differences ($p < 0.05$) between the groups *(analyzed by one-way ANOVA following Duncan test).*

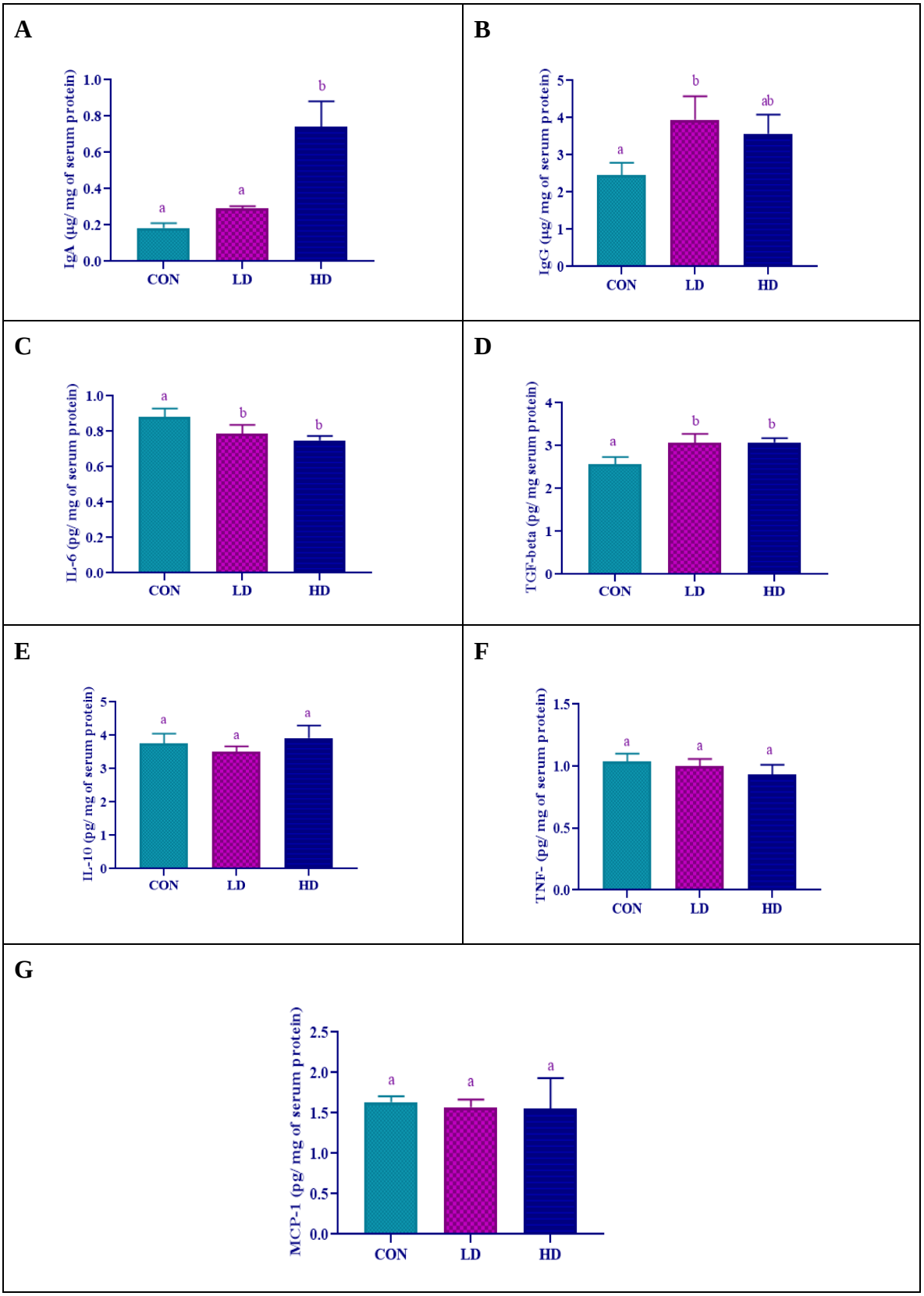

Fig. 4.50: Effect of subchronic exposure of NCDC 400 on immunoglobulins, cytokines, and chemokine levels in mice serum. (A) IgA; (B) IgG; (C) IL-6; (D) TGF-β (E) IL-10; (F) TNF-alpha; (G) MCP-1. Lowercase superscripts a and b indicate the significant differences ($p < 0.05$) between the groups *(analyzed by one-way ANOVA following Duncan test).*

Probiotics generally interact with the immune cells of lamina propria (LP) and mucosal-associated lymphoid tissue (MALT) of the gut. Besides the Microbe-associated Molecular Pattern (MAMP) and Pattern recognition receptor (PRR) based highly specific interaction of probiotics with host immune cells, the probiotics cross-talk with antigen-presenting cells (enterocytes and dendritic cells) in the epithelium as well as in Peyer's patches and thereby capture the antigen from the lumen which is further processed and presented to Treg cell response. Treg cells differentiate into effector cells like T helper cells (CD4+, known as Th) and cytotoxic T cells (CD8+) to produce cytokines. Later, the CD4+ T helper cells activate and regulate macrophages and B-cells to respond to the adaptive immune system (Azad *et al*., 2018). Therefore, the immunoregulatory activity of probiotics is more likely to be mediated by establishing an absolute balance between Th1 and Th2 response which lead to the upregulation of anti-inflammatory cytokines (for example; IL-10, TGF-beta) and downregulation of proinflammatory cytokines (TNF-α, IL-6, MCP-1) (Aparna Sudhakaran *et al*., 2013). Overall, the immunostimulatory or immunoregulatory effect of probiotics can be therefore assessed by quantifying the released cytokines, including interleukins (ILs), tumor necrosis factors (TNFs), interferons (IFNs), transforming growth factor (TGF), and chemokines from immune cells (Azad *et al*., 2018).

Objective 3: Evaluation of safety and efficacy of *Limosilactobacillus fermentum* NCDC 400 in an immunocompromised murine model

4.4.30. Development of cyclophosphamide (Cy) induced immunocompromised mice model

The development of animal models for biomedical research is vital for studying immunology, pathogenesis, safety, drug testing, virulence, diagnosis, and treatment of various microbial infections. Amongst the several laboratory animals, rodent models are considered most suitable for drug testing for their various advantages with mice being the species of choice. Creating a valid immunosuppressed animal model is required for comprehending the successful experimental infections of opportunistic microbes or safety of drugs under immune depleted state. For the induction of an immunocompromised model, cyclophosphamide (Cy) is most commonly used because of its antineoplastic and immunomodulatory roles. Cy is an alkylating agent, that kills both humoral and cellular immune cells in a cell cycle non-specific manner, meaning that they destroy the cell of various phases in the cell cycle (Koper *et al*., 2021). Moreover,

Cy can be converted into phosphoramide mustard and acrolein through the formation of two unstable transient intermediates, 4-hydroxycyclophosphamide and aldophosphamide with the assistance of liver cytochrome oxidase P450. These end products are reported to induce immune-suppression, genotoxicity, and oxidative stress.

Therefore, the selection of Cy dose as well as frequency of its administration is highly instrumental for the successful induction of an immunocompromised model. While developing such models, it is highly vital to select a specific Cy dose that can effectively suppress the immune status by meanwhile maintaining the long-term survival of the hosts to experiment on such animals. Although a handful of studies have been conducted on the development immunocompromised model using Cy, it lacks uniformity in the doses, duration, and route of administration of Cy (Huyan *et al*., 2011). Therefore, it was appropriate to optimize the dose and duration of Cy based on our experimental design as well as the test compound to be investigated on the model. Moreover, the previously reported Cy doses may not be effective for the experimental animals available at our facility. Several factors affect the immune suppression of animals, such as animal species, natural immune status, housing conditions, feeding practices, environmental conditions, etc. Hence, our goal was to exemplify a reliable Cy-induced immunosuppression model in Swiss Albino male mice for studying the bio-safety and efficacy of NCDC 400. Herein we optimized the Cy dose, duration, and frequency of administration for establishing an immunocompromised model.

4.4.30.1. Effect of different doses of Cy on body weight

The changes in the body weight of the mice after exposure to different doses of Cy are shown in **Table 4.29**. Compared to the mice in the control group (0 mg/kg BW), the body weight of the mice treated with Cy reduced considerably in a dose-specific manner. The highest body weight reduction was recorded in the mice administered with a high dose of Cy (150 mg/ kg BW) followed by 100 and 50 mg/ kg BW. Further, duration after Cy administration also seemed to have a significant ($p < 0.05$) role in determining the devastating effect of Cy on body weight. Because the reduction in the body weight of the mice was also found to be gradually declined with the progression in the duration of Cy administration from day 3 to day 17. Amongst, Cy dose of 150 mg/ kg BW significantly ($p < 0.05$) reduced the body weight of mice from 27.60 ± 0.44 g (day-3) to 21.50 ± 1.32 g (day-17) with no mortality being accounted. The reduction in the body weight of the animals could be affiliated with the toxicity effect of the drug on

various cellular tissues as well as a reduction in the feed and water intake by the animals. In fact, repeated Cy exposure to mice, especially at this 150 mg/ kg BW high dose, showed lethargy, reluctance to environmental activity, fur piloerection, and lackluster pelage. Our results are consistent with many previous reports. For example, Zhang *et al*. (2021), recorded a significant reduction in the body weight of mice treated with Cy at 40 mg/ kg BW for 5 consecutive days via intraperitoneal injection. In contrast, Hou *et al*. (2007) orally administrated as low as 10 mg/ kg BW dose of Cy for 30 consecutive days to achieve immune suppression and subsequently body weight reduction in Wistar rats. Overall, these observations conclusively suggest that irrespective of dose level and exposure period, reduction in body weight or growth was found to be an important marker of Cy toxicity.

4.4.30.2. Effect of different doses of Cy on spleen and thymus indices

The effect of different doses of Cy on the spleen index of mice has been presented in **Table 4.29**. In comparison with the control (0 mg/ Kg BW), the spleen index reduced significantly ($p < 0.05$) in the mice treated with a high dose of 150 mg/Kg BW only after three days (day 3) after the first exposure. Further, the reduction in the spleen index continued insignificantly till 12 days of Cy administration at 150 mg/Kg BW but ultimately reduced significantly ($p < 0.05$) to 0.21 ± 0.04. Moreover, there was a reduction in the spleen index of mice in two Cy-treated groups (50 and 100 mg Kg/ BW) over a course of time, but the results were not statistically significant. These results suggest that Cy is extremely noxious to the spleen which ultimately results in atrophy and other degenerative changes. These results are in agreement with Zhou *et al*. (2018) who also reported a reduction in the spleen index upon Cy administration at a very high dose of 200 mg/Kg BW for only one time. Likewise, Zhang *et al*. (2021) have also evidenced a significant reduction in the spleen index after intraperitoneal administration of Cy at 40 mg/kg BW for 5 consecutive days.

Similarly, the Cy administration significantly reduced the thymus index in a dose and time-specific manner (**Table 4.29**). As compared to the animals exempted from the Cy treatment (0 mg/Kg BW), the mice treated with 150 mg/ Kg BW showed a significant ($p < 0.05$) reduction in the thymus index after three days (0.09 ± 0.03) of first exposure to Cy. The spleen index of mice continued to be suppressed through the experiment over 17 days (0.11 ± 0.04) and thereby suggesting the immune suppressive and toxic effect of thymus upon three times repeated exposure to Cy.

Table 4.29: Effect of different doses of Cy on body weight and organ index (spleen and thymus) of mice

Cy Dose (mg/kg BW)	Body weight (g)				
	Day 3	**Day 6**	**Day 9**	**Day 12**	**Day 17**
0	$28.60^{aA} \pm 0.40$	$29.00^{aA} \pm 0.28$	$28.96^{a\,A} \pm 0.29$	$28.80^{aA} \pm 0.15$	$28.23^{aA} \pm 0.75$
50	$28.30^{aA} \pm 0.35$	$28.16^{abA} \pm 0.16$	$27.56^{abAB} \pm 0.69$	$27.43^{abAB} \pm 0.29$	$25.63^{abB} \pm 0.63$
100	$28.60^{aA} \pm 0.66$	$28.06^{abA} \pm 0.52$	$27.10^{abA} \pm 0.49$	$26.53^{bA} \pm 0.31$	$23.82^{bB} \pm 0.72$
150	$27.60^{aA} \pm 0.44$	$27.50^{bA} \pm 0.44$	$26.53^{bA} \pm 0.80$	$24.30^{cAB} \pm 1.32$	$21.50^{cB} \pm 1.32$
Cy Dose (mg/kg BW)	**Spleen index**				
0	$0.61^{aA} \pm 0.03$	$0.58^{aA} \pm 0.01$	$0.59^{aA} \pm 0.01$	$0.62^{aA} \pm 0.02$	$0.63^{aA} \pm 0.01$
50	$0.50^{aA} \pm 0.01$	$0.48^{bA} \pm 0.03$	$0.49^{abA} \pm 0.02$	$0.51^{aA} \pm 0.02$	$0.54^{abA} \pm 0.06$
100	$0.43^{aA} \pm 0.01$	$0.50^{abA} \pm 0.02$	$0.55^{abA} \pm 0.02$	$0.56^{aA} \pm 0.01$	$0.51^{abA} \pm 0.09$
150	$0.48^{aA} \pm 0.01$	$0.38^{bA} \pm 0.03$	$0.31^{bAB} \pm 0.07$	$0.35^{bAB} \pm 0.07$	$0.21^{bB} \pm 0.04$
Cy Dose (mg/kg BW)	**Thymus index**				
0	$0.18^{aA} \pm 0.03$	$0.20^{aA} \pm 0.01$	$0.16^{aA} \pm 0.03$	$0.17^{aA} \pm 0.02$	$0.23^{aA} \pm 0.02$
50	$0.17^{aA} \pm 0.04$	$0.10^{bA} \pm 0.01$	$0.12^{aA} \pm 0.03$	$0.15^{aA} \pm 0.02$	$0.18^{aA} \pm 0.01$
100	$0.11^{bA} \pm 0.01$	$0.09^{bA} \pm 0.01$	$0.08^{bA} \pm 0.01$	$0.12^{aA} \pm 0.03$	$0.16^{aA} \pm 0.02$
150	$0.09^{bA} \pm 0.03$	$0.09^{bA} \pm 0.01$	$0.07^{bA} \pm 0.03$	$0.10^{bA} \pm 0.01$	$0.11^{bA} \pm 0.04$

Note: Values are presented as the mean ± SEM (n = 3). Lowercase superscripts (a-c) represent the significant differences ($p < 0.05$) between different doses. Superscript letters in uppercase (A-B) represent significant differences between the days. *(Analyzed by one-way ANOVA following Duncan test separately as row and column wise)*

Similarly, a dose of 100 mg/ Kg BW was also found effective in reducing the thymus index until 9 days (0.08 ± 0.01) of first exposure to Cy but found ineffective after 12 days (0.12 ± 0.03) since the thymus index significantly ($p < 0.05$) enhanced after 12 days. This indicates that a Cy dose of 100 mg/ Kg BW or even less may not be effective in inducing immune suppression for a total of 17 days. Our results are consistent with the earlier reports wherein intraperitoneal administration of Cy (80 mg/kg BW Cy) intraperitoneally for 5 days significantly ($p < 0.05$) reduced the thymus index of mice (Huyan *et al*., 2011). Although most of the organs are affected by Cy, the spleen and thymus are the major immune tissues that are more sensitive to Cy action. Therefore, the weight and morphology of the thymus and spleen can reveal nonspecific immunity of the system (Zhang *et al*., 2021). Under normal conditions, the organ index does not vary. But when the animal is exposed to the toxicants, the sensitive and targeted organs may be badly damaged by the toxicants which can be assessed by determining the organ index. Overall, the reduction in the spleen and thymus indices observed in this study is the repercussion of immunosuppression in mice.

4.4.30.3. Effect of different doses of Cy on hematological parameters of mice

The changes in the blood parameters after Cy treatment were assessed to test the effect of Cy on white blood cells and red blood cells (**Table 4.30**). Accordingly, a dose-specific reduction in the WBC was recorded in the mice after Cy administration. The highest reduction (1.56×10^9/L) in the WBC was observed in the Cy 150 mg/Kg BW group while the lowest being recorded was 3.43×10^9/L for the 50 mg/Kg BW group. However, the animals administrated with a high dose of Cy 150 mg/Kg BW at three different frequencies maintained the WBC count in the suppressed state (1.63×10^9/L) until 17 days while the lowest dose of 50 mg/Kg BW group failed to maintain the immune suppressed conditions (6.06×10^9/L). The marked reduction in the WBC count suggests that the immune function of the animals was impaired and weakened substantially.

Lymphocytes, a subpopulation of WBC, constituting B and T cells, were also significantly impaired upon Cy administration in a dose-specific manner. A decreasing trend in the lymphocyte number was observed upon Cy treatment in all three doses. However, a high dose of 150 mg/Kg BW was enough to reduce the lymphocyte cell numbers to 1.56×10^9 /L after 3 days of the first Cy intervention. Upon subsequent

completion of 2 more doses of 150 mg/Kg BW, further reduction (0.63×10^9/ L) in the lymphocytes was recorded on 17th day.

Granulocytes, a class of WBC, comprising neutrophils, basophils, and eosinophils, were also shown a linearly decreasing trend with an increase in the Cy dose. Not surprisingly, the lowest dose (Cy: 50 mg/Kg BW) showed the least decline (0.40×10^9/L) in the granulocytes while the highest dose (Cy: 150 mg/Kg BW) showed a maximal reduction (0.86×10^9/L) in the granulocytes on 17th day. Although not significant compared to the control (0 mg/kg BW), an increase the granulocytes in all three Cy doses on the 12th day indicates the ineffective dose concentration and frequencies of Cy administration during the course of study. This partial recovery of granulocytes can be corroborated by the mobilization of hematopoietic progenitor cells (HPCs) in mice blood. It has been reported that Cy can increase the circulating HPCs by distressing the distribution of hematopoietic stem cells and mature progenitor cells (Neben *et al*., 1993). However, a further increase in the dose concentration and frequencies to suppress the rise in the granulocytes on the 12th would probably lead to mortality of animals as there was already a tremendous reduction in WBC being recorded on day 12.

A considerable reduction in the monocytes in a dose and duration-specific manner was evidenced upon Cy intervention in mice. In a similar passion as observed in other immune cells, 150 mg/ Kg BW dose of Cy significantly ($p < 0.05$) reduced the monocytes to 0.13×10^9 /L after 3 days of Cy injection. However, there was no increase in the monocyte count until day 17 was recorded. This suggests that this dose was sufficient to significantly suppress the monocytes to the desired level throughout the experiment. It has been reported that the bioactivated end products of Cy (phosphoramide mustard and acrolein) can alkylate the DNA and proteins. These end metabolites have a half-life of 6–9 h and can enter the plasma within 2–3 h. Within the circulatory system, they cause high level of toxicity to the rapidly dividing hematopoietic cells (Iqubal *et al*., 2020). Our results are consistent with Huyan *et al*. (2011), wherein the intraperitoneal administration of Cy 75-200 mg/Kg BW to Balb/c mice showed a decrease in the WBC and its subpopulation from day 1, attained the nadir on day 4, recovered on day 10, and decreased again on day 17 due to repeated administration of Cy.

Table 4.30: Effect of different doses of Cy on various hematological parameters of mice

Cy Dose (mg/kg BW)	WBC (10^9/ L)				
	Day 3	**Day 6**	**Day 9**	**Day 12**	**Day 17**
0	$8.03^{aA} \pm 0.33$	$8.26^{aA} \pm 1.51$	$5.46^{aB} \pm 0.53$	$8.40^{aA} \pm 0.30$	$8.36^{aA} \pm 0.33$
50	$3.43^{bB} \pm 0.47$	$4.5^{bAB} \pm 1.47$	$5.7^{aAB} \pm 1.53$	$7.16^{B} \pm 0.27$	$6.06^{bAB} \pm 0.59$
100	$3.60^{bA} \pm 0.66$	$3.73^{bA} \pm 0.64$	$4.43^{abA} \pm 1.51$	$5.00^{bA} \pm 0.28$	$3.30^{cA} \pm 0.36$
150	$1.56^{cA} \pm 0.29$	$3.63^{bB} \pm 0.61$	$1.33^{bA} \pm 0.58$	$1.90^{cA} \pm 0.66$	$1.63^{dA} \pm 0.20$
Cy Dose (mg/kg BW)	**Lymphocytes (10^9/ L)**				
0	$2.70^{aB} \pm 0.68$	$3.43^{aAB} \pm 0.62$	$2.43^{aB} \pm 0.27$	$4.83^{aA} \pm 0.63$	$5.06^{aA} \pm 0.61$
50	$1.26^{abA} \pm 0.26$	$2.06^{abAB} \pm 0.69$	$2.53^{aAB} \pm 0.63$	$4.13^{aB} \pm 0.66$	$1.70^{bAB} \pm 0.52$
100	$1.80^{abB} \pm 0.40$	$1.56^{bB} \pm 0.31$	$1.53^{abB} \pm 0.52$	$4.50^{aA} \pm 0.34$	$1.20^{bB} \pm 0.10$
150	$1.56^{bB} \pm 0.20$	$0.56^{bB} \pm 0.24$	$0.50^{bB} \pm 0.26$	$4.16^{aA} \pm 0.43$	$0.63^{bB} \pm 0.06$
Cy Dose (mg/kg BW)	**Granulocytes (10^9/ L)**				
0	$3.3^{aAB} \pm 0.81$	$4.03^{aAB} \pm 0.72$	$2.63^{aB} \pm 0.26$	$5.56^{abA} \pm 0.82$	$2.60^{aB} \pm 0.25$
50	$1.90^{abB} \pm 0.25$	$2.20^{abB} \pm 0.75$	$2.13^{abB} \pm 0.37$	$4.73^{bB} \pm 0.18$	$0.40^{bA} \pm 0.2$
100	$1.66^{abB} \pm 0.32$	$1.80^{bB} \pm 0.32$	$2.40^{abB} \pm 0.88$	$5.33^{aA} \pm 0.99$	$1.80^{aB} \pm 0.23$
150	$0.73^{bB} \pm 0.14$	$0.73^{bB} \pm 0.23$	$0.73^{bB} \pm 0.23$	$4.66^{bA} \pm 0.49$	$0.86^{bB} \pm 0.12$

Cy Dose (mg/kg BW)	**Monocytes (10^9/ L)**				
0	$0.63^{aAB} \pm 0.03$	$0.53^{aAB} \pm 0.03$	$0.41^{aA} \pm 0.01$	$0.90^{aA} \pm 0.15$	$0.63^{aAB} \pm 0.08$
50	$0.26^{bcA} \pm 0.03$	$0.26^{bA} \pm 0.03$	$0.36^{aA} \pm 0.14$	$0.40^{bA} \pm 0.05$	$0.50^{abA} \pm 0.17$
100	$0.33^{bA} \pm 0.03$	$0.36^{abA} \pm 0.06$	$0.50^{aA} \pm 0.20$	$0.46^{bA} \pm 0.03$	$0.30^{abA} \pm 0.11$
150	$0.13^{cA} \pm 0.03$	$0.26^{bB} \pm 0.08$	$0.13^{bB} \pm 0.08$	$0.66^{abB} \pm 0.06$	$0.13^{bB} \pm 0.03$
Cy Dose (mg/kg BW)	**RBC (10^{12} /L)**				
0	$9.21^{aA} \pm 0.45$	$9.30^{aA} \pm 0.29$	$8.66^{aA} \pm 0.35$	$7.89^{aA} \pm 0.56$	$9.32^{aA} \pm 0.53$
50	$7.35^{bAB} \pm 0.37$	$8.01^{aAB} \pm 0.24$	$8.60^{aA} \pm 0.23$	$6.31^{aB} \pm 0.92$	$7.51^{bAB} \pm 0.02$
100	$8.30^{abA} \pm 0.40$	$8.77^{aA} \pm 0.63$	$7.03^{aA} \pm 0.21$	$7.31^{aA} \pm 0.55$	$6.74^{bcA} \pm 0.52$
150	$7.23^{bA} \pm 0.27$	$8.11^{aA} \pm 0.38$	$5.68^{aA} \pm 1.69$	$7.48^{aA} \pm 0.65$	$5.68^{cA} \pm 0.33$
Cy Dose (mg/kg BW)	**HCT (%)**				
0	$41.1^{aA} \pm 2.87$	$40.20^{aA} \pm 1.02$	$38.76^{aA} \pm 2.85$	$35.8^{aA} \pm 1.78$	$37.83^{aA} \pm 0.61$
50	$31.83^{bAB} \pm 1.03$	$34.46^{bAB} \pm 0.85$	$37.26^{abA} \pm 0.13$	$30.90^{aAB} \pm 3.15$	$29.66^{bB} \pm 0.83$
100	$36.40^{abA} \pm 2.19$	$37.16^{abA} \pm 1.08$	$31.00^{abAB} \pm 2.11$	$31.06^{aAB} \pm 2.19$	$27.60^{bB} \pm 2.88$
150	$31.36^{bA} \pm 1.31$	$34.90^{bA} \pm 0.66$	$24.40^{bA} \pm 7.04$	$32.36^{aA} \pm 2.61$	$23.10^{bA} \pm 1.04$

Note: Values are presented as the mean ± SEM (n = 3). Lowercase superscripts (a-c) represent the significant differences ($p < 0.05$) between different doses. Superscript letters in uppercase (A-B) represent significant differences between the days. *(Analyzed by one-way ANOVA following Duncan test separately as row and column wise).*

Similar to our study, Warn *et al*. (2006) have also witnessed profound neutropenia (reduction of neutrophils, a subtype of granulocytes) 3 days after administration of Cy at 200 mg/Kg BW in CD1 mice. Further, our results regarding the dose-dependent induction of granulocytopenia and monocytopenia upon Cy administration are consistent with Van't Wout *et al*. (1989), wherein Cy administration to mice resulted in the severe reduction in the granulocytes and monocytes in the peripheral blood.

On the other hand, the RBC count also declined significantly ($p < 0.05$) after intraperitoneal administration of Cy at 150 mg/ Kg BW **(Table 4.30)**. However, the other two doses were found inappropriate and failed to lower the RBC. Compared to the control (Cy: 0 mg/kg BW) (9.32×10^{12} /L), the RBC count of animals administrated with 150 mg/ Kg BW Cy significantly ($p < 0.05$) decreased to 5.68×10^{12} /L on the 17^{th} day. These results align well with the HCT data which is a representation of the percentage of RBCs in the blood. The level of HCT declined significantly ($p < 0.05$) in the mice provided with 150 mg/ Kg BW Cy dose. In comparison with the control (37.83 ± 0.61%), the HCT values of mice administered with 150 mg/ Kg BW Cy dose reduced to (23.10 ± 1.04%) after 17 days of trial. Bone marrow is a vital component of the body responsible for maintaining immunity functions by fabricating the synthesis of WBC, RBC, and blood platelets. However, Cy induces myelosuppression and hematological toxicity by acting on bone marrow cells. It has been reported that Cy and its derived metabolized products can inhibit the DNA replication process of bone marrow cells and thereby halts the synthesis of peripheral blood cells (Iqubal *et al*., 2020). Our observations on the effect of Cy on RBC and HCT are highly similar to this supporting document. Moreover, these results are also in agreement with previous work suggesting the dose-specific distortive effect of Cy on RBC and HCT (Feng *et al*., 2016).

4.4.30.4. Effect of different doses of Cy on activities of enzymic antioxidants serum

The effect of Cy on the serum antioxidant enzymes *viz*. SOD, CAT, and GpX have been presented in **Table 4.31**. Although the level of serum SOD was found to be on a declining trend in the mice treated with Cy 50 and 100 mg/Kg BW, their statistical significance between the control (Cy: 0 mg /Kg BW) was found to be invariable. But we noticed a significant ($p < 0.05$) reduction in the serum SOD level after exposure to Cy 150 mg/Kg BW even after day 3 of the Cy injection. Further, the concentration of serum

SOD of mice administered with 150 mg/Kg BW was suppressed significantly throughout the experiment (until 17 days). Similarly, the serum CAT activity reduced insignificantly throughout the experimental tenure after exposure to Cy at 50 and 100 mg/Kg BW doses. However, a significant decline in the CAT level was recorded in the mice treated with Cy 150 mg/Kg BW. The levels of CAT after 3 and 17 days of Cy administration were found to be 0.17 ± 0.03 and 0.12 ± 0.04 ng/mL, respectively, while the control mice showed 0.31 ± 0.01 and 0.31 ± 0.05 ng/mL on the same days.

The perturbation in the serum GpX2 level was witnessed after the Cy intervention in mice **(Table 4.31)**. Although the two Cy doses lesser than 150 mg/Kg BW showed a reduction in the GpX2 activity, the results were insignificant. In fact, even exposure to a high dose of 150 mg/Kg BW could not affect the GpX2 level after 3 days of post-administration. However, a significant decrease in the serum GpX levels was found after day 9 and reached a nadir on day 17. This clearly suggests the resistance mechanism of GpX2 against the action of Cy and its metabolic products. The reason behind the increase in the serum GpX2 levels on day 9 may be related to enzyme saturation wherein there is a lack of reactive free active sites to combat the oxidative stress induced by the repetitive administration of Cy high dose. In support of this observation, McGown and Fox (1986) stated that resistance to alkylating agents has been associated with increased activity of the glutathione-dependent oxidoreductase (O/R) enzymes with subsequent elevation in the levels of glutathione.

Cy is an important anticancer drug that induces severe oxidative stress and inflammation in cells leading to DNA damage (DNA cross-linking) and apoptosis. The end products of Cy metabolism such as acrolein and phosphoramide mustard as well as the transient intermediates, 4-hydroxycyclophosphamide and aldophosphamide have been reported to generate toxic ROS such as superoxide radical ($O_2^{\bullet-}$), hydrogen peroxide (H_2O_2), hydroxyl radical ($^{\bullet}OH$), etc. (Jeelani *et al*., 2017). These ROS damages the enzymes and proteins including those that combat oxidative stress. The animal system has cellular defense (SOD, CAT, and GpX2) enzymes to confront the reactive oxygen species (ROS). SOD converts superoxide radicals into H_2O_2, which will dissociate into H_2O and O_2 in the presence of CAT. GSH also reduces the level of H_2O_2 by oxidizing itself to GSSG (oxidized glutathione) in presence of glutathione peroxidase (Wood *et al*., 2006).

Table 4.31: Effect of Cy administration on activities of enzymic antioxidants serum

Cy Dose (mg/kg BW)	SOD (ng/ mL)				
	Day 3	**Day 6**	**Day 9**	**Day 12**	**Day 17**
0	$20.93^{abA} \pm 1.14$	$19.51^{aA} \pm 2.99$	$20.48^{aA} \pm 1.71$	$29.29^{aA} \pm 2.70$	$19.17^{aA} \pm 3.05$
50	$26.96^{aA} \pm 3.30$	$13.91^{aB} \pm 4.21$	$15.92^{aB} \pm 1.01$	$17.20^{bB} \pm 1.53$	$14.44^{bB} \pm 0.18$
100	$15.17^{abA} \pm 6.88$	$11.44^{aA} \pm 2.70$	$13.46^{bA} \pm 3.02$	$12.79^{bA} \pm 7.02$	$15.48^{abA} \pm 3.64$
150	$10.58^{bA} \pm 1.23$	$9.44^{bA} \pm 3.82$	$11.06^{bA} \pm 3.08$	$10.69^{cA} \pm 1.59$	$11.18^{cA} \pm 0.19$
Cy Dose (mg/kg BW)	**CAT (ng/ mL)**				
0	$0.31^{aA} \pm 0.01$	$0.31^{aA} \pm 0.02$	$0.36^{aA} \pm 0.02$	$0.33^{aA} \pm 0.02$	$0.31^{aA} \pm 0.05$
50	$0.30^{aA} \pm 0.01$	$0.16^{aA} \pm 0.03$	$0.19^{bA} \pm 0.04$	$0.14^{bA} \pm 0.05$	$0.24^{aA} \pm 0.07$
100	$0.22^{abA} \pm 0.04$	$0.22^{aA} \pm 0.09$	$0.10^{bA} \pm 0.01$	$0.24^{abA} \pm 0.07$	$0.16^{bA} \pm 0.05$
150	$0.17^{bA} \pm 0.03$	$0.18^{aA} \pm 0.01$	$0.17^{bA} \pm 0.06$	$0.17^{abA} \pm 0.03$	$0.12^{bA} \pm 0.04$
Cy Dose (mg/kg BW)	**GpX2 (pg/ mL)**				
0	$1155.91^{aA} \pm 57.00$	$949.40^{aA} \pm 129.9$	$983.93^{aA} \pm 106.57$	$1572.2^{aA} \pm 249.4$	$812.58^{aA} \pm 64.04$
50	$1456.39^{aA} \pm 164.60$	$805.55^{aB} \pm 210.21$	$656.59^{abB} \pm 50.85$	$620.78^{abB} \pm 76.69$	$832.40^{aB} \pm 9.41$
100	$1868.25^{aA} \pm 99.86$	$682.80^{aA} \pm 99.86$	$783.18^{abA} \pm 50.79$	$430.26^{bA} \pm 30.86$	$620.00^{abA} \pm 118.26$
150	$1840.63^{aA} \pm 77.4$	$908.33^{aB} \pm 173.49$	$532.75^{bD} \pm 75.04$	$494.42^{bC} \pm 79.65$	$432.93^{bDC} \pm 36.02$

Note: Values are presented as the mean ± SEM (n = 3). Lowercase superscripts (a-c) represent the significant differences ($p < 0.05$) between different doses. Superscript letters in uppercase (A-D) represent significant differences between the days *(Analyzed by one-way ANOVA following Duncan test separately as row and column wise).*

However, excessive ROS stress may lead to the degradation of these enzymes leading to toxicity. In line with the above-stated mechanism, we noted the decline in the activity of these enzymes with an increase in the dose and frequency of the administration of Cy. Our results are consistent with Senthilkumar *et al*. (2006), who also evidenced the reduction in the activity of anti-oxidative enzymes *viz*. SOD, CAT, and GpX2 in rats after exposure to Cy 150 mg/kg BW. Based on these results, a Cy dose of 150 mg/kg BW was used for i.p injections to for three times with a gap of 6 days each to create an immunocompromized mice model.

4.4.31. Evaluation of safety and efficacy of NCDC 400 in Cy-induced immunocompromised mice model

4.4.31.1. General health parameters

As a part of assessing the general health status, the animals were monitored for changes in body weight, feed and water intake, salivation, diarrhoea, skin, fur, eyes, and behavior. There were no prominent signs of hypersalivation or lachrymation symptoms in any group including MC. Similarly, none of the animals in all four groups showed the symptoms of diarrhea. However, there was a trivial deterioration in the fur quality (lusterless) with thinning of fur being more noticeable in the MC group. Animals in the MC showed passive behavior, loss of appetite, tremors, convulsions, weakness, and lethargy (noticeable reduction in animal movement). Whereas, these general observations were not severe in LD and HD groups suggesting that NCDC 400 might have a protective role in ameliorating the Cy-induced toxic effects on animal physiology.

On the other hand, the animals showed considerable variations in body weight across the groups. Compare to the NC group, the Cy administration resulted in severe weight loss in the MC group throughout the experimental period. However, the weight loss during the experimental tenure in LD and HD groups was not severe compared to MC. No noticeable changes in the variations of body weight were recorded between LD and HD. When the weight gain or loss by the animals was computed at the end of the experiment, it was found that the MC group lost on an average of 3.3 g body weight while the LD and HD showed 2.09 and 1.8 g reduction in body weight. It is also evident from **Fig. 4.51** that Cy injections resulted in the disturbance in the normal feed and water intake by the experimental animals.

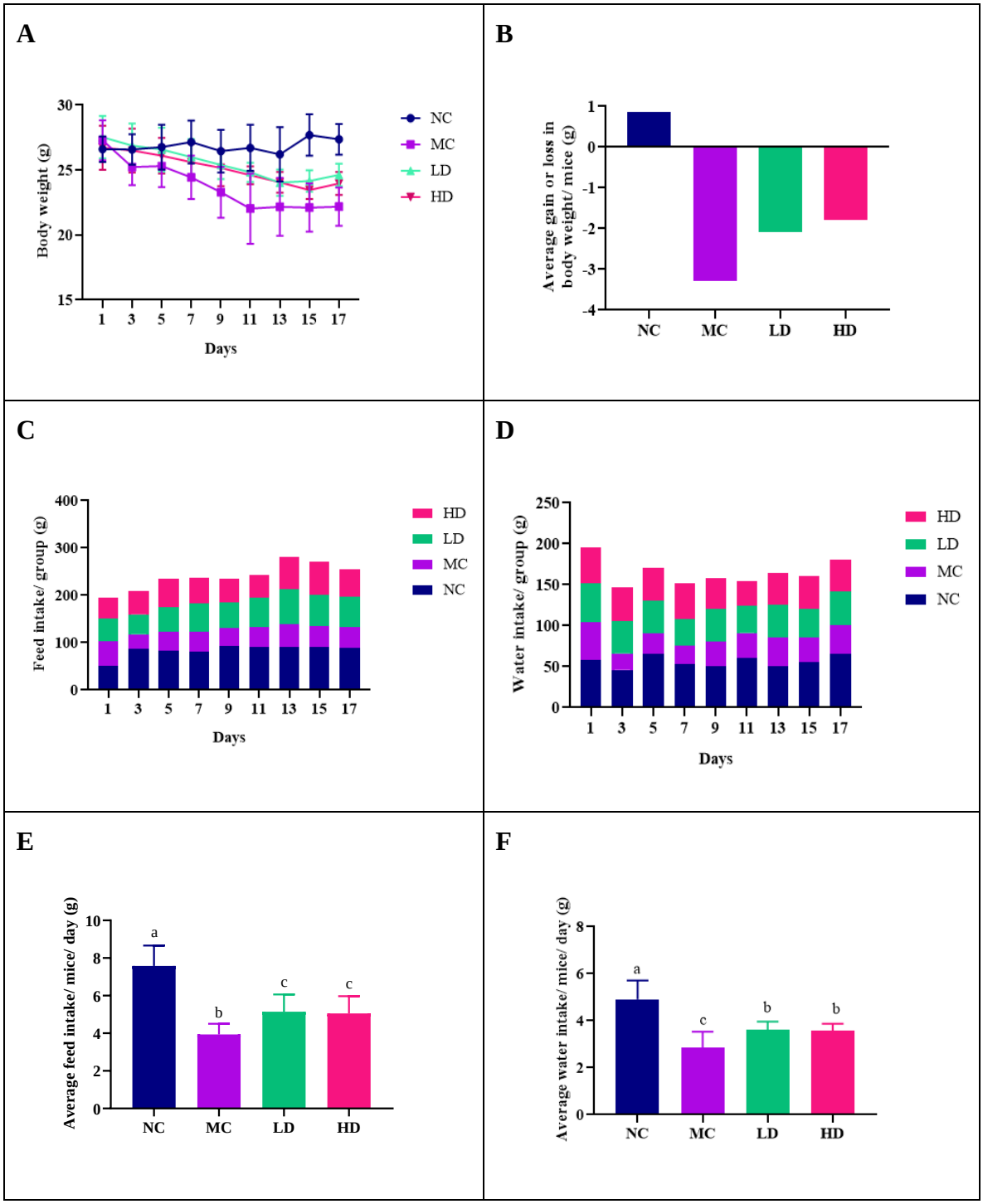

Fig. 4.51: Effect of oral administration of NCDC 400 on general health profile of immunocompromised mice. (A) Changes in body weight; (B) Gain/ loss in body weight; (C) Changes in daily feed intake/ group; (D) Changes in daily water intake/ group; (E) Average daily feed intake/ mouse; (F) Average daily water intake/ mouse. Here, NC, MC, LD, and HD refer to normal control, model control, low dose, and high dose, respectively. Error bars indicate the variations of eleven determinations in terms of the standard error of mean. Lowercase superscripts (a-c) represent the significant differences ($p < 0.05$) across the groups *(Analyzed by one-way ANOVA following Duncan test).*

Throughout the study, there was a sizable reduction in the feed and water intake in the MC group compared to NC, while improved gradually in the LD and HD groups. Compared to NC (7.57 ± 0.26 g), there was a significant ($p < 0.05$) reduction in the average daily feed intake per mouse in the MC (3.93 ± 0.13 g) but resumed significantly ($p < 0.05$) in both LD (5.14 ± 0.22 g) and HD (5.05 ± 0.22 g) groups. In a similar way, the MC (2.85 ± 0.16 g) group showed an appreciable ($p < 0.05$) reduction in the average daily water intake per mouse compared to NC (4.91 ± 0.19 g) but revamped significantly ($p < 0.05$) in LD (3.60 ± 0.08 g) and HD (3.57 ± 0.07 g) groups. These results are highly correlating with the body weight data wherein a proportionate reduction in the feed intake could be a prominent reason why the mice in MC exhibit excessive body weight loss. Whereas, the NCDC 400 administration either at low or high doses resulted in furtherance in the feed and water intake. An improved feed intake in NCDC 400 fed group could be ascribed to the microbes-mediated better feed conversion rate (FCR) which can be indirectly assessed by measuring the body weight. Probiotics have been reported to involve in the enzymatic digestion of food in the intestine of the host and thereby help in the better abortion of the nutrients (Cao *et al*., 2020). These findings are in-line with Mazkour *et al*. (2019) wherein oral supplementation of *Bacillus* probiotic mixture resulted in enhanced food intake which in turn improved FCR. In this regard, our observations are also consistent with the body weight data showing an improvement in body weight of mice in the LD and HD groups compared to the MC group. These results are in accordance with Meng *et al*. (2018), who also noticed that feeding *L. plantarum* KLDS1.0318 (5×10^7-10^9 CFU/mL) for 20 days significantly halted the drastic weight loss in the Cy-induced immune-suppressed BALB/c mice.

4.4.31.2. Organ index

The relative organ weights (organ indices) were determined for major organs (kidney, liver, spleen, brain, heart thymus, and lungs) at the end of the study. Drug injection significantly affected the organ index in the MC group. We observed a considerable ($p < 0.05$) decrease in the organ index of the kidney (1.12 ± 0.08), spleen (0.35 ± 0.01), brain (1.26 ± 0.10), and thymus (0.21 ± 0.02) of animals in MC group (**Fig. 4.52**). These observations are similar to the previous works reporting the decrease in the spleen, thymus, kidney, and thymus indices as well their atrophy upon Cy treatment (Zhou *et al*., 2018a; Liu *et al*., 2019). Our results are contradictory to the findings of Zhao *et al*. (2020), who observed spleen atrophy after Cy administration.

However, the increase or decrease in the organ volume can be directly linked with the dose and frequency of exposure to Cy (Cao *et al*., 2022). On the other hand, the animals exposed to NCDC 400 either at low or high doses did not influence the further reduction of the organ indices. Rather, the aforementioned tissues of the LD and HD groups demonstrated an improvement in the organ index towards normal weights, although not statistically significant in a few cases. The spleen and thymus are the important immune organs that deal with cellular and humoral immunity. The matured immune cells settle in the spleen and respond to the external antigenic stimulus. T-cells differentiation and maturation take place in the thymus. An increase in the weight of the spleen and thymus is an indication of the proliferation of lymphocytes in these organs. But certain drugs like Cy can hamper the proliferation and differentiation of lymphocytes in immune organs resulting in decreased spleen and thymus weight (Zhang *et al*., 2021). Hence, assessing the spleen and thymus indexes helps in understanding the immune-pharmacological mechanisms of test substances in animal models. In this study, NCDC 400 dosing (LD and HD) alleviated the atrophy of thymus and spleen by enhancing the thymus (LD: 0.33 ± 0.02 and HD: 0.31 ± 0.02) and spleen index (LD: 0.42 ± 0.02 and HD: 0.39 ± 0.02) loss in immunosuppressed mice and thereby hinting a preliminary clue on the immunomodulatory potential of the strain. Consistent with the previous work, immunomodulatory probiotic strains can display an increase in the spleen and thymus indexes in Cy-induced immunocompromised animal models. In a similar previous study, oral administration of *L. plantarum* KLDS1.0318 (5×10^9 CFU/mL for 20 days) to the immunocompromised mice significantly enhanced the spleen and thymus index compared to levamisole hydrochloride–treated mice (positive control) (Meng *et al*., 2018).

On the other hand, the Cy administration resulted in significant ($p < 0.05$) hypertrophy of the liver (6.4 ± 0.23), heart (0.66 ± 0.04), and lungs (1.72 ± 0.13), as evidenced by increased organ index (**Fig. 4.52**). This suggests the hepato-, cardiac-, and pulmonary toxic effects of Cy. The experiential data are in accord with the earlier reports highlighting the hypertrophy of the liver, heart, and lungs upon Cy intervention (Suddek *et al*., 2013; Cao *et al*., 2022; Elsayed *et al*., 2022). This is because; Cy induces vascular permeability and edema by altering the vascular endothelial cell structure (Elsayed *et al*., 2022).

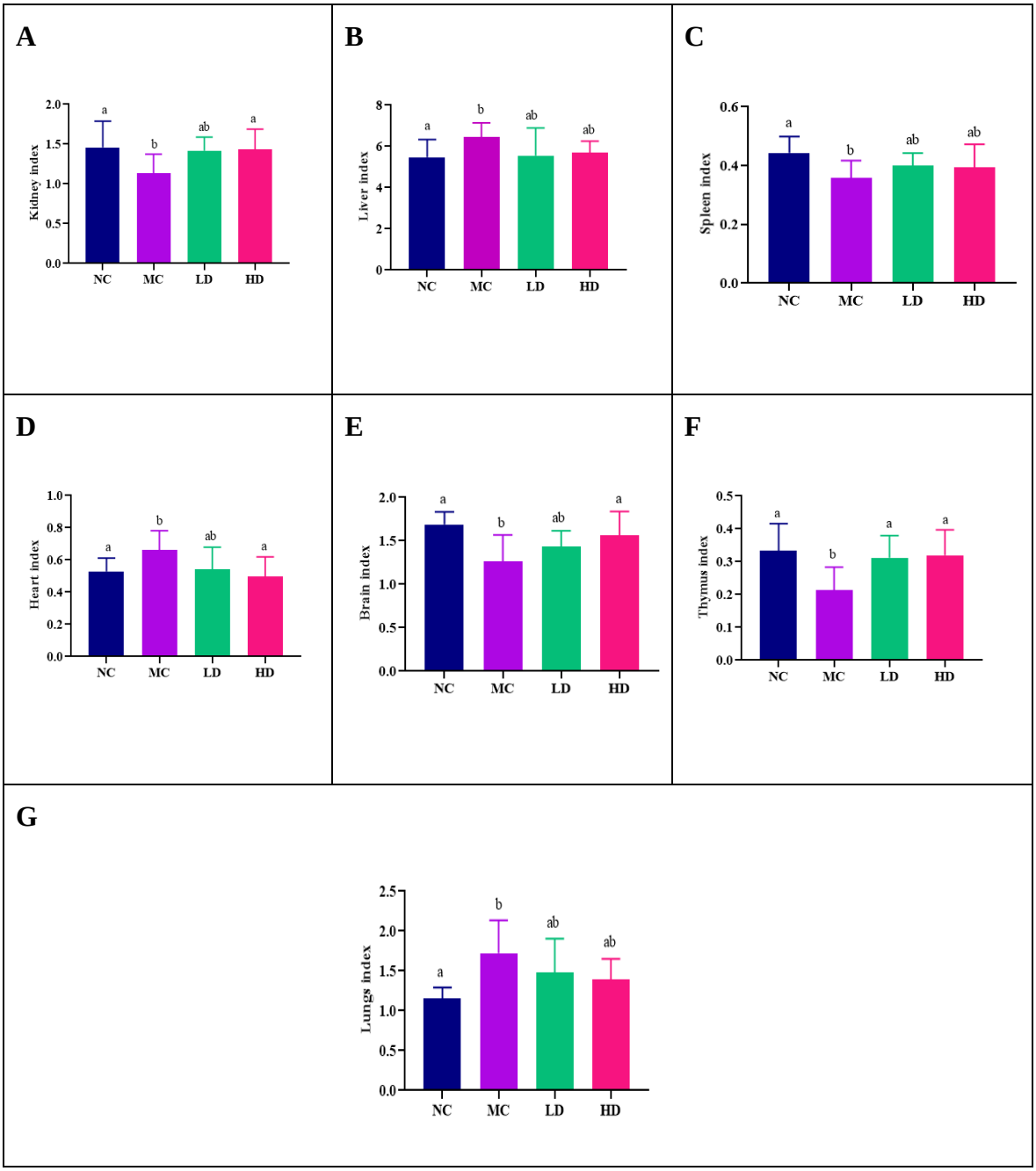

Fig. 4.52: Effect of oral administration of NCDC 400 on organ indices of immunocompromised mice. (A) Kidney index; (B) Liver index; (C) Spleen index; (D) Heart index; (E) Brain index; (F) Thymus index; (G) Lungs index. Error bars indicate the variations of eleven determinations in terms of the standard error of mean. Lowercase superscripts (a-b) represent the significant differences ($p < 0.05$) across the groups *(Analyzed by one-way ANOVA following Duncan test).*

But the extent of hypertrophy of the liver, heart, and lungs was lessened in LD and HD groups. Although not statistically significant, the trend towards normalizing the hypertrophy in NCDC 400 fed groups suggests its positive effects on health and physiology. Looking into this trend, it seems logical that a further increase in the duration of the feeding trial may result in normalizing the organ index up to a level of statistical significance.

4.4.31.3. Hematological analysis

The data apropos to the effect of NCDC 400 supplementation on hematological parameters of immunocompromised mice have been presented in **Table 4.32**. Compared to NC, the intraperitoneal Cy administration resulted in a marked decrease ($p < 0.05$) in the parameters like RBC, Hb HCT, PLT, WBC, LYM, MON, and GRAN in the MC group, suggesting that the immune system in the mice has suppressed. Although not significant when compared to NC, there was a slight decrease in MCV (42.83 ± 0.66 fL) and MCH (17.73 ± 1.10 pg) values in the MC group. However, the mice in the NCDC 400 supplemented groups (LD and HD) did not reveal any adverse changes (lowering the erythrocytes and immune cells) in the hematological parameters compared to MC suggesting its excellent safety and blood compatibility in immunocompromised mice. Compared to MC, although not significant, we found an increase in the WBC (LD: 2.03 $\times 10^9$/L and HD: 2.46$\times 10^9$/L), LYM (LD: 0.91$\times 10^9$/L and HD: 1.70$\times 10^9$/L), MON (LD: 0.18$\times 10^9$/L and HD: 0.21$\times 10^9$/L) and GRAN (LD: 0.90$\times 10^9$/L and HD: 0.63$\times 10^9$/L) counts in the LD and HD groups thereby signifying the important role of NCDC 400 in immune homeostasis and protection against immune suppression. In comparison with MC (0.13$\times 10^9$/L), the animals in LD (0.18$\times 10^9$/L) and HD (0.21$\times 10^9$/L) groups revealed an increase in the MON count, albeit not statistically significant. On the other hand, we observed a slight but not statistically significant increase in blood glucose level upon Cy treatment, suggesting that Cy or NCDC 400 may negligible influence on glucose metabolism. However, Cy has been earlier reported to induce diabetes by widespread destruction of pancreatic cells (β-cells), resulting in hyperglycaemia (Alenzi *et al*., 2010). But such effects were not severe in this study because the Cy dose and frequency of its exospores to mice to induce pancreatic toxicity may not reached to a sufficient level.

The hematopoietic system is a potential target of any toxic compounds and therefore is an excellent marker to measure the disease state of the animals. Toxic drugs like Cy act on the hematopoietic system and thereby disturb the synthesis of RBC and

WBC. WBC plays a vital role in protecting the host from invading pathogens by various innate and adaptive mechanisms. Considering the short life of WBC, a constant differentiation of hematopoietic stem cells in bone marrow is highly warranted. In contrast, Cy induces bone marrow toxicity and thereby reduces the differentiation of hematopoietic stem cells resulting in marked leukopenia and neutropenia. A similar hematopoietic depression involving the reduced blood elements like RBC, leukocytes, and platelets was observed in the MC group. In contrast, an improvement in the blood parameters in the LD and HD groups suggests an immunoprotective effect of NCDC 400 by augmenting the myeloid hematopoiesis. An improvement in the myelopoiesis in the LD and HD group can also be related to its anti-oxidant potential that would help overcome oxidative damage on the blood and other hematopoietic cells. Our results are in agreement with Gramajo Lopez *et al*. (2021), wherein oral administration of *L. rhamnosus* CRL 1505 and *L. plantarum* CRL1506 to Cy-induced immune-suppressed mice resulted in an effective and rapid improvement in the myelopoiesis in the bone marrow and which was reflected in the peripheral blood. Upon understanding the underlying mechanism, it was found that probiotics do not halt the apoptosis of bone marrow cells rather it enhances their proliferating capacity. Although not completely understood, it has been proposed that probiotics along with the beneficial gut microbiota shaped by the probiotic intervention participate in the myelopoiesis via IL-23/IL-17/G-CSF axis (Clarke *et al*., 2010). On the other hand, the MAMPs of probiotics are expected to interact with the TLR to regulate the formation of IL-17 and G-CSF that co-ordinate the granulopoiesis, which was reflected in this study by demonstrating the enhanced GRAN in the peripheral blood (**Table 4.32**). Other mechanisms have also been reported by researchers, where probiotic-derived metabolites and/ or their surface components like lipoteichoic acids are found to translocate into the systemic circulation and reach bone marrow (Clarke *et al*., 2010). This evidence provides proof that how probiotics can benefit the host by modulating bone marrow myelopoiesis and enhancing systemic innate immune function. In another study, researchers provide comprehensive information on probiotic-derived SCFA, especially, the propionate-mediated enhancement of the hematopoiesis of dendritic cells (DCs) precursors from bone marrow. The synthesized DCs exhibit an immense ability to activate Treg cells (Al-Qadami *et al*., 2022).

Table 4.32: Summary of hematological values of immunocompromised mice administrated with NCDC 400

Parameters	Unit	NC	MC	LD	HD
RBC	10^{12}/L	$8.73^{a} \pm 0.12$	$6.90^{b} \pm 0.05$	$7.39^{b} \pm 0.14$	$6.76^{b} \pm 0.25$
Hb	g/dL	$14.03^{a} \pm 0.20$	$11.83^{b} \pm 0.28$	$13.16^{b} \pm 0.37$	$12.90^{b} \pm 0.15$
HCT	%	$41.46^{a} \pm 1.4$	$29.7^{b} \pm 0.66$	$30.16^{b} \pm 0.64$	$30.3^{b} \pm 0.35$
MCV	fL	$46.46^{a} \pm 1.77$	$42.83^{a} \pm 0.66$	$41.5^{a} \pm 1.57$	$43.2^{a} \pm 0.36$
MCH	pg	$18.46^{a} \pm 0.31$	$17.73^{a} \pm 1.10$	$17.06^{a} \pm 0.61$	$17.5^{a} \pm 0.28$
PLT	10^{9}/L	$597.33^{a} \pm 8.22$	$234.00^{b} \pm 15.50$	$278.33^{b} \pm 11.83$	$250.00^{b} \pm 10.56$
PCT	%	$0.35^{a} \pm 0.02$	$0.33^{a} \pm 0.01$	$0.32^{a} \pm 0.011$	$0.37^{a} \pm 0.04$
WBC	10^{9}/L	$7.13^{a} \pm 0.28$	$1.36^{b} \pm 0.31$	$2.03^{b} \pm 0.47$	$2.46^{b} \pm 0.20$
LYM	10^{9}/L	$3.66^{a} \pm 0.13$	$0.43^{b} \pm 0.03$	$0.91^{b} \pm 0.26$	$1.70^{c} \pm 0.32$
MON	10^{9}/L	$0.43^{a} \pm 0.03$	$0.13^{b} \pm 0.03$	$0.18^{b} \pm 0.03$	$0.21^{b} \pm 0.10$
GRAN	10^{9}/L	$3.2^{a} \pm 0.30$	$0.73^{b} \pm 0.14$	$0.90^{b} \pm 0.25$	$0.63^{b} \pm 0.31$
Glucose	mg/ dL	$93.66^{a} \pm 2.20$	$95.00^{a} \pm 2.85$	$98.44^{a} \pm 2.75$	$95.11^{a} \pm 2.65$

Note: Values are presented as the mean ± SEM. Lowercase superscripts (a-b) represent the significant differences ($p < 0.05$) across the groups *(Analyzed by one-way ANOVA following Duncan test).*

4.4.30.4. Serum biochemistry analysis

A significant reduction ($p < 0.05$) in the liver functioning markers of immunocompromised was noticed after NCDC 400 supplementation at low and high doses (**Table 4.33**). Compared to the CON group, the level of serum ALT elevated significantly ($p < 0.05$) after Cy administration (MC: 111.16 ± 2.53 Unit/L) but reduced after NCDC 400 administration at low (LD: 88.46 ± 4.54 Unit/L) and high dose (HD: 80.89 ± 1.53 Unit/L). A similar considerable ($p < 0.05$) reduction in the AST concentration was also observed in the LD (92.53 ± 1.74 Unit/L) and HD (90.53 ± 4.03 Unit/L) group compared to the MC group (116.90 ± 7.46 Unit/L). In this study, an increase in the serum ALT and

AST levels after Cy intervention and its lowering effect upon NCDC 400 gavaging can also be correlated to an increase in the liver index in the MC group with a substantial decrease in the liver index parameter in LD and HD groups. Liver injury is one of the most common effects of Cy on the host. Therefore, elevation in the serum ALT and AST levels are considered valid markers to appraise liver function. These results are consistent with the previous findings of Zhang *et al*. (2022), who also evidenced a significant reduction in the ALT and AST levels after supplementation of *L. plantarum* Lp2 to the Cy-treated mice. The researchers proposed that the anti-oxidative and immunomodulatory properties of Lp2 could be a strong reason behind its ameliorative effects on Cy-induced liver damage. Among kidney functioning tests, there was a reduction in serum urea level in LD (52.66 ± 1.45 mg/dL) group compared to the animals in MC (67.00 ± 1.52 mg/dL). But no significant reduction in the Cy-induced serum creatinine elevation was observed in either LD (0.50 ± 0.10 mg/dL) or HD (0.41 ± 0.06 mg/dL) groups compared to MC (0.90 ± 0.03 mg/dL). Our results in this regard are in close alignment with Sengul *et al*. (2019), who also observed that oral probiotic supplementation (a consortium of *L. rhamnosus, L. fermentum,* and *L. brevis*) can alleviate the Cy-induced increase in the serum urea but not creatinine in rats. The authors interpreted that the immunomodulatory and anti-oxidative properties of these cultures might have halted the cellular oxidative damage in the kidney. In comparison with MC (755.00 ± 6.92 Unit/L), NCDC 400 supplementation at a high dose (693.00 ± 3.51 Unit/L) significantly ($p < 0.05$) reduced the serum LDH level. However, a similar effect was not seen in the LD group suggesting that a low dose may not be effective in curbing the Cy-induced toxicity in mice. This suggests the anti-toxic/ protective effects of NCDC 400 at relatively higher doses. These results are similar to Wang *et al*. (2019), who reported that LAB-based probiotic intervention reduced the Cy exacerbated serum LDH levels in the piglet model.

The level of serum proteins improved significantly ($p < 0.05$) in the LD (6.22 ± 0.03 g/dL) and HD (6.18 ± 0.09 g/dL) groups compared to the MC group (4.99 ± 0.44 g/dL), approaching that of NC group (7.45 ± 0.16 g/dL). The decrease in the total serum protein in the MC group can be correlated to the lowered feed intake as well as the suppressed immune system. In a similar way, an elevation in serum protein after NCDC 400 intervention may be linked with a concomitant increase in feed intake in LD and HD groups. The serum proteins are vital to ascertain clinical and biochemical indicators in pre-

clinical studies. Serum proteins are the indirect markers to assess the immune status of the host as the decrease in serum proteins has a direct positive correlation with the suppressed immune system (Zhang *et al*., 2021). These results are similar to the findings of Lv *et al*. (2020), who also reported a significant decline in the serum total protein content upon Cy intervention but improved significantly upon probiotic treatment. On the other hand, we observed no obvious changes in serum calcium and phosphorus levels across all groups. In fact, Cy administration had a negligible effect on the serum calcium and phosphorus levels of mice.

With regard to the serum lipid profile, oral supplementation of NCDC 400 to Cy-treated mice at low (LD: 98.66 ± 1.22 mg/dL) and high doses (HD: 96.59 ± 3.05 mg/dL) curtailed the serum triglycerides level significantly ($p < 0.05$) compared to MC group (117.00 ± 3.51). Further, there was a significant ($p < 0.05$) increase in the serum cholesterol level in the MC group (202.3 ± 3.13 mg/dL) compared to the NC group (160.33 ± 8.16 mg/dL) which may be due to Cy-induced toxicity and altered liver metabolism. In response to the NCDC 400 administration, there was a considerable ($p < 0.05$) decrease in the serum total cholesterol of the animals in the LD (173.90 ± 6.99 mg/dL) and HD (183.11 ± 4.81 mg/dL) groups. Amongst the different types of cholesterol, LDL cholesterol level reduced significantly ($p < 0.05$) in the LD and HD groups compared to the MC group. Whereas, there were no significant variations in the HDL-cholesterol were noted after NCDC 400 supplementation at low (LD: 63.11 ± 2.19 mg/ dL) and high doses (HD: 62.94 ± 2.11 mg/ dL) compared to MC (66.83 ± 1.45 mg/ dL). It is well known that oxidative stress requires different lipids (e.g., triglycerides, cholesterol, and LDL-cholesterol), which are transported into cells after binding to their respective receptors. Moreover, the dysregulation in the liver metabolism during the Cy treatment leads to impaired cellular lipid metabolism. Accordingly, our are similar to the previous studies indicating a significant increase in the plasma total cholesterol, triglycerides, and LDL content of Cy-treated rats and subsequent reversal of this effect upon supplementation of some plant-based anti-oxidants (Alenzi *et al*., 2010). Overall, although NCDC 400 supplementation to immunocompromised mice reduced the atherogenic index to some extent, the values were not statistically significant. Taken together, NCDC 400 supplementation to immunocompromised mice did not induce any elevation in the toxicity markers in mice suggesting its tolerability in immunosuppressed hosts. In fact, NCDC 400

supplementation, preferably at a high dose, had ameliorated the Cy-induced systemic toxicity.

Table 4.33: Serum biochemical analysis of immunocompromised mice fed with different doses of NCDC 400

Parameters	Unit	NC	MC	LD	HD
ALT/ SGPT	Unit/ L	$50.05^{a} \pm 4.97$	$111.16^{c} \pm 2.53$	$88.46^{b} \pm 4.54$	$80.89^{b} \pm 1.53$
AST/ SGOT	Unit/ L	$54.12^{a} \pm 1.26$	$116.90^{c} \pm 7.46$	$92.53^{b} \pm 1.74$	$90.53^{b} \pm 4.03$
Urea	mg/ dL	$42.00^{a} \pm 1.52$	$67.00^{c} \pm 1.52$	$52.66^{b} \pm 1.45$	$60.16^{c} \pm 1.30$
Creatinine	mg/ dL	$0.38^{a} \pm 0.01$	$0.90^{a} \pm 0.03$	$0.50^{a} \pm 0.10$	$0.41^{a} \pm 0.06$
LDH	Unit/ L	$217.33^{a} \pm 8.35$	$755.00^{c} \pm 6.92$	$711.00^{c} \pm 10.13$	$693.00^{b} \pm 3.51$
Total protein	g/ dL	$7.45^{c} \pm 0.16$	$4.99^{a} \pm 0.44$	$6.22^{b} \pm 0.03$	$6.18^{b} \pm 0.09$
Calcium	mg/ dL	$10.87^{a} \pm 0.16$	$11.96^{a} \pm 0.55$	$10.35^{a} \pm 0.78$	$10.03^{a} \pm 0.92$
Phosphorous	mg/ dL	$13.63^{a} \pm 0.26$	$13.61^{a} \pm 0.32$	$13.53^{a} \pm 0.39$	$13.39^{a} \pm 0.46$
Triglycerides	mg/ dL	$85.15^{a} \pm 0.90$	$117.00^{c} \pm 3.51$	$98.66^{b} \pm 1.22$	$96.59^{b} \pm 3.05$
Total cholesterol	mg/ dL	$160.33^{a} \pm 8.16$	$202.3^{b} \pm 3.13$	$173.90^{a} \pm 6.99$	$183.11^{ab} \pm 4.81$
LDL-cholesterol	mg/ dL	$65.91^{b} \pm 8.12$	$112.13^{a} \pm 3.12$	$97.75^{a} \pm 6.11$	$100.85^{a} \pm 5.83$
HDL-cholesterol	mg/ dL	$75.72^{b} \pm 1.64$	$66.83^{a} \pm 1.45$	$63.11^{a} \pm 2.19$	$62.94^{a} \pm 2.11$
VLDL-cholesterol	mg/ dL	$17.03^{a} \pm 0.18$	$23.4^{c} \pm 0.70$	$19.73^{b} \pm 0.24$	$19.31^{b} \pm 0.61$
Atherogenic index	-	$0.76^{a} \pm 0.02$	$1.68^{b} \pm 0.06$	$1.55^{b} \pm 0.15$	$1.54^{b} \pm 0.07$

Note: Values are presented as the mean ± SEM. Lowercase superscripts (a-c) represent the significant differences ($p < 0.05$) across the groups *(Analyzed by one-way ANOVA following Duncan test).*

4.4.30.5. Gut health indices and short-chain fatty acids

The effect of supplementation of NCDC 400 on mouse faecal pH has been shown in **Fig. 4.53**. Compared to NC, the faecal pH increased significantly ($p \leq 0.05$) in the MC

group (7.60 ± 0.30) and returned to normal after supplementation of NCDC 400 at low (LD: 6.1 ± 0.11) and high doses (HD: 5.68 ± 0.18). These results are in accordance with the faecal lactate concentrations. The faecal lactate concentration decreased significantly ($p \leq 0.05$) in the MC (0.70 ± 0.19 μmol/g) group while increased gradually after NCDC 400 supplementation in a dose-specific manner (LD: 2.03 ± 0.16 and HD: 2.50 ±0.29 μmol/g).

On the other hand, the faecal ammonia increased considerably ($p < 0.05$) in the MC group (7.61 ± 0.26 mol/g) and decreased in the LD (3.72 ± 0.39 μmol/g) and HD (4.94 ± 0.50 μmol/g) groups significantly ($p \leq 0.05$). These results indicate that the Cy administration may shift the gut econiche toward neutral to alkaline pH conditions that support the proliferation of opportunistic pathogens. However, supplementation of NCDC 400 redirected and maintained the acidic intestinal conditions that do not support the growth of pathobionts in the gut. Ammonia is an important metabolite in the gut, majorly generally produced by pathogenic microbes during protein and urea metabolism. Ammonia is reported to demonstrate harmful effects and potential carcinogenicity on intestinal epithelial cells. The reduction in the faecal ammonia in the NCDC 400 fed groups (LD and HD) could be due to two reasons; (i) the exclusion of ammonia-producing harmful pathogens from the gut, or (ii) at the intestinal low pH conditions, gut microbes may promote the use of ammonia as the nitrogen source and thereby alleviate the intestinal ammonia level (Xie *et al*., 2016). It was reported that the intestinal lower pH is highly essential in restraining the growth of pathogens by affecting their enzymatic actions. Our results concur with the findings of Meng *et al*. (2019), who also observed a concomitant decrease in the intestinal/ faecal pH and ammonia after supplementation of probiotic *L. plantarum* KLDS1.0318 at 10^9 CFU/mouse/day for 20 days in a Cy-induced immunocompromised murine model. Another previous study has also highlighted that oral administration of a probiotic product (NCU116) containing 10^{10} CFU/g *Bifidobacterium* BB12 for nearly 20 days reduced the intestinal pH and ammonia in the Cy-treated mice (Xie *et al*., 2016). Thus, our results demonstrate that NCDC 400 intervention could be useful to maintain the gut environment healthy by suppressing ammonia and promoting lactate production.

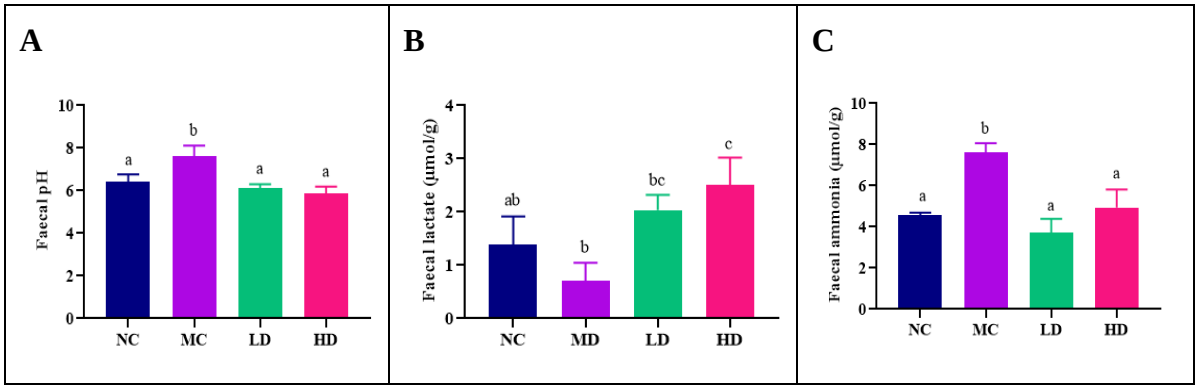

Fig. 4.53: Effect of NCDC 400 supplementation on faecal pH (A), lactate (B), and ammonia (C) in immunocompromised mice. Lowercase superscripts (a-c) represent the significant differences ($p < 0.05$) across the groups *(Analyzed by one-way ANOVA following Duncan test).*

However, it is worth mentioning that not only the lactate influence the reduction of faecal pH but also Short Chain Fatty Acids (SCFAs) play important role in maintaining reduced pH and ammonia concentrations in the gut. The effect of oral supplementation of NCDC 400 on faecal SCFA has been shown in **Fig 4.54**. Compared to NC, the concentrations of acetate (3.02 ± 0.24 µmol/ g), butyrate (0.61 ± 0.02 µmol/ g), and total SCFA (4.67 ± 0.12 µmol/ g) concentrations decreased significantly ($p \leq 0.05$) in the MC group. However, the oral intervention of NCDC 400 at low and high doses (LD and HD) showed a significant ($p \leq 0.05$) increase in the acetate, butyrate, and total SCFAs concentrations while the level of propionate improved considerably ($p \leq 0.05$) in the HD group. On the other hand, the total SCFAs content decreased markedly ($p \leq 0.05$) in the MC group but increased significantly ($p \leq 0.05$) upon supplementation of NCDC 400 (LD: 12.25 ± 0.89 and HD: 20.44 ± 2.46 µmol/g) in a dose-specific manner. Increased faecal SCFAs could also explain why the faecal pH decreased upon NCDC 400 supplementation in LD and HD groups. These results are in close alignment with the previous observation wherein *L. plantarum* KLDS1.0318 administration to Cy-induced immunocompromised mice model resulted in an improvement in the feacal SCFA *viz*. acetic acid, propionic acid, butyric acid, and valeric acid (Meng *et al*., 2019). The increase total SCFAs upon NCDC 400 supplementation to immunocompromised mice could be attributed to the saccharolytic fermentation of complex carbohydrates either solely by the test bacterium or the gut microbiota that has fostered upon NCDC 400 intervention. SCFAs are reported to interact with free fatty acid receptors (FFARs) in the gut and thereby maintain intestinal epithelial integrity, mucus secretion, and mucosal immunity to protect against intestinal-related diseases (Xie *et al*., 2016).

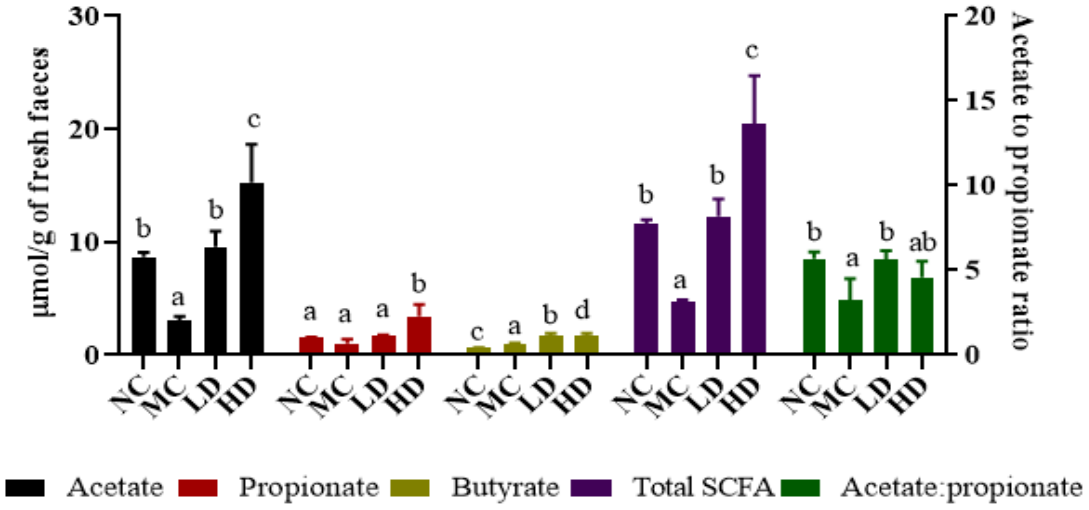

Fig. 4.54: Effect of oral NCDC 400 supplementation on faecal SCFAs in immunocompromised mice. Lowercase superscripts (a-c) represent the significant differences ($p < 0.05$) across the groups *(Analyzed by one-way ANOVA following Duncan test).*

4.4.30.6. Caecal harmful enzymes

In comparison with the NC group, the activities of caecal beta-glucosidase (16.23 ± 0.88 Unit/ g) and beta-glucuronidase (14.15 ± 0.82 Unit/ g) increased significantly ($p \leq 0.05$) in the MC group probably because of the susceptibility of immune-suppressed mice to resist the intestinal colonization of pathogens that produce harmful enzymes. In contrast, there was a considerable ($p \leq 0.05$) reduction in the beta-glucosidase and beta-glucuronidase activities in the caecal samples of the LD and HD groups (**Fig. 4.55**). This suggests that NCDC 400 administration may induce suitable physicochemical conditions by reducing the faecal beta-glucosidase and beta-glucuronidase activity because of anti-colonization ability against the gut pathobionts. Our results agreed with the findings of Shokryazdan *et al.* (2016), wherein the oral gavaging of *L. fermentum* HM3 and *L. buchneri* FD2 individually or their consortium at 10^{10} CFU/kg BW/day for 14-day and 28-day significantly ($p \leq 0.05$) reduced the caecal beta-glucosidase and beta-glucuronidase activities. Similarly, Chaiongkarn *et al.* (2019) have also observed a marked reduction in the β-glucuronidase activity in rat feces fed with probiotic *L. fermentum* TISTR 2514 and *P. acidilactici* TISTR 2612 at 9 $\log_{10}$ CFU/ mL for 8 weeks along with prebiotics (manno-oligosaccharides and rice syrup-oligosaccharides).

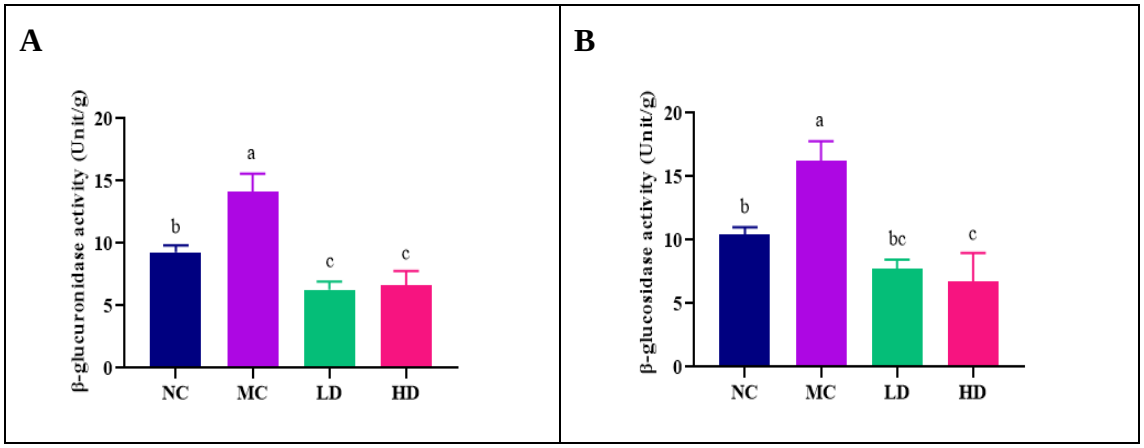

Fig. 4.55: Effect of oral supplementation of NCDC 400 on caecal beta-glucuronidase (A) and beta-glucosidase (B) in immunocompromised mice model. Lowercase superscripts (a-c) represent the significant differences ($p < 0.05$) across the groups *(Analyzed by one-way ANOVA following Duncan test).*

4.4.30.7. Histopathological analysis

The histopathological examination of spleen tissue showed that the NC groups had white pulp and red pulp. The white pulp consisted of lymphoid aggregation and the surrounding area made up of vascular tissue formed the red pulp. The white pulp showed the germinal center and the central blood vessel whereas the red pulp consisted of sinusoids, RBCs, occasional megakaryocytes, and other blood cells. Examination of spleen derived from the MC group revealed moderate to severe atrophy of the white pulp (comprising of periarteriolar lymphatic sheath (PALS), marginal zone, and the follicles). There was a mild to moderate level of increased extramedullary hematopoiesis (EMH) with a predominant increase in megakaryocytes (platelet precursors). Megakaryocytes were observed as large cells with a single lobulated nucleus. A mild to moderate accumulation of yellowish-brown granular pigment within the macrophages was observed in the red pulp (**Fig. 4.56**). To confirm the nature of yellowish brown granular pigment within the macrophages, the spleen from all the groups were subjected to Pearl's Prussian blue staining. Based on the positive staining, the pigment was identified as hemosiderin where the iron pigment appeared as Prussian blue color against the pink background (**Fig. 4.57**). However, the oral gavage administration of *L. fermentum* NCDC 400 to immunocompromised mice at 10^8 CFU/day (LD) and 10^{10} CFU/day (HD) for 15 days resulted in the reversal of histopathological changes observed in immunocompromised mice such as atrophy of white pulp, increased extramedullary hematopoiesis and increased accumulation of hemosiderin in macrophages on

microscopic examination of the spleen. As compared to the MC group, the morphology of spleens from LD and HD groups had returned to normalcy which was similar or comparable to that of the NC groups.

No considerable variations were recorded in the intestinal histology across all four groups (**Fig. 4.58**). Cy administration (MC group) did not alter the epithelial architecture and cellular arrangement of small and large intestinal tissues. The jejunum was examined as a representative part of the small intestine, which revealed mucosa, submucosa, muscularis, and serosa layers. The mucosa was lined by simple columnar epithelium evaginating into tall cylindrical villi with lamina propria as the core and crypts at their base. Submucosa showed loose fibrous connective tissue with blood vessels and the muscularis had 2 layers of muscular lining, the inner circular and the outer longitudinal. The outer layer was surrounded by thin serosa. The colon was examined as a representative part of the large intestine, where the layers were similar to that of the small intestine. Unlike the small intestine, there were mucosal folds in the colon over which the villi were present. Numerous goblet cells were seen in the epithelial lining of the villi and the crypts. The muscularis layers were thick as compared to the small intestine.

On examination of the kidney, the cortex, medulla, and papillary regions were noticed. The microscopic picture revealed glomerus with Bowman's capsule, proximal and convoluted tubules lined by simple cuboidal epithelium, and collecting ducts. Occasionally the blood vessels were also noticed. However tubular unilateral basophilia minimal (blue coloration of kidney tube) was observed in the MC and LD groups but the same was not witnessed in the HD group suggesting the protective effect of NCDC 400 at the high dose on kidney morphology as well as its functioning. The parenchyma of the liver showed cords of hepatocytes surrounding the central vein radiating towards the portal area. The portal area consisted of the portal vein, portal artery, and bile ducts. Between the hepatic cords, the sinusoidal spaces were lined by endothelial cells and occasional kupffer cells. However, the vacuolation of hepatocyte minimal was noticed in the MC group but not in LD and HD groups (**Table 4.34**). These manifestations suggest that NCDC 400 may have a hepato-protective effect. Overall, the histopathology results may be correlated with the clinical findings, hematology, serum biochemistry, organ indices, and other relevant data of the study.

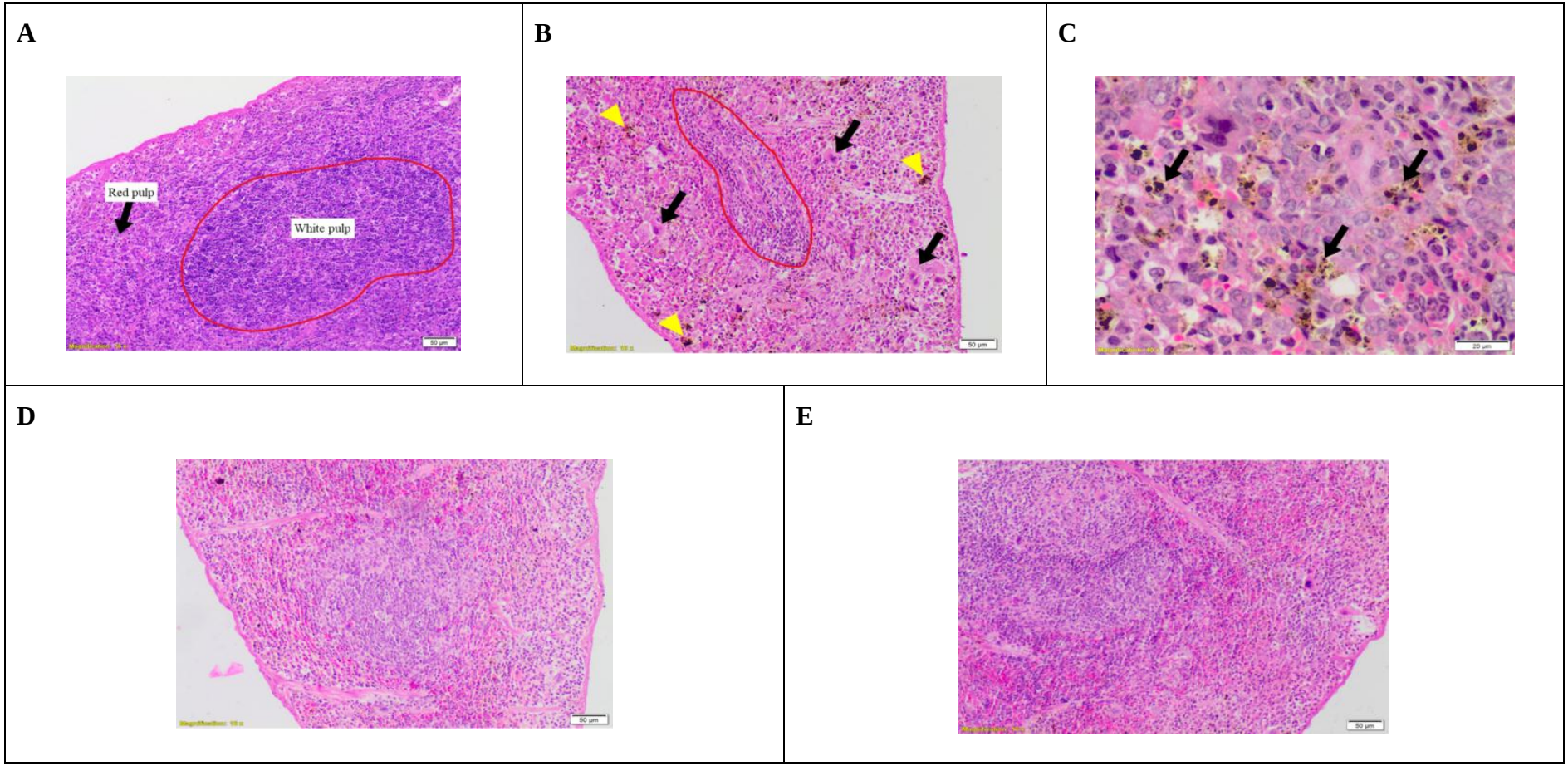

Fig. 4.56: Microscopic views of spleen tissue of different experimental groups stained with H and E. (A) NC; (B) MC (100 X) ; (C) MC (400 X) (D) LD; (E) HD. Red marks indicate atrophy of the white pulp; Black indicates EMH, predominantly megakaryocyte; Yellow heads show increased pigmentation.

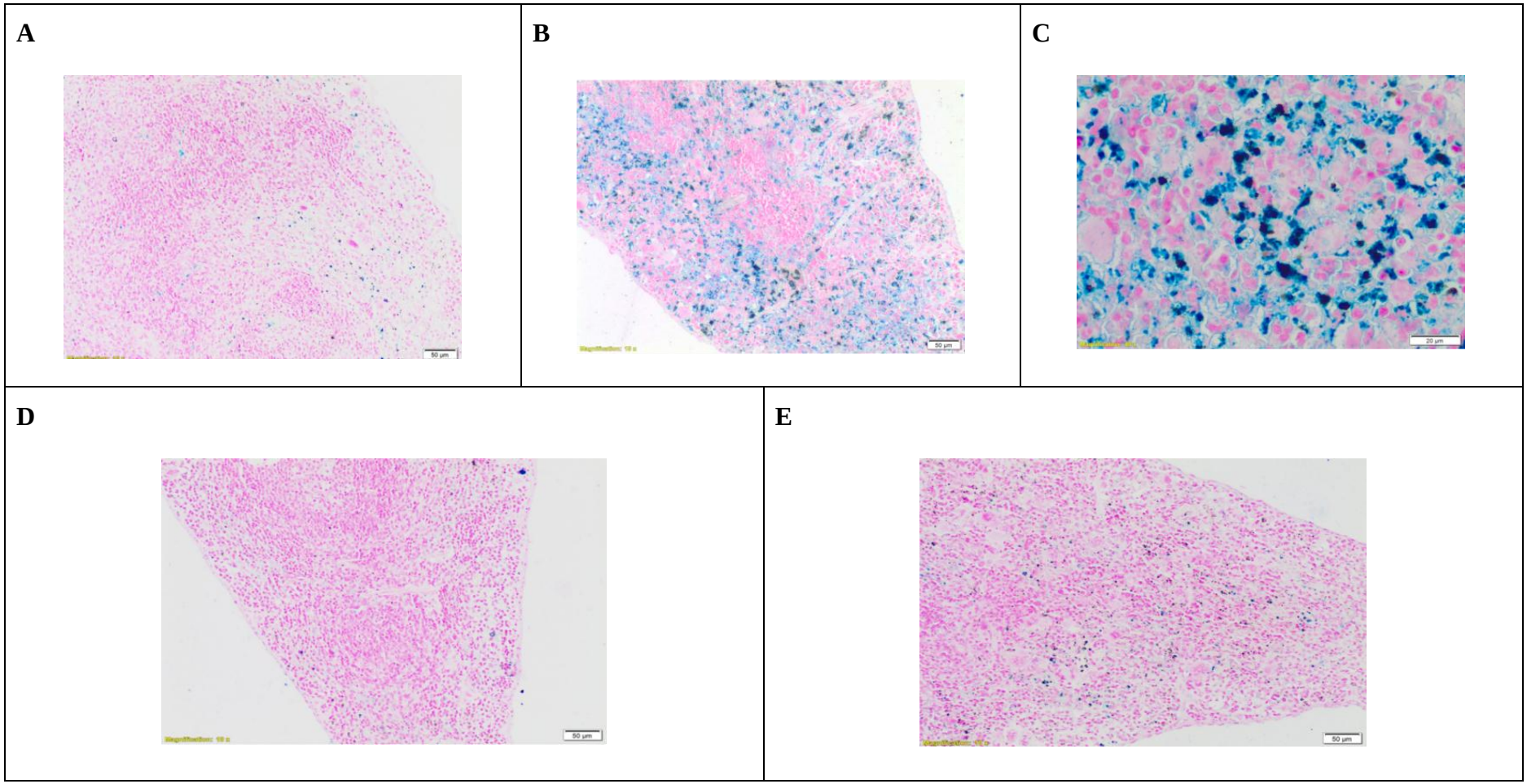

Fig. 4.57: Microscopic views of spleen tissue of different experimental groups stained with Pearl's Prussian blue. (A) NC; (B) MC (100 X); (C) MC (400 X) (D) LD; (E) HD.

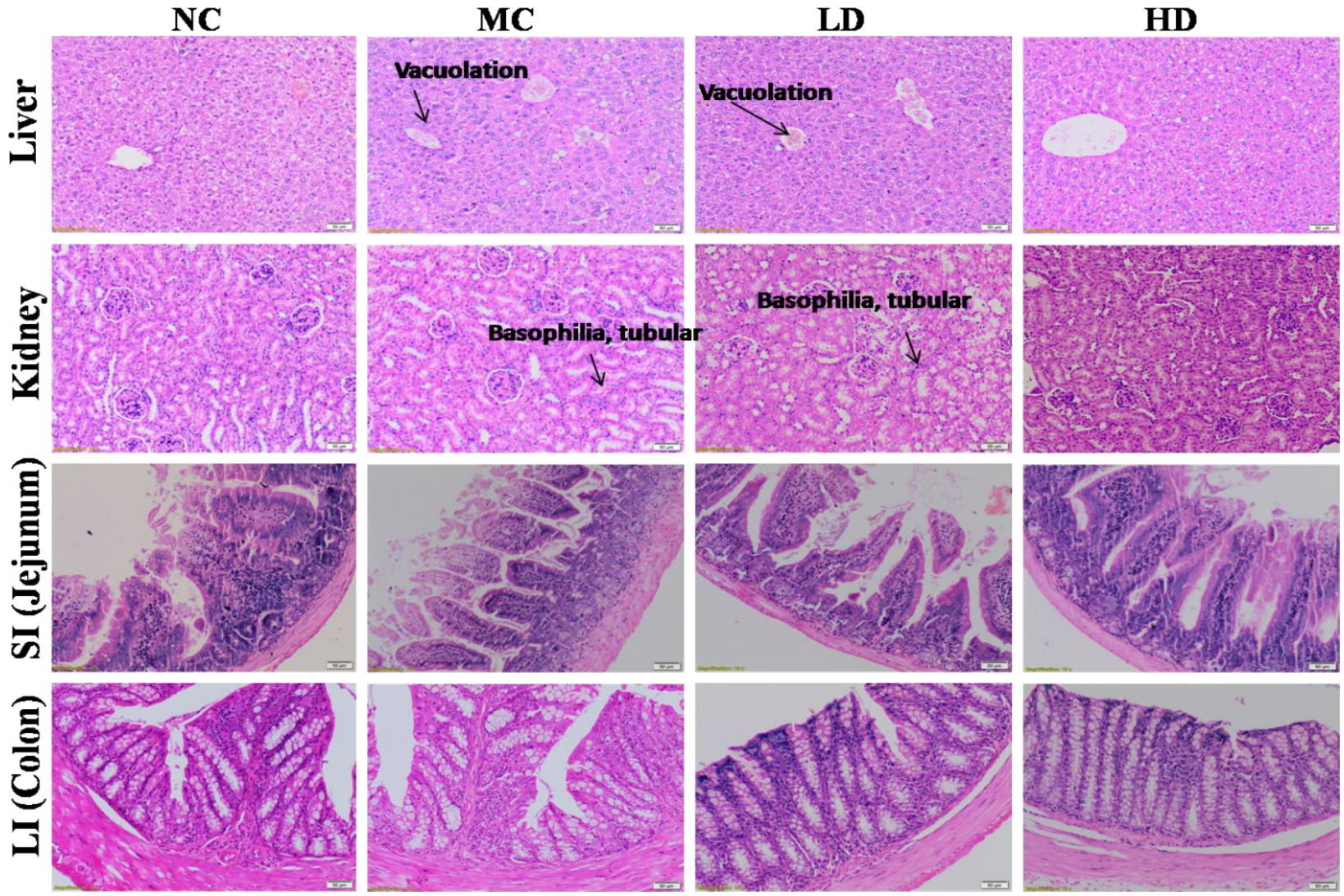

Fig. 4.58: Photomicrographs (100 X) of various experimental groups stained with H and E

Our results in this regard are in close alignment with Lv *et al*. (2021), who observed hemosiderin deposition in the spleen of mice treated with Cy, but lowered tremendously in the CBLEB probiotic (*Bifidobacterium*, *Lactobacillus*, and *Bacillus*) fed group. Similarly, normalization of tissue morphology of the liver was also witnessed upon oral administration of CBLEB probiotics to Cy-treated rats.

Table 4.34: Summary of histopathological findings of safety assessment of *L. fermentum* NCDC 400 in immunocompromised mice model

Group		**NC**	**MC**	**LD**	**HD**
No. of mice examined/group		3	3	3	3
Dose (CFU/mice/day)		0	0	10^8	10^{10}
Organs / Lesions	**Mode of Death**	**TS**	**TS**	**TS**	**TS**
Small intestine (Jejunum)		N	N	N	N
Large intestine (Colon)		N	N	N	N
Spleen		N	L	N	L
a. Increased Extramedullary hematopoiesis, minimal		-	-	-	1
mild		-	3	-	-
moderate		-	2	-	-
b. Pigment, Increased mild		-	3	-	-
moderate		-	2	-	-
c. Atrophy, white pulp moderate		-	3	-	-
severe		-	1	-	-
Kidney		N	L	L	N
Basophilia, tubular, Unilateral, minimal		-	1	1	-
Liver		N	L	N	N
Vacuolation, hepatocyte, minimal		-	1	-	-

4.4.30.8. Gut barrier integrity and bacterial translocation assay

Bacterial translocation to extra-intestinal organs is considered detrimental to the survivability of the host because of sepsis. Hence, the effect of NCDC 400 on the gut mucosa was conducted by translocation assay as well as by conducting a detailed microscopic examination of intestinal tissues. The blood collected from the experimental animals of all groups was sterile, suggesting the absence of NCDC 400-mediated sepsis or bacteremia. In line with this observation, the values of LD and HD groups for the blood Procalcitonin Test, a test whose values rise during bacterial translocation/ sepsis, were also comparable with the NC values. This further validates the absence of any bacteria in the systemic circulation (blood). Similarly, no bacterial colonies were observed after the plating of heart tissue homogenate. However, the plating of other organs like the liver, spleen, lungs, and kidney resulted in the formation of relatively a limited number of colonies on the MRS agar (**Table 4.35)**. However, their genotypic identification using the colony PCR approach revealed no amplified bands specific to *L. fermentum* (**Fig. 4.59**). Since species-specific PCR confirmed the absence of *L. fermentum* molecular identity, we therefore did not further perform RAPD-based characterization of those isolates for strain-level discrimination. Overall, the percentage incidence of NCDC 400 translocation was calculated to be zero (**Table 4.35**). Nevertheless, the incidence of other bacterial translocation to visceral tissues but their absence in blood indicates the cross-contamination during animal dissection, handling, and processing. Given the fact that every organ contains its own microflora, the obtained bacterial colonies on the MRS agar could be considered indigenous microbes of the mice.

In analogy with these observations, a detailed microscopic examination of the small intestine (jejunum) and large intestinal (colon) tissues of all experimental groups showed no signs of distortion in epithelial architecture, inflammation, necrosis, and local toxicity. The morphology of villi was normal and there were no remarkable changes in the arrangement of epithelial cells. There were no signs of enterocyte breach in the epithelial lining of the mucosa. No incidences of neutrophil or mononuclear cell infiltration were recorded across all the groups. Furthermore, the underlying connective tissues of the mucosa demonstrated no distortion in the submucosa, muscularis, and serosa suggesting no evidence of test bacterial leaching into the bloodstream via the gastrointestinal route.

Table 4.35: The incidence of NCDC 400 translocation during 15 days exposure to immunocompromised mice

Sample	NC	MC	LD	HD	No. of colonies used for PCR from LD	No. of colonies used for PCR from HD	No. of confirmed colonies by PCR	% Translocation
	Colonies on MRS agar				Colonies used for PCR approach			
Blood	Nil/3	Nil/3	Nil/3	Nil/3	-	-	0	0
Heart	Nil/3	Nil/3	Nil/3	Nil/3	-	-	0	0
Liver	12/3	29/3	8/3	15/3	8	10	0	0
Kidney	Nil	4/3	Nil	Nil	-	-	0	0
Spleen	17 /3	20/3	6/3	10/3	6	10	0	0
Lungs	Nil /3	11 /3	Nil/3	12/3	-	10	0	0

Note: Values of colonies on MRS agar are presented as the sum of the total number of colonies on MRS agar from each organ (n=3) / total number of animals tested per group.

These results, therefore, indicate that NCDC 400 does not exhibit local toxicity and mucosal damage at its primary adhesion site. Our results are in agreement with Meleh *et al*. (2020) wherein after acute exposure to *L. reuteri* 29B (1×10^{10} CFU/mouse/day), the researchers found few colonies of indigenous microflora in different organs of mice but none of them have matched the molecular identity of test probiotic strain (*L. reuteri* 29B). On the contrary, Pradhan *et al*. (2019b), found the mediated bacterial translocation of *L. plantarum* MTCC 5690 and *L. fermentum* MTCC 5689 to extra-intestinal organs while assessing their safety in the colitis mice model. This could be because of the extensive damage of intestinal morphology in the DSS/TNBS-induced colitis mice model which was unseen in Cy-induced immunocompromised mice.

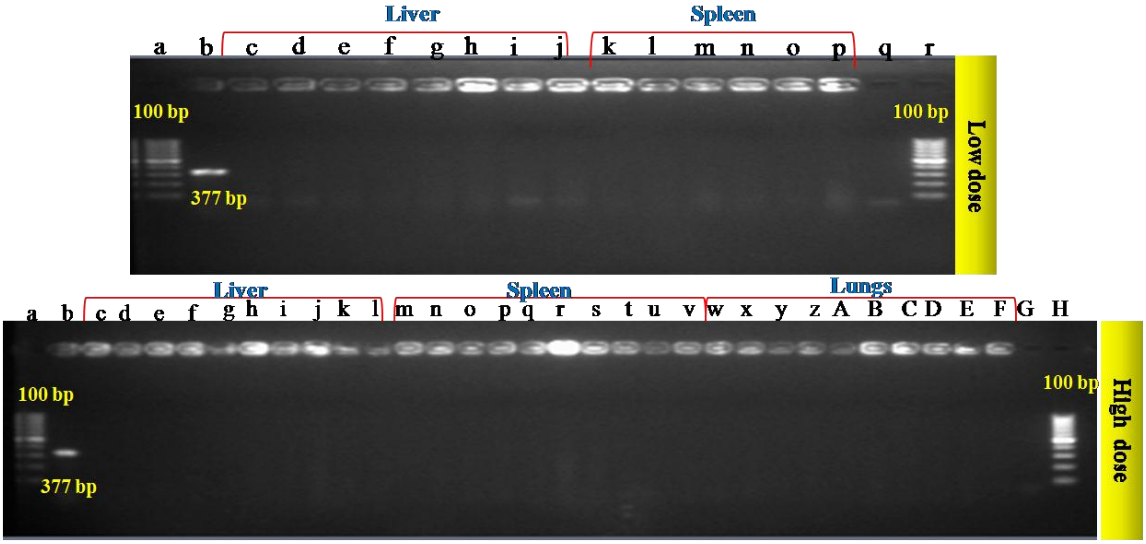

Fig. 4.59: Gel image displaying the absence of *L. fermentum* isolates cultured from mice tissues of LD and HD groups. a, r, H: 100 bp DNA ladder; b: Positive control (NCDC 400); q, G: Non-template control.

4.4.30.9. Splenocyte proliferation assay

Splenocyte proliferation in response to corresponding mitogens is most commonly determined while determining the efficacy of immunomodulatory agents. The proliferation of spleen cells in response to with and without LPS or ConA treatment is presented in **Fig**. **4.60.** In this study, ConA and LPS are used as stimulants to induce T cell and B cell proliferation, respectively. We observed no significant changes in the splenocyte proliferation without T or B cell stimulation. Regardless of the stimulant, the proliferation of spleen cells decreased significantly ($p \leq 0.05$) in the MC group (ConA: 1.06 ± 0.13; LPS: 0.63 ± 0.08). However, it is worth mentioning that the capability of splenocytes isolated from NCDC 400 fed groups (LD and HD) to proliferate in response

to LPS and ConA stimulation was restored compared to the MC group. Although not statistically significant, we noticed an increase in the spleen cells proliferation in the LD (1.84±0.12) and HD (1.72±0.48) groups upon stimulation with ConA stimulation. Similarly, there was an increasing trend in the spleen cell proliferation index in the LD (1.51±0.37) and HD (1.23±0.09) groups after LPS stimulation. These results indicate that NCDC 400 can recover the splenocyte proliferation in response to both T and B lymphocytes in immunocompromised mice. Hence, this strain could augment humoral as well as cell-mediated immunity, and thereby it may exhibit potential immune-related activity. These results are constant with the findings of Park and Lee (2018), who also found that 2 weeks of repeated dose oral administration of *Weissella cibaria* JW15 at 10^8-10^9 cells to Cy-induced immunocompromised mice would enhance splenocytes proliferation after LPS and ConA stimulation for 72 h. Our results are in agreement with Meng *et al*. (2018), who also evidenced that *L. plantarum* KLDS1.0318 (10^9 CFU/mL/day) feeding for 20 days to immunocompromised mice increases T-cell specific spleen lymphocyte proliferation.

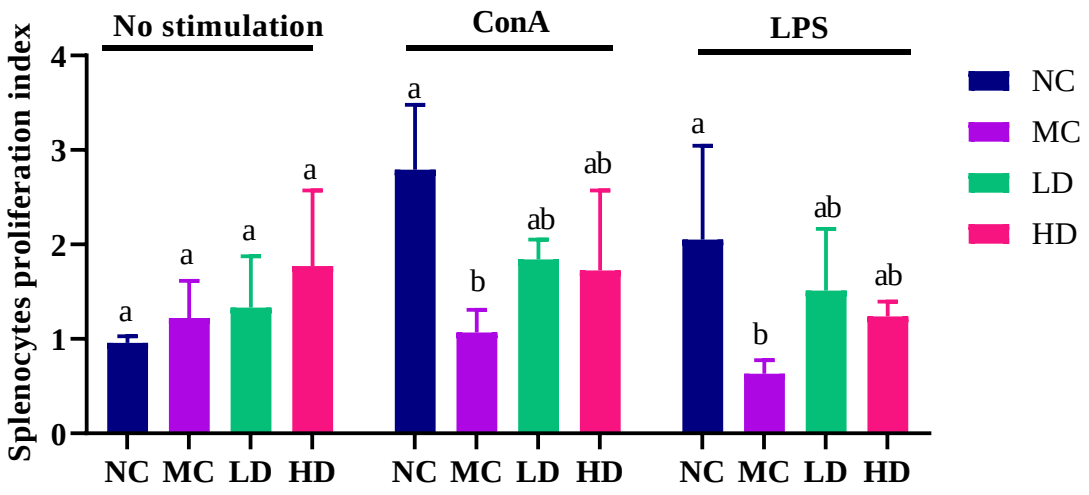

Fig. 4.60: Effects of NCDC 400 on the proliferation of splenocytes in immunocompromised mice. Lowercase superscripts (a-b) represent the significant differences ($p < 0.05$) across the groups *(Analyzed by one-way ANOVA following Duncan test).*

4.4.30.10. Immune markers in serum

The levels of serum IgA and IgG were assayed across all groups to determine the effect of NCDC 400 on the humoral immunity of Cy-treated mice (**Fig. 4.61**). Compared to the NC group, the MC showed a significant ($p \leq 0.05$) decline in the serum IgA

(0.19±0.02 µg/mg) and IgG (1.75±0.36 µg/mg) levels suggesting Cy-mediated immune suppression. However, interventions with NCDC 400 in low (LD) and high doses (HD) resulted in an elevation in the IgA and IgG levels of mice significantly ($p \leq 0.05$), thereby approaching the values of NC. Hence, these results suggest that NCDC 400 supplementation could help in the quick restoration of the IgA and IgG levels in immunocompromised mice. Humoral immunity, which is mediated by B lymphocytes, plays a significant role in the defense mechanism of the body against various infections/ antigens. Immunoglobulins are the protein response molecules produced after successful maturation (proliferation and differentiation) of B cells in response to a specific antigen. Amongst, IgG is the most plentiful antibody present in sera. This plays a significant role in the phagocytosis of macrophages. On the other side, serum IgA has been reported to trigger the effector protein that removes exogenous microorganisms (Zhang *et al*., 2021). NCDC 400 administration resulted in significant improvement in these antibodies compared to the MC group. These results inferred that NCDC 400 can augment the humoral immune response by enhancing immunoglobulin production through sustaining immune homeostasis (reversing the immune disorder). Similar results were also obtained by Choi *et al*. (2018), wherein oral *L. plantarum* nF1 (4×10^{10} CFU/kg BW) supplementation for 15 days to Cy-treated immunocompromised mice demonstrated an elevation in serum immunoglobulin level.

Furthermore, the levels of IL-6, TNF-alpha, TGF-beta, IL-10, MCP-1, and NO were determined in serum to further investigate the immunomodulatory capability of NCDC 400. In this regard, the MC group showed a significant ($p \leq 0.05$) decrease in the serum IL-6 (0.73 ± 0.02 pg/mg) and TNF-α (0.94 ± 0.02 pg/mg) levels when compared to the NC group. In contrast, oral gavage administration of NCDC 400 resulted in an increase in the serum IL-6 and TNF-α concentration in the LD and HD groups, but the values were not statistically significant. Likewise, serum IL-10 level decreased markedly in the MC group (1.96 ± 0.17 pg/mg) but increased significantly ($p \leq 0.05$) (approaching towards the values of NC group) in the LD (2.96 ± 0.21 pg/mg) and HD (2.69 ± 0.12 pg/mg) groups. This suggests the immunomodulatory activity of NCDC 400 in the *in vivo* system. On the other hand, although NCDC 400 supplementation showed an increasing trend in the TGF-beta in LD (1.73 ± 0.13 pg/mg) and HD (1.81± 0.23 pg/mg) groups, the values were found insignificant when compared to the MC group (1.56 ± 0.20 pg/mg).

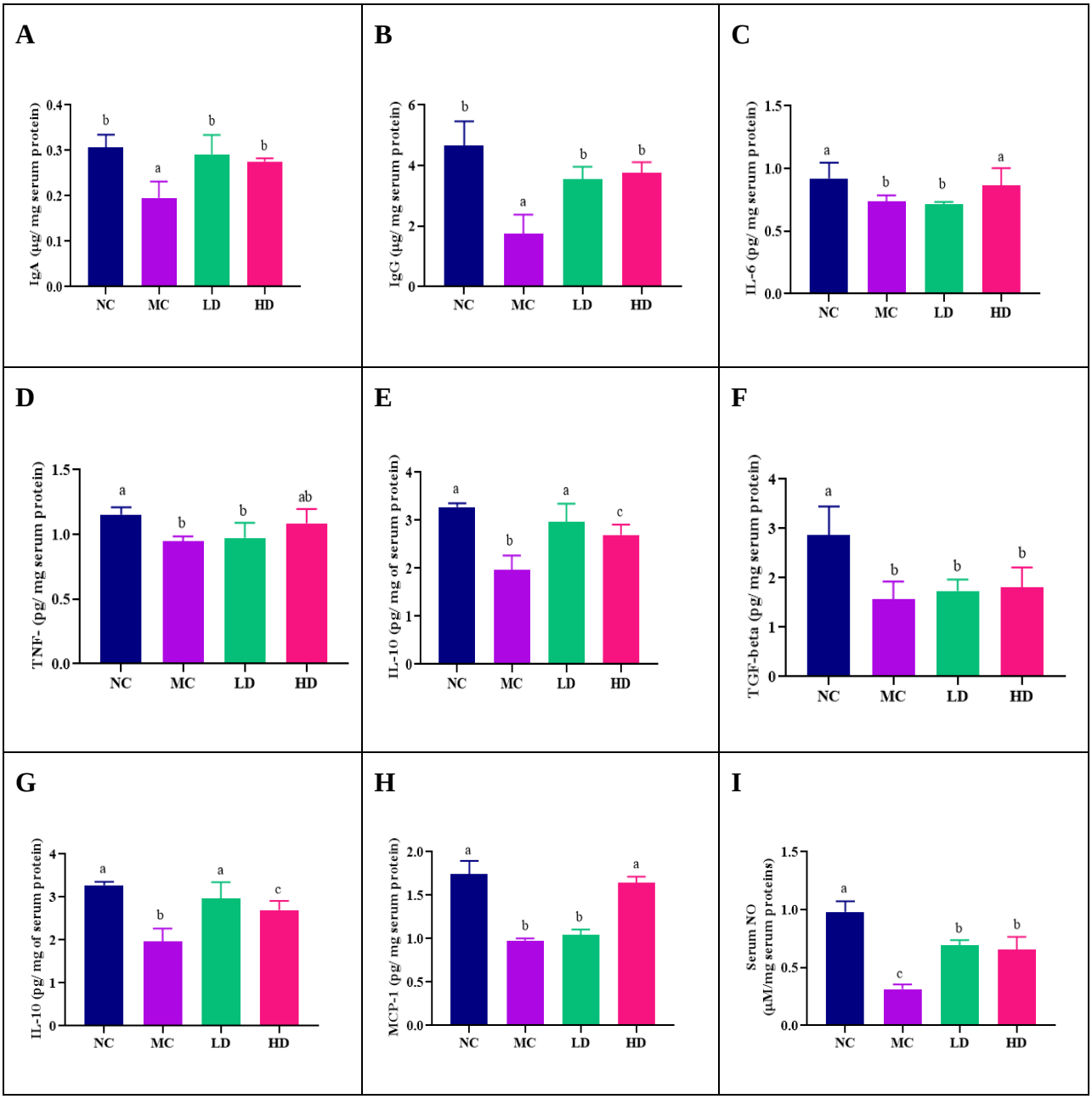

Fig. 4.61: Effects of NCDC 400 on serum immunoglobulins, cytokines, chemokine, and NO release in immunocompromised mice. (A) IgA; (B) IgG; (C) IL-6; (D) TNF-alpha; (E) IL-10; (F) TGF-beta; (G) IL-10; (H) MCP-1; (I) NO release. Lowercase superscripts (a-c) represent the significant differences ($p < 0.05$) across the groups *(Analyzed by one-way ANOVA following Duncan test).*

Cy-administration to mice (MC group) resulted in decrease in the serum MCP-1 (0.97 ± 0.01 pg/mg), which is in agreement with a corresponding reduction in the monocyte concentration in the blood samples of the MC group. Interestingly, NCDC 400 supplementation enhanced the serum MCP-1 levels considerably ($p \leq 0.05$) in the HD (1.64 ± 0.04 pg/mg) but not in the LD (1.04 ± 0.03 pg/mg) group. This suggests that a

high dose of NCDC 400 (10^{10} CFU/mice/day) may be more effective in enhancing the immune response of the host. The serum NO level also decreased noticeably ($p \leq 0.05$) in response to the Cy administration to mice (MC: 0.31± 0.02 μM/mg). However, NCDC 400 administration resulted in a significant ($p \leq 0.05$) increase in the serum NO level in a dose-dependent manner (LD: 0.69 ± 0.02 μM/mg and HD: 0.65 ± 0.06 μM/mg). Overall, these results conclusively suggest that NCDC 400 administration could improve the immune responses by enhancing the secretion of cytokines, chemokine, and NO in the systemic circulation of immunocompromised mice. Our results pertaining to serum cytokine response as well as NO level after NCDC 400 supplementation are in agreement with earlier works suggesting an elevation in IL-10, TGF-beta, IL-6, TNF-alpha, MCP-1, and NO levels after oral supplementation of different potential probiotic strains to Cy-induced immune-suppressed mice in a dose-strain-duration specific manner (Lin *et al*., 2008; Meng *et al*., 2018; Gao *et al*., 2021; Kim *et al*., 2022).

4.4.30.11. Serum oxidative markers

In comparison with the NC group, the level of serum SOD, CAT and GpX2 decreased significantly ($p < 0.05$) in the MC group due to their destruction during the oxidative stress (free radicals, reactive oxygen species, superoxide molecules) induced by Cy administration (**Fig. 4.62)**. However, the concentrations of serum GpX2 increased significantly ($p \leq 0.05$) in the LD and HD groups while the level of SOD increased significantly ($p \leq 0.05$) only in the HD group. Although not statistically significant, the NCDC 400 supplementation in the low (LD group) and high doses (HD group) increased the serum CAT level compared to the MC group. This is an indication of an excellent anti-oxidant ability of NCDC 400 as a whole or its EPS molecule, which was even proved in previous studies conducted in our lab (data unpublished). An excellent anti-oxidant activity of NCDC 400 may be correlated to the free radicals scavenging ability of NCDC 400 that would otherwise involve the oxidative damage of enzymes and other biological membranes. SOD involves in dismutation of superoxide ($O_2^{\bullet-}$) to hydrogen peroxide H_2O_2. Catalase is another important anti-oxidant heme enzyme that converts reactive oxygen species like hydrogen peroxide to water and oxygen and thereby nullifies the toxic effects of hydrogen peroxide on biological macromolecules. GPx-2 is an intracellular antioxidant enzyme that converts hydrogen peroxide to water by reducing the glutathione to reduced glutathione (Nowak *et al*., 2019). Therefore, these enzymes constitutively work in the *in vivo* system to confront oxidative stress. An increase in the

level of these enzymes in the serum after NCDC 400 suggests its potential to overcome oxidative stress induced by Cy administration. These results commemorate the findings of Zhang *et al*. (2022), who also reported an increased serum SOD, CAT, and other anti-oxidative markers upon oral gavage administration of *L. plantarum* Lp2 (10^9 CFU/mL/mice) to Cy-treated mice model for 10 days. Our results are also in agreement with Sengul *et al*. (2019), who reported an excellent *in vivo* anti-oxidant activity of probiotic strains (*L. plantarum* and *L. fermentum*) in Cy-treated rats.

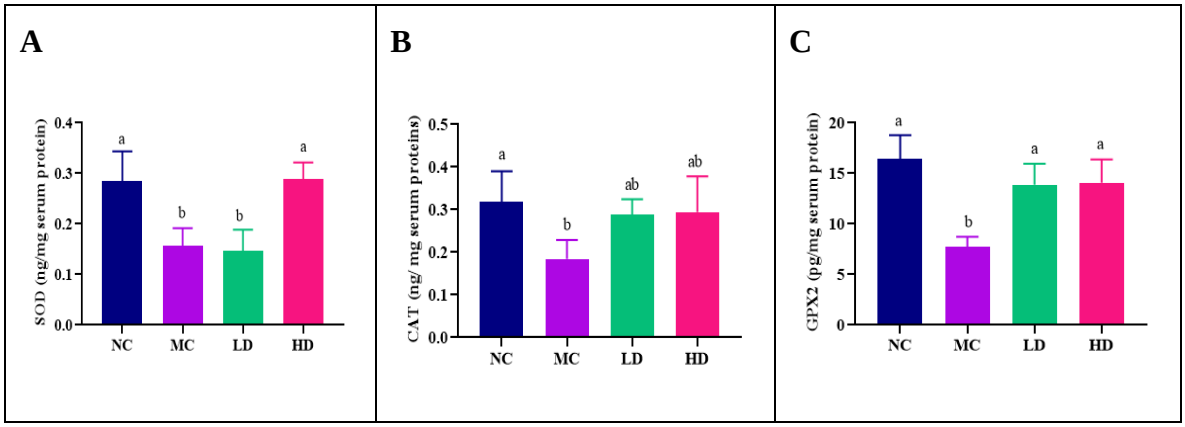

Fig. 4.62: Effects of oral supplementation of NCDC 400 on serum oxidative markers in Cy-induced immunocompromised mice. (A) SOD; (B) CAT; (C) GpX2. Lowercase superscripts (a-b) represent the significant differences ($p < 0.05$) across the groups *(Analyzed by one-way ANOVA following Duncan test).*

4.4.30.12. Macrophage functioning tests

When compared to the NC group, the Cy administration significantly ($p \leq 0.05$) reduced the phagocytic ability of macrophages in the MC group (**Fig. 4.63)**. However, the percentage of yeast engulfing capacity (phagocytosis) increased considerably ($p \leq 0.05$) upon NCDC 400 supplementation in the LD and HD groups. However, there was no considerable difference among different doses of NCDC 400 in demonstrating the phagocytic ability since LD and HD had no significant variations in exhibiting yeast engulfing knack (refer **Fig. 4.64**) for visualization of microscopic views). These results are comparable with the results of the pinocytosis assay. The pinocytic ability of the MC group reduced dramatically ($p \leq 0.05$) when compared to NC. But regardless of the NCDC 400 dose administered, there was a significant increase ($p \leq 0.05$) in the pinocytic ability of macrophages in both the LD and HD groups. These results are well correlated with the corresponding release of β-glucosidase, β-glucuronidase, and NO release in the macrophage culture medium.

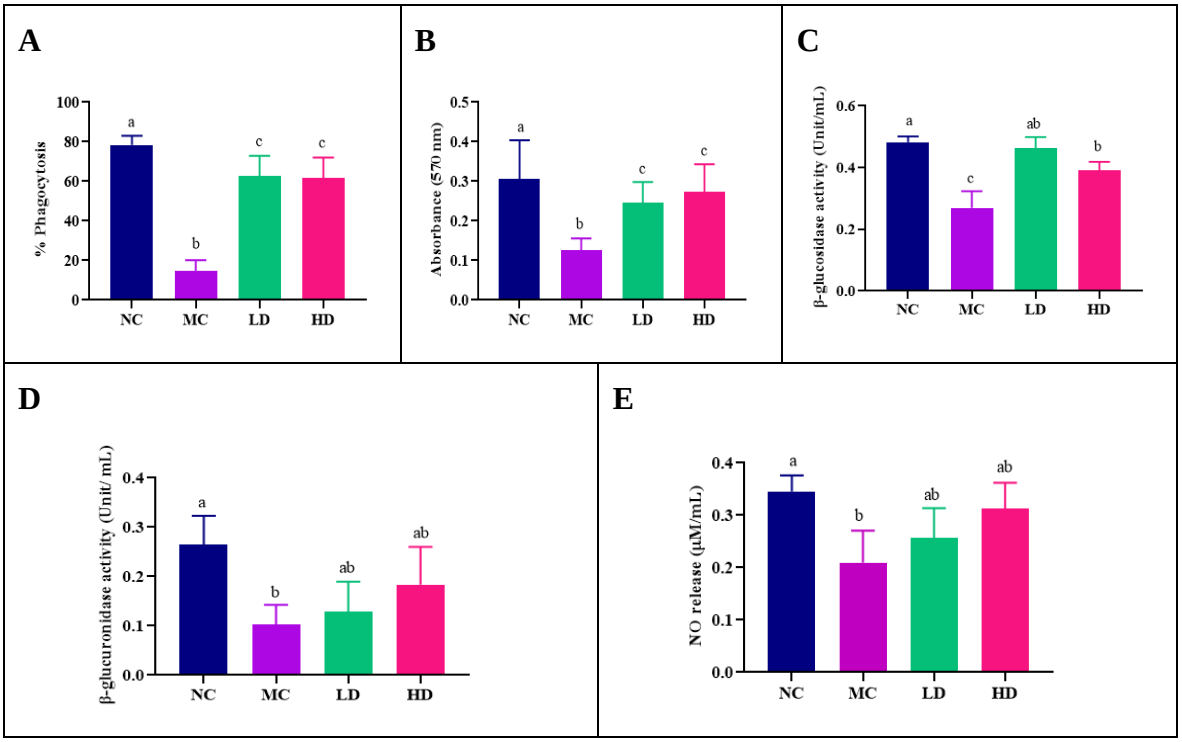

Fig. 4.63: Effects of oral supplementation of NCDC 400 on peritoneal macrophage functioning parameters in Cy-induced immunocompromised mice. (A) Phagocytosis; (B) Pinocytosis; (C) β-Glucosidase; (D) β-glucuronidase; (E) NO release. Lowercase superscripts (a-c) represent the significant differences ($p < 0.05$) across the groups *(Analyzed by one-way ANOVA following Duncan test).*

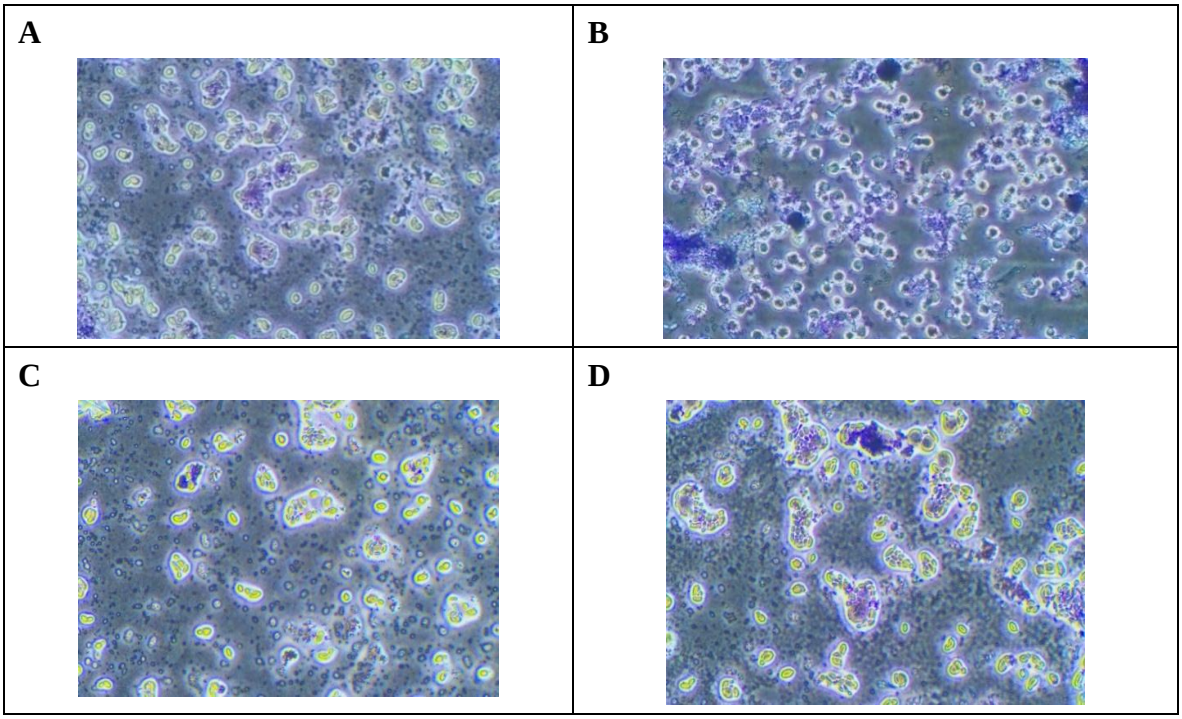

Fig. 4.64: Micrographs (400 X) suggesting the effects of oral supplementation of NCDC 400 on yeast engulfing capacity of peritoneal macrophages in Cy-induced immunocompromised mice. (A) NC; (B) MC; (C) LD; (D) HD.

Compared to the NC group, the activities of β-glucosidase and β-glucuronidase, as well as NO release decreased significantly ($p \leq 0.05$) in the MC group. Although not significant, we found an increasing trend in the values representing the release of β-glucosidase, β-glucuronidase, and NO in the culture medium of macrophages derived from the LD and HD groups. This further validates the NCDC 400 mediated upsurge in the phagocytic/ yeast engulfing capability of macrophages in Cy-treated mice. β-glucosidase and β-glucuronidase are among the few important lysosomal enzymes of macrophages that help degradation of the engulfed yeast cells. Therefore, the release of these enzymes in the medium during phagocytosis may be considered the best markers to assay macrophage functioning (Tusl *et al*., 1983). On the other hand, the activated macrophages in response to the yeast exposure trigger the oxidative burst and bacterial killing via nitric inducible oxide synthase (iNOS) which results in the production of elevated levels of NO during the active phagocytosis process (Slauch, 2011). The results in this regard are in agreement with Salva *et al*. (2014), who reported that oral administration of *L. casei* CRL431 (10^8 cells/mouse/day) for 10 days significantly enhanced the phagocytic capability of macrophages in Cy-induced immunocompromised mice model. Similarly, oral administration of *L. plantarum* KLDS1.0318 (5×10^9 CFU/mL/mice; 0.2 mL/day) for 20 days significantly enhanced the pinocytosis of mice peritoneal macrophages in the immunocompromised mice model. Our results are comparable with Nanjundaiah *et al*. (2020), who demonstrated an increased NO level in the culture medium of macrophage previously treated with *L. rhamnosus* GG and thereby inferred that LGG may influence suppressing the total microbial load in macrophage.

4.4.30.13. Genotoxicity tests

4.4.30.13.a. Micronucleus assay

In comparison with NC, the bone marrow cells obtained from MC groups showed a significant ($p \leq 0.05$) increase in micronuclei formation (**Fig. 4.65)**. This is because Cy is a potent genotoxic compound and exhibits its toxicity mainly on the bone marrow cells and thereby altering the blood parameters. Cy and it is *in vivo*-derived metabolites like 4-hydroxycyclophosphamide are reported to exhibit cytostatic effects by the alkylation of DNA at the N7 position of guanine. This results in the breakdown of the nucleus by DNA–DNA cross-links, DNA–protein cross-links, single-strand breaks, and double-stranded breaks (Voelcker *et al*., 2020). However, NCDC 400 administration in different doses (high and low) showed no significant changes in the frequency of micronuclei

formation when compared to MC. However, it is worth pointing out that NCDC 400 administration (LD and HD group) did not further increase the micronucleus formation in the reticulocytes of the bone marrow cells compared to the MC group. This suggests the lack of clastogenicity/ genotoxic potential of NCDC 400 even in low and high doses. Our results are similar to Pradhan *et al*. (2019a) who reported no genotoxic effect of *L. plantarum* Lp91 and *L. fermentum* Lf1 (10^{12} CFU/mouse) upon oral administration to healthy mice for 21 days. Our results are also comparable with previous work wherein the researchers reported that the single-dose oral probiotic administration of freeze-dried powder containing *L. rhamnosus* LCR177, *B. adolescentis* BA286, and *P. acidilactici* PA318 at a dose of 1.25, 2.5, and 5.0 g/kg BW did not show the frequency of reticulocytes and micronucleated reticulocytes (Chiu *et al*., 2013).

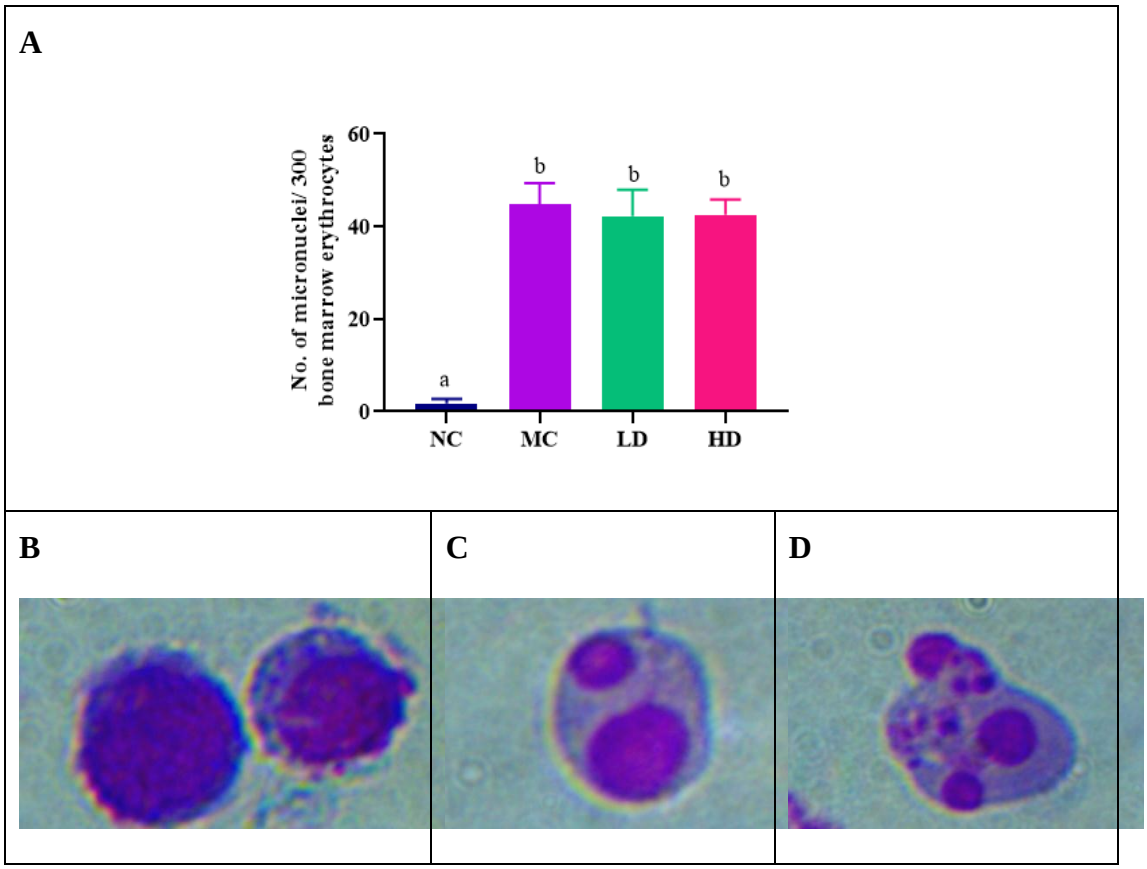

Fig. 4.65: Effects of oral supplementation of NCDC 400 on Cy-induced genotoxicity in immunocompromised mice. (A) Bar graph representing the micronucleus formation by bone marrow cells derived from different experimental groups; (B) Bone marrow cell demonstrating single nucleus; (C) and (D) Bone marrow cell with multiple micronuclei. Lowercase superscripts (a-b) represent the significant differences ($p < 0.05$) across the groups *(Analyzed by one-way ANOVA following Duncan test).*

4.4.30.13.b. Chromosomal aberration assay

The chromosomal aberration assay was carried out to investigate the effect of NCDC 400 on adverse effects on the chromosomal structure. As presented in **Fig. 4.66,** compared to NC, the Cy administration (well-proved genotoxic compound) has significantly ($p \leq 0.05$) increased the total number of chromosomal aberrations in terms of their structure (structural aberrations) but not the numbers (numerical aberrations) in MC group.

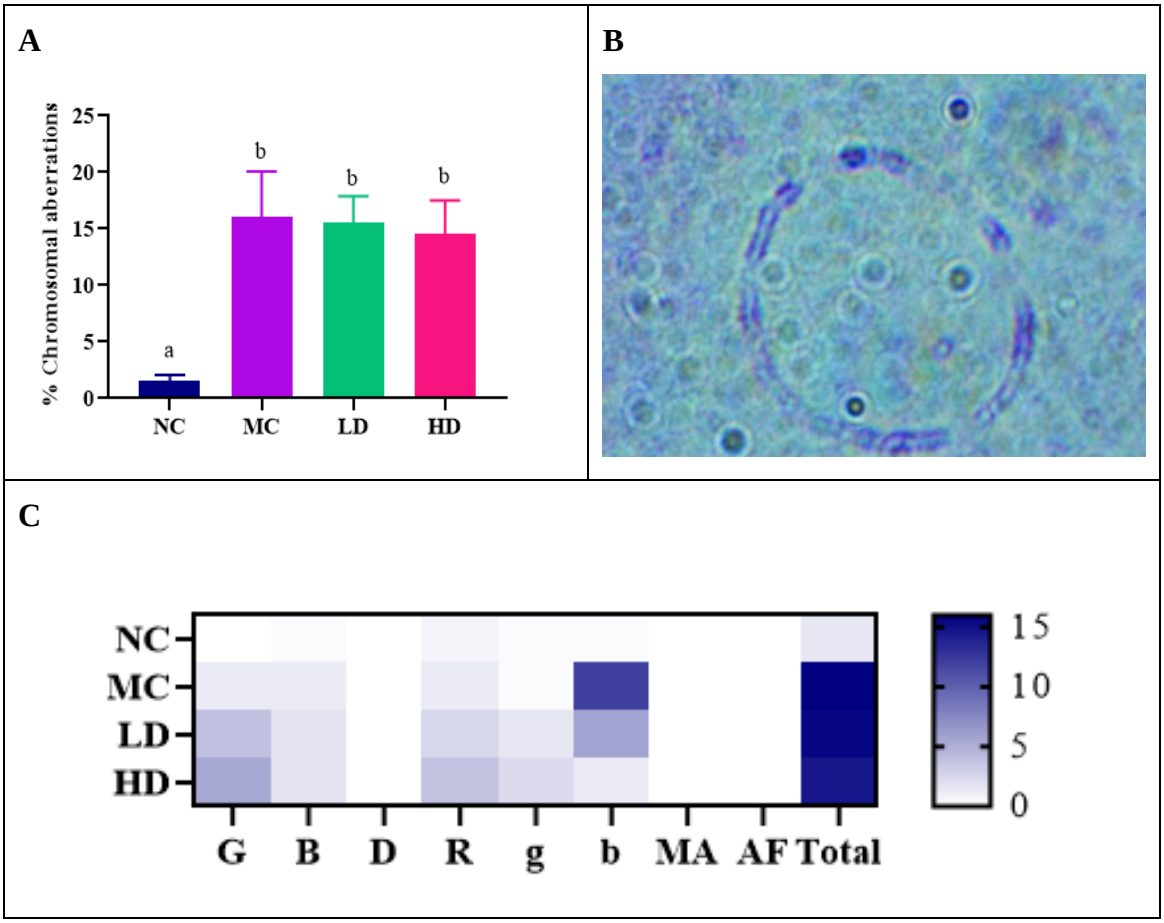

Fig. 4.66: Effects of oral supplementation of NCDC 400 on Cy-induced chromosomal aberration in immunocompromised mice. (A) Bar graph representing percentage chromosomal aberrations by bone marrow cells derived from different experimental groups; (B) Chromosomal metaphase spread; (C) Heatmap showcasing the different types of Cy-induced structural aberrations in the chromosome of bone marrow cells derived from in all experimental groups, wherein the abbreviations in the heatmap are provided here:- G: Chromosomal gap; B: Chromosomal break; D: Dicentric; R: Ring; G: Chromatid gap; b: Chromatid break; MA: Multiple aberrations; AF: Acentric fragment. Lowercase superscripts (a-b) represent the significant differences ($p < 0.05$) across the groups *(Analyzed by one-way ANOVA following Duncan test).*

However, low and high doses of NCDC 400 administration to immunocompromised mice did not induce any further increase in chromosomal aberrations (such as chromosomal gap, chromosomal break, dicentric, ring; chromatid gap, chromatid break, multiple aberrations, acentric fragment) suggesting that NCDC 400 was devoid of genotoxic ability. Our results in this regard are in agreement with previous work reporting the absence of chromosomal aberrations in mammalian somatic cells after exposure to freeze-dried powder containing *L. rhamnosus* LCR177, *B. adolescentis* BA286, and *P. acidilactici* PA318 at a dose of 1.25, 2.5, and 5.0 g/kg BW (Chiu *et al*., 2013). In congruent with this observation, Pradhan *et al*. (2019a) have also found no test strain-related chromosomal aberrations in bone marrow cells after oral administration of *L. plantarum* Lp91 and *L. fermentum* Lf1 (10^{12} CFU/mouse) to healthy mice for 21 days.

4.4.30.14. Faecal microbiome analysis

The effect of oral administration of NCDC 400 in different doses on gut microbial composition in immunocompromised mice was evaluated by using 16S rRNA metagenomic analysis. The effect of NCDC 400 gavaging on faecal microbiota α-diversity was evaluated by the number of ASVs and the Chao1 and Shannon indices. Although no significant reduction in the ASVs was observed in the NC and MC groups, there was an increase in the ASVs in the LD and HD groups, albeit statistically insignificant (p = 0.965) (**Fig. 4.67**). In a similar way, bacterial species richness (Chao-1 index) increased in the LD and HD groups but was found statistically insignificant (p = 0.84). However, we observed no observable difference in the bacterial evenness (Shannon index) between MC and LD but decreased in the HD group irrespective of NCDC 400 administration at a high dose, which could be due to the small sample size (n=3). Furthermore, NCDC 400 intervention at LD and HD induced the microbiome β-diversity configuration shift considerably [but statistically insignificantly (p = 0.85)].

The Bray–Curtis (BC) dissimilarity is used to locate the microbiome similarities between the test groups and is varied between 0 and 1, where 0 means the two groups may have the same composition (that is they share all the species), and 1 means the two groups do not share any species. Groups where BC is intermediate (0.5) suggest that two groups may share equal microbes (Ricotta and Podani, 2017). In this regard, the BC index between NC v/s. LD and NC v/s. HD was 0.2 to 1.0, respectively (**Table 4.36**). This suggests that NCDC 400 supplementation at high doses may be beneficial in

diversifying the gut microbiome of even healthy individuals. The BC index between NC v/s. MC was 0.70 suggesting that Cy administration might have considerably influenced in shifting the microbial species in the gut milieu, which was also recorded in the microbiome composition in terms of the relative abundance of major bacterial phyla. However, the BC index between MC v/s. LD and MC v/s. HD was 0.20 and 0.59, respectively. These values indicate that NCDC 400 supplementation, more preferably at HD, may help in more efficiently ameliorating the gut microbial dysbiosis by augmenting the gut microbial profile via fostering gut microbiota diversification.

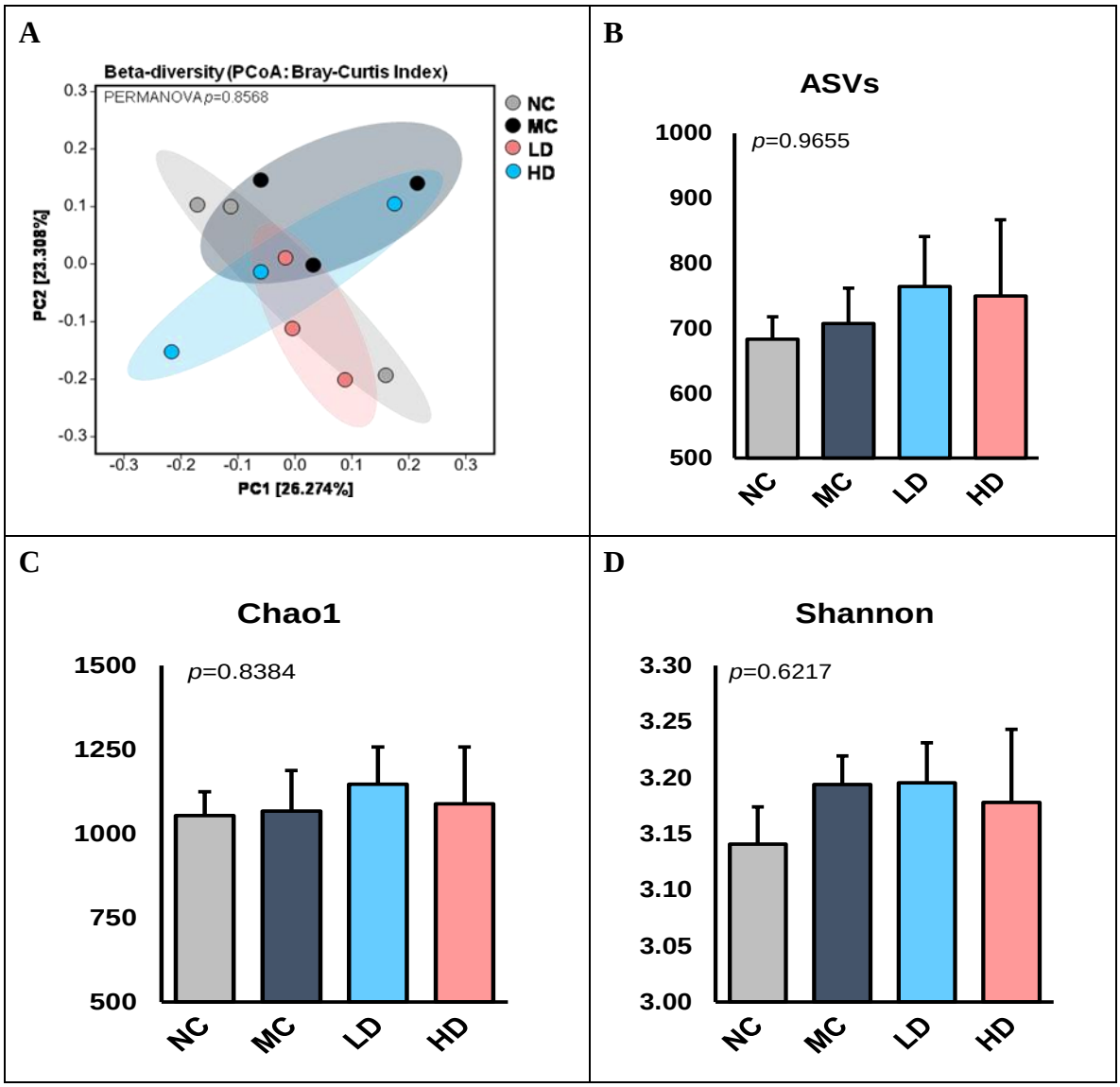

Fig. 4.67: Effects of oral administration of NCDC 400 on gut microbiome composition in immunocompromised mice. Microbiome beta-diversity arrays demonstrated by principal component analysis (A), ASVs (B), and alpha-diversity indices of bacterial species richness and evenness (C and D). Error bars indicate the variations of three determinations in terms of the standard error of mean.

The principal coordinate plot of β-diversity based on Bray–Curtis (BC) dissimilarity, which accounts for the relative abundance of species/ taxa shared among the groups, represented 49.48% of the total variance, among which PC1 contributed 26.27% and 23.30% on the vertical axis (PC2), highlighting the degree of variations between groups. The distance between NC and MC plots was nearly close to each other, suggesting that Cy administration might have the least influence on gut microbiota perturbation, which could be due to the low sample size. However, the distance between the LD and HD plots on the axis was far from the MC group, suggesting that NCDC 400 supplementation to immunocompromised mice resulted in improvement in the gut microbial profile by taxa/ species diversification.

Table 4.36: Compilation of community dissimilarities (β-diversity) estimate between the groups by pairwise Bray-Curtis dissimilarity index

	NC	MC	LD	HD
NC	-	0.709	0.209	1
MC	0.709	-	0.594	0.798
LD	0.209	0.594	-	
HD	1	0.798	1	-

In terms of major bacterial phyla **(Fig. 4.68)**, Firmicutes and Bacteroidetes were dominant across all the groups, accounting for > 75% of taxonomic units. There was an increase in the levels of *Firmicutes* and *Proteobacteria*, and a decrease in the *Bacteroidetes, Saccharibacteria* and *Actinobacteria* was found in the MC group. These observations are highly similar to a previous study reporting an increase in *Firmicutes* and Proteobacteria as well as a decrease in Bacteroidetes after Cy administration to mice (Xu and Zhang, 2015). However, oral NCDC 400 administration (LD and HD groups) to immunocompromised mice maintained the normal levels of Firmicutes and increased the *Bacteroidetes*, *Saccharibacteria*, *Actinobacteria*, and *Verrucomicrobiota*. It is worth mentioning that NCDC 400 feeding resulted in a considerable reduction in Proteobacteria and this explains why there was a considerable reduction in the caecal harmful enzymes reduced in the LD and HD groups in the previous assays. Albeit found statistically insignificant, the *Firmicutes*/ *Bacteroidetes* (F/B) ratio was increased in the MC group and reduced sizably in the LD and HD groups. Similarly, a previous study by

Xue *et al*. (2022) reported an increase in the F/B ratio in the gut microbiota of Cy-treated mice which was allivated upon oro-gastic administration of *L. acidophilus* LA85 at the dose of 1×10^{8} CFU/ mL, 1×10^{9} CFU/ mL, and 1×10^{10} CFU/ mL.

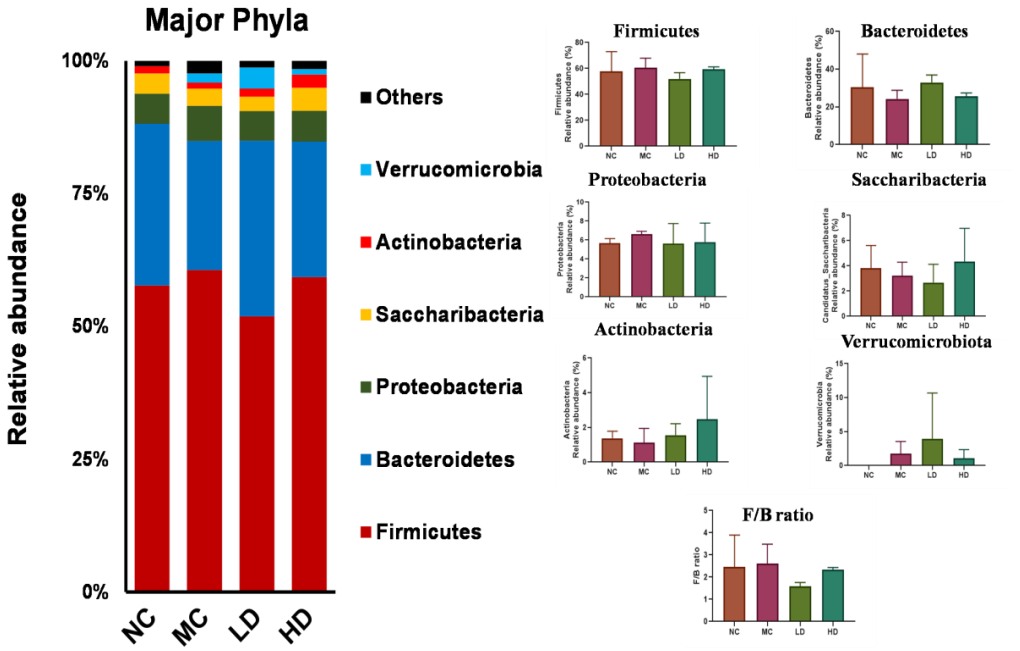

Fig. 4.68: Distinct arrays of gut microbiota composition at phyla level and *Firmicutes/ Bacteroidetes* (F/B) ratio in different experimental groups of mice.

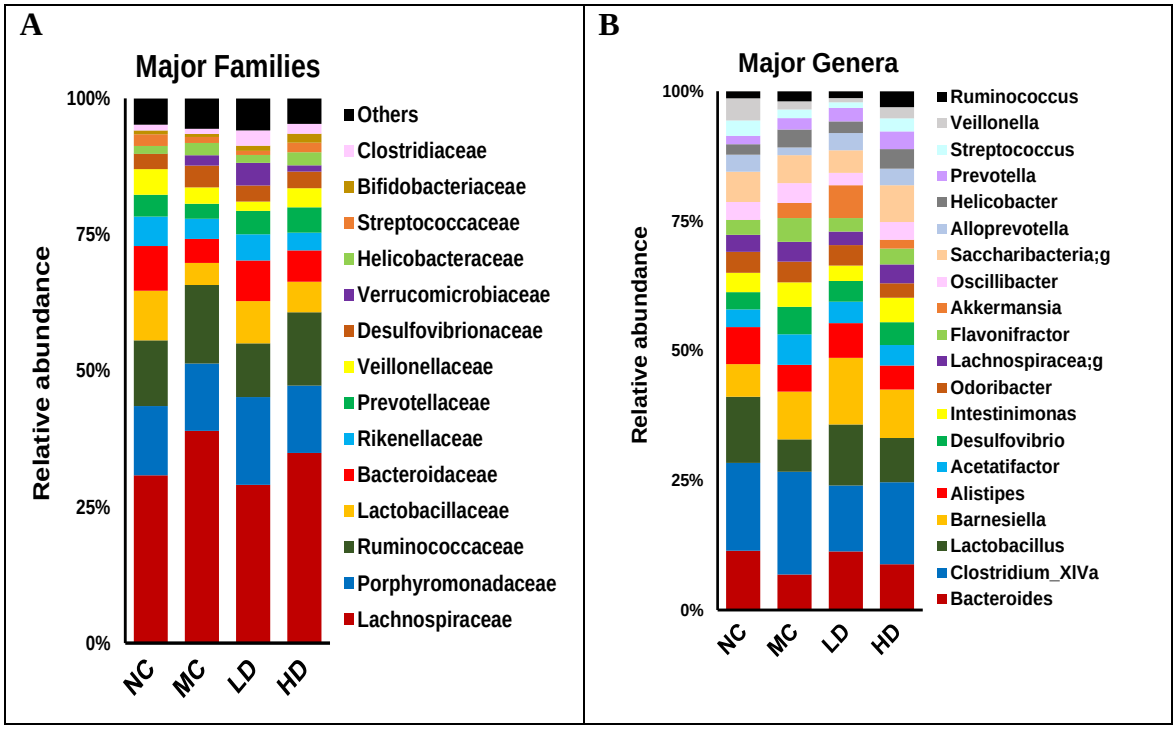

Fig. 4.69: Gut microbiota abundance at families (A) and genera (B) level in different experimental groups of mice.

At the family level **(Fig. 4.69A)**, there was an increase in the *Porphyromonadaceae*, *Ruminococcaceae*, *Lactobacillaceae*, *Bacteroidaceae*, *Rickenellaceae*, *Prevotellaceae*, *Verrucomicrobiaceae*, and *Clostridiaceae* in the LD and HD groups when compared to either NC or MC groups. These results are in line with previous reports that underscore that Cy administration diminishes the aforementioned beneficial bacterial families but was restored successfully after probiotic/ prebiotic intervention (Kong *et al*., 2020). In a human trial, an increased abundance of *Rikenellaceae* and *Porphyromonadaceae* has been associated with a healthier metabolic profile in the Italian elderly (Tavella *et al*., 2021). The family *Verrucomicrobiaceae* consists of *A. muciniphila*, an important member of next-generation probiotics, reported to produce butyrate, which enhances gut barrier integrity and reduces inflammation (Zhang *et al*., 2019).

In terms of major bacterial genera **(Fig. 4.69B)**, we noticed an increase in the important genera *viz*. *Bacteroides*, *Lactobacillus*, *Barnesiella*, *Alistipes*, *Odoribacteria*, *Lachnospiracea*:g, *Akkermansia*, *Saccharibacteria*:g, *Alloprevotella*, *Streptococcus*, *Veillonella*, and *Ruminococcus* in the LD or HD groups when compared to NC or MC groups. It is important to note that most of these genera belong to next-generation probiotics whose increased abundance has been associated with a positive state of health (Chang *et al*., 2019; Singh and Natraj, 2021). Moreover, these genera have been reported to produce SCFAs by utilizing the complex carbohydrates/ prebiotics in the diet (Kaźmierczak-Siedlecka *et al*., 2022). This perhaps justifies why the level of caecal total SCFAs increased significantly in the LD and HD groups. These results are in agreement with several previous reports suggesting an increase in beneficial microflora such as *Lactobacillus*, *Lachnospiraceae*:*g*, and other beneficial genera as well as their metabolites after oral probiotic administration (Xie *et al*., 2016; Lv *et al*., 2021).

Overall, the microbiome analysis suggests that NCDC 400 administration to the Cy-treated immunocompromised mice helps replenish the beneficial gut microbiota whose abundance and diversity decrease during the immunocompromised state. A shift toward NCDC 400-mediated eubiosis in the mice gut could be linked to the direct gut microbial modulation or by stimulation of specific gut microflora by the exopolysaccharide produced by the strain (EPS 400). A similar effect was observed in a recent previous study from our lab, wherein oral gavage administration of EPSRam12

(*Lacticaseibacillus rhamnosus* Ram12) to D-gal induced oxidative stress mice model decreased the gut dysbiosis by enriching the abundance of SCFAs-producing microbial genera *Prevotella*, *Clostridium*, *Intestinimonas*, and *Acetatifactor* while decreasing the potential pathobionts including *Helicobacter* (Kumari *et al*., 2022).

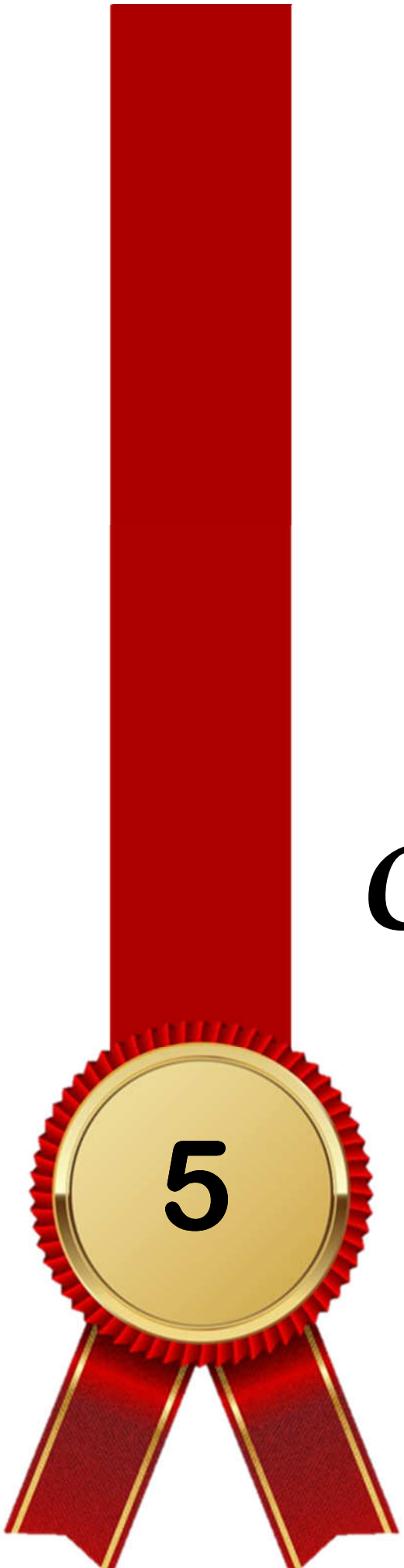

Summary & Conclusion

SUMMARY AND CONCLUSION

The present investigation was contemplated to evaluate the safety and toxicology of an indigenous probiotic *L. fermentum* NCDC 400 for its prospective safe use as functional biotherapeutics. The present study amalgamated an array of *in vitro, in silico,* and *in vivo* experiments using healthy and immunocompromised mice models to establish the safety of the test strain. The salient findings that emerged from this study are underpinned below:

Objective 1: Assessment of *L. fermentum* NCDC 400 for safety aspects using *in vitro* methods.

- The species-specific PCR using LF1 and LF2 primers resulted in the formation of an expected amplicon size of 337 bp which reconfirms the molecular identity of the strain under investigation as *L. fermentum*.
- The RAPD fingerprinting of the test strain using M13 primer resulted in the formation of two intense bands of above 1 kb, one at 400 bp, and three prominent faint bands appeared between 300-400 bp. However, amplification with OPA5 resulted in two faint bands above 1 kb.
- Plasmid profiling of NCDC 400 demonstrated two plasmids of approximate size 8 kb (plasmid A) and 5 kb (plasmid B) at the current physiological stage of the bacterium.
- Hemolytic activity by streaking on blood agar and spectrophotometric method did not reveal any hemolytic activity by NCDC 400. Moreover, the membrane integrity of RBCs treated with the NCDC 400 was unaffected and thereby suggested the absence of hemolytic activity.
- NCDC 400 did not exhibit DNase activity since there was a clear absence of a pinkish zone around the agar wells treated with NCDC 400 cell-free supernatant.
- In contrast to *S. aureus* ATCC 25923 (positive control), the test strain NCDC 400 displayed coagulase negative phenotype since it failed to coagulate the human plasma.

- Compared to the positive control (*P. aeruginosa* NCDC 105), the test strain (NCDC 400) could produce a relatively lesser amount of ammonia (0.02 ± 0.01 μg/mL) which may not be harmful at such a lower concentration.
- NCDC 400 was devoid of gelatinase activity since it could not able to liquefy the nutrient gelatin.
- NCDC 400 showed the yellow-colored negative reaction on Christenson urea agar suggesting that NCDC 400 was devoid of urease activity.
- NCDC 400 fails to produce a pink ring after the addition of Kovac's reagent to the tryptophan culture medium, suggesting that NCDC 400 do not produce indole.
- The test strain was negative for the phenylalanine production test that assays the production of phenylpyruvate with the action of phenylalaninase.
- NCDC 400 fails to utilize the specific substrate p-nitrophenyl-β-D-glucopyranoside and p-nitrophenyl-β-D-glucuronide to produce yellow color reaction suggesting that the test strain was free from beta-glucosidase and beta-glucuronidase activity.
- NCDC 400 produced L-lactate as principal isomeric form of lactic acid which contributes to 0.71 ± 0.04 g/ L. On the contrary, the D-lactate produced by NCDC 400 was relatively low (0.21 ± 0.02 g/ L).
- NCDC 400 was sensitive to the antagonistic actions of human serum. Three hours of exposure to human serum resulted in 3.36 ± 0.23 logarithmic reductions in the viability of NCDC 400.
- In contrast to a positive control (collagen), NCDC 400 was devoid of platelet aggregation phenotype.
- The test strain was unable to produce the tyramine, cadaverine, histamine, and putrescine by degradation of respective amino acids such as tyrosine, lysine, histidine, and arginine, as tested by decarboxylase broth method, pH measurement method, decarboxylase agar method, and HPLC method.
- NCDC 400 did not show the mucin degradation ability as it failed to grow in the basal medium containing mucin as only the carbon source. SDS-PAGE analysis

following silver straining of mucin treated with NCDC 400 showed an intact mucin band which was absent in the faecal flora (positive control). Similarly, the PAS straining of SDS-PAGE gel indicated the mucin smear in the lanes loaded with the mucin treated with NCDC 400 or negative control, while the smear disappeared in the faecal flora-treated mucin. Moreover, ATR-FTIR spectra of mucin treated with NCDC 400 were well preserved and unaltered. These findings indicate the absence of mucin degradation phenotype in NCDC 400.

- NCDC 400 showed an excellent adhesion to Caco-2 cells and mucin corresponding to 15.60 ± 2.88 and 14.40 ± 0.83% relative adhesion, respectively.
- Upon testing by MTT assay, neutral red assay, and trypan blue exclusion assay, the NCDC 400 (10^8-10^{11} CFU/ mL) was found to be non-cytotoxic to Caco-2 cells.
- In comparison with positive control *E. coli* (12.94 ± 1.56% transflux), the test strain NCDC 400 did not alter the phenol red transflux across (< 2.5% transflux) the completely differentiated and polarized Caco-2 cell monolayer cultured on transwell insert, suggesting that NCDC 400 do not ruin the gut barrier integrity.
- In the antibiotic susceptibility test, NCDC 400 was sensitive to a total of 27 antibiotics of different classes, except for vancomycin, for which intermediary resistance was demonstrated.
- MICs of different antibiotics toward NCDC 400 were determined by E-strips. The test strain was sensitive to all the eight antibiotics (Kanamycin, Ampicillin, Gentamicin, Streptomycin, Clindamycin, Tetracycline, Erythromycin, and Chloramphenicol) enlisted by EFSA for heterofermentative lactobacilli for food/ probiotic applications.
- The targeted PCR approach confirmed the absence of 14 ARGs confirming resistance towards tetracycline (*TetO* and *TetM*), erythromycin (*ermA, ermB, ermC, msrA,* and *ermf*), aminoglycoside-modifying-enzyme genes (*ant(6')-Ia, aph(3')-IIIa,* and *aac(6')-le-apha (2'')-Ia*), chloramphenicol (*CatA8*), multidrug resistance efflux (*emeA*), beta-lactam (*blaTEM*), and *Int-Tn* (*Tn916/Tn1545*), either in genomic DNA or in the plasmid DNA. Similarly, NCDC 400 was also free from virulence genes that encode coagulase (*Coa*), nuclease (*nucA*), and gelatinase (*gelE*).

- The whole genome analysis of NCDC 400 for mining of potential antibiotic-resistant genes (ARGs) using RGI, ResFinder, ARG-ANNOT, and CARD databases suggests the absence of potential ARGs of public health concern. Most of resistance genes predicted by these pipelines were responsible for intrinsic resistance which lacks lateral transferability.
- Analysis of NCDC 400 whole genome sequences for virulence factors through VFDB and Pathogen Finder databases suggested that NCDC 400 is non-pathogenic to humans and carries no virulence determinants.
- Analysis of prophage sequences in the whole genome of NCDC 400 by the PHASTER tool suggested 2 incomplete prophage sequences that lack lateral transferability.
- Analysis of CRISPR regions in the NCDC 400 whole genome by CRISPRFinder/ CRISPRcasFinder suggested 1 confirmed and 2 questionable CRISPR sequences.
- The whole genome of NCDC 400 was free from OriT regions that initiate the horizontal gene transfers.
- The functional annotation of the NCDC 400 whole genome by Prokka and RAST as well as their validation through universally accepted and updated databases like UniProt/ NCBI-BLAST/ CARD/ VFDB suggested the absence of potential genes conferring virulence traits, harmful enzymes, and adverse metabolites.

Objective 2: Toxicological evaluation of *Limosilactobacillus fermentum* NCDC 400 in the murine model.

- Three independent oral toxicity tests *viz*. acute/ 14 days repeated dose toxicity, subacute toxicity study (28 days), and subchronic toxicity study (90 days) were conducted according to OECD guidelines with slight modifications. *L*. *fermentum* NCDC 400 was orally administrated daily to the mice for different durations (14, 28, and 90 days as per OECD guidelines) at low (LD: 10^8 CFU/mouse/day) and high doses (HD: 10^{10} CFU/mouse/day).
- Oral administration of NCDC 400 at 10^8 (Low dose) and 10^{10} (High dose) cells for 14 (acute), 28 (subacute), and 90 (subchronic) days did not induce treatment-related toxicity signs in terms of their sleep, salivation, diarrhea, skin, fur, eyes, and behavior.

- There were no treatment-related changes in feed and water intake as well as the body weight of animals in all three oral toxicity studies.
- Exposure to NCDC 400 at different doses did not result in any gross pathological changes in organs and their organ indices in the murine model.
- Oral administration of NCDC 400 did not adversely affect the hematological parameters such as RBC, Hb, HCT, MCV, MCH, MCHC, MPV, WBC, DLC, and fasting glucose levels either at the low or high dose in all three studies.
- No treatment and dose-related changes in the serum biochemistry parameters like ALT, AST, urea, creatinine, LDH, total protein, calcium, phosphorous, and serum lipid profile were observed in all three studies.
- Oral gavaging of NCDC 400 for the different experimental periods significantly ($p < 0.05$) improved the faecal parameters by reducing the faecal pH and ammonia and elevating the faecal lactate.
- Repeated administration of different doses of NCDC 400 significantly ($p < 0.05$) lowered the caecal harmful enzymes (beta-glucosidase, beta-glucuronidase, and tryptophanase) and improved the caecal SCFAs (acetate, propionate, and butyrate) content in the dose and duration specific manner.
- Oro-gastric administration of NCDC 400 elevated the serum IgA and IgG response in a dose and duration-specific manner but did not trigger the adverse immune reactions that provoke the pro-inflammatory response. Administration of NCDC 400 maintained a dynamic balance between pro- and anti-inflammatory cytokines (decrease in IL-6 and TNF-alpha, increase in IL-10, TGF-beta with no change in MCP-1) in healthy mice.
- Episodes of NCDC 400-mediated bacterial translocation to blood and extra-intestinal organs like the liver, spleen, kidney, and lungs were not witnessed in all three oral toxicity studies.
- Acute, sub-acute, and sub-chronic exposure of NCDC 400 to healthy mice at low and high doses did not foster any treatment-related histological changes in the various tissues/ organs like brain, kidney, liver, heart, lungs, spleen, small intestine, and large intestine.

Objective 3: Evaluation of safety and efficacy of *Limosilactobacillus fermentum* NCDC 400 in an immunocompromised murine model.

- In the development of immunocompromised mice model, three groups out of four mice groups (0, 50, 100, and 150 mg/kg BW) received Cy treatment at doses of 50, 100, and 150 mg/kg BW intraperitoneally (i.p.) on 1, 7 and 14 days while control while 0 mg/kg BW received only PBS via i.p. route. Further, three animals per group were dissected on the 3, 6, 9, 12, and 17th days for analysis purposes.
- Compared to animals in the 0 mg/ kg BW group, the body weight of animals significantly ($p < 0.05$) reduced after the Cy administration in a dose-dependent manner. However, a significant ($p < 0.05$) reduction in the animal body weight from day-6 was observed only in a group where Cy administration was higher (150 mg/kg BW).
- Similarly, the spleen and thymus indices of the animals significantly ($p < 0.05$) reduced after the Cy administration in a dose-dependent manner. However, a significant reduction in the immune organ indices from day-6 was observed only in a group where Cy administration was higher (150 mg/kg BW).
- The hematological parameters like WBC, lymphocytes, granulocyte, monocytes, RBC, and HCT values reduced drastically after the Cy administration. But a significant ($p < 0.05$) reduction in aforementioned hematological parameters from day-3 without any increase till 17 days was observed only in the mice group administrated with Cy at 150 mg/kg BW.
- The levels of serum oxidative markers like SOD, CAT, and GpX2 reduced considerably after the Cy administration. Nevertheless, a significant ($p < 0.05$) reduction in the SOD and CAT from day-3 (GpX2 reduced significantly from day 9) without any increase till 17 days was observed only in the mice group treated with Cy at 150 mg/kg BW.
- Owing to these findings, a Cy dose of 150 mg/kg BW was used for the development of an immunocompromised model to study the safety and efficacy of NCDC 400.

- To study the safety and efficacy of NCDC 400 in an immunocompromised mice model, three out of four mice groups (NC, MC, LD, and HD) received Cy administration via i.p. route on 1, 7, and 15th day. NCDC 400 was orally administrated at 10^8 and 10^{10} CFU/mouse/day for LD and HD groups, respectively, for 15 days (from the 3rd to the 17th day). However, NC and MC groups received only PBS orally during the experimental duration.
- The animals in the MC groups showed reduced body weight with a simultaneous reduction in feed and water intake while the severity of weight reduction was reduced in LD and HD groups because of a parallel increase in feed and water intake.
- Abnormal increase (liver, heart, and lungs) or decrease (kidney, spleen, brain, and thymus) in the organ index was witnessed in the MC group but tended towards normalization with respect to their indices in the LD and HD groups.
- Hematological parameters like RBC, Hb, HCT, PLT, WBC, LYM, MON and GRAN were reduced significantly ($p < 0.05$) in the MC group. However, no significant improvements in these parameters were observed after NCDC 400 supplementation either at low or high doses. Although not statistically significant, WBC, LYM, MON, and GRAN values were in increasing trend in the LD and HD groups compared to the MC group. The parameters like glucose and PCT were unaltered even after Cy or NCDC 400 administration.
- The liver (ALT and AST) and kidney (urea and creatinine) functioning markers as well as LDH increased significantly ($p < 0.05$) in the MC groups but reduced after NCDC 400 administration considerably in the LD and HD groups. On the contrary, the serum total protein decreased significantly ($p < 0.05$) in the MC group (4.99 ± 0.44 g/dL) but increased in the LD (6.22 ± 0.03 g/dL) and HD (6.18 ± 0.09 g/ dL) group. Similarly, the serum total lipid profile increased considerably in the MD group but decreased slightly in the LD and HD groups.
- There was an increase in the faecal pH (decreased lactate and SCFAs), ammonia, and harmful intestinal enzymes (beta-glucuronidase and beta-glucosidase) activity in the MC group but decreased considerably ($p < 0.05$) in the NCDC 400 fed groups (LD and HD groups).

- There no incidences of NCDC 400-mediated bacterial translocation to the blood and extra-intestinal organs were observed across the groups.
- No adverse immunological reactions or mortalities were observed upon NCDC 400 supplementation to immunocompromised mice.
- The levels of serum NO, IgA, IgG, and other inflammatory cytokines and chemokines decreased markedly in the MC group. However, their levels tended toward normal in the NCDC 400 fed groups (LD and HD) in a dose-specific manner.
- The splenocyte proliferation (T or B cells) index reduced considerably in the MC group, but improved considerably in the LD and HD groups, although not statistically significant.
- The activities of peritoneal macrophages such as phagocytosis and pinocytosis, and their related markers decreased substantially in the MC but increased significantly ($p < 0.05$) upon NCDC 400 supplementation in low and high doses.
- A marked increase in genotoxicity (micronucleus formation and chromosomal structural aberrations) was observed in the bone marrow cells of animals in the MC group. However, no further significant increase or decrease in the genotoxic effect was observed after NCDC 400 intervention in low and high doses.
- Cy administration significantly ruined the histological features of the liver, kidney, and spleen. However, these changes were reversed in the LD and HD groups. Nevertheless, Cy administration did not affect intestinal histological features since there was no tissue distortions/ inflammation in the MC groups
- Cy administration did not significantly lower the ASVs, alpha diversity, and beta diversity compared to NC which is probably due to the small sample size. However, NCDC 400 administration positively influenced the gut microbiota by demonstrating an increasing trend in ASV, alpha diversity (Chao1 and Shannon index), and beta diversity compared to NC and MC.
- NCDC 400 intervention resulted in the enrichment or fostering of beneficial saccharolytic microbes, including NGPs that produce short-chain fatty acids, while declining the pathobionts (proteobacteria phylum) in gut.

Conclusion

Albeit the members of LAB enjoy the GRAS status, the mounting evidence on LAB-mediated adverse health effects in the immunocompromised subjects calls for rigorous and in-depth safety analysis of food-grade bacteria or any potential probiotic strains before clinical/ food applications. Hence, the current study aimed at an in-depth bio-safety assessment of *L. fermentum* NCDC 400 whose probiotic functionalities have been previously established. *In vitro* and computational studies suggested that NCDC 400 was non-pathogenic or non-virulent and free from concerning antibiotic resistance issues of public health significance. *In vivo* toxicological studies (acute, subacute, and subchronic oral toxicity tests) on this strain at low and high doses resulted in no-treatment-related toxicity either in terms of physiological behaviors or clinical parameters (hematology, clinical biochemistry, histopathology, and immune status) of mice. *L. fermentum* NCDC 400 was well tolerated in the immunocompromised mice model and did not foster any adverse effects like genotoxicity even at a high dose (10^{10} CFU/mouse/day). Owing to these findings, a dose of 10^{10} CFU/mouse/day may be considered NOEL (No Observable Effect Level) in both healthy and immunocompromised mice. Overall, the results that emerged from this study underscore the safe and non-toxic behavior of *L. fermentum* NCDC 400 and thereby call for and may facilitate further human clinical trials.

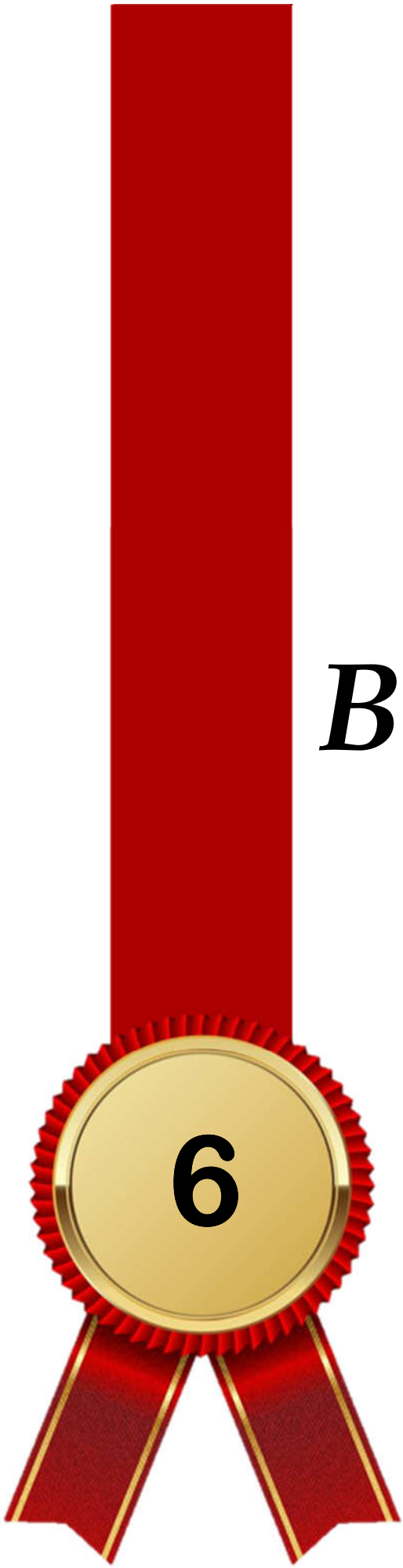

Bibliography

BIBLIOGRAPHY

Abe Sato, S.T., Marques, J.M., da Luz de Freitas, A., Sanches Progenio, R.C., Nunes, M.R.T., Mota de Vasconcelos Massafra, J., Gomes Moura, F. and Rogez, H. (2021). Isolation and genetic identification of endophytic lactic acid bacteria from the *Amazonian açai* fruits: Probiotics features of selected strains and their potential to inhibit pathogens. *Frontiers in Microbiology*, **11**: 610524.

Abe, F., Muto, M., Yaeshima, T., Iwatsuki, K., Aihara, H., Ohashi, Y. and Fujisawa, T. (2010). Safety evaluation of probiotic bifidobacteria by analysis of mucin degradation activity and translocation ability. *Anaerobe*, **16**: 131-136.

Abfalter, C.M., Schmidt, T.P. and Wessler, S. (2015). Proteolytic activities expressed by gastrointestinal pathogens *Bacillus cereus*, *Listeria monocytogenes* and *Enterococcus faecium* in different growth phases. *British Microbiology Research Journal*, **7**: 62.

Adawi, D., Molin, G., Ahrné, S. and Jeppsson, B. (2002). Safety of the probiotic strain *Lactobacillus plantarum* DSM 9843 (strain 299v) in an endocarditis animal model. *Microbial Ecology in Health and Disease*, **14**: 50-53.

Agrawal, S., Tuchman, E.S., Bruce, M.J. and Theodorou, M.E. (2020). Fatal *Lactobacillus* endocarditis in a patient with transcatheter aortic valve replacement. *BMJ Case Reports CP*, **13**: 236835.

Ajam, M., Adam, O., Yeddi, A., Kahlid, M., Shokr, M. and Afonso, L. (2019). Prosthetic aortic valve endocarditis in a patient with Birt-Hogg-Dube syndrome due to *Lactobacillus paracasei*. *Cardiology Research*, **10:** 245.

Akram, M., Ali, S.A., Behare, P. and Kaul, G. (2022). Dietary intake of probiotic fermented milk benefits the gut and reproductive health in mice fed with an obesogenic diet. *Food and Function*, **13**(2): 737-752.

Akram, M.F.S., Ashraf, M., Ali, S. and Kazmi, S.I. (2017). Isolation of Gram-positive bacteria from different sources and evaluation of their probiotic properties. *Journal of Medical Microbiology and Infectious Diseases*, **5:** 12-16.

Al Atya, A.K., Drider-Hadiouche, K., Ravallec, R., Silvain, A., Vachee, A. and Drider, D. (2015). Probiotic potential of *Enterococcus faecalis* strains isolated from meconium. *Frontiers in Microbiology*, **6**: 227.

Alayande, K.A., Aiyegoro, O.A., Nengwekhulu, T.M., Katata-Seru, L. and Ateba, C.N. (2020). Integrated genome-based probiotic relevance and safety evaluation of *Lactobacillus reuteri* PNW1. *Plos One*, **15**: 0235873.

Alenzi, F.Q., El-Bolkiny, Y.E.S. and Salem, M.L. (2010). Protective effects of Nigella sativa oil and thymoquinone against toxicity induced by the anticancer drug cyclophosphamide. *British Journal of Biomedical Science*, **67**(1): 20-28.

AlGburi, A., Volski, A., Cugini, C., Walsh, E.M., Chistyakov, V.A., Mazanko, M.S., Bren, A.B., Dicks, L.M. and Chikindas, M.L. (2016). Safety properties and probiotic potential of *Bacillus subtilis* KATMIRA1933 and *Bacillus amyloliquefaciens* B-1895. *Advances in Microbiology*, **6:** 432-452.

Al-Qadami, G.H., Secombe, K.R., Subramaniam, C.B., Wardill, H.R. and Bowen, J.M. (2022). Gut Microbiota-Derived Short-Chain Fatty Acids: Impact on Cancer Treatment Response and Toxicities. *Microorganisms*, **10**(10): 2048.

Álvarez-Cisneros, Y.M. and Ponce-Alquicira, E. (2018). Antibiotic resistance in lactic acid bacteria. In *Antimicrobial Resistance-A Global Threat*. IntechOpen.

Ambesh, P., Stroud, S., Franzova, E., Gotesman, J., Sharma, K., Wolf, L. and Kamholz, S. (2017). Recurrent *Lactobacillus* bacteremia in a patient with leukemia. *Journal of Investigative Medicine High Impact Case Reports*, **5**: 2324709617744233.

An, H., Douillard, F.P., Wang, G., Zhai, Z., Yang, J., Song, S., Cui, J., Ren, F., Luo, Y., Zhang, B. and Hao, Y. (2014). Integrated transcriptomic and proteomic analysis of the bile stress response in a centenarian-originated probiotic *Bifidobacterium longum* BBMN68. *Molecular & Cellular Proteomics*, **13**: 2558-2572.

An, H.M., Park, S.Y., Lee, D.K., Kim, J.R., Cha, M.K., Lee, S.W., Lim, H.T., Kim, K.J. and Ha, N.J. (2011). Antiobesity and lipid-lowering effects of *Bifidobacterium* spp. in high fat diet-induced obese rats. *Lipids in Health and Disease*, **10**(1): 1-8.

Ansari, F., Pourjafar, H., Tabrizi, A. and Homayouni, A. (2020). The effects of probiotics and prebiotics on mental disorders: a review on depression, anxiety, Alzheimer, and autism spectrum disorders. *Current Pharmaceutical Biotechnology*, **21**: 555-565.

Aparna Sudhakaran, V., Panwar, H., Chauhan, R., Duary, R.K., Rathore, R.K., Batish, V.K. and Grover, S. (2013). Modulation of anti-inflammatory response in

lipopolysaccharide stimulated human THP-1 cell line and mouse model at gene expression level with indigenous putative probiotic lactobacilli. *Genes and Nutrition*, **8**(6): 637-648.

Ara, K., Meguro, S., Hase, T., Tokimitsu, I., Otsuji, K., Kawai, S., Ito, S. and Iino, H. (2002). Effect of spore-bearing lactic acid-forming bacteria (*Bacillus coagulans* SANK 70258) administration on the intestinal environment, defecation frequency, fecal characteristics and dermal characteristics in humans and rats. *Microbial Ecology in Health and Disease*, **14**(1): 4-13.

Arellano, K., Vazquez, J., Park, H., Lim, J., Ji, Y., Kang, H.J., Cho, D., Jeong, H.W. and Holzapfel, W.H. (2020). Safety evaluation and whole-genome annotation of *Lactobacillus plantarum* strains from different sources with special focus on isolates from green tea. *Probiotics and Antimicrobial Proteins*, **12**: 1057-1070.

Aristimuño Ficoseco, C., Mansilla, F.I., Maldonado, N.C., Miranda, H., Fátima Nader-Macias, M.E. and Vignolo, G.M. (2018). Safety and growth optimization of lactic acid bacteria isolated from feedlot cattle for probiotic formula design. *Frontiers in Microbiology*, **9**: 2220.

Aryantini, N.P.D., Yamasaki, E., Kurazono, H., Sujaya, I.N., Urashima, T. and Fukuda, K. (2017). *In vitro* safety assessments and antimicrobial activities of *Lactobacillus rhamnosus* strains isolated from a fermented mare's milk. *Animal Science Journal*, **88**: 517-525.

Asan-Ozusaglam, M. and Gunyakti, A. (2021). A new probiotic candidate bacterium from human milk: *Limosilactobacillus vaginalis* MA-10. *Acta Alimentaria*, **50**: 13-21.

Aydoğan, S., Dilli, D., Özyazici, A., Aydin, N., Şimşek, H., Orun, U.A. and Aksoy, Ö.N. (2022). *Lactobacillus rhamnosus* sepsis associated with probiotic therapy in a term infant with congenital heart disease. *Fetal and Pediatric Pathology*, **41**(5): 823-827.

Azad, M., Kalam, A., Sarker, M. and Wan, D. (2018). Immunomodulatory effects of probiotics on cytokine profiles. *BioMed Research International*, **2018**: 1-10

Azmal Ali, S., Kumar, S., Mohanty, A.K. and Behare, P. (2018). Draft genome sequence of *Lactobacillus fermentum* NCDC 400, isolated from a traditional Indian dairy product. *Genome Announcements*, **6**(2): e01492-17.

Bahrehvar, S., Barzegari, A.A., Khezri, S. and Nejati, V. (2021a). Safety Assessment of *Lactobacillus paracasei* IBRC-M 11110 in Wistar rats: a subacute 28-day toxicity study. *Medical Laboratory Journal*, **15**: 19-26.

Bahrehvar, S., Khezri, S., Barzegari, A.A. and Nejati, V. (2021b). Safety assessment of a new strain of *Lactobacillus pentosus* (IBRC= 11143) as a candidate probiotic. *Pharmaceutical and Biomedical Research*, **7**: 37-46.

Baker, L.M., Webberley, T.S., Masetti, G., Hughes, T.R., Marchesi, J.R., Jack, A.A., Joyce, T.S.C., Allen, M.D., Plummer, S.F., Michael, D.R. and Ramanathan, G. (2021). A genome guided evaluation of the Lab4 probiotic consortium. *Genomics*, **113**: 4028-4038.

Ballini, A., Santacroce, L., Cantore, S., Bottalico, L., Dipalma, G., De Vito, D., Saini, R. and Inchingolo, F. (2018). Probiotics improve urogenital health in women. *Open Access Macedonian Journal of Medical Sciences*, **6**: 1845.

Baloch, M.N., Siddiqui, R., Zafar, U., Haider, F., Mojgani, N. and Eijaz, S. (2019). Persistence and safety assessment of novel probiotic strain *Lactobacillus plantarum* 1 strain Lp86 and Lp36 in *Salmonella typhi* infected mice. *Pakistan Journal of Pharmaceutical Sciences*, **32**: 1261-1267.

Ban, O.H., Oh, S., Park, C., Bang, W.Y., Lee, B.S., Yang, S.Y., Chae, S.A., Jung, Y.H., and Yang, J. (2020). Safety assessment of *Streptococcus thermophilus* IDCC 2201 used for product manufacturing in Korea. *Food Science & Nutrition*, ***8***: 6269-6274.

Banerjee, G., Nandi, A., and Ray, A.K. (2017). Assessment of hemolytic activity, enzyme production and bacteriocin characterization of *Bacillus subtilis* LR1 isolated from the gastrointestinal tract of fish. *Archives of Microbiology*, **199**: 115-124.

Bang, W.Y., Ban, O.H., Lee, B.S., Oh, S., Park, C., Park, M.K., Jung, S.K., Yang, J. and Jung, Y.H. (2021). Genomic-, phenotypic-, and toxicity-based safety assessment and probiotic potency of *Bacillus coagulans* IDCC 1201 isolated from green malt. *Journal of Industrial Microbiology and Biotechnology*, **48**: kuab026.

Barba-Vidal, E., Castillejos, L., López-Colom, P., Rivero Urgell, M., Moreno Muñoz, J.A. and Martín-Orúe, S.M. (2017). Evaluation of the probiotic strain *Bifidobacterium longum* subsp. *infantis* CECT 7210 capacities to improve

health status and fight digestive pathogens in a piglet model. *Frontiers in Microbiology*, **8**: 533.

Baumgartner, A., Kueffer, M., Simmen, A. and Grand, M. (1998). Relatedness of *Lactobacillus rhamnosus* Strains Isolated from Clinical Specimens and Such from Food-stuffs, Humans and Technology. *LWT-Food Science and Technology*, **31**(5): 489-494.

Behare, P.V., Singh, R., Nagpal, R. and Rao, K.H. (2013). Exopolysaccharides producing *Lactobacillus fermentum* strain for enhancing rheological and sensory attributes of low-fat dahi. *Journal of Food Science and Technology*, **50**(6): 1228-1232.

Bhardwaj, A., Gupta, H., Kapila, S., Kaur, G., Vij, S. and Malik, R.K. (2010). Safety assessment and evaluation of probiotic potential of bacteriocinogenic *Enterococcus faecium* KH 24 strain under *in vitro* and *in vivo* conditions. *International Journal of Food Microbiology*, **141**: 156-164.

Bharti, V., Mehta, A., Singh, S., Jain, N. and Ahirwal, L. (2015). Cytotoxicity of live whole cell, heat killed cell and cell free extract of *Lactobacillus* strain in U-87 human glioblastoma cell line and MCF-7 breast cancer cell line. *International Journal of Probiotics and Prebiotics*, **10**: 153-158.

Bhat, M.I., Kapila, S. and Kapila, R. (2020). *Lactobacillus fermentum* (MTCC-5898) supplementation renders prophylactic action against *Escherichia coli* impaired intestinal barrier function through tight junction modulation. *LWT-Food Science and Technology*, **123**: 109-118.

Bhat, M.I., Singh, V.K., Sharma, D., Kapila, S. and Kapila, R. (2019a). Adherence capability and safety assessment of an indigenous probiotic strain *Lactobacillus rhamnosus* MTCC-5897. *Microbial Pathogenesis*, **130**: 120-130.

Bhat, M.I., Sowmya, K., Kapila, S. and Kapila, R. (2019b). *Escherichia coli* K12: an evolving opportunistic commensal gut microbe distorts barrier integrity in human intestinal cells. *Microbial Pathogenesis*, **133**: 103545.

Birri, D.J., Brede, D.A., Tessema, G.T. and Nes, I.F. (2013). Bacteriocin production, antibiotic susceptibility and prevalence of haemolytic and gelatinase activity in faecal lactic acid bacteria isolated from healthy Ethiopian infants. *Microbial Ecology*, **65:** 504-516.

Bisanz, J.E., Macklaim, J.M., Gloor, G.B. and Reid, G. (2014). Bacterial metatranscriptome analysis of a probiotic yogurt using an RNA-Seq approach. *International Dairy Journal*, **39**: 284-292.

Bocci, A., Sebastiani, B., Trotta, F., Federici, E. and Cenci, G. (2015). *In vitro* inhibition of 4-nitroquinoline-1-oxide genotoxicity by probiotic *Lactobacillus rhamnosus* IMC501. *Journal of Microbiology* and *Biotechnology*, **25**: 1680-1686.

Bonham, K.S., Wolfe, B.E. and Dutton, R.J. (2017). Extensive horizontal gene transfer in cheese-associated bacteria. *Elife*, **6**: 22144.

Boumis, E., Capone, A., Galati, V., Venditti, C. and Petrosillo, N. (2018). Probiotics and infective endocarditis in patients with hereditary hemorrhagic telangiectasia: a clinical case and a review of the literature. *BMC Infectious Diseases*, **18**: 65.

Božič, J.T., Butinar, L., Marušič, M.B., Korte, D. and Vodopivec, B.M. (2021). Determination of biogenic amines formation by autochthonous lactic acid bacteria from 'Refošk'grapes using different analytical methods. *LWT-Food Science and Technology*, **156**: 112908.

Burns, A.J. and Rowland, I.R. (2004). Antigenotoxicity of probiotics and prebiotics on faecal water-induced DNA damage in human colon adenocarcinoma cells. *Mutation Research/Fundamental and Molecular Mechanisms of Mutagenesis*, **551**: 233-243.

Bustos, A.Y., de Valdez, G.F., Fadda, S. and Taranto, M.P. (2018). New insights into bacterial bile resistance mechanisms: the role of bile salt hydrolase and its impact on human health. *Food Research International*, **112**: 250-262.

Byakika, S., Mukisa, I.M., Byaruhanga, Y.B. and Muyanja, C., (2019). A review of criteria and methods for evaluating the probiotic potential of microorganisms. *Food Reviews International*, **35**(5): 427-466.

Cai, Y., Liu, L., Xia, M., Tian, C., Wu, W., Dong, B. and Chu, X. (2022). SEDDS facilitate cinnamaldehyde crossing the mucus barrier: the perspective of mucus and Caco-2/HT29 co-culture models. *International Journal of Pharmaceutics*, **614**: 121461.

Caldini, G., Trotta, F., Corsetti, A. and Cenci, G. (2008). Evidence for *in vitro* anti-genotoxicity of cheese non-starter lactobacilli. *Antonie Van Leeuwenhoek*, **93**: 51.

Câmara, S.P.A., Dapkevicius, A., Silva, C.C.G., Malcata, F.X. and LN Enes Dapkevicius, M. (2020). Artisanal Pico cheese as reservoir of *Enterococcus*

species possessing virulence and antibiotic resistance properties: Implications for food safety. *Food Biotechnology*, **34**: 25-41.

Campagne, J., Guichard, J.F., Moulhade, M.C., Kawski, H. and Maurier, F. (2020). *Lactobacillus* endocarditis: a case report in France and literature review. *IDCases*, **21**: 00811.

Cao, L., Du, J., Nie, Z., Jia, R., Yin, G., Xu, P., Ding, W. and Xu, G. (2022). Alteration of endoplasmic reticulum stress, inflammation and anti-oxidative status in cyclophosphamide-damaged liver of Nile tilapia (Oreochromis niloticus). *Comparative Biochemistry and Physiology*, **254**: 109271.

Cao, X., Tang, L., Zeng, Z., Wang, B., Zhou, Y., Wang, Q., Zou, P. and Li, W. (2020). Effects of probiotics BaSC06 on intestinal digestion and absorption, antioxidant capacity, microbiota composition, and macrophage polarization in pigs for fattening. *Frontiers in Veterinary Science*, **7**: 570-593.

Casarotti, S.N., Carneiro, B.M., Todorov, S.D., Nero, L.A., Rahal, P. and Penna, A.L.B. (2017). *In vitro* assessment of safety and probiotic potential characteristics of *Lactobacillus* strains isolated from water buffalo mozzarella cheese. *Annals of Microbiology*, **67**: 289-301.

Celebioglu, H.U., Olesen, S.V., Prehn, K., Lahtinen, S.J., Brix, S., Abou Hachem, M. and Svensson, B. (2017). Mucin-and carbohydrate-stimulated adhesion and subproteome changes of the probiotic bacterium *Lactobacillus acidophilus* NCFM. *Journal of Proteomics*, **163**: 102-110.

Chaiongkarn, A., Dathong, J., Phatvej, W., Saman, P., Kuancha, C., Chatanon, L. and Moonmungmee, S. (2019). Characterization of prebiotics and their synergistic activities with *Lactobacillus* probiotics for β-glucuronidase reduction. *Science Asia*, **45**(6): 538-546.

Chakravarty, S., Parashar, A. and Acharyya, S. (2019). *Saccharomyces cerevisiae* sepsis following probiotic therapy in an infant. *Indian Pediatrics*, **56**: 971-972.

Chang, C.J., Lin, T.L., Tsai, Y.L., Wu, T.R., Lai, W.F., Lu, C.C. and Lai, H.C. (2019). Next generation probiotics in disease amelioration. *Journal of Food and Drug Analysis*, **27**(3): 615-622.

Cherifi, S., Robberecht, J. and Miendje, Y. (2004). *Saccharomyces cerevisiae* fungemia in an elderly patient with *Clostridium difficile* colitis. *Acta Clinica Belgica*, **59**: 223-224.

Chiang, M.C., Chen, C.L., Feng, Y., Chen, C.C., Lien, R. and Chiu, C.H. (2021). *Lactobacillus rhamnosus* sepsis associated with probiotic therapy in an extremely preterm infant: Pathogenesis and a review for clinicians. *Journal of Microbiology, Immunology and Infection*, **54**: 575-580.

Chin, S.C., Abdullah, N., Siang, T.W. and Wan, H.Y. (2005). Plasmid profiling and curing of Lactobacillus strains isolated from the gastrointestinal tract of chicken. *Journal of Microbiology*, **43**(3): 251-256.

Chiu, Y.J., Nam, M.K., Tsai, Y.T., Huang, C.C. and Tsai, C.C. (2013). Genotoxicity assessment of multispecies probiotics using reverse mutation, mammalian chromosomal aberration, and rodent micronucleus tests. *The Scientific World Journal*, **2013**: 1-7.

Choi, D.W., Jung, S.Y., Kang, J., Nam, Y.D., Lim, S.I., Kim, K.T. and Shin, H.S. (2018). Immune-enhancing effect of nanometric *Lactobacillus plantarum* nF1 (nLp-nF1) in a mouse model of cyclophosphamide-induced immunosuppression. *Journal of Microbiology and Biotechnology*,**28**(2): 218-226.

Chokesajjawatee, N., Santiyanont, P., Chantarasakha, K., Kocharin, K., Thammarongtham, C., Lertampaiporn, S., Vorapreeda, T., Srisuk, T., Wongsurawat, T., Jenjaroenpun, P. and Nookaew, I. (2020). Safety assessment of a nham starter culture *Lactobacillus plantarum* BCC9546 via whole-genome analysis. *Scientific Reports*, **10**: 1-12.

Cirrincione, S., Neumann, B., Zühlke, D., Riedel, K. and Pessione, E. (2019). Detailed soluble proteome analyses of a dairy-isolated *Enterococcus faecalis*: A possible approach to assess food safety and potential probiotic value. *Frontiers in Nutrition*, **6**: 71.

Clarke, T. B., Davis, K. M., Lysenko, E. S., Zhou, A. Y., Yu, Y. and Weiser, J. N. (2010). Recognition of peptidoglycan from the microbiota by Nod1 enhances systemic innate immunity. *Nature Medicine*, **16**: 228–231.

Collins, J., van Pijkeren, J.P., Svensson, L., Claesson, M.J., Sturme, M., Li, Y., Cooney, J.C., van Sinderen, D., Walker, A.W., Parkhill, J. and Shannon, O. (2012). Fibrinogen-binding and platelet-aggregation activities of a *Lactobacillus salivarius* septicaemia isolate are mediated by a novel fibrinogen-binding protein. *Molecular Microbiology*, **85**: 862-877.

Comerlato, C.B., Zhang, X., Walker, K., Brandelli, A. and Figeys, D. (2020). Comparative proteomic analysis reveals metabolic variability of probiotic *Enterococcus durans* during aerobic and anaerobic cultivation. *Journal of Proteomics*, **220**: 103764.

Copeland, D.R., McVay, M.R., Dassinger, M.S., Jackson, R.J. and Smith, S.D. (2009). Probiotic fortified diet reduces bacterial colonization and translocation in a long-term neonatal rabbit model. *Journal of Pediatric Surgery*, **44**: 1061-1064.

Cuffaro, B., Assohoun, A.L., Boutillier, D., Súkeníková, L., Desramaut, J., Boudebbouze, S., Salomé-Desnoulez, S., Hrdý, J., Waligora-Dupriet, A.J., Maguin, E. and Grangette, C. (2020). *In vitro* characterization of gut microbiota-derived commensal strains: Selection of *Parabacteroides distasonis* strains alleviating TNBS-induced colitis in mice. *Cells*, **9**: 2104.

Cui, Y., Hu, T., Qu, X., Zhang, L., Ding, Z. and Dong, A. (2015). Plasmids from food lactic acid bacteria: diversity, similarity, and new developments. *International Journal of Molecular Sciences*, **16**(6): 13172-13202.

Cui, Y., Wang, S., Ding, S., Shen, J. and Zhu, K. (2020). Toxins and mobile antimicrobial resistance genes in *Bacillus* probiotics constitute a potential risk for One Health. *Journal of Hazardous Materials*, **382**: 121-266.

Daniel, C., Poiret, S., Goudercourt, D., Dennin, V., Leyer, G. and Pot, B. (2006). Selecting lactic acid bacteria for their safety and functionality by use of a mouse colitis model. *Applied and Environmental Microbiology*, **72**: 5799-5805.

de Jesus, L.C.L., de Jesus Sousa, T., Coelho-Rocha, N.D., Profeta, R., Barroso, F.A.L., Drumond, M.M., Mancha-Agresti, P., Ferreira, Ê., Brenig, B., Aburjaile, F.F. and Azevedo, V. (2022). Safety evaluation of Lactobacillus delbrueckii subsp. lactis CIDCA 133: a health-promoting bacteria. *Probiotics and Antimicrobial Proteins*, **14**(5): 816-829.

de LeBlanc, A.D.M., del Carmen, S., Chatel, J.M., Azevedo, V., Langella, P., Bermudez-Humaran, L. and LeBlanc, J.G. (2016). Evaluation of the biosafety of recombinant lactic acid bacteria designed to prevent and treat colitis. *Journal of Medical Microbiology*, **65**: 1038-1046.

de Souza, B.M.S., Borgonovi, T.F., Casarotti, S.N., Todorov, S.D. and Penna, A.L.B. (2019). *Lactobacillus casei* and *Lactobacillus fermentum* strains isolated from mozzarella cheese: probiotic potential, safety, acidifying kinetic parameters

and viability under gastrointestinal tract conditions. *Probiotics and Antimicrobial Proteins*, **11**: 382-396.

De Vries, M.C., Vaughan, E.E., Kleerebezem, M. and de Vos, W.M., (2006). *Lactobacillus plantarum*—survival, functional and potential probiotic properties in the human intestinal tract. *International Dairy Journal*, **16**(9): 1018-1028.

Deepika Priyadarshani, W.M. and Rakshit, S.K. (2011). Screening selected strains of probiotic lactic acid bacteria for their ability to produce biogenic amines (histamine and tyramine). *International Journal of Food Science and Technology*, **46:** 2062-2069.

Deng, F., Chen, Y., Sun, T., Wu, Y., Su, Y., Liu, C., Zhou, J., Deng, Y. and Wen, J. (2021). Antimicrobial resistance, virulence characteristics and genotypes of *Bacillus* spp. from probiotic products of diverse origins. *Food Research International*, **139**: 109949.

Dey, D.K., Khan, I. and Kang, S.C. (2019). Anti-bacterial susceptibility profiling of *Weissella confusa* DD_A7 against the multidrug-resistant ESBL-positive *E. coli*. *Microbial Pathogenesis*, **128**: 119-130.

Dhanani, A.S. and Bagchi, T., (2013). The expression of adhesin EF-Tu in response to mucin and its role in L actobacillus adhesion and competitive inhibition of enteropathogens to mucin. *Journal of Applied Microbiology*, ***115***(2): 546-554.

Dickson, E.M., Riggio, M.P. and Macpherson, L. (2005). A novel species-specific PCR assay for identifying *Lactobacillus fermentum*. *Journal of Medical Microbiology*, **54**(3): 299-303.

Diehl, R., Ferrara, F., Müller, C., Dreyer, A.Y., McLeod, D.D., Fricke, S. and Boltze, J. (2017). Immunosuppression for *in vivo* research: state-of-the-art protocols and experimental approaches. *Cellular and Molecular Immunology*, **14**: 146-179.

Divisekera, D.M., Samarasekera, J.K.R., Hettiarachchi, C., Maharjan, R., Gooneratne, J., Iqbal Choudhary, M., Gopalakrishnan, S., Wahab, A. and Mazumdar, S.D. (2021). Oral toxicity evaluation of probiotic strains isolated from Finger millet [Eleusine coracana (L.) Gaertn.] in Wistar rat models (in vivo). *Archives of Ecotoxicology*, **3**: 91-102.

Dlamini, Z.C., Langa, R.L., Aiyegoro, O.A. and Okoh, A.I. (2019). Safety evaluation and colonisation abilities of four lactic acid bacteria as future probiotics. *Probiotics and Antimicrobial Proteins*, **11**: 397-402.

Doeun, D., Davaatseren, M. and Chung, M.S. (2017). Biogenic amines in foods. *Food Science and Biotechnology*, **26**: 1463-1474.

Domingos-Lopes, M.F.P., Stanton, C., Ross, P.R., Dapkevicius, M.L.E. and Silva, C.C.G. (2017). Genetic diversity, safety and technological characterization of lactic acid bacteria isolated from artisanal Pico cheese. *Food Microbiology*, **63**: 178-190.

Doron, S. and Snydman, D.R. (2015). Risk and safety of probiotics. *Clinical Infectious Diseases*, **60**: S129-S134.

Dos Santos, C.I., Campos, C.D., Nunes-Neto, W.R., do Carmo, M.S., Nogueira, F.A., Ferreira, R.M., Costa, E.P., Gonzaga, L.F., Araújo, J.M., Monteiro, J.M. and Monteiro, C.R.A. (2021). Genomic Analysis of *Limosilactobacillus fermentum* ATCC 23271, a Potential Probiotic Strain with Anti-Candida Activity. *Journal of Fungi*, **7**: 794.

Druart, C., Plovier, H., Van Hul, M., Brient, A., Phipps, K.R., de Vos, W.M. and Cani, P.D. (2020). Toxicological safety evaluation of pasteurized *Akkermansia muciniphila*. *Journal of Applied Toxicology*, **41**: 276-290.

Dubbert, S., Klinkert, B., Schimiczek, M., Wassenaar, T.M., and Bünau, R.V. (2020). No genotoxicity is detectable for *Escherichia coli* strain Nissle 1917 by standard in vitro and in vivo tests. *European Journal of Microbiology and Immunology*, **10**: 11-19.

Duc, K.M., Kang, B.G., Lee, C., Park, H.J., Park, Y.M., Joung, Y.H. and Bang, I.S. (2020). The small protein CydX is required for Cytochrome bd quinol oxidase stability and function in Salmonella enterica Serovar Typhimurium: a Phenotypic Study. *Journal of Bacteriology*, **202**(2): e00348-19.

EFSA Panel on Additives and Products or Substances used in Animal Feed (FEEDAP). (2012). Guidance on the assessment of bacterial susceptibility to antimicrobials of human and veterinary importance. *EFSA Journal*, **10**: 2740.

Elsayed, F.F., Elshenawy, W.M., Khalifa, E.M., Rizq, M.R. and Abdelaziz, R.R. (2022). Ameliorative effect of flavocoxid on cyclophosphamide-induced cardio and neurotoxicity via targeting the GM-CSF/NF-κB signaling pathway. *Environmental Science and Pollution Research*, **29**: 1-17.

Endo, K., Mine, Y., Shuto, T., Taji, T., Murayama, T. and Nikawa, H. (2020). Comprehensive analysis of transcriptional profiles in oral epithelial-like cells

stimulated with oral probiotic *Lactobacillus* spp. *Archives of Oral Biology*, **118**: 104832.

Endres, J.R., Qureshi, I., Farber, T., Hauswirth, J., Hirka, G., Pasics, I. and Schauss, A.G. (2011). One-year chronic oral toxicity with combined reproduction toxicity study of a novel probiotic, *Bacillus coagulans*, as a food ingredient. *Food and Chemical Toxicology*, **49**: 1174-1182.

Erginkaya, Z.E.R.R.İ.N., Turhan, E.U. and Tatlı, D. (2018). Determination of antibiotic resistance of lactic acid bacteria isolated from traditional Turkish fermented dairy products. *Iranian Journal of Veterinary Research*, **19**: 53.

Fareez, I.M., Lim, S.M. and Ramasamy, K. (2019). Microencapsulated *Lactobacillus plantarum* LAB12 showed no sign of acute or sub-chronic toxicity in vivo. *Probiotics and Antimicrobial Proteins*, **11**: 447-459.

Feng, L., Huang, Q., Huang, Z., Li, H., Qi, X., Wang, Y., Liu, Z., Liu, X. and Lu, L. (2016). Optimized animal model of cyclophosphamide-induced bone marrow suppression. *Basic & Clinical Pharmacology and Toxicology*, **119**(5): 428-435.

Fernández-Murga, M.L. and Sanz, Y. (2016). Safety assessment of *Bacteroides uniformis* CECT 7771 isolated from stools of healthy breast-fed infants. *PLoS One*, **11**: 0145503.

Fochesato, A.S., Martínez, M.P., Escobar, F.S., García, G., Dogi, C.A. and Cavaglieri, L.R. (2020). Cytotoxicity in Vero cells and cytokines analyses in Balb/c mice as safety assessments of the probiotic mixture *Saccharomyces cerevisiae* RC016 and *Lactobacillus rhamnosus* RC007 for use as a feed additive. *Letters in Applied Microbiology*, **71**: 400-404.

Forsythe, P. (2011). Probiotics and lung diseases. *Chest*, **139**(4): 901-908.

Fu, X., Lyu, L., Wang, Y., Zhang, Y., Guo, X., Chen, Q. and Liu, C. (2022). Safety assessment and probiotic characteristics of *Enterococcus lactis* JDM1. *Microbial Pathogenesis*, **163**: 105380.

Fuller, R. (1992). History and development of probiotics. In R. Fuller (Eds.), *Probiotics* (1-8). Springer, Dordrecht.

Ganguly, N.K., Bhattacharya, S.K., Sesikeran, B., Nair, G.B., Ramakrishna, B.S., Sachdev, H.P.S., Batish, V.K., Kanagasabapathy, A.S., Muthuswamy, V., Kathuria, S.C. and Katoch, V.M. (2011). ICMR-DBT guidelines for evaluation of probiotics in food. *Indian Journal of Medical Research*, **134**(1): 22-25.

Gao, D., Liu, Z., Liu, F., Chen, L., Wang, W., Ma, J., Xu, C., Jiang, Z. and Hou, J. (2021). Study of the immunoregulatory effect of *Lactobacillus rhamnosus* 1.0320 in immunosuppressed mice. *Journal of Functional Foods*, **79**: 104423.

Garle, M.J., Fentem, J.H. and Fry, J.R. (1994). *In vitro* cytotoxicity tests for the prediction of acute toxicity *in vivo*. *Toxicology in vitro*, **8**: 1303-1312.

Gavriely, S., Richter, S. and Zucker, I. (2022). Mucin-Based Composites for Efficient Mercuric Biosorption. *Advanced Sustainable Systems*, **6**(7): 2200081.

Gawande, K., Kolhekar, M., Kumari, M., Kapila, S., Sharma, P., Ali, S.A. and Behare, P.V. (2021). Lactic acid bacteria based purified exopolysaccharide showed viscofying and hypercholesterolemic capabilites. *Food Hydrocolloids for Health*, **1**: 100042.

Geier, M.S., Butler, R.N., Giffard, P.M. and Howarth, G.S. (2007). *Lactobacillus fermentum* BR11, a potential new probiotic, alleviates symptoms of colitis induced by dextran sulfate sodium (DSS) in rats. *International Journal of Food Microbiology*, **114**: 267-274.

Ghasemi, A., Hedayati, M. and Biabani, H. (2007). Protein precipitation methods evaluated for determination of serum nitric oxide end products by the Griess assay. *Journal of Medical Sciences Research*, **2**(15): 29-32.

Gómez del Pulgar, E.M., Benítez-Páez, A. and Sanz, Y. (2020). Safety assessment of *Bacteroides uniformis* CECT 7771, a symbiont of the gut microbiota in infants. *Nutrients*, **12**: 551.

Gonzalez Pereyra, M.L., Dogi, C., Torres Lisa, A., Wittouck, P., Ortíz, M., Escobar, F., Bagnis, G., Yaciuk, R., Poloni, L., Torres, A. and Dalcero, A.M. (2014). Genotoxicity and cytotoxicity evaluation of probiotic *Saccharomyces cerevisiae* RC 016: a 60-day subchronic oral toxicity study in rats. *Journal of Applied Microbiology*, **117**: 824-833.

Gorbach, S., Doron, S. and Magro, F., (2017). *Lactobacillus rhamnosus* GG. In *The microbiota in gastrointestinal pathophysiology* (79-88). Academic Press.

Gore, S. and Tucker, K. (2020). Bloodstream infections with typical probiotic organisms. *Infection Control and Hospital Epidemiology*, **41**: 22-s22.

Goyal, C. (2018). *Whole Genome Sequencing of Lactobacillus Reuteri LR6 and Validation of Its Unique Features* (Doctoral dissertation, NDRI).

Gramajo Lopez, A., Gutiérrez, F., Saavedra, L., Hebert, E.M., Alvarez, S. and Salva, S. (2021). Improvement of myelopoiesis in cyclophosphamide-

immunosuppressed mice by oral administration of viable or non-viable lactobacillus strains. *Frontiers in Immunology*, **12**: 647049.

Gueimonde, M., Ouwehand, A.C. and Salminen, S. (2004). Safety of probiotics. *Scandinavian Journal of Nutrition*, **48**(1): 42-48.

Gueimonde, M., Sánchez, B., de los Reyes-Gavilán, C.G. and Margolles, A. (2013). Antibiotic resistance in probiotic bacteria. *Frontiers in Microbiology*, **4**: 202.

Gupta, M., Pattanaik, A.K., Singh, A., Sharma, S. and Jadhav, S.E. (2021a). An appraisal of the gut health modulatory effects of a calf faecal-origin probiotic *Lactobacillus salivarius* CPN60 using Wistar rats with dextran sulfate sodium-induced colitis. *Journal of the Science of Food and Agriculture*, **101**(4): 1340-1348.

Gupta, M., Pattanaik, A.K., Singh, A., Sharma, S., Jadhav, S.E., Kumar, A. and Verma, A.K. (2021b). Functional and probiotic characterization of *Ligilactobacillus salivarius* CPN60 isolated from calf faeces and its appraisal in rats. *Journal of Bioscience and Bioengineering*, **132**(6): 575-584.

Haghighat, L. and Crum-Cianflone, N.F. (2016). The potential risks of probiotics among HIV-infected persons: Bacteraemia due to *Lactobacillus acidophilus* and review of the literature. *International Journal of Std and Aids*, **27**: 1223-1230.

Han, J.S., Back, S.M., Cho, J.W., Park, H.J., Kim, W.J., Park, S.H., Noh, J.H., Kim, Y.B. and Lee, B.S. (2021). Genotoxicity and subchronic general toxicity assessments of *Lactobacillus curvatus* WiKim 38 using Sprague-Dawley rats. *Food and Chemical Toxicology*, **152**: 112199.

Haro, C. and Medina, M. (2019). *Lactobacillus casei* CRL 431 improves endothelial and platelet functionality in a pneumococcal infection model. *Beneficial Microbes*, **10**: 533-541.

He, F. (2011). Laemmli-sds-page. *Bio-protocol*, **1**:e80-e80.

Hill, C., Guarner, F., Reid, G., Gibson, G.R., Merenstein, D.J., Pot, B., Morelli, L., Canani, R.B., Flint, H.J., Salminen, S. and Calder, P.C. (2014). Expert consensus document: The International Scientific Association for Probiotics and Prebiotics consensus statement on the scope and appropriate use of the term probiotic. *Nature Reviews Gastroenterology and Hepatology*, **11**: 506.

Hou, F.X., Yang, H.F., Yu, T. and Chen, W. (2007). The immunosuppressive effects of 10mg/ kg cyclophosphamide in Wistar rats. *Environmental Toxicology and Pharmacology*, **24**(1): 30–36.

Huang, H., Lai, W., Cui, M., Liang, L., Lin, Y., Fang, Q., Liu, Y. and Xie, L. (2016). An evaluation of blood compatibility of silver nanoparticles. *Scientific Reports*, **6**(1): 1-15.

Hummel, A.S., Hertel, C., Holzapfel, W.H. and Franz, C.M. (2007). Antibiotic resistances of starter and probiotic strains of lactic acid bacteria. *Applied and Environmental Microbiology*, **73**: 730-739.

Huyan, X.H., Lin, Y.P., Gao, T., Chen, R.Y. and Fan, Y.M. (2011). Immunosuppressive effect of cyclophosphamide on white blood cells and lymphocyte subpopulations from peripheral blood of Balb/c mice. *International Immunopharmacology*, **11**: 1293-1297.

Ihedioha, J.I., Ugwuja, J.I., Noel-Uneke, O.A., Udeani, I.J. and Daniel-Igwe, G. (2012). Reference values for the haemotology profile of conventional grade outbred albino mice (*Mus musculus*) in Nsukka, Eastern Nigeria. *Animal Research International*, **9**(2): 1-10.

Iqubal, A., Syed, M.A., Haque, M.M., Najmi, A.K., Ali, J. and Haque, S.E. (2020). Effect of nerolidol on cyclophosphamide-induced bone marrow and hematologic toxicity in Swiss albino mice. *Experimental Hematology*, **82**: 24-32.

Isa, K., Oka, K., Beauchamp, N., Sato, M., Wada, K., Ohtani, K., Nakanishi, S., McCartney, E., Tanaka, M., Shimizu, T. and Kamiya, S. (2016). Safety assessment of the *Clostridium butyricum* MIYAIRI 588® probiotic strain including evaluation of antimicrobial sensitivity and presence of *Clostridium toxin* genes *in vitro* and teratogenicity *in vivo*. *Human & Experimental Toxicology*, **35**: 818-832.

Ishibashi, N. and Yamazaki, S. (2001). Probiotics and safety. *American Journal of Clinical Nutrition*, **73**(2): 465s-470s.

Jarocki, P., Komoń-Janczara, E., Glibowska, A., Dworniczak, M., Pytka, M., Korzeniowska-Kowal, A., Wzorek, A. and Kordowska-Wiater, M. (2020). Molecular routes to specific identification of the *Lactobacillus casei* group at the species, subspecies and strain level. *International Journal of Molecular Sciences*, **21**(8): 2694.

Jaglin, M., Rhimi, M., Philippe, C., Pons, N., Bruneau, A., Goustard, B., Daugé, V., Maguin, E., Naudon, L. and Rabot, S. (2018). Indole, a signaling molecule

produced by the gut microbiota, negatively impacts emotional behaviors in rats. *Frontiers in Neuroscience*, **12**: 216.

Jayashree, S., Karthikeyan, R., Nithyalakshmi, S., Ranjani, J., Gunasekaran, P. and Rajendhran, J. (2018). Anti-adhesion property of the potential probiotic strain *Lactobacillus fermentum* 8711 against methicillin-resistant *Staphylococcus aureus* (MRSA). *Frontiers in Microbiology*, **9**: 411.

Jeelani, R., Khan, S.N., Shaeib, F., Kohan-Ghadr, H.R., Aldhaheri, S.R., Najafi, T., Thakur, M., Morris, R. and Abu-Soud, H.M. (2017). Cyclophosphamide and acrolein induced oxidative stress leading to deterioration of metaphase II mouse oocyte quality. *Free Radical Biology and Medicine*, **110**: 11-18.

Jiang, Q., He, X., Shui, Y., Lyu, X., Wang, L., Xu, L., Chen, Z., Zou, L., Zhou, X., Cheng, L. and Li, M. (2021). D-Alanine metabolic pathway, a potential target for antibacterial drug designing in *Enterococcus faecalis*. *Microbial Pathogenesis*, **158**: 105078.

Junior, W.J.F.L., Guerra, A.F., Tarrah, A., da Silva Duarte, V., Giacomini, A., Luchese, R.H. and Corich, V. (2020). Safety and stability of two potentially probiotic lactobacillus strains after *in vitro* gastrointestinal transit. *Probiotics and Antimicrobial Proteins*, **12:** 657–666.

Kaktcham, P.M., Temgoua, J.B., Zambou, F.N., Diaz-Ruiz, G., Wacher, C. and Pérez-Chabela, M.D.L. (2018). *In vitro* evaluation of the probiotic and safety properties of bacteriocinogenic and non-bacteriocinogenic lactic acid bacteria from the intestines of Nile tilapia and common carp for their use as probiotics in aquaculture. *Probiotics and antimicrobial proteins*, **10**(1): 98-109.

Kang, M.S., Yeu, J.E. and Hong, S.P. (2019). Safety evaluation of oral care probiotics Weissella cibaria CMU and CMS1 by phenotypic and genotypic analysis. *International Journal of Molecular Sciences*, **20**(11): 2693.

Kapila, S., Sinha, P.R. and Singh, S., (2007). Influence of feeding fermented milk and non-fermented milk containing *Lactobacillus casei* on immune response in mice. *Food and agricultural immunology*, **18**(1): 75-82.

Kato, K., Funabashi, N., Takaoka, H., Kohno, H., Kishimoto, T., Nakatani, Y., Matsumiya, G. and Kobayashi, Y. (2016). *Lactobacillus paracasei* endocarditis in a consumer of probiotics with advanced and severe bicuspid aortic valve stenosis complicated with diffuse left ventricular mid-layer fibrosis. *International Journal of Cardiology*, **224**: 157-161.

Kaur, G., Ali, S.A., Kumar, S., Mohanty, A.K. and Behare, P. (2017). Label-free quantitative proteomic analysis of *Lactobacillus fermentum* NCDC 400 during bile salt exposure. *Journal of Proteomics*, **167**: 36-45.

Kaźmierczak-Siedlecka, K., Skonieczna-Żydecka, K., Hupp, T., Duchnowska, R., Marek-Trzonkowska, N. and Połom, K. (2022). Next-generation probiotics–do they open new therapeutic strategies for cancer patients?. *Gut Microbes*, **14**(1): 2035659.

Kerrigan, S.W. (2015). Platelet interactions with bacteria. In *The Non-Thrombotic Role of Platelets in Health and Disease*. Intech Open.

Khalkhali, S. and Mojgani, N. (2018). *In vitro* and *in vivo* safety analysis of *Enterococcus faecium* 2C isolated from human breast milk. *Microbial Pathogenesis*, **116**: 73-77.

Kim, H.J. and Kang, S.A. (2020). Antibiotic resistance and safety assessment of *Enterococcus faecium* CKDB003 for using as probiotics. *The Korean Journal of Food and Nutrition*, **33**: 223-236.

Kim, J.Y., Kim, J.Y., Kim, H., Moon, E.C., Heo, K., Shim, J.J. and Lee, J.L. (2022). Probiotic strains *Bifidobacterium animalis* ssp. *lactis* HY8002 and *Lactobacillus plantarum* HY7717 improved immunosuppression in cyclophosphamide-treated mice. *Journal of Animal Science and Technology*, **24**: 1-10.

Kim, K.M., Jung, T.S., Ok, S., Ko, C.Y. and Kang, J.S. (2012). Evaluation of genotoxicity of *Bacillus mojavensis* KJS-3 on culture supernatant for use as a probiotic. *Molecular and Cellular Toxicology*, **8**: 77-81.

Kim, K.T., Yang, S.J. and Paik, H.D. (2021). Probiotic properties of novel probiotic *Levilactobacillus brevis* KU15147 isolated from radish kimchi and its antioxidant and immune-enhancing activities. *Food Science and Biotechnology*, **30**: 257-265.

Kim, M.J., Jeon, D.G., Lim, Y. and Jang, I. (2022). Effects of prebiotics in combination with probiotics on intestinal hydrolase activity, microbial population and immunological biomarkers in SD rats fed an AIN-93G diet. *Laboratory Animal Research*, **38**(1): 1-10.

Kim, M.J., Ku, S., Kim, S.Y., Lee, H.H., Jin, H., Kang, S., Li, R., Johnston, T.V., Park, M.S. and Ji, G.E. (2018). Safety evaluations of *Bifidobacterium bifidum* BGN4

and *Bifidobacterium longum* BORI. *International Journal of Molecular Sciences*, **19**(5): 1422.

Kim, T., Mondal, S.C., Jeong, C.R., Kim, S.R., Ban, O.H., Jung, Y.H., Yang, J. and Kim, S.J. (2021). Safety evaluation of *Lactococcus lactis* IDCC 2301 isolated from homemade cheese. *Food Science and Nutrition*, **10**(1): 1-8.

Kirjavainen, P.V., Tuomola, E.M., Crittenden, R.G., Ouwehand, A.C., Harty, D.W., Morris, L.F., Rautelin, H., Playne, M.J., Donohue, D.C. and Salminen, S.J. (1999). In vitro adhesion and platelet aggregation properties of bacteremia-associated lactobacilli. *Infection and immunity*, **67**(5): 2653-2655.

Klein, G., Schanstra, J.P., Hoffmann, J., Mischak, H., Siwy, J. and Zimmermann, K. (2013). Proteomics as a quality control tool of pharmaceutical probiotic bacterial lysate products. *PloS One*, **8**: 66682.

Klein, R., Nagy, O., Tóthová, C. and Chovanová, F. (2020). Clinical and diagnostic significance of lactate dehydrogenase and its isoenzymes in animals. (2022). *Veterinary Medicine International*, **2020**: 1-11.

Kochan, P., Chmielarczyk, A., Szymaniak, L., Brykczynski, M., Galant, K., Zych, A., Pakosz, K., Giedrys-Kalemba, S., Lenouvel, E. and Heczko, P.B. (2011). *Lactobacillus rhamnosus* administration causes sepsis in a cardiosurgical patient—is the time right to revise probiotic safety guidelines?. *Clinical Microbiology and Infection*, **17**: 1589-1592.

Kong, X., Duan, W., Li, D., Tang, X. and Duan, Z. (2020). Effects of polysaccharides from Auricularia auricula on the immuno-stimulatory activity and gut microbiota in immunosuppressed mice induced by cyclophosphamide. *Frontiers in Immunology*, **11**: 595700.

Koper, K., Wileński, S. and Koper, A. (2021). Advancements in cancer chemotherapy. *Physical Sciences Reviews*, 12: 206.

Koppel, N., Rekdal, V.M. and Balskus, E.P. (2017). Chemical transformation of xenobiotics by the human gut microbiota. *Science*, **356**: 2770.

Koskenniemi, K., Laakso, K., Koponen, J., Kankainen, M., Greco, D., Auvinen, P., Savijoki, K., Nyman, T.A., Surakka, A., Salusjärvi, T. and de Vos, W.M. (2011). Proteomics and transcriptomics characterization of bile stress response in probiotic *Lactobacillus rhamnosus* GG. *Molecular and Cellular Proteomics*, **10**: S1-S18.

Ku, S., Yang, S., Lee, H.H., Choe, D., Johnston, T.V., Ji, G.E. and Park, M.S. (2020). Biosafety assessment of *Bifidobacterium animalis* subsp. *lactis* AD011 used for human consumption as a probiotic microorganism. *Food Control*, **117**: 106985.

Kumari, M., Dasriya, V.L., Nataraj, B.H., Nagpal, R. and Behare, P.V. (2022). *Lacticaseibacillus rhamnosus*-Derived Exopolysaccharide Attenuates D-Galactose-Induced Oxidative Stress and Inflammatory Brain Injury and Modulates Gut Microbiota in a Mouse Model. *Microorganisms*, **10**(10): 2046.

Kusumitha, S., Aeron, V. and Chidambaram, R. (2020). Prebiotics and Probiotics in the Formulation of Infant Foods. In Tomy J. G. (Eds.), *Food Science, Technology and Nutrition for Babies and Children* (35-57). Springer, Cham.

Lee, B.S., Ban, O.H., Bang, W.Y., Chae, S.A., Oh, S., Park, C., Lee, M., Kim, S.J., Yang, J. and Jung, Y.H. (2021). Safety assessment of *Lactobacillus reuteri* IDCC 3701 based on phenotypic and genomic analysis. *Annals of Microbiology*, **71**: 1-6.

Lee, D.K., Park, S.Y., Jang, S., Baek, E.H., Kim, M.J., Huh, S.M., Choi, K.S., Chung, M.J., Kim, J.E., Lee, K.O. and Ha, N.J. (2011). The combination of mixed lactic acid bacteria and dietary fiber lowers serum cholesterol levels and fecal harmful enzyme activities in rats. *Archives of Pharmacal Research*, **34**(1): 23-29.

Lee, D.Y., Seo, Y.S., Rayamajhi, N., Kang, M.L., Lee, S.I. and Yoo, H.S. (2009). Isolation, characterization, and evaluation of wild isolates of *Lactobacillus reuteri* from pig feces. *The Journal of Microbiology*, **47**(6): 663-672.

Lee, Y.R., Bang, W.Y., Baek, K.R., Kim, G.H., Kang, M.J., Yang, J. and Seo, S.O. (2022). Safety Evaluation by Phenotypic and Genomic Characterization of Four Lactobacilli Strains with Probiotic Properties. *Microorganisms*, **10**(11): 2218.

Lefevre, M., Racedo, S.M., Denayrolles, M., Ripert, G., Desfougères, T., Lobach, A.R., Simon, R., Pélerin, F., Jüsten, P. and Urdaci, M.C. (2017). Safety assessment of *Bacillus subtilis* CU1 for use as a probiotic in humans. *Regulatory Toxicology and Pharmacology*, **83**: 54-65.

Lengliz, S., Abbassi, M.S., Rehaiem, A., Ben Chehida, N. and Najar, T. (2021). Characterization of bacteriocinogenic *Enterococcus* isolates from wild and

laboratory rabbits for the selection of autochthonous probiotic strains in Tunisia. *Journal of Applied Microbiology*, **131**: 1474-1486.

Leong, K.W. and Ding, J.L. (2014). The unexplored roles of human serum IgA. *DNA and Cell Biology*, **33**(12): 823-829.

Lewis, S.P., Lewis, A.T. and Lewis, P.D. (2013). Prediction of glycoprotein secondary structure using ATR-FTIR. *Vibrational Spectroscopy*, **69**: 21-29.

Li, A., Wang, Y., Li, Z., Qamar, H., Mehmood, K., Zhang, L., Liu, J., Zhang, H. and Li, J. (2019). Probiotics isolated from yaks improves the growth performance, antioxidant activity, and cytokines related to immunity and inflammation in mice. *Microbial Cell Factories*, **18**(1): 1-12.

Li, B., Jin, D., Etareri Evivie, S., Li, N., Yan, F., Zhao, L., Liu, F. and Huo, G. (2017). Safety assessment of *Lactobacillus helveticus* KLDS1. 8701 based on whole genome sequencing and oral toxicity studies. *Toxins*, **9**: 301.

Li, B., Zhan, M., Evivie, S.E., Jin, D., Zhao, L., Chowdhury, S., Sarker, S.K., Huo, G. and Liu, F. (2018). Evaluating the safety of potential probiotic *Enterococcus durans* KLDS6. 0930 using whole genome sequencing and oral toxicity study. *Frontiers in Microbiology*, **9**: 1943.

Li, M., Wang, Y., Cui, H., Li, Y., Sun, Y. and Qiu, H.J. (2020). Characterization of lactic acid Bacteria Isolated from the gastrointestinal tract of a wild boar as potential probiotics. *Frontiers in Veterinary Science*, **7**: 49.

Liang, S., Gao, D., Liu, H., Wang, C. and Wen, J. (2018). Metabolomic and proteomic analysis of D-lactate-producing *Lactobacillus delbrueckii* under various fermentation conditions. *Journal of Industrial Microbiology and Biotechnology*, **45**: 681-696.

Liao, P.L., Wu, C.C., Chen, T.Y., Tsai, Y.C., Peng, W.S., Yang, D.J. and Kang, J.J. (2019). Toxicity studies of *Lactobacillus plantarum* PS128TM isolated from spontaneously fermented mustard greens. *Foods*, **8**: 668.

Lin, T.L., Shu, C.C., Lai, W.F., Tzeng, C.M., Lai, H.C. and Lu, C.C. (2019). Investiture of next generation probiotics on amelioration of diseases–strains do matter. *Medicine in Microecology*, **1**: 00002.

Lin, Y.C., Chen, Y.T. and Chen, M.J. (2018). Lack of mutagenicity, genotoxicity and developmental toxicity in safety assessment tests of *Lactobacillus mali* APS1. *PLoS One*, **13**: 0208881.

Lin, Y.P., Thibodeaux, C.H., Peña, J.A., Ferry, G.D. and Versalovic, J. (2008). Probiotic Lactobacillus reuteri suppress proinflammatory cytokines via c-Jun. *Inflammatory Bowel Diseases*, **14**(8): 1068-1083.

Liong, M.T. (2008). Safety of probiotics: translocation and infection. *Nutrition Reviews*, **66**: 192-202.

Liu, J., Wang, Y., Li, A., Iqbal, M., Zhang, L., Pan, H., Liu, Z. and Li, J. (2020). Probiotic potential and safety assessment of *Lactobacillus* isolated from yaks. *Microbial Pathogenesis*, **145**: 104213.

Liu, X., Zhang, Z., Liu, J., Wang, Y., Zhou, Q., Wang, S. and Wang, X. (2019). Ginsenoside Rg3 improves cyclophosphamide-induced immunocompetence in Balb/c mice. *International Immunopharmacology*, **72**: 98-111.

Lorencová, E., Buňková, L., Matoulková, D., Dráb, V., Pleva, P., Kubáň, V. and Buňka, F. (2012). Production of biogenic amines by lactic acid bacteria and bifidobacteria isolated from dairy products and beer. *International Journal of Food Science and Technology*, **47**: 2086-2091.

Louis, P., Hold, G.L. and Flint, H.J. (2014). The gut microbiota, bacterial metabolites and colorectal cancer. *Nature Reviews Microbiology*, **12**: 661-672.

Lu, H., Zhao, W., Liu, W.H., Sun, T., Lou, H., Wei, T., Hung, W.L. and Chen, Q. (2021). Safety Evaluation of *Bifidobacterium lactis* BL-99 and *Lacticaseibacillus paracasei* K56 and ET-22 in vitro and in vivo. *Frontiers in Microbiology*, **12**: 686541.

Lutgendorff, F., Trulsson, L.M., van Minnen, L.P., Rijkers, G.T., Timmerman, H.M., Franzén, L.E., Gooszen, H.G., Akkermans, L.M., Soderholm, J.D. and Sandstrom, P.A. (2008). Probiotics enhance pancreatic glutathione biosynthesis and reduce oxidative stress in experimental acute pancreatitis. *American Journal of Physiology-Gastrointestinal and Liver Physiology*, **295**: G1111-G1121.

Lv, L., Mu, D., Du, Y., Yan, R. and Jiang, H. (2021). Mechanism of the Immunomodulatory Effect of the Combination of Live *Bifidobacterium, Lactobacillus, Enterococcus,* and *Bacillus* on Immunocompromised Rats. *Frontiers in Immunology*, **12**: 2342.

Ma, Q., Fu, Y., Sun, H., Huang, Y., Li, L., Yu, Q., Dinnyes, A. and Sun, Q. (2017). Antimicrobial resistance of *Lactobacillus* spp. from fermented foods and human gut. *LWT-Food Science and Technology*, **86**: 201-208.

Magni, C., de Felipe, F.L., López, P. and de Mendoza, D. (1996). Characterization of an insertion sequence-like element identified in plasmid pCIT264 from *Lactococcus lactis* subsp. *lactis* biovar *diacetylactis*. *FEMS Microbiology Letters*, **136**(3): 289-295.

Mann, S., Park, M.S., Johnston, T.V., Ji, G.E., Hwang, K.T. and Ku, S. (2021a). Isolation, Characterization and Biosafety Evaluation of *Lactobacillus fermentum* OK with Potential Oral Probiotic Properties. *Probiotics and Antimicrobial Proteins*, **13**(5): 1363-1386.

Mann, S., Park, M.S., Johnston, T.V., Ji, G.E., Hwang, K.T. and Ku, S. (2021b). Oral probiotic activities and biosafety of *Lactobacillus gasseri* HHuMIN D. *Microbial Cell Factories*, **20**(1): 1-24.

Mathur, S. and Singh, R. (2005). Antibiotic resistance in food lactic acid bacteria—a review. *International Journal of Food Microbiology*, **105**(3): 281-295.

Mazkour, S., Shekarforoush, S.S. and Basiri, S. (2019). The effects of supplementation of *Bacillus subtilis* and *Bacillus coagulans* spores on the intestinal microflora and growth performance in rat. *Iranian Journal of Microbiology*, **11**(3): 260.

Mbye, M., Baig, M.A., AbuQamar, S.F., El-Tarabily, K.A., Obaid, R.S., Osaili, T.M., Al-Nabulsi, A.A., Turner, M.S., Shah, N.P. and Ayyash, M.M. (2020). Updates on understanding of probiotic lactic acid bacteria responses to environmental stresses and highlights on proteomic analyses. *Comprehensive Reviews in Food Science and Food Safety*, **19**: 1110-1124.

McGown, A.T. and Fox, B.W. (1986). A proposed mechanism of resistance to cyclophosphamide and phosphoramide mustard in a Yoshida cell line *in vitro*. *Cancer Chemotherapy and Pharmacology*, **17**(3): 223-226.

Meini, S., Laureano, R., Fani, L., Tascini, C., Galano, A., Antonelli, A. and Rossolini, G.M. (2015). Breakthrough *Lactobacillus rhamnosus* GG bacteremia associated with probiotic use in an adult patient with severe active ulcerative colitis: case report and review of the literature. *Infection*, **43**: 77-781.

Meleh, H.U., Choo, S., Desa, M.N.M., Chew, S.Y., Rangasamy, P., Hassan, H. and Than, L.T.L. (2020). Isolation and safety characterisation of lactobacilli strains with antimicrobial properties as potential probiotics for human use. *LWT-Food Science and Technology*, **13**: 109796.

Meng, Y., Li, B., Jin, D., Zhan, M., Lu, J. and Huo, G. (2018). Immunomodulatory activity of *Lactobacillus plantarum* KLDS1. 0318 in cyclophosphamide-treated mice. *Food and Nutrition Research*, **62**:1296.

Meng, Y., Wang, J., Wang, Z., Zhang, G., Liu, L., Huo, G. and Li, C. (2019). *Lactobacillus plantarum* KLDS1. 0318 ameliorates impaired intestinal immunity and metabolic disorders in cyclophosphamide-treated mice. *Frontiers in Microbiology*, **10**: 731.

Mercha, I., Lakram, N., Kabbour, M.R., Bouksaim, M. and Zkhiri, F. (2020). Probiotic and technological features of *Enterococcus* and *Weissella* isolates from camel milk characterised by an Argane feeding regimen. *Archives of Microbiology*, **202:** 2207–2219.

Minasyan, H. (2019). Sepsis: mechanisms of bacterial injury to the patient. *Scandinavian Journal of Trauma, Resuscitation and Emergency Medicine*, **27**(1): 1-22.

Moffett, J.R., Arun, P., Puthillathu, N., Vengilote, R., Ives, J.A., Badawy, A.A. and Namboodiri, A.M. (2020). Quinolinate as a marker for kynurenine metabolite formation and the unresolved question of NAD+ synthesis during inflammation and infection. *Frontiers in Immunology*, **11**: 31.

Mora, D. and Arioli, S. (2014). Microbial urease in health and disease. *PLoS Pathogens*, **10**(12): 1004472.

Morovic, W., Roper, J.M., Smith, A.B., Mukerji, P., Stahl, B., Rae, J.C. and Ouwehand, A.C. (2017). Safety evaluation of HOWARU® Restore (*Lactobacillus acidophilus* NCFM, *Lactobacillus paracasei* Lpc-37, *Bifidobacterium animalis* subsp. *lactis* Bl-04 and *B. lactis* Bi-07) for antibiotic resistance, genomic risk factors, and acute toxicity. *Food and Chemical Toxicology*, **110**: 316-324.

Motro, Y. and Moran-Gilad, J. (2017). Next-generation sequencing applications in clinical bacteriology. *Biomolecular Detection and Quantification*, **14**: 1-6.

Mroczynska, M. and Libudzisz, Z.D.Z.I.S.Ł.A.W.A. (2010). Beta-glucuronidase and beta-glucosidase activity of *Lactobacillus* and *Enterococcus* isolated from human feces. *Polish Journal of Microbiology*, **59**: 265-269.

Muftuoglu, M.A.T., Isikgor, S., Tosun, S. and Saglam, A. (2006). Effects of probiotics on the severity of experimental acute pancreatitis. *European Journal of Clinical Nutrition*, **60**: 464-468.

Muñoz, M.D.C.C., Benomar, N., Ennahar, S., Horvatovich, P., Lerma, L.L., Knapp, C.W., Gálvez, A., and Abriouel, H. (2016). Comparative proteomic analysis of a potentially probiotic *Lactobacillus pentosus* MP-10 for the identification of key proteins involved in antibiotic resistance and biocide tolerance. *International Journal of Food Microbiology*, **222**: 8-15.

Muñoz-Atienza, E., Landeta, G., de las Rivas, B., Gómez-Sala, B., Muñoz, R., Hernández, P.E., Cintas, L.M. and Herranz, C. (2011). Phenotypic and genetic evaluations of biogenic amine production by lactic acid bacteria isolated from fish and fish products. *International Journal of Food Microbiology*, **146**: 212-216.

Nadelman, P., Magno, M.B., Masterson, D., da Cruz, A.G. and Maia, L.C. (2018). Are dairy products containing probiotics beneficial for oral health? A systematic review and meta-analysis. *Clinical Oral Investigations*, **22**: 2763-2785.

Nagpal, R. and Yadav, H. (2017). Bacterial translocation from the gut to the distant organs: an overview. *Annals of Nutrition and Metabolism*, **71**: 11-16.

Nagpal, R., Kumar, A., Kumar, M., Behare, P.V., Jain, S. and Yadav, H. (2012). Probiotics, their health benefits and applications for developing healthier foods: a review. *FEMS Microbiology Letters*, **334**: 1-15.

Nagpal, R., Wang, S., Ahmadi, S., Hayes, J., Gagliano, J., Subashchandrabose, S., Kitzman, D.W., Becton, T., Read, R. and Yadav, H. (2018). Human-origin probiotic cocktail increases short-chain fatty acid production via modulation of mice and human gut microbiome. *Scientific Reports*, **8**(1): 1-15.

Nanjundaiah, Y.S., Wright, D.A., Baydoun, A.R., Khaled, Z., Ali, Z., Dean, P. and Sarker, M.H. (2020). Modulation of Macrophage Function by *Lactobacillus*-Conditioned Medium. *Frontiers in Cell and Developmental Biology*, **8**: 723.

Naqvi, S.S.B., Nagendra, V. and Hofmeyr, A. (2018). Probiotic related *Lactobacillus rhamnosus* endocarditis in a patient with liver cirrhosis. *IDCases*, **13**: 00439.

Nascimento, L.C.S., Casarotti, S.N., Todorov, S.D. and Penna, A.L.B. (2019). Probiotic potential and safety of enterococci strains. *Annals of Microbiology*, **69**: 241-252.

Nataraj, B.H., Ali, S.A., Behare, P.V. and Yadav, H. (2020). Postbiotics-parabiotics: The new horizons in microbial biotherapy and functional foods. *Microbial Cell Factories*, **19**(1): 1-22.

Nawaz, M., Wang, J., Zhou, A., Ma, C., Wu, X., Moore, J.E., Millar, B.C. and Xu, J. (2011). Characterization and transfer of antibiotic resistance in lactic acid bacteria from fermented food products. *Current Microbiology*, **62**: 1081-1089.

Neben, S., Marcus, K. and Mauch, P. (1993). Mobilization of hematopoietic stem and progenitor cell subpopulations from the marrow to the blood of mice following cyclophosphamide and/or granulocyte colony-stimulating factor. *Blood*, **81**(7): 1960–1967.

Neut, C., Mahieux, S. and Dubreuil, L.J. (2017). Antibiotic susceptibility of probiotic strains: Is it reasonable to combine probiotics with antibiotics?. *Médecine Et Maladies Infectieuses*, **47**: 477-483.

Niles, A.L., Moravec, R.A. and Riss, T.L. (2008). Update on *in vitro* cytotoxicity assays for drug development. *Expert Opinion on Drug Discovery*, **3**: 655-669.

Nissilä, E., Douillard, F.P., Ritari, J., Paulin, L., Järvinen, H.M., Rasinkangas, P., Haapasalo, K., Meri, S., Jarva, H. and De Vos, W.M. (2017). Genotypic and phenotypic diversity of *Lactobacillus rhamnosus* clinical isolates, their comparison with strain GG and their recognition by complement system. *PLoS One*, **12**: 0176739.

Nithya, V., Muthukumar, S.P. and Halami, P.M. (2012). Safety assessment of *Bacillus licheniformis* Me1 isolated from milk for probiotic application. *International Journal of Toxicology*, **31**: 228-237.

Nitzsche, R., Köhler, J., Kreikemeyer, B. and Oehmcke-Hecht, S. (2016). *Streptococcus pyogenes* escapes killing from extracellular histones through plasminogen binding and activation by streptokinase. *Journal of Innate Immunity*, **8**: 589-600.

Nowak, A., Paliwoda, A. and Błasiak, J. (2019). Anti-proliferative, pro-apoptotic and anti-oxidative activity of *Lactobacillus* and *Bifidobacterium* strains: A review of mechanisms and therapeutic perspectives. *Critical Reviews in Food Science and Nutrition*, **59**(21): 3456-3467.

Núñez, I.N., Galdeano, C.M., de LeBlanc, A.D.M. and Perdigón, G. (2014). Evaluation of immune response, microbiota, and blood markers after probiotic bacteria administration in obese mice induced by a high-fat diet. *Nutrition*, **30**(11-12): 1423-1432.

O'Bryan, C.A., Pak, D., Crandall, P.G., Lee, S.O. and Ricke, S.C. (2013). The role of prebiotics and probiotics in human health. *Journal of Probiotics and Health*, **1**(2): 1000108.

Ocvirk, S. and O'Keefe, S.J. (2017). Influence of bile acids on colorectal cancer risk: potential mechanisms mediated by diet-gut microbiota interactions. *Current Nutrition Reports*, **6**: 315-322.

OECD. (1995). Organization for economic cooperation and development: OECD guidelines for the testing of chemicals. Test guideline 408. Repeated dose 90-day oral toxicity study in rodent. Paris: OECD.

OECD. (2008a). Organization for economic cooperation and development: OECD guidelines for the testing of chemicals. Test guideline 425. Acute oral toxicity-up-and-down procedure. Paris: OECD.

OECD. (2008b). Organization for economic cooperation and development: OECD guidelines for the testing of chemicals. Test guideline 407. Repeated dose 28-day oral toxicity study in rodents. Paris: OECD.

OECD. (2016a). Organization for economic cooperation and development: OECD guidelines for the testing of chemicals. Test guideline 474. *In vivo* mammalian erythrocyte micronucleus test. Paris: OCED.

OECD. (2016b). Organization for economic cooperation and development: OECD guidelines for the testing of chemicals. Test guideline 489. *In vivo* mammalian alkaline comet assay. Paris: OCED.

OECD. (2016c). Organization for economic cooperation and development: OECD guidelines for the testing of chemicals. Test guideline 475. Mammalian Bone Marrow Chromosomal aberration test. Paris: OCED.

OECD. (2018a). Organization for economic cooperation and development: OECD guidelines for the testing of chemicals. Test guideline 452. Chronic toxicity studies. Paris: OECD.

OECD. (2018b). Organization for economic cooperation and development: OECD guidelines for the testing of chemicals. Test guideline 414. Prenatal developmental toxicity study, Paris: OECD.

Ollagnier-de Choudens, S., Loiseau, L., Sanakis, Y., Barras, F. and Fontecave, M. (2005). Quinolinate synthetase, an iron–sulfur enzyme in NAD biosynthesis. *FEBS Letters*, **579**(17): 3737-3743.

Osman, A., Taipale, M., Najjar, M. and Osman, B. (2019). *Lactobacillus paracasei* endocarditis of bioprosthetic aortic valve presenting with recurrent embolic strokes. *Access Microbiology*, **1**: 000038.

Ozen, M. and Dinleyici, E.C. (2015). The history of probiotics: the untold story. *Beneficial Microbes*, **6**: 159-165.

Özkan, E.R., Demirci, T. and Akın, N. (2021). *In vitro* assessment of probiotic and virulence potential of Enterococcus faecium strains derived from artisanal goatskin casing Tulum cheeses produced in central Taurus Mountains of Turkey. *LWT-Food Science and Technology*, **141**: 110908.

Panicker, A.S., Ali, S.A., Anand, S., Panjagari, N.R., Kumar, S., Mohanty, A.K. and Behare, P.V. (2018). Evaluation of some *in vitro* probiotic properties of *Lactobacillus fermentum* Strains. *Journal of Food Science and Technology*, **55**(7): 2801-2807.

Park, H.E. and Lee, W.K. (2018). Immune enhancing effects of *Weissella cibaria* JW15 on BALB/c mice immunosuppressed by cyclophosphamide. *Journal of Functional Foods*, **49**: 518-525.

Pasala, S., Singer, L., Arshad, T. and Roach, K. (2020). *Lactobacillus* endocarditis in a healthy patient with probiotic use. *IDCases*, **22**: 00915.

Pavan, S., Desreumaux, P. and Mercenier, A. (2003). Use of mouse models to evaluate the persistence, safety, and immune modulation capacities of lactic acid bacteria. *Clinical and Diagnostic Laboratory Immunology*, **10**: 696-701.

Pepoyan, A.Z., Balayan, M.H., Malkhasyan, L., Manvelyan, A., Bezhanyan, T., Paronikyan, R., Tsaturyan, V.V., Tatikyan, S., Kamiya, S. and Chikindas, M.L. (2019). Effects of probiotic *Lactobacillus acidophilus* strain INMIA 9602 Er 317/402 and putative probiotic lactobacilli on DNA damages in the small intestine of Wistar rats *in vivo*. *Probiotics and Antimicrobial Proteins*, **11**: 905-909.

Poloni, V.L., Bainotti, M.B., Vergara, L.D., Escobar, F., Montenegro, M. and Cavaglieri, L. (2021). Influence of technological procedures on viability, probiotic and anti-mycotoxin properties of *Saccharomyces boulardii* RC009, and biological safety studies. *Current Research in Food Science*, **4**: 132-140.

Porwal, M., Khan, N.A. and Maheshwari, K.K. (2017). Evaluation of acute and subacute oral toxicity induced by ethanolic extract of *Marsdenia tenacissima* leaves in experimental rats. *Scientia Pharmaceutica*, **85**(3): 29.

Pospiech, A. and Neumann, B. (1995). A versatile quick-prep of genomic DNA from gram-positive bacteria. *Trends in Genetics*, **11**(6): 217-218.

Pradhan, D., Singh, R., Tyagi, A., Rashmi, H.M., Batish, V.K. and Grover, S. (2019a). Assessing safety of *Lactobacillus plantarum* MTCC 5690 and *Lactobacillus fermentum* MTCC 5689 using *in vitro* approaches and an *in vivo* murine model. *Regulatory Toxicology and Pharmacology*, **101**: 1-11.

Pradhan, D., Singh, R., Tyagi, A., Rashmi, H.M., Batish, V.K. and Grover, S. (2019b). Assessing the safety and efficacy of *Lactobacillus plantarum* MTCC 5690 and *Lactobacillus fermentum* MTCC 5689 in colitis mouse model. *Probiotics and Antimicrobial Proteins*, **11**: 910-920.

Pragya, P., Kaur, G., Ali, S.A., Bhatla, S., Rawat, P., Lule, V., Kumar, S., Mohanty, A.K. and Behare, P. (2017). High-resolution mass spectrometry-based global proteomic analysis of probiotic strains *Lactobacillus fermentum* NCDC 400 and RS2. *Journal of Proteomics*, **152**: 121-130.

Prajapati, J.B. and Nair, B.M. (2008). The history of fermented foods. In Edward R. (Eds.), *Handbook of fermented functional foods* (pp.1-24). CRC Press.

Prete, R., Long, S.L., Gallardo, A.L., Gahan, C.G., Corsetti, A. and Joyce, S.A. (2020). Beneficial bile acid metabolism from *Lactobacillus plantarum* of food origin. *Scientific Reports*, **10**: 1-11.

Prete, R., Tofalo, R., Federici, E., Ciarrocchi, A., Cenci, G. and Corsetti, A. (2017). Food-associated *Lactobacillus plantarum* and yeasts inhibit the genotoxic effect of 4-Nitroquinoline-1-Oxide. *Frontiers in Microbiology*, **8**: 2349.

Priyanka, V., Ramesha, A., Gayathri, D. and Vasudha, M. (2021). Molecular characterization of non-biogenic amines producing *Lactobacillus plantarum* GP11 isolated from traditional pickles using HRESI-MS analysis. *Journal of Food Science and Technology*, **58**: 2216-2226.

Quail, M.A., Smith, M., Coupland, P., Otto, T.D., Harris, S.R., Connor, T.R., Bertoni, A., Swerdlow, H.P. and Gu, Y. (2012). A tale of three next generation sequencing platforms: comparison of Ion Torrent, Pacific Biosciences and Illumina MiSeq sequencers. *BMC Genomics*, **13**: 1-13.

Qureshi, N., Gu, Q. and Li, P. (2020). Whole genome sequence analysis and in vitro probiotic characteristics of a *Lactobacillus* strain *Lactobacillus paracasei* ZFM54. *Journal of Applied Microbiology*, **129**: 422-433.

Radulović, Z., Petrović, T., Nedović, V., Dimitrijević, S., Mirković, N., Petrušić, M. and Paunović, D. (2010). Characterization of autochthonous Lactobacillus paracasei strains on potential probiotic ability. *Mljekarstvo: časopis za unaprjeđenje proizvodnje i prerade mlijeka*, **60**(2): 86-93.

Ragul, K., Kandasamy, S., Devi, P.B. and Shetty, P.H. (2019). Safety and stability assessment of potential probiotic strains from fermented mango brine pickle. *Probiotics and Antimicrobial Proteins*, **12**: 1039–1044.

Rani, K., Ali, S.A., Kaul, G. and Behare, P.V. (2022). Protective effect of probiotic and prebiotic fermented milk containing *Lactobacillus fermentum* against obesity-induced hepatic steatosis and inflammation. *Journal of Food Biochemistry*, **46**:14509.

Rao, S.S., Rehman, A., Yu, S. and De Andino, N.M. (2018). Brain fogginess, gas and bloating: a link between SIBO, probiotics and metabolic acidosis. *Clinical and Translational Gastroenterology*, **9**: 162.

Rasouli, B.S., Ghadimi-Darsajini, A., Nekouian, R. and Iragian, G.R. (2017). *In vitro* activity of probiotic *Lactobacillus reuteri* against gastric cancer progression by downregulation of urokinase plasminogen activator/urokinase plasminogen activator receptor gene expression. *Journal of Cancer Research and Therapeutics*, **13**: 246.

Rastogi, S., Mittal, V. and Singh, A. (2019). *In vitro* evaluation of probiotic potential and safety assessment of *Lactobacillus mucosae* strains isolated from Donkey's lactation. *Probiotics and Antimicrobial Proteins*, **12:** 1045–1056.

Ravcheev, D.A. and Thiele, I. (2017). Comparative genomic analysis of the human gut microbiome reveals a broad distribution of metabolic pathways for the degradation of host-synthetized mucin glycans and utilization of mucin-derived monosaccharides. *Frontiers in Genetics*, **8**:111.

Razmgah, N., Mojgani, N. and Torshizi, M.A.T. (2016). Probiotic potential and virulence traits of bacillus and lactobacillus species isolated from local honey sample in Iran. *IOSR Journal of Pharmacy and Biological Sciences*, **11**(5): 87-95.

Ricotta, C. and Podani, J. (2017). On some properties of the Bray-Curtis dissimilarity and their ecological meaning. *Ecological Complexity*, **31**: 201-205.

Riquelme, A.J., Calvo, M.A., Guzmán, A.M., Depix, M.S., García, P., Pérez, C., Arrese, M. and Labarca, J.A. (2003). *Saccharomyces cerevisiae* fungemia after

Saccharomyces boulardii treatment in immunocompromised patients. *Journal of Clinical Gastroenterology*, **36**: 41-43.

Rokana, N., Mallappa, R.H., Batish, V.K. and Grover, S. (2017). Interaction between putative probiotic *Lactobacillus* strains of Indian gut origin and Salmonella: impact on intestinal barrier function. *LWT-Food Science and Technology*, **84**: 851-860.

Romero, M. (2020). Detection of extracellular nuclease activity during lag and exponential growth phases of *Lactobacillus casei*. *Acta Microscopica*, **29**: 2051-2056.

Rossi, F., Amadoro, C. and Colavita, G. (2019). *Lactobacillus* strains as opportunistic pathogens: a review, *Microorganisms*, **7**: 126.

Ruas-Madiedo, P., Gueimonde, M., Fernández-García, M., Clara, G. and Margolles, A. (2008). Mucin degradation by *Bifidobacterium* strains isolated from the human intestinal microbiota. *Applied and Environmental Microbiology*, **74**: 1936-1940.

Ruiz-Capillas, C. and Herrero, A.M. (2019). Impact of biogenic amines on food quality and safety. *Foods*, **8**: 62.

Ruiz-Perez, C.A., Conrad, R.E. and Konstantinidis, K.T. (2021). MicrobeAnnotator: a user-friendly, comprehensive functional annotation pipeline for microbial genomes. *BMC Bioinformatics*, **22**(1): 1-16.

Rzepkowska, A., Zielińska, D., Ołdak, A., and Kołożyn-Krajewska, D. (2017). Safety assessment and antimicrobial properties of the lactic acid bacteria strains isolated from polish raw fermented meat products. *International Journal of Food Properties*, **20**: 2736-2747.

Saif, F.A.A. and Sakr, E.A. (2020). Characterization and bioactivities of exopolysaccharide produced from probiotic *Lactobacillus plantarum* 47FE and *Lactobacillus pentosus* 68FE. *Bioactive Carbohydrates and Dietary Fibre*, **24**: 100231.

Saleh, I.D., Zain, H.H., Husni, I., Salih, N.D. and Gopalan, H. (2017). A locally synthesized probiotic for maintaining immune system functions in immunocompromised NZW rabbits. *World Journal of Pharmacy and Pharmaceutical Sciences*, **6**: 111-124.

Salva, S., Marranzino, G., Villena, J., Agüero, G. and Alvarez, S. (2014). Probiotic *Lactobacillus* strains protect against myelosuppression and

immunosuppression in cyclophosphamide-treated mice. *International Immunopharmacology*, **22**(1): 209-221.

Salvetti, E., Orrù, L., Capozzi, V., Martina, A., Lamontanara, A., Keller, D., Cash, H., Felis, G.E., Cattivelli, L., Torriani, S. and Spano, G. (2016). Integrate genome-based assessment of safety for probiotic strains: *Bacillus coagulans* GBI-30, 6086 as a case study. *Applied Microbiology and Biotechnology*, **100**: 4595-4605.

Samelis, J., Bleicher, A., Delbès-Paus, C., Kakouri, A., Neuhaus, K. and Montel, M.C. (2011). FTIR-based polyphasic identification of lactic acid bacteria isolated from traditional Greek Graviera cheese. *Food Microbiology*, **28**: 76-83.

Samtiya, M., Bhat, M.I., Gupta, T., Kapila, S. and Kapila, R. (2020). Safety assessment of potential probiotic *Lactobacillus fermentum* MTCC-5898 in murine model after repetitive dose for 28 days (Sub-Acute Exposure). *Probiotics and antimicrobial proteins*, **12**(1): 259-270.

Sanders, M.E., Akkermans, L.M., Haller, D., Hammerman, C., Heimbach, J.T., Hörmannsperger, G. and Huys, G. (2010). Safety assessment of probiotics for human use. *Gut Microbes*, **1**: 164-185.

Santino, I., Alari, A., Bono, S., Teti, E., Marangi, M., Bernardini, A., Magrini, L., Di Somma, S. and Teggi, A. (2014). *Saccharomyces cerevisiae* fungemia, a possible consequence of the treatment of *Clostridium difficile* colitis with a probioticum. *International Journal of Immunopathology and Pharmacology*, **27**: 143-146.

Saroj, D.B. and Gupta, A.K. (2020). Genome based safety assessment for *Bacillus coagulans* strain LBSC (DSM 17654) for probiotic application. *International Journal of Food Microbiology*, **318**: 108523.

Sen, S. and Mansell, T.J. (2020). Yeasts as probiotics: Mechanisms, outcomes, and future potential. *Fungal Genetics and Biology*, **137**: 103333.

Senan, S., Prajapati, J.B. and Joshi, C.G. (2015). Feasibility of genome-wide screening for biosafety assessment of probiotics: a case study of *Lactobacillus helveticus* MTCC 5463. *Probiotics and Antimicrobial Proteins*, **7**: 249-258.

Sengul, E., Gelen, S.U., Yıldırım, S., Çelebi, F. and Çınar, A. (2019). Probiotic bacteria attenuates cisplatin-induced nephrotoxicity through modulation of oxidative stress, inflammation and apoptosis in rats. *Asian Pacific Journal of Tropical Biomedicine*, **9**(3): 116.

Senthilkumar, S., Yogeeta, S.K., Subashini, R. and Devaki, T. (2006). Attenuation of cyclophosphamide induced toxicity by squalene in experimental rats. *Chemico-biological Interactions*, **160**(3): 252-260.

Sharma, A., Lee, S. and Park, Y.S. (2020). Molecular typing tools for identifying and characterizing lactic acid bacteria: a review. *Food Science and Biotechnology*, **29**: 1301-1318.

Sharma, P., Tomar, S.K., Sangwan, V., Goswami, P. and Singh, R. (2016). Antibiotic resistance of Lactobacillus sp. isolated from commercial probiotic preparations. *Journal of Food Safety*, **36**(1): 38-51.

Shekh, S.L., Dave, J.M. and Vyas, B.R.M. (2016). Characterization of *Lactobacillus plantarum* strains for functionality, safety and γ-amino butyric acid production. *LWT-Food Science and Technology*, **74**: 234-241.

Sherid, M., Samo, S., Sulaiman, S., Husein, H., Sifuentes, H. and Sridhar, S. (2016). Liver abscess and bacteremia caused by lactobacillus: role of probiotics? Case report and review of the literature. *BMC Gastroenterology*, **16**: 138.

Shimura, M., Mizuma, M., Nakagawa, K., Aoki, S., Miura, T., Takadate, T., Ariake, K., Maeda, S., Kawaguchi, K., Masuda, K. and Ishida, M. (2021). Probiotic-related bacteremia after major hepatectomy for biliary cancer: a report of two cases. *Surgical Case Reports*, **7**: 1-8.

Shin, M., Ban, O.H., Jung, Y.H., Yang, J. and Kim, Y. (2021). Genomic characterization and probiotic potential of Lactobacillus casei IDCC 3451 isolated from infant faeces. *Letters in Applied Microbiology*, **72**: 578-588.

Shokryazdan, P., Faseleh Jahromi, M., Liang, J.B., Kalavathy, R., Sieo, C.C. and Ho, Y.W. (2016). Safety assessment of two new *Lactobacillus* strains as probiotic for human using a rat model. *PLoS One*, **11**: 0159851.

Shu Q. and Gill H.S. (2001). A dietary probiotic (*Bifidobacterium lactis* HN019) reduces the severity of *Escherichia coli* O157:H7 infection in mice. *Medical Microbiology and Immunology*, **189**: 147–52.

Singer, B.H., Dickson, R.P., Denstaedt, S.J., Newstead, M.W., Kim, K., Falkowski, N.R., Erb-Downward, J.R., Schmidt, T.M., Huffnagle, G.B. and Standiford, T.J. (2018). Bacterial dissemination to the brain in sepsis. *American Journal of Respiratory and Critical Care Medicine*, **197**(6): 747-756.

Singh, A., Kumar, S., Vinay, V.V., Tyagi, B., Choudhury, P.K., Rashmi, H.M., Banakar, P.S., Tyagi, N. and Tyagi, A.K. (2021). Autochthonous *Lactobacillus* spp.

isolated from Murrah buffalo calves show potential application as probiotic. *Current Research in Biotechnology*, **3**: 109-119.

Singh, M., Kumar, S., Banakar, P.S., Vinay, V.V., Das, A., Tyagi, N. and Tyagi, A.K. (2021). Synbiotic formulation of *Cichorium intybus* root powder with *Lactobacillus acidophilus* NCDC15 and *Lactobacillus reuteri* BFE7 improves growth performance in Murrah buffalo calves via altering selective gut health indices. *Tropical Animal Health and Production*, **53**(2): 1-9.

Singh, T.P. and Natraj, B.H. (2021). Next-generation probiotics: a promising approach towards designing personalized medicine. *Critical Reviews in Microbiology*, **47**(4): 479-498.

Singh, T.P., Kaur, G., Malik, R.K., Schillinger, U., Guigas, C. and Kapila, S. (2012). Characterization of intestinal *Lactobacillus reuteri* strains as potential probiotics. *Probiotics and Antimicrobial Proteins*, **4**: 47-58.

Singhi, S.C. and Baranwal, A. (2008). Probiotic use in the critically ill. *The Indian Journal of Pediatrics*, **75**: 621-627.

Singracha, P., Niamsiri, N., Visessanguan, W., Lertsiri, S. and Assavanig, A. (2017). Application of lactic acid bacteria and yeasts as starter cultures for reduced-salt soy sauce (moromi) fermentation. *LWT-Food Science and Technology*, **78**: 181-188.

Sirichoat, A., Flórez, A.B., Vázquez, L., Buppasiri, P., Panya, M., Lulitanond, V. and Mayo, B. (2020). Antibiotic susceptibility profiles of lactic acid bacteria from the human vagina and genetic basis of acquired resistances. *International Journal of Molecular Sciences*, **21**: 2594.

Skvortsov, E., Mukhammadiev, R., Mukhammadiev, R., Valiullin, L. and Rud, V. (2021). Study of the reproductive toxicity of probiotic strains on laboratory animals. *Earth and Environmental Science*, **663**: 012034.

Slauch, J.M. (2011). How does the oxidative burst of macrophages kill bacteria? Still an open question. *Molecular Microbiology*, **80**(3): 80-583.

Sohn, Y.W. (2016). Guidelines for standardization for quality of *Lactobacillus* products. *National Institute of Food and Drug Safety Evaluation*.

Solga, S.F. (2003). Probiotics can treat hepatic encephalopathy. *Medical Hypotheses*, **61**(2): 307-313.

Soltani, S., Hammami, R., Cotter, P.D., Rebuffat, S., Said, L.B., Gaudreau, H., Bédard, F., Biron, E., Drider, D. and Fliss, I. (2021). Bacteriocins as a new generation

of antimicrobials: Toxicity aspects and regulations. *FEMS Microbiology Reviews*, **45**: 039.

Somashekaraiah, R., Shruthi, B., Deepthi, B.V. and Sreenivasa, M.Y. (2019). Probiotic properties of lactic acid bacteria isolated from neera: a naturally fermenting coconut palm nectar. *Frontiers in Microbiology*, **10**: 1382.

Son, S.H., Jeon, H.L., Yang, S.J., Sim, M.H., Kim, Y.J., Lee, N.K., and Paik, H.D. (2018). Probiotic lactic acid bacteria isolated from traditional Korean fermented foods based on β-glucosidase activity. *Food Science and Biotechnology*, **27**: 123-129.

Sonpal, N., Tsai, R., Vinod, J., Satchi, M., Vadada, D. and Chun, A. (2010). *Saccharomyces cerevisiae* gungemia after *Saccharomyces boulardii* treatment in an immunocompetent patient: 954. *American Journal of Gastroenterology*, **105**: S345.

Sornsenee, P., Singkhamanan, K., Sangkhathat, S., Saengsuwan, P. and Romyasamit, C. (2021). Probiotic Properties of *Lactobacillus* Species Isolated from Fermented Palm Sap in Thailand. *Probiotics and Antimicrobial Proteins*, **13**: 957-969.

Sotoudegan, F., Daniali, M., Hassani, S., Nikfar, S. and Abdollahi, M. (2019). Reappraisal of probiotics' safety in human. *Food and Chemical Toxicology*, **129**: 22-29.

Sowmya, K., Bhat, M.I., Bajaj, R., Kapila, S. and Kapila, R., 2019. Antioxidative and anti-inflammatory potential with trans-epithelial transport of a buffalo casein-derived hexapeptide (YFYPQL). *Food Bioscience*, **28**: 151-163.

Srivastava, U., Nataraj, B.H., Kumari, M., Kadyan, S., Puniya, A.K., Behare, P.V. and Nagpal, R. (2022). Antioxidant and immunomodulatory potency of *Lacticaseibacillus rhamnosus* NCDC24 fermented milk-derived peptides: A computationally guided in-vitro and ex-vivo investigation. *Peptides*, **155**: 170843.

Steppe, M., Van Nieuwerburgh, F., Vercauteren, G., Boyen, F., Eeckhaut, V., Deforce, D., Haesebrouck, F., Ducatelle, R. and Van Immerseel, F. (2014). Safety assessment of the butyrate-producing *Butyricicoccus pullicaecorum* strain 25-3T, a potential probiotic for patients with inflammatory bowel disease, based on oral toxicity tests and whole genome sequencing. *Food and Chemical Toxicology*, **72**: 129-137.

Stogios, P. J. and Savchenko, A. (2020). Molecular mechanisms of vancomycin resistance. *Protein Science*, **29**(3): 654-669.

Suddek, G.M., Ashry, N.A. and Gameil, N.M. (2013). Thymoquinone attenuates cyclophosphamide-induced pulmonary injury in rats. *Inflammopharmacology*, **21**(6): 427-435.

Tan, H., Wang, C., Zhang, Q., Tang, X., Zhao, J., Zhang, H., Zhai, Q. and Chen, W. (2020). Preliminary safety assessment of a new *Bacteroides fragilis* isolate. *Food and Chemical Toxicology*, **135**: 110934.

Tang, L., Song, S., Hu, C., Lam, J.C.W., Liu, M., Zhou, B., Lam, P.K. and Chen, L. (2020). Unexpected observations: Probiotic administration greatly aggravates the reproductive toxicity of perfluorobutanesulfonate in zebrafish. *Chemical Research in Toxicology*, **33**: 1605-1608.

Tao, S., Tao, S., Cheng, Y., Liu, J., Ma, L. and Fu, P. (2019). Effects of probiotic supplements on the progression of chronic kidney disease: A meta-analysis. *Nephrology*, **24**: 1122-1130.

Tarrah, A., da Silva Duarte, V., de Castilhos, J., Pakroo, S., Junior, W.J.F.L., Luchese, R.H., Guerra, A.F., Rossi, R.C., Ziegler, D.R., Corich, V. and Giacomini, A. (2019). Probiotic potential and biofilm inhibitory activity of *Lactobacillus casei* group strains isolated from infant feces. *Journal of Functional Foods*, **54**: 489-497.

Tavella, T., Rampelli, S., Guidarelli, G., Bazzocchi, A., Gasperini, C., Pujos-Guillot, E., Comte, B., Barone, M., Biagi, E., Candela, M. and Nicoletti, C. (2021). Elevated gut microbiome abundance of Christensenellaceae, Porphyromonadaceae and Rikenellaceae is associated with reduced visceral adipose tissue and healthier metabolic profile in Italian elderly. *Gut Microbes*, **13**: 1880221.

Terai, T., Kato, K., Ishikawa, E., Nakao, M., Ito, M., Miyazaki, K., Kushiro, A., Imai, S., Nomura, Y., Hanada, N. and Okumura, T. (2020). Safety assessment of the candidate oral probiotic *Lactobacillus crispatus* YIT 12319: Analysis of antibiotic resistance and virulence-associated genes. *Food and Chemical Toxicology*, **140**: 111278.

Thakur, N., Sharma, C., Rokana, N., Singh, B.P., Gulhane, R.D., Mishra, S.K., Khatkar, S.K., Puniya, A.K. and Panwar, H. (2018). *In vitro* Assessment of Antibiotic Resistance Pattern among *Lactobacillus* Strains Isolated from Goat

Milk. *Internal Journal of Current Microbiology and Applied Science*, **7**(1): 2108-2116.

Thumu, S.C.R. and Halami, P.M. (2020). *In vivo* safety assessment of *Lactobacillus fermentum* strains, evaluation of their cholesterol-lowering ability and intestinal microbial modulation. *Journal of the Science of Food and Agriculture*, **100**: 705-713.

Thygesen, J.B., Glerup, H. and Tarp, B. (2012). *Saccharomyces boulardii* fungemia caused by treatment with a probioticum. *Case Reports*, **2012**: 0620114412.

Todić, M., Bakić, S., Begović, B., Krošnjar, S. and Zulić, I. (2003). Food and water consumption in assessment of acute oral toxicity of HEPALIP FORTE in rats. *Bosnian Journal of Basic Medical Sciences*, **3**(4): 47-53.

Todorov, S.D., Stojanovski, S., Iliev, I., Moncheva, P., Nero, L.A. and Ivanova, I.V. (2017). Technology and safety assessment for lactic acid bacteria isolated from traditional Bulgarian fermented meat product" lukanka". *Brazilian Journal of Microbiology*, **48**: 576-586.

Tofalo, R., Perpetuini, G., Schirone, M. and Suzzi, G. (2016). Biogenic amines: Toxicology and health effect.

Toomey, N., Monaghan, Á., Fanning, S. and Bolton, D.J. (2009). Assessment of horizontal gene transfer in lactic acid bacteria–a comparison of mating techniques with a view to optimising conjugation conditions. *Journal of Microbiological Methods*, **77**: 23-28.

Toropov, V., Demyanova, E., Shalaeva, O., Sitkin, S. and Vakhitov, T. (2020). Whole-genome sequencing of *Lactobacillus helveticus* D75 and D76 confirms safety and probiotic potential. *Microorganisms*, **8:** 329.

Tseng, W.T., Shih, T.W., Liu, S.H. and Pan, T.M. (2015). Safety and mutagenicity evaluation of Vigiis 101 powder made from *Lactobacillus paracasei* subsp. *paracasei* NTU 101. *Regulatory Toxicology and Pharmacology*, **71**: 148-157.

Tusl, M., Vyskocil, A., Dürrer, I., Aulika, B.V., Litvinov, N.N. and Merkur'Eva, R.V. (1983). Importance of the functional state of alveolar macrophages of the lungs for hygienic evaluation of protective reactions and cell damage due to atmospheric pollution. *Journal of Hygiene, Epidemiology, Microbiology, and Immunology*, **27**(3): 259-263.

Ukelis, U., Kramer, P.J., Olejniczak, K. and Mueller, S.O. (2008). Replacement of *in vivo* acute oral toxicity studies by *in vitro* cytotoxicity methods: Opportunities,

limits and regulatory status. *Regulatory Toxicology and Pharmacology*, **51**: 108-118.

Urshev, Z. and Yungareva, T. (2021). Initial safety evaluation of *Enterococcus faecium* LBB. E81. *Biotechnology and Biotechnological Equipment*, **35:** 11-17.

Van Herreweghen, F., De Paepe, K., Marzorati, M. and Van de Wiele, T. (2020). Mucin as a functional niche is a more important driver of *in vitro* gut microbiota composition and functionality than supplementation of *Akkermansia muciniphila*. *Applied and Environmental Microbiology*, **87:** 1-36.

Vankerckhoven, V., Huys, G., Vancanneyt, M., Vael, C., Klare, I., Romond, M.B., Entenza, J.M., Moreillon, P., Wind, R.D., Knol, J. and Wiertz, E. (2008). Biosafety assessment of probiotics used for human consumption: recommendations from the EU-PROSAFE project. *Trends in Food Science and Technology*, **19**: 102-114.

Vankerckhoven, V., Moreillon, P., Piu, S., Giddey, M., Huys, G., Vancanneyt, M., Goossens, H. and Entenza, J.M. (2007). Infectivity of *Lactobacillus rhamnosus* and *Lactobacillus paracasei* isolates in a rat model of experimental endocarditis. *Journal of Medical Microbiology*, **56**: 1017-1024.

Van't Wout, J.W., Linde, I., Leijh, P.C.J. and Van Furth, R. (1989). Effect of irradiation, cyclophosphamide, and etoposide (VP-16) on number of peripheral blood and peritoneal leukocytes in mice under normal conditions and during acute inflammatory reaction. *Inflammation*, **13**(1): 1-14.

Ventoulis, I., Sarmourli, T., Amoiridou, P., Mantzana, P., Exindari, M., Gioula, G. and Vyzantiadis, T.A. (2020). Bloodstream infection by *Saccharomyces cerevisiae* in two COVID-19 patients after receiving supplementation of *Saccharomyces* in the ICU. *Journal of Fungi*, **6**: 98.

Verma, A. and Shukla, G. (2013). Probiotics *Lactobacillus rhamnosus* GG, *Lactobacillus acidophilus* suppresses DMH-induced procarcinogenic fecal enzymes and preneoplastic aberrant crypt foci in early colon carcinogenesis in Sprague Dawley rats. *Nutrition and Cancer*, **65**: 84-91.

Vesterlund, S., Vankerckhoven, V., Saxelin, M., Goossens, H., Salminen, S. and Ouwehand, A.C. (2007). Safety assessment of *Lactobacillus* strains: presence of putative risk factors in faecal, blood and probiotic isolates. *International Journal of Food Microbiology*, **116:** 325-331.

Visk, D. (2015). Will advances in preclinical in vitro models lower the costs of drug development?. *Applied In Vitro Toxicology*, **1**(1): 79-82.

Voelcker, G. (2020). The mechanism of action of cyclophosphamide and its consequences for the development of a new generation of oxazaphosphorine cytostatics. *Scientia Pharmaceutica*, **88**(4): 42.

Wang, J., Da, R., Tuo, X., Cheng, Y., Wei, J., Jiang, K., Lv, J., Adediji, O.M., and Han, B. (2019). Probiotic and safety properties screening of *Enterococcus faecalis* from healthy Chinese infants. *Probiotics and Antimicrobial Proteins*, **12**: 1115–1125.

Wang, J., Karnati, P.K., Takacs, C.M., Kowalski, J.C. and Derbyshire, K.M. (2005). Chromosomal DNA transfer in Mycobacterium smegmatis is mechanistically different from classical Hfr chromosomal DNA transfer. *Molecular Microbiology*, **58**(1): 280-288.

Wang, J., Wu, T., Fang, X., Min, W. and Yang, Z. (2018). Characterization and immunomodulatory activity of an exopolysaccharide produced by Lactobacillus plantarum JLK0142 isolated from fermented dairy tofu. *International Journal of Biological Macromolecules*, **115**: 985-993.

Wang, K., Cao, G., Zhang, H., Li, Q. and Yang, C. (2019). Effects of Clostridium butyricum and *Enterococcus faecalis* on growth performance, immune function, intestinal morphology, volatile fatty acids, and intestinal flora in a piglet model. *Food and function*, **10**(12): 7844-7854.

Wang, M.L., Zhang, Y., Fan, M., Guo, Y.J., Ren, W.D. and Luo, E.J. (2013). A rabbit model of right-sided *Staphylococcus aureus* endocarditis created with echocardiographic guidance. *Cardiovascular Ultrasound*, **11**: 3.

Wang, Y., Liang, Q., Lu, B., Shen, H., Liu, S., Shi, Y., Leptihn, S., Li, H., Wei, J., Liu, C. and Xiao, H. (2021). Whole-genome analysis of probiotic product isolates reveals the presence of genes related to antimicrobial resistance, virulence factors, and toxic metabolites, posing potential health risks. *BMC Genomics*, **22**: 1-12.

Warn, P.A., Sharp, A., Mosquera, J., Spickermann, J., Schmitt-Hoffmann, A., Heep, M. and Denning, D.W. (2006). Comparative *in vivo* activity of BAL4815, the active component of the prodrug BAL8557, in a neutropenic murine model of disseminated Aspergillus flavus. *Journal of Antimicrobial Chemotherapy*, **58**(6): 1198-1207.

Wei, Y.X., Zhang, Z.Y., Liu, C., Malakar, P.K. and Guo, X.K. (2012). Safety assessment of Bifidobacterium longum JDM301 based on complete genome sequences. *World Journal of Gastroenterology*, **18**(5): 479.

Wenning, M., Büchl, N.R. and Scherer, S. (2010). Species and strain identification of lactic acid bacteria using FTIR spectroscopy and artificial neural networks. *Journal of Biophotonics*, **3**: 493-505.

Wiggins, T., Kumar, S., Markar, S.R., Antonowicz, S. and Hanna, G.B. (2015). Tyrosine, Phenylalanine, and Tryptophan in Gastroesophageal Malignancy: A Systematic ReviewAmino Acids in Gastroesophageal Cancer. *Cancer Epidemiology, Biomarkers and Prevention*, **24**(1): 32-38.

Wood, L.G., Gibson, P.G. and Garg, M.L. (2006). A review of the methodology for assessing *in vivo* antioxidant capacity. *Journal of the Science of Food and Agriculture*, **86**(13): 2057-2066.

Wray, W., Boulikas, T., Wray, V.P. and Hancock, R. (1981). Silver staining of proteins in polyacrylamide gels. *Analytical Biochemistry*, **118**(1): 197-203.

Xie, J., Nie, S., Yu, Q., Yin, J., Xiong, T., Gong, D. and Xie, M. (2016). *Lactobacillus plantarum* NCU116 attenuates cyclophosphamide-induced immunosuppression and regulates Th17/Treg cell immune responses in mice. *Journal of Agricultural and Food Chemistry*, **64**(6): 1291-1297.

Xie, J.H., Fan, S.T., Nie, S.P., Yu, Q., Xiong, T., Gong, D. and Xie, M.Y. (2016). *Lactobacillus plantarum* NCU116 attenuates cyclophosphamide-induced intestinal mucosal injury, metabolism and intestinal microbiota disorders in mice. *Food and function*, **7**(3): 1584-1592.

Xu, W., Yang, W., Wang, Y., Wang, M., Zhang, M. (2020). Structural and biochemical analyses of β-N-acetylhexosaminidase Am0868 from *Akkermansia muciniphila* involved in mucin degradation. *Biochemical and Biophysical Research Communications*, **529:** 876-881.

Xu, X. and Zhang, X. (2015). Effects of cyclophosphamide on immune system and gut microbiota in mice. *Microbiological Research*, **171**: 97-106.

Xue, L., He, J., Gao, N., Lu, X., Li, M., Wu, X., Liu, Z., Jin, Y., Liu, J., Xu, J. and Geng, Y. (2017). Probiotics may delay the progression of nonalcoholic fatty liver disease by restoring the gut microbiota structure and improving intestinal endotoxemia. *Scientific Reports*, **7**: 45176.

Xue, L., Li, Z., Xue, J., Wang, H., Wu, T., Liu, R., Sui, W. and Zhang, M. (2022). *Lactobacillus acidophilus* LA85 ameliorates cyclophosphamide-induced immunosuppression by modulating Notch and TLR4/NF-κB signal pathways and remodeling the gut microbiota. *Food and Function*, **13**(15): 8107-8118.

Yasmin, I., Saeed, M., Khan, W.A., Khaliq, A., Chughtai, M.F.J., Iqbal, R., Tehseen, S., Naz, S., Liaqat, A., Mehmood, T. and Ahsan, S. (2020). *In vitro* probiotic potential and safety evaluation (hemolytic, cytotoxic Activity) of *Bifidobacterium* Strains isolated from raw camel milk. *Microorganisms*, **8**: 354.

Yazdankhah, S.P., Eckner, K.F., Halvorsen, R., Kapperud, G., Lassen, J.F., Narvhus, J., Nesbakken, T., Robertson, L., Rosnes, J.T., Skjerdal, T. and Skjerve, E. (2014). Guidelines for assessment of safety aspects of probiotic (food) products. Opinion of the panel on Biological Hazards of the Norwegian Scientific Committee for Food Safety. *VKM Report*.

Zankari, E. (2014). Comparison of the web tools ARG-ANNOT and ResFinder for detection of resistance genes in bacteria. *Antimicrobial Agents and Chemotherapy*, **58**(8): 4986-4986.

Zeba, F., Yirerong, J., Assali, M., Tewary, G. and Amanda Noska, M.D. (2018). A double whammy: *Lactobacillus acidophilus* bacteremia and subsequent *Lactobacillus rhamnosus* prosthetic valve infective endocarditis in an elderly diabetic patient. *Rhode Island Medical Journal*, **101**: 32-35.

Zeng, Y., Li, Y., Wu, Q.P., Zhang, J.M., Xie, X.Q., Ding, Y., Cai, S.Z., Ye, Q.H., Chen, M.T., Xue, L. and Wu, S. (2020). Evaluation of the Antibacterial Activity and Probiotic Potential of *Lactobacillus plantarum* Isolated from Chinese Homemade Pickles. *Canadian Journal of Infectious Diseases and Medical Microbiology*, **2020:** 1-11.

Zhang, B., Lynch, B., Zhao, J., Guo, Y. and Mak, A. (2020). *Lactobacillus rhamnosus* MP108: Toxicological evaluation. *Journal of Food Science*, **86:** 228-241.

Zhang, F., Jiang, M., Wan, C., Chen, X., Chen, X., Tao, X., Shah, N.P. and Wei, H. (2016). Screening probiotic strains for safety: evaluation of virulence and antimicrobial susceptibility of enterococci from healthy Chinese infants. *Journal of Dairy Science*, **99**: 4282-4290.

Zhang, J., Gao, S., Li, H., Cao, M., Li, W. and Liu, X. (2021). Immunomodulatory effects of selenium-enriched peptides from soybean in

cyclophosphamide-induced immunosuppressed mice. *Food Science and Nutrition*, **9**(11): 6322-6334.

Zhang, N., Tian, Y., Wang, Y., Fan, Y., Zhang, Y., Xing, X., Nan, B., Ai, Z., Li, X. and Wang, Y. (2022). Ameliorative effect of *Lactobacillus plantarum* Lp2 against cyclophosphamide-induced liver injury in mice. *Food and Chemical Toxicology*, **169:** 113433.

Zhang, T., Li, Q., Cheng, L., Buch, H. and Zhang, F. (2019). *Akkermansia muciniphila* is a promising probiotic. *Microbial Biotechnology*, **12**(6): 1109-1125.

Zhang, Z., Pan, T., Liu, C., Shan, X., Xu, Z., Hong, H., Lin, H., Chen, J. and Sun, H. (2021). Cyclophosphamide induced physiological and biochemical changes in mice with an emphasis on sensitivity analysis. *Ecotoxicology and Environmental Safety*, **211**: 111889.

Zhao, J., Gong, L., Wu, L., She, S., Liao, Y., Zheng, H., Zhao, Z., Liu, G. and Yan, S. (2020). Immunomodulatory effects of fermented fig (Ficus carica L.) fruit extracts on cyclophosphamide-treated mice. *Journal of Functional Foods*, **75**: 104219.

Zheng, J., Wittouck, S., Salvetti, E., Franz, C.M., Harris, H.M., Mattarelli, P., O'Toole, P.W., Pot, B., Vandamme, P., Walter, J. and Watanabe, K. (2020). A taxonomic note on the genus *Lactobacillus*: Description of 23 novel genera, emended description of the genus *Lactobacillus* Beijerinck 1901, and union of Lactobacillaceae and Leuconostocaceae. *International Journal of Systematic and Evolutionary Microbiology*, **70**: 2782-2858.

Zheng, M., Zhang, R., Tian, X., Zhou, X., Pan, X. and Wong, A. (2017). Assessing the risk of probiotic dietary supplements in the context of antibiotic resistance. *Frontiers in Microbiology*, **8**: 908.

Zhou, J.S., Rutherfurd, K.J. and Gill, H.S. (2005). Inability of probiotic bacterial strains *Lactobacillus rhamnosus* HN001 and *Bifidobacterium lactis* HN019 to induce human platelet aggregation *in vitro*. *Journal of Food Protection*, **68**: 2459-2464.

Zhou, X., Dong, Q., Kan, X., Peng, L., Xu, X., Fang, Y. and Yang, J. (2018a). Immunomodulatory activity of a novel polysaccharide from Lonicera japonica in immunosuppressed mice induced by cyclophosphamide. *PloS One*, **13**(10): 0204152.

Zhou, Y., Chen, X., Yi, R., Li, G., Sun, P., Qian, Y. and Zhao, X. (2018b). Immunomodulatory effect of tremella polysaccharides against cyclophosphamide-induced immunosuppression in mice. *Molecules*, **23**(2): 239.

Zielińska, D., Sionek, B. and Kołożyn-Krajewska, D. (2018). Safety of probiotics. In Alina M.H., and Alexandru M.G. (Eds.), *Diet, Microbiome and Health* (131-161). Academic Press.

Annexure

ANNEXURE-I

Standard curves for the estimation of various experimental parameters in the study

A. Ammonia

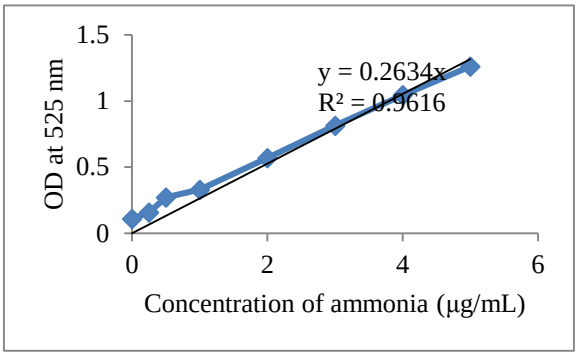

B. P-nitrophenol

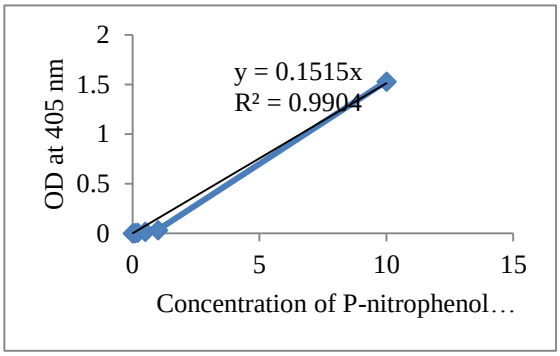

C. Nitrate

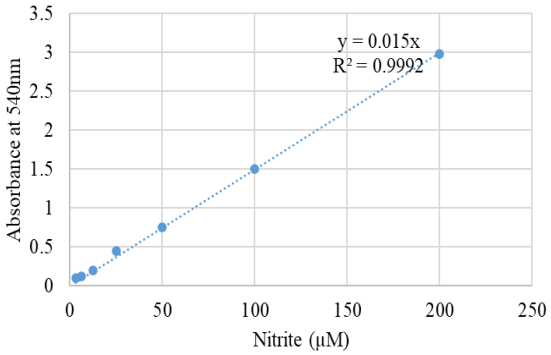

D. IgA

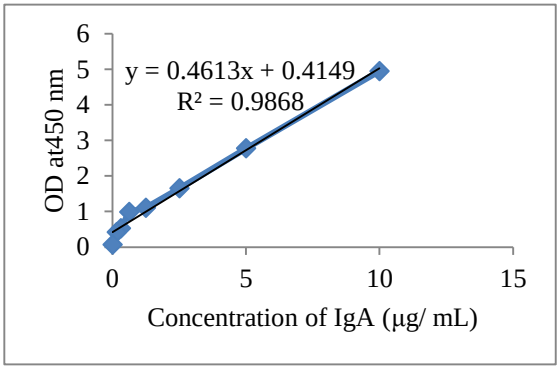

E. IgG

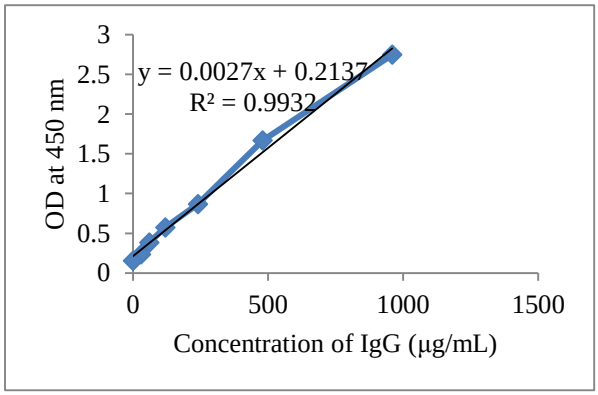

F. TGF-beta

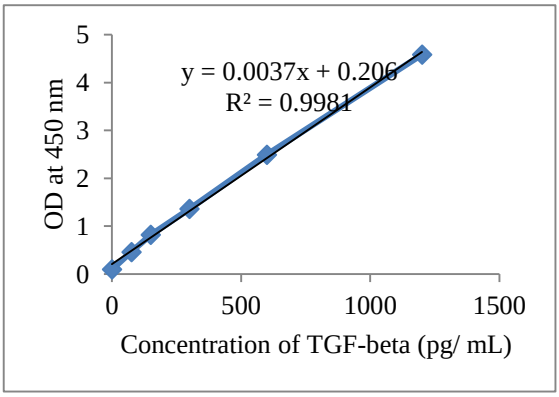

G. IL-6

H. IL-10

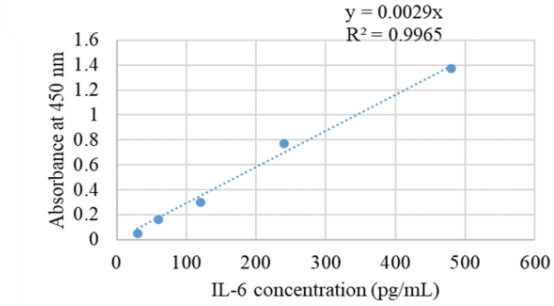

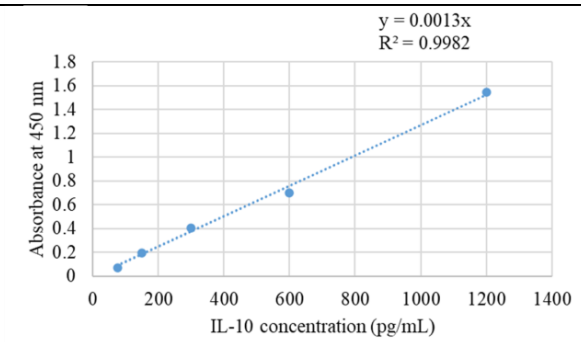

I. TNF-alpha

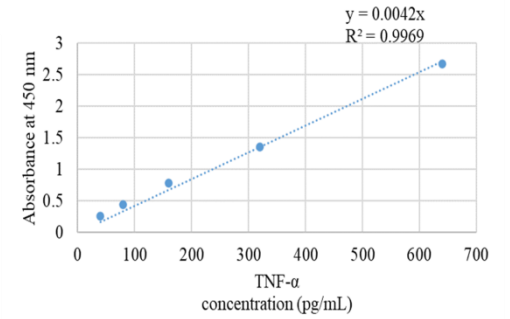

J. MCP-1

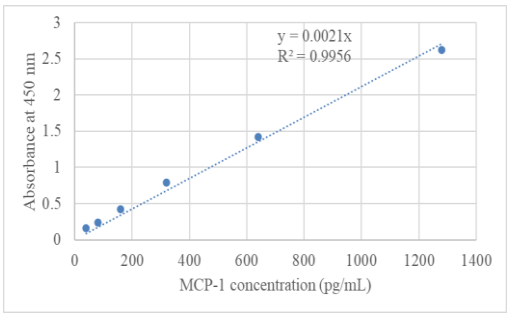

K. SOD

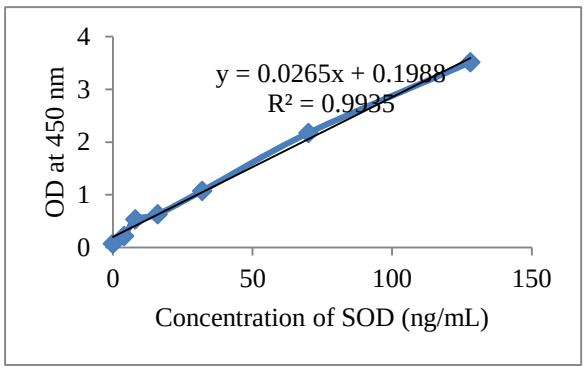

L. CAT

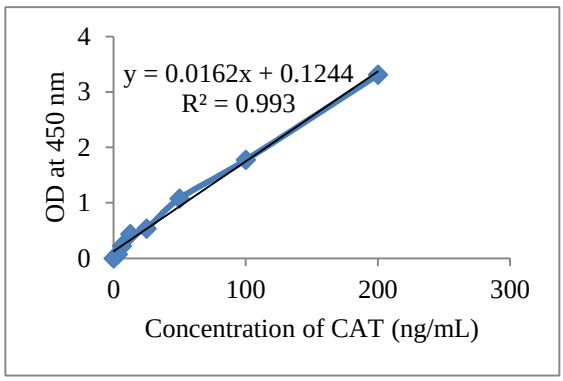

M. GpX2

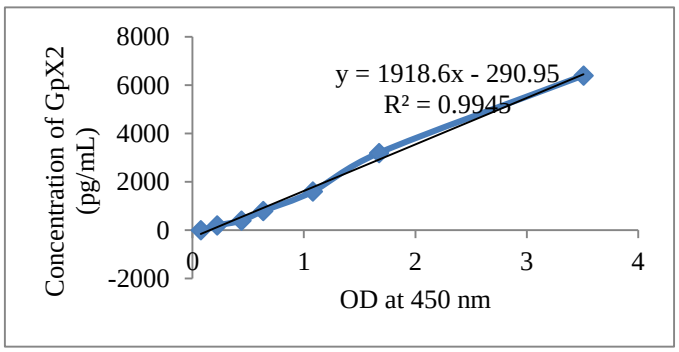

ANNEXURE-II

1. List of antibiotics used to evaluate the antibiotic susceptibility of NCDC 400

Antibiotics	Symbol/ concentration
Kanamycin	K (30 mcg)
Ofloxacin	OF (5 mcg)
Linezolid	LZ (30 mcg)
Clindamycin	CD (2 mcg)
Tetracycline	TE (30 mcg)
Chloramphenicol	C (30 mcg)
Oxacillin	OX (1 mcg)
Teicoplanin	TEI (10 mcg)
Vancomycin	VA (30 mcg)
Penicillin	P (10 Units)
Amikacin	AK (30 mcg)
Gentamicin	GEN (10 mcg)
Clarithromycin	CLR (15 mcg)
Co-Trimoxazole	COT (25 mcg)
Netillin	NET (30 mcg)
Cefaclor	CF (30 mcg)
Cefotaxime	CTX (30 mcg)
Azithromycin	AZM (5 mcg)
Ampicillin/Cloxacillin	AX (10 mcg)
Ampicillin/Sulbactam	A/S (10/10 mcg)
Ciprofloxacin	CIP (5 mcg)
Amoxyclav	AMC (30 mcg)
Novobiocin	NV (5 mcg)
Erythromycin	E (15 mcg)
Cefadroxil	CFR (30 mcg)
Ampicillin	AMP (30 mcg)
Cephalothin	CEP (30 mcg)

2. List of antibiotics (E-strips) used to determine the minimum MICs against NCDC 400

Antibiotics	Symbol	Range tested (mcg/mL)
Cephalotin	CE	0.016-256
Azithromycin	AZ	0.016-256
Amoxicillin	AC	0.016-256
Levofloxacin	LE	0.002-32
Ceftriaxone	CTR	0.016-256
Nitrofurantoin	NIT	0.032-512
Kanamycin	KAN	0.016-256
Cefotaxime	CTX	0.016-256
Cefuroxime	CXM	0.016-256
Ampicillin	AMP	0.016-256
Gentamicin	HLG	0.064-1024
Nalidixic acid	NAL	0.016-256
Clarithromycin	CH	0.016-256
Penicillin	PEN	0.002-32
Amoxyclav	AMC	0.016-256
Cefoperazone	CFP	0.016-256
Ampicillin	AB	0.016-256
Cefepime	CPM	0.016-256
Teicoplanin	TEI	0.016-256
Doxycycline	DOX	0.016-256
Cefaclor	CEC	0.016-256
Oxacillin	OXA	0.016-256
Amoxicillin	AMX	0.016-256
Streptomycin	SM	0.064-1024
Ciprofloxacin	CI	0.002-32
Ceftazidime	TZ	0.016-256
Roxithromycin	ROX	0.016-256
Clindamycin	CLN	0.016-256
Cefepime	CPM	0.016-256
Vancomycin	VAN	0.016-256
Tetracyclin	TET	0.016-256
Norfloxacin	NEX	0.016-256
Erythromycin	E	0.001-32
Chlormphenical	C	0.016-256

ANNEXURE-III

This current section includes the composition of bacteriological media, saline/ diluents, buffers used in the current investigation.

1. De mann rogosa and sharpe (MRS) broth

Components	Quantity
Peptone	10.0 g
Beef extract	10.0 g
Yeast extract	5.0 g
Dextrose	20.0 g
Dipotassium hydrogen phosphate	2.0 g
Sodium acetate	5.0 g
Ammonium citrate	2.0 g
Magnesium sulfate	0.1 g
Manganese sulfate	0.05 g
Tween 80	1.0 g
Distilled water	1000 mL
pH	6.5±0.2
Storage temperature	2-8ºC
Sterilization conditions	121ºC/15 min/15 psi

Note: Used for cultivation of *Lactobacilli*

2. M-17 broth

Components	Quantity
Pancreatic digest of casein	5.0 g
Soy peptone	5.0 g
Beef extract	5.0 g
Yeast extract	2.5 g
Ascorbic acid	0.5 g
Magnesium Sulfate	0.25 g
Disodium-β-glycerophosphate	19 g
Distilled water	1000 mL
pH	7.1 ± 0.2

3. DNase Test Agar

Components	Quantity
Tryptone	15.0 g
Soya Peptone	5.0 g
Deoxyribonucleic acid (DNA)	2.0 g
Sodium chloride	5.0 g
Dipotassium hydrogen phosphate	15.0 g
Toluidine blue	0.1 g
Agar powder	18.0 g
Distilled water	1000 mL
pH	7.3±0.2
Storage temperature	10-30ºC
Sterilization conditions	121ºC/15 min/15 psi

Note: Used for detection of deoxyribonuclease activity of bacteria, fungi and especially for the identification of pathogenic Staphylococci

4. Blood agar base

Components	Quantity
Proteose peptone	15.0 g
Live extract	2.5 g
Yeast extract	5.0 g
Sodium chloride	5.0 g
Agar powder	18.0 g
Distilled water	1000 mL
pH	7.4±0.2
Storage temperature	10-30ºC
Sterilization conditions	121ºC/15 min/15 psi
5-10% blood should be supplemented after the media get autoclaved and cooled to 37ºC	

Note: Used for identification of hemolytic activity of fastidious pathogenic microorganisms

5. Brain Heart Infusion (BHI) Broth (Himedia)

Components	Quantity
HM infusion powder	12.5 g
BHI powder	5.0 g
Proteose peptone	10.0 g
Dextrose	2.0 g
Sodium chloride	5.0 g
Disodium phosphate	2.5 g
pH	7.4±0.2
Distilled water	1000 mL
Storage temperature	10-30ºC
Sterilization conditions	121ºC/15 min/15 psi

Note: Used for cultivation of fastidious pathogenic microorganisms

6. Brain Heart Infusion (BHI) agar

Components	Quantity
HM infusion powder	12.5 g
BHI powder	5.0 g
Proteose peptone	10.0 g
Dextrose	2.0 g
Sodium chloride	5.0 g
Disodium phosphate	2.5 g
Agar- agar	15.0 g
pH	7.4±0.2
Distilled water	1000 mL
Storage temperature	10-30ºC
Sterilization conditions	121ºC/15 min/15 psi

Note: Used for cultivation of fastidious pathogenic microorganisms/ faecal flora

7. Physiological saline

Components	Quantity
Sodium chloride	8.5 g
Distilled water	1000 mL
pH	7.0±0.2
Sterilization	121ºC/15 min/15 psi

Note: Used as diluent in the serial dilution process

8. Phosphate buffered saline (PBS)

Components	Concentration
Potassium Chloride	0.0027 M
Sodium Chloride	0.137 M
Distilled water	200 mL
pH	7.4
Sterilization	121ºC/15 min/15 psi

9. Sodium EDTA Tris (SET) buffer

Components	Concentration
75 mM Sodium chloride	22.2 g
25 mM EDTA	7.26 g
20 mM Tris base	1.8 g
Distilled water	100 mL
pH	7.5
Sterilization	121ºC/15 min/15 psi

10. SDS solution (10%)

Components	Quantity
SDS	10 g
Distilled water	100 mL

11. 5 M NaCl

Components	Quantity
NaCl	29.22 g
Distilled water	100 mL

12. Tris-EDTA (TE) buffer

Components	Quantity
Tris (10 mM)	0.121 g
Di-Sodium EDTA (1 mM)	0.037 g
Distilled water	100 mL

13. Tris Acetate EDTA (TAE) buffer (50 X) (Stock solution)

Components	Quantity
Tris	24.20 g
0.5 M Di-sodium EDTA	10 mL
Glacial acetic acid	5.71 mL
Distilled water	100 mL

Note: The working solution was prepared by diluting the 1 mL of stock solution with 49 mL of distilled water.